



University
of Glasgow

Kennedy, Ashleigh (2015) *An investigation of the effects of fentanyl on respiratory control*. PhD thesis.

<http://theses.gla.ac.uk/5998/>

Copyright and moral rights for this thesis are retained by the author

A copy can be downloaded for personal non-commercial research or study, without prior permission or charge

This thesis cannot be reproduced or quoted extensively from without first obtaining permission in writing from the Author

The content must not be changed in any way or sold commercially in any format or medium without the formal permission of the Author

When referring to this work, full bibliographic details including the author, title, awarding institution and date of the thesis must be given

An investigation of the effects of fentanyl on respiratory control

Ashleigh Kennedy

B.Sc (Hons), M.Res

A Thesis submitted in fulfilment of the requirements for the degree of Doctor of Philosophy to the Institute of Neuroscience and Psychology, College of Medical, Veterinary and Life Sciences, University of Glasgow, September, 2014



**University
of Glasgow**

Abstract

Respiration is a complex rhythmic motor behaviour that metabolically supports all physiological processes in the body and is continuous throughout the life of mammals. A failure to generate a respiratory rhythm can be fatal. Understanding how the respiratory rhythm is generated by the brainstem presents a substantial challenge within the field of respiratory neurobiology. Studies utilising *in vitro* and *in vivo* rodent models have provided compelling evidence that a small bilateral region of the ventrolateral medulla, known as the preBötzinger complex (preBötC), is the site for respiratory rhythmogenesis. There is also evidence to suggest a second distinct neuronal group, the retrotrapezoid nucleus/parafacial respiratory group (RTN/pFRG), plays a specialised role in respiratory rhythm generation in the neonatal rodent. During early life in rodents and humans, the respiratory system is immature and an irregular breathing pattern is generated, making this period of life potentially vulnerable to external perturbations. However a step in maturity occurs early in life after which breathing becomes regular. Currently, the underlying mechanisms involved in respiratory rhythm generation during early life are not fully understood. It is hypothesised that the RTN/pFRG functions as the dominant respiratory rhythm generating oscillator during early life when the respiratory system is immature, after which the preBötC becomes the dominant rhythm generator. However, how the preBötC and the RTN/pFRG interact *in vivo* to produce rhythmic breathing during postnatal development remains elusive.

The first aim of this thesis was to assess postnatal maturation of breathing patterns in the mouse using non-invasive whole body plethysmography. Between postnatal day (P) 2 and P3, a critical maturation step occurred, whereby breathing transitioned from an unstable and dysrhythmic pattern to a regular and robust pattern. The second aim of the thesis was to investigate the influence of this postnatal maturation on central respiratory control. Mu (μ) opioid receptor agonists are known respiratory depressants. The activity of the preBötC is depressed by μ opioids *in vitro*. Furthermore, fentanyl, a potent μ opioid receptor agonist, evokes respiratory frequency depression *in vivo* by exclusively targeting and depressing preBötC neurons. Conversely, the RTN/pFRG is insensitive to μ opioids. Accordingly, fentanyl was utilised as a pharmacological tool to selectively perturb the preBötC *in vivo* throughout postnatal development and through to early adulthood. The acute respiratory depressive effects of fentanyl were measured in order to investigate the level of involvement of the preBötC in respiratory rhythm generation throughout this

critical developmental time period. Based on the general hypothesis that the preBötC functions as the dominant respiratory rhythm generator when the respiratory system has matured, it was hypothesised that mice would be more susceptible to the respiratory depressive effects of fentanyl after the maturation step has occurred i.e. the respiratory sensitivity to fentanyl would be age-dependent. Initially, mice were repeatedly exposed to fentanyl throughout postnatal development. However, fentanyl failed to induce a respiratory depression at all postnatal ages, suggesting repeated exposure had induced a rapid desensitisation to fentanyl's respiratory effects. The study design was consequently altered to allow the hypothesis to be sufficiently tested, whereby different mice were studied on each postnatal day i.e. each mouse was only exposed to fentanyl once. This study revealed a trend towards an age-dependent increase in respiratory sensitivity to fentanyl, where mice displayed a heightened respiratory frequency depression in response to fentanyl after the maturation step had occurred from P3 onwards. This data therefore lends support to the hypothesis that the preBötC functions as the dominant respiratory rhythm generator post-maturation.

In the clinical setting fentanyl is widely utilised for treating chronic and acute pain. However, despite the potent respiratory depressive actions of fentanyl, the long-term respiratory consequences of repeated exposure remain unexplored both clinically and pre-clinically. Owing to the immaturity of the respiratory system and the corresponding fragile nature of breathing patterns during neonatal life in mammals, a further aim of the thesis was to determine the long-term effects of fentanyl exposure during this vulnerable respiratory time period in the mouse. To establish if the postnatal age of fentanyl-exposure influences long-term respiratory effects, fentanyl exposure during juvenile life, which is regarded as being post-respiratory maturation, was also assessed. Neonatal mice were exposed to fentanyl (0.04 mg/kg daily) from P1-P5 and juvenile mice were exposed from P9-P13. When mice reached adulthood, baseline respiratory activity and the respiratory response to a subsequent fentanyl challenge were assessed during wakefulness and under anaesthesia. When awake, neonatal-exposed mice exhibited a reduced baseline respiratory frequency and an attenuated respiratory sensitivity to fentanyl. Under anaesthesia, neonatal-exposed mice displayed a depressed baseline minute ventilation and a high frequency of spontaneous augmented breaths. In direct contrast to the wakeful state, when anaesthetised, neonatal-exposed mice exhibited a striking hypersensitivity to the acute respiratory depressive actions of fentanyl. In all neonatal-exposed mice, fentanyl evoked a respiratory failure. In juvenile-exposed mice, baseline respiratory activity remained

unaltered in the wakeful state and fentanyl also failed to induce a respiratory depression. When anaesthetised, baseline minute ventilation remained unchanged and the high occurrence of augmented breaths exhibited by the neonatal-exposed mice was not observed. Unlike the wakeful state, fentanyl evoked a depression of respiratory activity in the juvenile-exposed mice when anaesthetised, however the augmented sensitivity to fentanyl and consequential respiratory arrest displayed by the neonatal-exposed was not observed. This data indicates that the anaesthetised state is more susceptible to respiratory depression. Furthermore, the data suggests that neonatal life represents a time period that is particularly vulnerable to the respiratory effects of opioid depression. The final aim of the thesis was to determine the long-term effects of neonatal fentanyl exposure on neurokinin-1 (NK1R) and μ opioid receptor expression within the ventral respiratory column (VRC), a region of the ventrolateral medulla comprising the preBötC. Neonatal-exposed mice exhibited significantly less NK1R and μ opioid receptor expressing cells in the region of the preBötC. This data suggests that repeated fentanyl exposure in neonatal life induces a long-term downregulation of these receptors.

In conclusion, fentanyl's acute respiratory effects were age-dependent, which lends supports to the hypothesis that the preBötC functions as the dominant rhythm generator post-maturation. Furthermore, this thesis highlights the vulnerabilities of neonatal life to the lasting effects of opioid respiratory depression, whilst also providing invaluable insight into state-dependent respiratory modulation and depression.

Contents

Title Page	i
Abstract	ii
List of Figures	xiii
List of Tables	xviii
Acknowledgements	xix
Author's Declaration	xx
Abbreviations	xxi
Chapter 1. Introduction	25
1.1 Respiration: An essential function	26
1.2 Investigating central respiratory control	26
1.3 Early central respiratory control studies	27
1.4 Respiratory neurons and their location in the brainstem	27
1.5 The preBötzing complex and respiratory rhythm generation	30
1.5.1 Location and identification of preBötC neurons	33
1.5.2 PreBötC neuronal projections	35
1.5.3 PreBötC lesioning	35
1.5.4 Mechanisms of respiratory rhythm generation in the preBötC	36
1.5.4.1 Pacemaker hypothesis	37
1.5.4.2 Group-pacemaker hypothesis	38
1.5.5 Prenatal development of the preBötC	39
1.5.5.1 Anatomical development of the preBötC	39
1.5.5.2 Functional development of the preBötC	39
1.5.6 Transgenic mouse models	40
1.5.7 Human preBötC	41
1.6 The retrotrapezoid nucleus/parafacial respiratory group	42
1.6.1 RTN/pFRG and respiratory rhythm generation	42
1.6.2 Prenatal development of the RTN/pFRG	45
1.6.3 RTN/pFRG and active expiration	46

1.6.4 RTN/pFRG and chemosensitivity	47
1.7 Chemosensitivity	47
1.7.1 Central chemosensitivity	47
1.7.1.1 RTN/pFRG	48
1.7.1.2 Serotonergic neurons	49
1.7.1.3 Locus coeruleus	49
1.7.2 Peripheral chemosensitivity	50
1.8 Developmental plasticity and respiratory activity in early life	50
1.9 Opioids and respiratory depression	53
1.9.1 The preBötC and opioid-induced respiratory depression	55
1.10 Thesis aims	59
Chapter 2. Methods	61
2.1 Animals	62
2.2 Fentanyl injections	62
2.3 Whole body plethysmography	62
2.3.1 Neonatal and juvenile plethysmography	63
2.3.2 Adult plethysmography	65
2.4 Neonatal/juvenile behavioural assessments	67
2.5 Analysis of plethysmograph respiratory traces	67
2.5.1 Respiratory frequency, tidal volume and minute ventilation	67
2.5.2 Neonatal and juvenile breathing patterns	68
2.6 Anaesthetised preparations	72
2.6.1 General surgical preparation	72
2.6.2 Respiratory airflow measurements	72
2.6.3 Respiratory musculature EMG measurements	73
2.6.4 Analysis of airflow and GG_{EMG} activity	74
2.7 Perfusion fixation	76
2.8 Cryostat sectioning	76
2.9 Fluorescent immunohistochemistry	77
2.9.1 Staining protocol	77

Chapter 3. Postnatal Maturation of Central Respiratory Control	80
3.1 Introduction	81
3.1.1 Study aims and rationale	83
3.2 Methods	85
3.2.1 Animals	85
3.2.2 Study design	85
3.2.3 Respiratory measurements	86
3.2.4 Respiratory analysis	87
3.2.5 Behavioural assessments	87
3.2.6 Statistical analysis	88
3.3 Results of study 1: Investigation of postnatal changes in respiratory activity of mice	88
3.3.1 Respiratory traces	88
3.3.2 Quantification of postnatal changes in respiratory activity	92
3.3.2.1 Apnoeas	92
3.3.2.2 Hyperpnoeas	92
3.3.2.3 Hiccups	93
3.3.2.4 Respiratory frequency	98
3.4 Discussion of study 1: Investigation of postnatal changes in respiratory activity of mice	101
3.4.1 Respiratory activity undergoes significant postnatal changes	101
3.4.1.1 Apnoeas	101
3.4.1.2 Hyperpnoeic breathing	102
3.4.1.3 Hiccups	104
3.4.1.4 Respiratory frequency	104
3.4.2 Critical developmental time window between P2 and P3	105
3.4.3 Study limitations and future directions	105
3.5 Results of study 2. Susceptibility of postnatal breathing patterns to fentanyl: A longitudinal study	107
3.5.1 Behavioural assessments	107
3.5.2 Respiratory traces	109
3.5.3 Respiratory frequency	111

3.5.4 Tidal volume	111
3.6 Results of Study 3. Susceptibility of postnatal breathing patterns to fentanyl:	
A single exposure Study	114
3.6.1 Behavioural assessments	114
3.6.2 Plethysmography respiratory traces	116
3.6.3 Respiratory frequency	118
3.6.4 Tidal volume	122
3.7 Discussion of studies 2 and 3	124
3.7.1 Repeated exposure induced an acute respiratory tolerance to fentanyl	124
3.7.2 Respiratory sensitivity to fentanyl was age-dependent	127
3.7.3 Study limitations and points to consider	130
3.7.4 Summary	132
Chapter 4. Long-term respiratory effects of repeated fentanyl exposure in neonatal and juvenile mice	133
4.1 Introduction	134
4.1.1 Study aims and rationale	135
4.1.2 Hypotheses	136
4.2 Methods	137
4.2.1 Animals	137
4.2.2 Study design	137
4.2.3 Repeated fentanyl exposure	138
4.2.4 Definition of experimental groups	138
4.2.5 Respiratory recording in awake adult mice	141
4.2.5.1 Baseline breathing and acute respiratory response to fentanyl challenge	141
4.2.5.2 Chemosensitivity experiments	141
4.2.6 Respiratory analysis in awake adult mice	142
4.2.6.1 Baseline breathing and acute respiratory response to fentanyl challenge	142
4.2.6.2 Chemoresponses	142

4.2.7 Statistical analysis of respiratory variables in awake adult mice	143
4.2.8 Respiratory recording in anaesthetised adult mice	143
4.2.9 Respiratory analysis in anaesthetised adult mice	144
4.2.10 Statistical analysis of respiratory variables in anaesthetised adult mice	144
4.3 Results of study 4: Investigation of the long-term respiratory effects of repeated fentanyl exposure in the neonatal mouse	145
4.3.1 Animal body weights	145
4.3.2 Baseline respiratory parameters of awake adult mice	146
4.3.3 Acute fentanyl challenge in awake mice	148
4.3.3.1 Respiratory frequency	148
4.3.3.2 Tidal volume	149
4.3.3.3 Minute ventilation	150
4.3.3.4 Plethysmography respiratory traces	157
4.3.4 Chemosensitivity	159
4.3.5 Baseline respiratory parameters of adult mice under anaesthesia	161
4.3.6 Augmented breaths	163
4.3.7 Acute fentanyl challenge in anaesthetised mice	165
4.3.7.1 Respiratory frequency	165
4.3.7.2 Tidal volume and minute ventilation	166
4.3.7.3 Genioglossus activity	166
4.3.7.4 Physiological traces from anaesthetised preparations	172
4.4 Results of study 5: Investigation of the long-term respiratory effects of repeated fentanyl exposure in the juvenile mouse	175
4.4.1 Animal body weights	175
4.4.2 Baseline respiratory parameters of awake adult mice	176
4.4.3 Acute fentanyl challenge in awake mice	178
4.4.3.1 Respiratory frequency	178
4.4.3.2 Tidal volume	179
4.4.3.3 Minute ventilation	180
4.4.3.4 Plethysmography respiratory traces	187
4.4.4 Baseline respiratory parameters of adult mice under anaesthesia	189
4.4.5 Augmented breaths	191

4.4.6 Acute fentanyl challenge in anaesthetised mice	192
4.4.6.1 Respiratory frequency	192
4.4.6.2 Tidal volume and minute ventilation	192
4.4.6.3 Genioglossus activity	193
4.4.6.4 Physiological traces from anaesthetised preparations	198
4.5 Discussion	201
4.5.1 Wakeful state: resting breathing	201
4.5.1.1 Neonatal fentanyl exposure induced lasting changes in resting breathing during wakefulness	201
4.5.1.2 Neonatal fentanyl exposure does not alter respiratory response to hypercapnia or hypoxia	202
4.5.1.3 Juvenile fentanyl exposure did not induce lasting changes in resting breathing during wakefulness	204
4.5.2 Wakeful state: acute respiratory response to fentanyl	204
4.5.2.1 Neonatal-exposed mice exhibited a reduced sensitivity to fentanyl during wakefulness	204
4.5.2.2 Juvenile-exposed mice exhibited a reduced sensitivity to fentanyl during wakefulness	207
4.5.3 Anaesthetised state: resting breathing	208
4.5.3.1 Neonatal fentanyl exposure induced lasting changes in resting breathing under anaesthesia	208
4.5.3.2 Juvenile fentanyl exposure induced lasting changes in resting breathing under anaesthesia	212
4.5.4 Anaesthetised state: acute respiratory response to fentanyl	213
4.5.4.1 Neonatal-exposed mice exhibited a heightened sensitivity to fentanyl under anaesthesia	213
4.5.4.2 Juvenile-exposed mice did not exhibit an altered sensitivity to fentanyl under anaesthesia	215
4.5.5 Neonatal life is vulnerable to repeated fentanyl exposure	216
4.5.6 Future experimental studies	218
4.5.7 Limitations and technical issues	220
4.5.8 Summary	220

Chapter 5. Long-term respiratory effects of repeated fentanyl exposure in the neonatal mouse: Immunohistochemical analysis of the ventral respiratory column	222
5.1 Introduction	223
5.1.1 Study 6 aims and rationale	224
5.2 Methods	225
5.2.1 Animals	225
5.2.2 Chronic fentanyl exposure	225
5.2.3 Perfusion fixation and cryostat sectioning	225
5.2.4 Antibody combinations	226
5.2.4.1 NK1R immunostaining	226
5.2.4.2 μ opioid receptor immunostaining	226
5.2.4.3 Phox2b immunostaining	226
5.2.5 Immunofluorescent imaging and quantification	227
5.2.6 Statistical analysis	228
5.3 Results	232
5.3.1 NK1R expression throughout the VRC	232
5.3.2 μ opioid receptor expression throughout the VRC	237
5.3.3 μ opioid receptor expression outside the VRC	241
5.3.4 Phox2b expression throughout the VRC	242
5.4 Discussion	243
5.4.1 Neonatal-exposed mice exhibited a reduction in NK1R expression within the preBötC	243
5.4.2 NK1R expression within the RTN/pFRG was unaltered	245
5.4.3 Neonatal-exposed mice exhibited a striking reduction in μ opioid receptor expression within the VRC	245
5.4.4 Study limitations and technical issues	249
5.4.5 Immunohistochemical analysis of juvenile-exposed brains	250
5.4.6 Summary	251

Chapter 6. General Conclusions	253
6.1 Critical respiratory maturational time window	254
6.2 Repeated exposure induces an acute respiratory tolerance to fentanyl	255
6.3 Fentanyl-induced respiratory depression is age-dependent	255
6.4 Neonatal life is vulnerable to repeated fentanyl exposure	256
6.5 Fentanyl exposure in neonatal life induces long-term changes in μ opioid receptor expression within the VRC	258
6.6 Behavioural state and respiratory activity	258
6.7 Future Directions	259
6.8 Concluding remarks	259
References	261
Appendix I	286

List of Figures

Figure 1-1. Schematic illustrations showing the location of the principal respiratory neurons in the rodent brainstem.	28
Figure 1-2. Schematic illustration of a medullary slice preparation that contains the preBötC and generates a respiratory-like rhythm.	32
Figure 1-3. μ opioid receptor expressing neurons are found within the preBötC.	34
Figure 1-4. Disordered breathing exhibited by awake adult rats after bilateral ablation of the preBötC.	36
Figure 1-5. Naloxone eliminates apnoeas and increases respiratory frequency in <i>Krox-20</i> null mutant mice.	45
Figure 1-6. Schematic illustration of the two proposed respiratory rhythm generators in early postnatal life.	52
Figure 1-7. Schematic illustration of the structure of the μ opioid receptor.	54
Figure 1-8. Systemically administered fentanyl mediates respiratory frequency depression by directly targeting the preBötC.	57
Figure 1-9. μ opioid receptor agonists suppress the activity of NK1R-expressing inspiratory preBötC neurons <i>in vitro</i> .	58
Figure 2-1. Whole body plethysmography apparatus used for neonatal and juvenile mice.	63
Figure 2-2. Whole body plethysmography apparatus used for adult mice.	66
Figure 2-3. Calculation of respiratory frequency from plethysmograph trace.	69
Figure 2-4. Calculation of tidal volume from plethysmograph trace.	70
Figure 2-5. Representative respiratory traces illustrating various neonatal breathing patterns.	71
Figure 2-6. Calculation of respiratory frequency from airflow trace.	75
Figure 2-7. Schematic diagram illustrating how brainstem sections were split into 4 groups.	78
Figure 2-8. Schematic diagram illustrating the principle of tyramide signal amplification (TSA) in immunohistochemistry.	79
Figure 3-1. Representative respiratory traces illustrating postnatal maturation of breathing patterns.	90

Figure 3-2. Representative respiratory traces illustrating hiccup breathing patterns in a P1 and P5 mouse.	91
Figure 3-3. Number of apnoeas exhibited throughout postnatal development.	94
Figure 3-4. Number of hyperpnoeas exhibited throughout postnatal development.	95
Figure 3-5. Number of hiccups exhibited throughout postnatal development.	96
Figure 3-6. Changes in average respiratory frequency (bpm) throughout postnatal development.	99
Figure 3-7. Coefficient of variation (CV) of respiratory frequency throughout postnatal development.	100
Figure 3-8. Representative plethysmography respiratory traces illustrating the effects of saline and fentanyl in P1, P2, P5 and P11 mice.	110
Figure 3-9. Acute changes in respiratory frequency in response to saline or fentanyl throughout postnatal life.	112
Figure 3-10. Acute changes in tidal volume (Vt) in response to saline or fentanyl throughout postnatal life.	113
Figure 3-11. Representative plethysmography respiratory traces illustrating the effects of saline and fentanyl in P1, P2, P3 and P30 mice.	117
Figure 3-12. Absolute changes in respiratory frequency in response to saline or fentanyl throughout postnatal life.	120
Figure 3-13. Relative change in respiratory frequency in response to saline or fentanyl throughout postnatal life.	121
Figure 3-14. Relative change in tidal volume in response to saline or fentanyl throughout postnatal life.	123
Figure 4-1. Experimental protocols undertaken in study 4.	139
Figure 4-2. Experimental protocols undertaken in study 5.	140
Figure 4-3. Baseline respiratory parameters of adult control and neonatal-exposed mice during wakefulness.	147
Figure 4-4. Changes in respiratory frequency in response to a single fentanyl challenge in control and neonatal-exposed mice when awake.	151
Figure 4-5. Percentage change in respiratory frequency in response to a single fentanyl challenge in control and neonatal-exposed mice when awake.	152
Figure 4-6. Changes in tidal volume (Vt) in response to a single fentanyl challenge in control and neonatal-exposed mice when awake.	153

Figure 4-7. Percentage change in tidal volume (V_t) in response to a single fentanyl challenge in control and neonatal-exposed mice when awake.	154
Figure 4-8. Changes in minute ventilation (V_e) in response to a single fentanyl challenge in control and neonatal-exposed mice when awake.	155
Figure 4-9. Percentage change in minute ventilation (V_e) in response to a single fentanyl challenge in control and neonatal-exposed mice when awake.	156
Figure 4-10. Representative respiratory traces before and after fentanyl challenge in control and neonatal-exposed mice.	158
Figure 4-11. Respiratory responses of control and neonatal-exposed mice to hypercapnic and hypoxic stimuli in the wakeful state.	160
Figure 4-12. Baseline respiratory parameters of adult control and neonatal-exposed mice under anaesthesia.	162
Figure 4-13. Examples of baseline GG_{EMG} and ABD_{EMG} activity.	163
Figure 4-14. Number of augmented breaths exhibited by control and neonatal-exposed mice under anaesthesia.	164
Figure 4-15. Changes in respiratory frequency in response to a fentanyl challenge in control and neonatal-exposed mice under anaesthesia.	168
Figure 4-16. Changes in tidal volume (V_t) in response to a fentanyl challenge in control and neonatal-exposed mice under anaesthesia.	169
Figure 4-17. Changes in minute ventilation (V_e) in response to a fentanyl challenge in control and neonatal-exposed mice under anaesthesia.	170
Figure 4-18. Changes in genioglossus amplitude in response to a fentanyl challenge in control and neonatal-exposed mice under anaesthesia.	171
Figure 4-19. Representative airflow and GG_{EMG} trace taken from a control mouse administered 0.02 mg/kg fentanyl under anaesthesia.	173
Figure 4-20. Representative airflow and GG_{EMG} trace taken from a neonatal-exposed mouse administered 0.02 mg/kg fentanyl under anaesthesia.	174
Figure 4-21. Baseline respiratory parameters of adult control and juvenile-exposed mice during wakefulness.	177
Figure 4-22. Changes in respiratory frequency in response to a single fentanyl challenge in control and juvenile-exposed mice when awake.	181

Figure 4-23. Percentage change in respiratory frequency in response to a single fentanyl challenge in control and juvenile-exposed mice when awake.	182
Figure 4-24. Changes in tidal volume (V_t) in response to a single fentanyl challenge in control and juvenile-exposed mice when awake.	183
Figure 4-25. Percentage change in tidal volume (V_t) in response to a single fentanyl challenge in control and juvenile-exposed mice when awake.	184
Figure 4-26. Changes in minute ventilation (V_e) in response to a single fentanyl challenge in control and juvenile-exposed mice when awake.	185
Figure 4-27. Percentage change in minute ventilation (V_e) in response to a single fentanyl challenge in control and juvenile-exposed mice when awake.	186
Figure 4-28. Representative respiratory traces before and after a fentanyl challenge taken from control and juvenile-exposed mice.	188
Figure 4-29. Baseline respiratory parameters of adult control and juvenile-exposed mice under anaesthesia.	190
Figure 4-30. Number of augmented breaths exhibited by control and juvenile-exposed mice under anaesthesia.	191
Figure 4-31. Changes in respiratory frequency in response to a fentanyl challenge in control and juvenile-exposed mice under anaesthesia.	194
Figure 4-32. Changes in tidal volume (V_t) in response to a fentanyl challenge in control and juvenile-exposed mice under anaesthesia.	195
Figure 4-33. Changes in minute ventilation (V_e) in response to a fentanyl challenge in control and juvenile-exposed mice under anaesthesia.	196
Figure 4-34. Changes in GG amplitude in response to a fentanyl challenge in control and juvenile-exposed mice under anaesthesia.	197
Figure 4-35. Representative airflow and GG _{EMG} trace taken from a control mouse administered 0.02 mg/kg fentanyl under anaesthesia.	199
Figure 4-36. Representative airflow and GG _{EMG} trace taken from a juvenile-exposed mouse administered 0.02 mg/kg fentanyl under anaesthesia.	200
Figure 5-1. The rostrocaudal extent of the ventral respiratory column (VRC) analysed.	229

Figure 5-2. Method of cell counting within the region of the VRC containing the preBötC.	230
Figure 5-3. Method of cell counting within the region of the RTN/pFRG.	231
Figure 5-4. Fluorescent images showing NK1R expressing cells within the preBötC of control (A) and neonatal-exposed (B) mice.	234
Figure 5-5. Fluorescent images showing NK1R expressing cells within the RTN/pFRG of control (A) and neonatal-exposed (B) mice.	235
Figure 5-6. Number of NK1R immunopositive cells throughout the VRC in control and neonatal-exposed mice.	236
Figure 5-7. Fluorescent images showing μ opioid receptor expressing cells within the preBötC of control (A) and neonatal-exposed (B) mice.	238
Figure 5-8. Fluorescent images showing a lack of μ opioid receptor expressing cells within the RTN/pFRG of control and neonatal-exposed mice.	239
Figure 5-9. Number of μ opioid receptor immunopositive cells throughout the VRC in control and neonatal-exposed mice.	240
Figure 5-10. Fluorescent images showing μ opioid receptor expressing cells within the hypoglossal nucleus of control and neonatal-exposed mice.	241
Figure 5-11. Fluorescent images showing Phox2b expressing cells within the RTN/pFRG of control (A) and neonatal-exposed (B) mice.	242

List of Tables

Table 3-1. Percentage of mice displaying apnoeas, hyperpnoeas and hiccups at each postnatal age.	97
Table 3-2. Assessment of body temperature before and after saline or fentanyl administration.	108
Table 3-3. Assessment of righting reflex before and after saline or fentanyl administration.	108
Table 3-4. Mastication rate before and after saline or fentanyl administration.	109
Table 3-5. Assessment of body temperature before and after saline or fentanyl administration.	115
Table 3-6. Assessment of righting reflex before and after saline or fentanyl administration.	115
Table 3-7. Mastication rate before and after saline or fentanyl administration.	116
Table 4-1. Average body weights of control and neonatal-exposed mice.	145
Table 4-2. Average body weights of control and juvenile-exposed mice.	175
Table 4-3. Summary of the long-term respiratory effects of repeated fentanyl exposure in the neonatal and juvenile mouse.	221

Acknowledgements

I would first and foremost like to thank my supervisor, Dr Leanne McKay for not only giving me the opportunity to conduct research in her lab but also for her continued support and guidance throughout the duration of my PhD. It has been greatly appreciated. I would also like to extend my thanks to Professor I Mhairi Macrae for her guidance and advice during my thesis write up.

Thank you to all the staff at the Wellcome Surgical Institute. Everyone has been very supportive and I feel privileged to have worked alongside you all. A special thanks goes to Linda Carberry and Vicky King for their assistance during my immunohistochemistry studies.

A massive thank you goes to my Garscube friends: Emma B, Lisa, Tristan, Emma M, Vicky, Emma R and Dave. Thank you all for keeping me sane during the challenging times and for making this experience so enjoyable. I hope the wall of appreciation continues to flourish!

Finally, I wish to thank my parents and my boyfriend, Stephen, without whom, completing my research and writing this thesis would have been a more difficult task. Your endless support and encouragement has been unrivalled. I dedicate my thesis to you.

Author's Declaration

I declare that, except where explicit reference is made to the contribution of others, this dissertation is the result of my own work and has not been submitted for any other degree at the University of Glasgow or any other institution.

Ashleigh Kennedy,

September 2014

Abbreviations

μ -OR	μ opioid receptor
2-DG	2-deoxyglucose
5-HT	Serotonin
ABD	Abdominal muscle
ABD _{EMG}	Abdominal muscle EMG activity
AMPA	Amino-3-hydroxy-5-methyl-4-isoxazolepropionate
ANOVA	Analysis of variance
A.u	Arbitrary units
<i>Atoh1</i>	<i>Atonal homolog 1</i>
ATP	Adenosine triphosphate
BC	Böttinger complex
Bpm	Breaths per minute
BrdU	5-bromo-2-deoxyuridine
C4	Cervical spinal nerve 4
CCHS	Congenital central hypoventilation syndrome
ChAT	Choline acetyltransferase
CNS	Central nervous system
CO ₂	Carbon dioxide
CPG	Central pattern generator
cVRG	Caudal ventral respiratory group
DAMGO	d-Ala(2),NMePhe(4),Gly-ol(5)enkephalin
<i>Dbx1</i>	<i>developing brain homeobox protein 1</i>

DRG	Dorsal respiratory group
E	Embryonic day
EEG	Electroencephalography
EMG	Electromyography
e-pF	Embryonic parafacial oscillator
FBMs	Fetal breathing movements
FFA	Flufenamic acid
GABA	γ -aminobutyric acid
GAD67	Glutamic acid decarboxylase 67
GG	Genioglossus
GG _{EMG}	Genioglossus EMG activity
GlyT2	Glycine transporter 2
GPCRs	G protein coupled receptors
GRKs	G protein-coupled receptor kinases
H ₂ O ₂	Hydrogen peroxide
HEB	Hyperpnoeic episodic breathing
IHC	Immunohistochemistry
I _{NaP}	Persistent sodium current
I.p	Intraperitoneal
K-F	Kö llicker-Fuse
<i>Lbx1</i>	<i>Ladybird homeobox homolog 1</i>
LC	Locus coeruleus
LRN	Lateral reticular nucleus
<i>MafB</i>	<i>v-maf musculoaponeurotic fibrosarcoma oncogene homologue B</i>

NA	Nucleus ambiguus
NDS	Normal donkey serum
NK1R	Neurokinin-1 receptor
NMS	Neonatal maternal separation
NTS	Nucleus tractus solitarius
nREM	Non-rapid eye movement
NTS	Nucleus tractus solitarius
O ₂	Oxygen
P	Postnatal day
PB	Phosphate buffer
PBc	Parabrachial complex
PBS	Phosphate buffered saline
PBST	Phosphate buffered saline with 0.3% Triton X-100
Phox2b	Paired-like homeobox 2b
PreBötC	PreBötzinger complex
Pre-I	Pre-inspiratory
PRG	Pontine respiratory group
PKA	Protein kinase A
PKC	Protein kinase C
REM	Rapid eye movement
RTN/pFRG	Retrotrapezoid nucleus/parafacial respiratory group
rVRG	Rostral ventral respiratory group
scNA	Subcompact formation of the nucleus ambiguus
SIDS	Sudden infant death syndrome

SP	Substance P
SP-SAP	Substance P conjugated to saporin
SST	Somatostatin
TSA	Tyramide Signal Amplification
Ttot	Total breath time
Ve	Minute ventilation
VGLUT2	Vesicular glutamate transporter 2
VII	Facial motor nucleus
VLM	Ventrolateral medulla
VRC	Ventral respiratory column
VRG	Ventral respiratory group
Vt	Tidal volume
XII	Hypoglossal nucleus

Chapter 1.

Introduction

1.1 Respiration: An essential function

Respiration is a unique and fundamental physiological process in mammals and is continuous throughout life. It is a stringently controlled rhythmic motor output that functions to maintain blood oxygen (O_2), carbon dioxide (CO_2) and pH, essential to mammalian survival. Mammals have a high metabolic rate and therefore require a constant, rich supply of O_2 . In humans, the demand for O_2 can rapidly change (e.g. triples during modest movements) and as a result, respiration must be highly labile, constantly responding and adapting to environmental and behavioural stimuli. Furthermore, it must also be coordinated with other complex behaviours such as speech, coughing, sneezing and swallowing. Given that irreversible brain damage can occur after only a few minutes of low blood O_2 , respiration must be unremitting. Despite the vital role of respiration in sustaining life, the underlying neuronal mechanisms by which the respiratory motor rhythm is generated and also modulated are still largely unknown, and identifying these mechanisms represents an important challenge in the field of respiratory neurobiology.

1.2 Investigating central respiratory control

It has been long established that the brainstem is the neural basis for the automatic control of breathing. The ultimate goal of respiratory research is to fully understand normal and pathological breathing in humans; however investigating the neural control of breathing in humans is limited. Invasive techniques are impractical due to the small size of the neural structures within the brainstem, as well as ethical considerations. Furthermore, non-invasive neuroimaging of the brainstem is difficult, owing to the brainstem's compact structure and extensive blood vessel innervation. Consequently, much of the existing knowledge of central respiratory control is derived from experimental studies undertaken in non-primate animal models, with rodents being the current model of choice. Respiratory control is particularly amenable to experimental research since respiratory activity that is present in the whole animal, including rhythmic respiratory neural and motor output, can be recorded in highly reduced vertebrate preparations (Smith et al., 1991).

1.3 Early central respiratory control studies

Early investigations in the field of respiratory neurobiology found that respiratory movements persisted after complete removal of the cerebrum in rabbits and were only abolished when the brainstem was removed. In addition, specific lesions within the medulla induced a cessation of respiratory activity, leading to the conclusion that the circuitry essential for respiratory control was located within the medulla (LeGallois, 1813). In 1868, Hering and Breuer discovered that inflation and deflation of the lung initiated breathing reflexes which indicated that afferent inputs from the periphery could modulate central respiratory control (Hering and Breuer, 1868). The importance of the brainstem in ventilatory control was further acknowledged in 1923, by Lumsden (Lumsden, 1923), who performed brain transections in the anaesthetised cat. A transection through the medullary-cervical junction evoked a complete cessation of respiratory function, supporting the theory that the brainstem contains critical respiratory centres. Further transections identified the caudal pons and rostral medulla as an apneusis centre, believed to produce prolonged inspiratory pauses and identified the rostral pons as a pneumotaxic site i.e. the site for normal rhythmic breathing. The introduction of single-cell recordings further advanced respiratory research allowing individual medullary neurons to be recorded from. This led to the description of respiratory neurons, defined as such because their firing pattern corresponded with particular phases of the respiratory cycle (Salmoiraghi and Burns, 1960). The primary focus of subsequent research was identifying the neural networks responsible for the generation of the respiratory rhythm.

1.4 Respiratory neurons and their location in the brainstem

Breathing is generated and modulated by a complex neural circuitry within the brainstem. There are distinct clusters of respiratory-related and functionally interacting neurons located bilaterally within the pons in an area defined as the pontine respiratory group (PRG), and in the medulla within a region named the dorsal respiratory group (DRG) and the ventral respiratory column (VRC). The VRC is located in the ventrolateral medulla and extends from the upper spinal cord through to the facial motor nucleus. Figure 1-1 illustrates the location of the main respiratory neurones in the rodent brainstem.

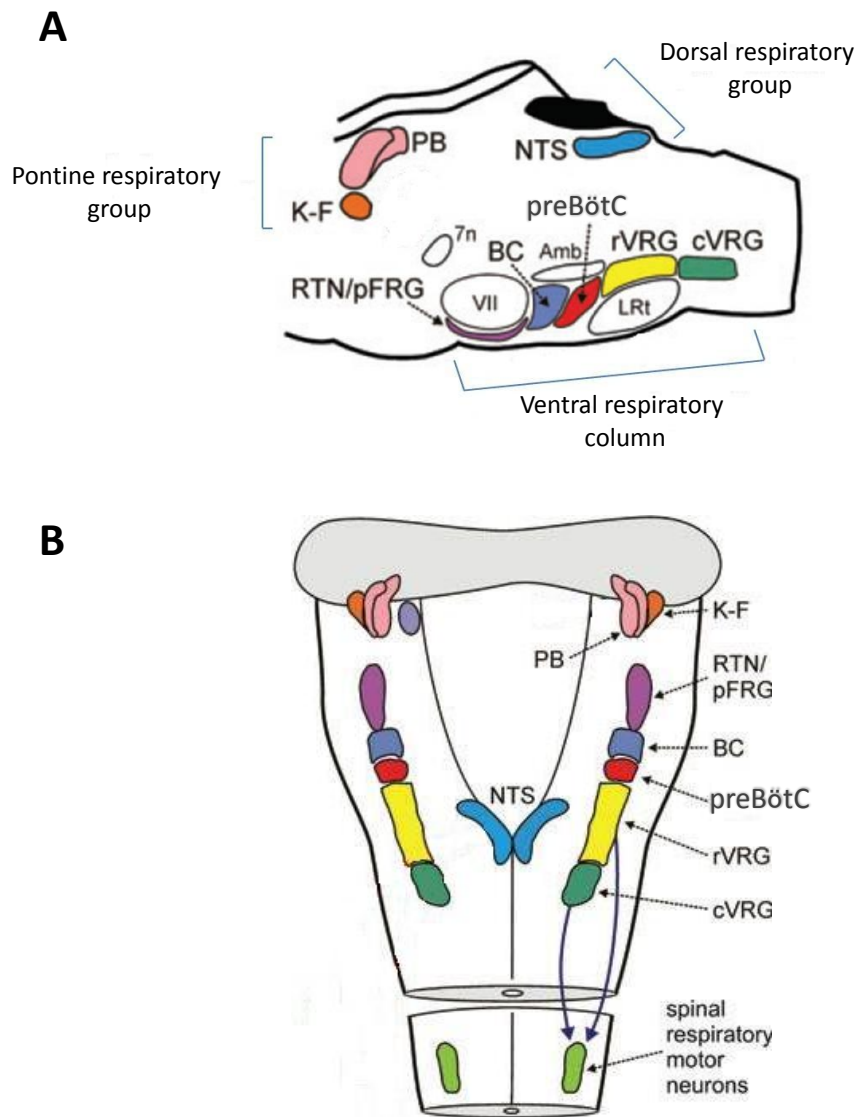


Figure 1-1. Schematic illustrations showing the location of the principal respiratory neurons in the rodent brainstem. Parasagittal view (A) and horizontal, dorsal view (B) of the brainstem showing the pontine respiratory group, the dorsal respiratory group and the rostro-caudally distributed respiratory neurons within the ventral respiratory column. Abbreviations: 7n, facial nerve; Amb, nucleus ambiguus; BC, Bötzing complex; cVRG, caudal ventral respiratory group, K-F, Kölliker-Fuse nucleus; LRT, lateral reticular nucleus; NTS, nucleus tractus solitarius; PB, parabrachial complex; preBötC, preBötzinger complex; RTN/pFRG, retrotrapezoid nucleus/parafacial respiratory group; rVRG, rostral ventral respiratory group; VII, facial motor nucleus. Modified from Spyer (2009).

Within the PRG, the Kölliker-Fuse (K-F) and the parabrachial complex (PBc) are the main respiratory nuclei. The exact role of the pons in neural control of breathing remains elusive, but studies suggest it plays a modulatory role to shape and adapt the respiratory pattern. Anatomical and electrophysiological tracing studies have shown that the pontine nuclei have synaptic inputs into the medulla (Gang et al., 1995; Ezure et al., 1998; Jiang et al., 2004) and computational modelling studies suggest these areas regulate the output from the preBötzinger complex (Rybak et al., 2004). Electrical stimulation and glutamate injection into the PBc and K-F neurons has revealed that the lateral PBc modulates the inspiratory phase whereas the medial PBc and K-F modulates the expiratory phase (Lara et al., 1994). The K-F has also been proposed to control the transition from inspiration to expiration, as lesioning and pharmacological manipulation of this nucleus extends the duration of inspiration (Dutschmann et al., 2004; Dutschmann and Herbert, 2006). Furthermore, transection of the pons below the PBc evokes an apneusis breathing pattern (Feldman and Gautier, 1976), further indicating the role of the pons in modulating inspiratory activity. The K-F also comprises pharyngeal premotor neurons that act to regulate upper airway resistance (Dutschmann and Herbert, 2006).

The DRG is located within the nucleus tractus solitarius (NTS) and provides an important interface between afferent information from the periphery and the brain circuitry. In terms of respiratory control, the NTS functions to relay afferent inputs allowing for modulation of respiratory activity. The NTS receives vagal inputs from lung and airway mechanoreceptors, peripheral chemoreceptors as well as other visceral sensory afferent inputs. NTS neurons project and terminate in the pons, the VRC of the medulla and the spinal cord (Alheid et al., 2011).

The ventral respiratory group (VRG) is located within the rostro-caudally arranged VRC and is subdivided into a caudal and rostral region. The caudal ventral respiratory group (cVRG) contains excitatory expiratory bulbospinal premotor neurons that innervate spinal thoracic and lumbar motoneurons (Shen and Duffin, 2002), thereby shaping the patterns of expiratory motor output. The rostral ventral respiratory group (rVRG) comprises mainly excitatory bulbospinal premotor inspiratory neurons that project to both spinal phrenic motoneurons that in turn innervate the diaphragm (Dobbins and Feldman, 1994) and to external intercostal motoneurons in the thoracic spinal cord (Stornetta et al., 2003a).

Rostral to the VRG, resides the preBötzinger complex (preBötC). This small bilateral cluster of glutamatergic interneurons is considered the principal site of respiratory rhythm generation (Smith et al, 1991) and will be discussed in detail in section 1.5.

The Bötzing complex (BC) is located directly rostral to the preBötC and caudal to the facial motor nucleus. This neuronal group comprises mainly inhibitory expiratory neurons (Smith et al., 2007), including glycinergic and GABAergic neurons (Ezure et al., 2003) that provide widespread inhibitory projections throughout the VRC (Jiang and Lipski, 1990) and to spinal phrenic motoneurons (Tian et al., 1998). The BC neurons are believed to inhibit inspiratory neurons allowing the switch between inspiration and expiration (Smith et al., 2007).

In the most rostral region of the VRC lies the retrotrapezoid nucleus/parafacial respiratory group (RTN/pFRG), a cluster of neurons situated in close proximity to the facial motor nucleus and the ventral medullary surface. The RTN/pFRG has been implicated in both the generation of respiratory rhythm in early life (Onimaru and Homma, 2003) as well as central chemoreception (Mulkey et al., 2004; Guyenet et al., 2005) and will be fully discussed in section 1.6.

1.5 The preBötzinger complex and respiratory rhythm generation

Understanding where and how the rhythmic motor pattern of breathing is generated has fascinated scientists for decades, and consequently a great deal of research has been dedicated to uncovering this. There is now extensive evidence that a bilateral cluster of neurons known as the preBötzinger complex (preBötC), located in the ventrolateral medulla, are fundamental to respiratory rhythmogenesis. The preBötC has long been postulated to contain the kernel for respiratory rhythm generation (Smith et al., 1991). The advent of the isolated rodent brainstem spinal cord (*en bloc*) preparation and the rhythmically active medullary slice preparation have greatly facilitated the study of the preBötC and significantly advanced the understanding of the functional role of this neural group. The neonatal rat brainstem-spinal cord preparation continues to generate a respiratory-like rhythmic motor output that can be recorded from electrodes positioned on the hypoglossal and phrenic nerve rootlets. The hypoglossal nerve innervates the genioglossus and the phrenic nerve innervates the diaphragm, two inspiratory muscles. Recording this motor activity is therefore a measure of inspiratory activity. Serial

transections of this brainstem-spinal cord preparation in a rostral and caudal direction do not abolish the respiratory rhythm until a transection is made through the mid medulla, where the preBötC is located (Smith et al., 1991). The isolated neonatal rodent medullary slice preparation preserves the preBötC as well as hypoglossal respiratory motoneurons, and continues to generate a respiratory-like rhythm that is comparable to the rhythmic activity recorded from the more intact brainstem-spinal cord preparation (Smith et al., 1991). Intracellular recordings of preBötC neurons in the slice preparation reveal intrinsic rhythmogenic activity that occurs simultaneously with inspiratory hypoglossal motor output (Figure 1-2). This further suggests the preBötC plays a role in respiratory rhythmogenesis and generates the inspiratory rhythm. PreBötC neurons are consequently referred to as being inspiratory modulated. Microinjection of 6-cyano-7-nitroquinoxaline-2,3-dione (CNQX), a non-N-methyl-D-aspartate glutamate receptor antagonist into the preBötC in the slice preparation decreases and then eliminates the oscillatory respiratory output (Smith et al., 1991). This indicates that glutamatergic neurotransmission within the preBötC is essential for respiratory rhythm generation. These landmark experiments were the first to identify the preBötC as being necessary and sufficient for generating the inspiratory rhythm that in turn generates inspiratory motor output *in vitro*, indicating the preBötC functions as an oscillator driving inspiration. In light of these findings, an extensive array of studies within the field of respiratory neurobiology was then conducted in an attempt to further uncover the role of the preBötC in respiratory rhythm generation.

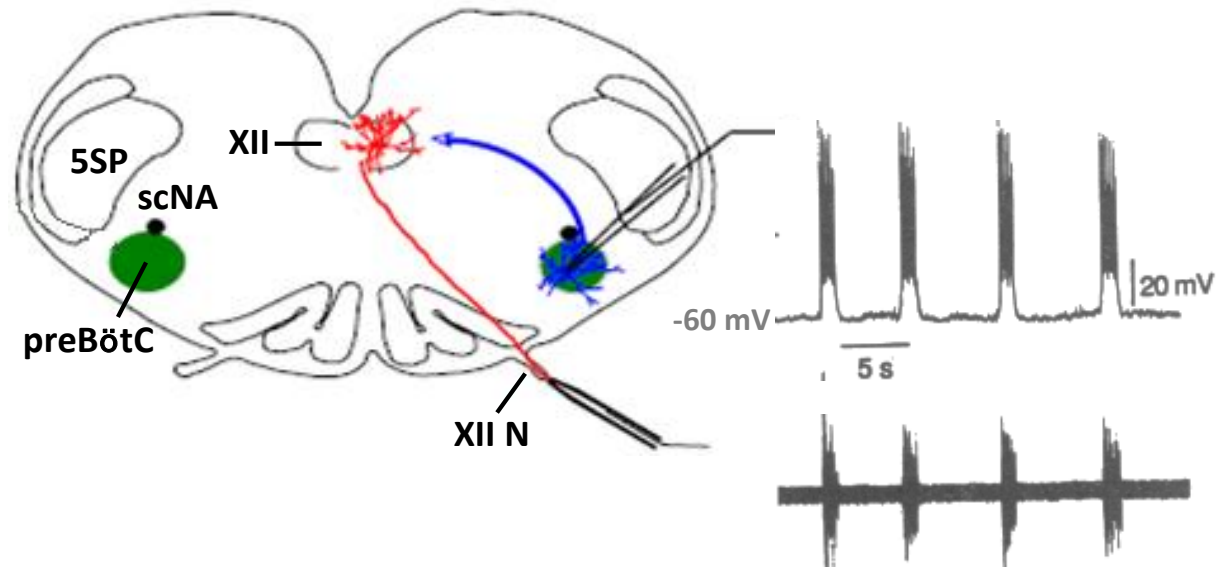


Figure 1-2. Schematic illustration of a medullary slice preparation that contains the preBötC and generates a respiratory-like rhythm. The preBötC sends neural signals to the hypoglossal nucleus (XII) which in turn drives the hypoglossal nerve (XII N). Respiratory-related rhythmic activity can be intracellularly recorded from individual preBötC neurons (top trace) or extracellularly recorded from the XII N. Note that the oscillatory activity of the preBötC occurs concurrently with the hypoglossal inspiratory motor output suggesting the preBötC drives inspiratory rhythm. 5SP, spinal trigeminal nucleus; preBötC, preBötzinger complex; scNA, subcompact formation of the nucleus ambiguus. Modified from Smith et al. (1991).

1.5.1 Location and identification of preBötC neurons

Elucidating the precise location and rostrocaudal boundaries of the preBötC has received a great deal of attention. Gray and colleagues (1999) investigated the effects of various peptides on rhythmic respiratory activity of the preBötC. Application of the neuropeptide substance P (SP) directly into the preBötC in the neonatal medullary slice preparation initiated an increase in the frequency of the endogenous respiratory bursting. It was concluded that the powerful respiratory excitation is mediated through the membrane neurokinin-1 receptor (NK1R) given that SP is the natural ligand for this receptor. Immunohistochemical analyses of the VRC in the rat have revealed that neurons within the level of the preBötC express high levels of NK1R (Gray et al., 1999; Guyenet and Wang, 2001; Wang et al., 2001a; Guyenet et al., 2002); thus the NK1R has been proposed as an anatomical marker for preBötC neurons. The NK1R-expressing preBötC neurons have also been shown to express vesicular glutamate transporter 2 (VGLUT2) and are immunoreactive for glutamate indicating that the preBötC neurons are glutamatergic and therefore excitatory (Liu et al., 2001; Guyenet et al., 2002; Stornetta et al., 2003b), which further supports the work of Smith and colleagues (1991). Likewise, few NK1R expressing preBötC neurons express glutamic acid decarboxylase 67 (GAD67), a γ -aminobutyric acid (GABA) synthetic enzyme or glycine transporter 2 (GlyT2), indicating the neurons are not inhibitory (Wang et al., 2001a). Application of the synthetic μ opioid receptor agonist d-Ala(2),NMePhe(4),Gly-ol(5)encephalin (DAMGO) directly into the preBötC in the medullary slice preparation evokes a significant depression of rhythmic inspiratory motor output. Furthermore, histological analyses have found a distinct population of NK1R-expressing preBötC neurons co-express the μ opioid receptor (Gray et al., 1999) (Figure 1-3), which explains the sensitivity of the preBötC to opioids. A subset of NK1R-expressing preBötC express the neuropeptide somatostatin (Stornetta et al., 2003b) and the glycoprotein reelin (Tan et al., 2012) which further facilitates the anatomical delineation and *in vivo* targeting of this neuronal group. Neurons within the preBötC are also predominantly propriobulbar (Guyenet et al., 2002) i.e. they originate and terminate in the brainstem. Within the rostral VRC, preBötC neurons are found to reside in the region ventral to the subcompact formation of the nucleus ambiguus (scNA) (Gray et al., 1999). From the extensive research, it is apparent that the preBötC consists of a heterogenous population of neurons whose function depends on glutamate-mediated synaptic connections.

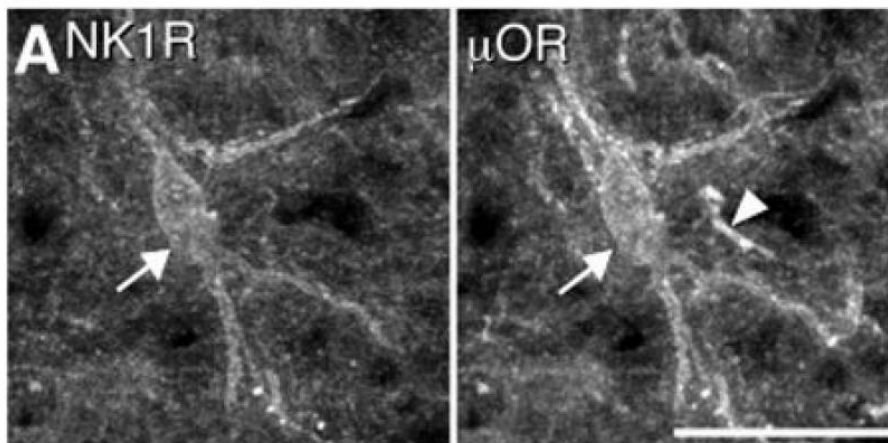
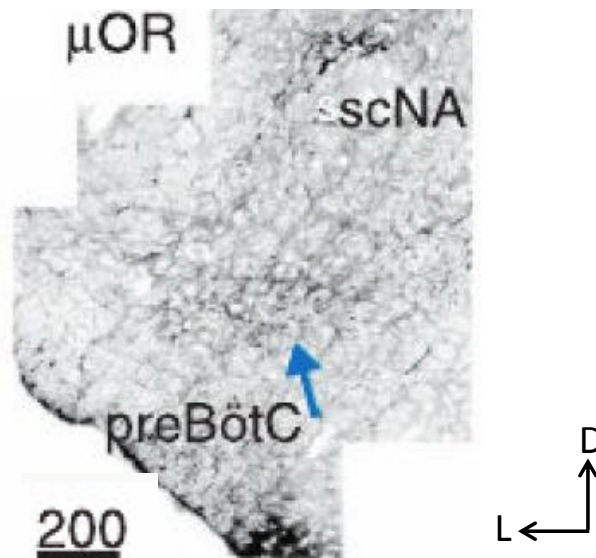


Figure 1-3. μ opioid receptor expressing neurons are found within the preBötC. Top: confocal image illustrating μ opioid receptor immunohistochemical staining within the preBötC i.e. the region ventral to the subcompact nucleus ambiguus. Bottom: confocal images illustrating NK1R expression on a preBötC cell soma and μ opioid receptor expression on a preBötC cell soma and process. Arrow indicates co-expression of NK1R and μ opioid receptor. Arrow head indicates absence of co-expression. Top scale bar= 200 μ m, bottom scale bar= 25 μ m. μ -OR, μ opioid receptor; scNA; subcompact nucleus ambiguus. Reproduced from Gray et al. (1999).

1.5.2 PreBötC neuronal projections

Elucidating the projections of the preBötC within the brainstem is vital in order to establish the role these neurons play in central respiratory control. Acute silencing a subset of preBötC neurons that express somatostatin (SST) induces a persistent apnoea in the adult rat indicating the importance of these neurons in respiratory control (Tan et al., 2008). These SST expressing, glutamatergic preBötC neurons have been further investigated in an attempt to establish their connectivity within the brainstem. They have been found to exhibit extensive projections throughout the brainstem in the adult rat (Tan et al., 2010). Specifically, these neurons project to the BC, rostral and caudal VRG, RTN/pFRG, NTS, DRG and the contralateral preBötC. This widespread connectivity with other principal respiratory brainstem nuclei confirms the integral role the preBötC plays in central respiratory control in the adult rodent.

1.5.3 PreBötC lesioning

Lesioning the preBötC and studying the respiratory effects can provide information regarding the functional importance of the preBötC *in vivo*. Bilateral microinjection of tetrodotoxin, a sodium channel blocker, into the preBötC in anaesthetised cats evokes an irreversible inactivation of the neurons and causes an abolition of phrenic nerve activity and a persistent apnoea (Ramirez et al., 1998). This suggests the preBötC is the source of respiratory rhythm. NK1R-expressing preBötC neurons can be ablated by substance P conjugated to the neurotoxin saporin (SP-SAP). SP is the natural ligand for the NK1R and when bound, internalisation of the receptor occurs. This means the neurotoxin conjugate is also taken into the cell thereby destroying it. The bilateral ablation of NK1R-expressing preBötC neurons (> 80%) using SP-SAP in adult rats *in vivo*, results in a profound deterioration in breathing during wakefulness, characterised by an ataxic pattern (Gray et al., 2001) (Figure 1-4). Furthermore, these irreversible breathing abnormalities are first observed during sleep before they progress into wakefulness (McKay et al., 2005). Interestingly, a unilateral preBötC lesion results in breathing disturbances during sleep only (McKay and Feldman, 2008). Bilateral preBötC lesioning also depresses the ventilatory response to hypercapnia and alters the hypoxic respiratory response (Gray et al., 2001), whereas unilateral ablation has no effect on chemoresponses (McKay and Feldman, 2008). Taken together, these studies signify the fundamental and dominant role the preBötC plays in generating a reliable and robust respiratory rhythm in the adult rodent

in vivo. Moreover, these studies suggest that pathological breathing patterns tend to first manifest in more depressed states e.g. sleep. However, in contrast to these findings, a gradual bilateral destruction of preBötC neurons in adult goats does not induce a disturbed breathing phenotype under normoxic and normocapnic conditions. The researchers suggest that plasticity changes within the respiratory network allows sufficient respiratory rhythm to continue that is capable of maintaining blood gas homeostasis in the absence of the preBötC (Krause et al., 2009). This data suggests that if enough time is given, respiratory network reconfiguration can overcome a defective or absent preBötC.



Figure 1-4. Disordered breathing exhibited by awake adult rats after bilateral ablation of the preBötC. Top: respiratory recording showing normal, rhythmic breathing of a control mouse. Bottom: ataxic breathing pattern is exhibited by mouse with ablated preBötC (preBötC⁻). Reproduced from Gray et al. (2001).

1.5.4 Mechanisms of respiratory rhythm generation in the preBötC

Rhythmic motor behaviours including breathing are produced by central pattern generators (CPGs) which are neural circuits capable of generating rhythmic activity in the absence of sensory or descending inputs (Marder and Calabrese, 1996). The activity of CPGs must be able to be modulated by central and peripheral inputs. This is particularly important for respiratory motor output which needs to adapt quickly to changes in metabolic needs in order to sustain life. Unravelling the mechanisms that underlie respiratory rhythm generation has been at the forefront of respiratory research for decades. The highly reduced medullary slice preparation which contains the preBötC is ideally suited to experimentally investigate rhythm generation. Currently, there are two main hypotheses for the mechanism of preBötC rhythm generation. The first is the pacemaker hypothesis, which asserts that respiratory rhythmogenesis is exclusively generated by intrinsic pacemaker

neurons within the preBötC. The second is the group-pacemaker hypothesis which proposes that respiratory rhythm generation is reliant on recurrent excitation between preBötC neurons which leads to population bursting, and does not require specialised pacemaker neurons.

1.5.4.1 Pacemaker hypothesis

Respiratory rhythm continues *in vitro* after the blockade of chloride-mediated inhibition, which suggests rhythm generation is not dependent on postsynaptic inhibition (Feldman and Smith, 1989). This finding led to the hypothesis that pacemaker neurons must generate the rhythm (Feldman and Smith, 1989; Smith et al., 1991; Brockhaus and Ballanyi, 1998). PreBötC pacemaker neurons that depend on persistent sodium currents (I_{NaP}) have been identified (Smith et al., 1991; Johnson et al., 1994). These neurons are voltage-dependent, and are antagonised by riluzole, a I_{NaP} blocker (Del Negro et al., 2002). A second type of pacemaker activity that is sensitive to the calcium ion channel blocker, cadmium, was identified in the preBötC (Thoby-Brisson and Ramirez, 2001). Further work demonstrated that this pacemaker mechanism depends on calcium activated nonspecific and voltage-insensitive cation currents (I_{CAN}) (Del Negro et al. 2005; Pena et al. 2004). Experiments employing pharmacological interventions have been employed to better understand the potential contribution of pacemaker neurons to respiratory rhythm generation. Drugs that block either or both I_{NaP} and I_{CAN} , have been utilised and the resultant changes in network activity are measured to determine if either or both types of pacemaker neurons generate respiratory rhythm. Within the preBötC, only 5% of neurons are found to rely on I_{NaP} . (Del Negro et al., 2005). Application of riluzole to the medullary slice preparation containing the preBötC from neonatal rats does not affect the frequency of rhythmic motor output (Del Negro et al., 2005). This finding is not congruent with the theory that I_{NaP} pacemakers are essential to rhythm generation. Riluzole does however prevent fictive gasping (slower frequency bursting) under anoxic conditions *in vitro* suggesting that respiratory rhythm generation during gasping is exclusively reliant on I_{NaP} (Pena et al., 2004; Paton et al., 2006). This proposes that the contribution of pacemaker neurons in respiratory rhythmogenesis may be state-dependent. The coapplication of riluzole and the I_{CAN} blocker, flufenamic acid (FFA), abolishes respiratory rhythm *in vitro* (Pena et al., 2004; Del Negro et al., 2005). It was therefore suggested that I_{CAN} dependent pacemakers are important for driving respiratory rhythm *in vitro*. However given that almost all preBötC neurons express I_{NaP} and I_{CAN} (Del Negro et al., 2002), these drugs will reduce the overall

excitability within the preBötC. This means that the loss of rhythm could be due to riluzole and FFA lowering excitability of all other neurons as well as pacemakers themselves. As a result it is difficult to make definitive conclusions regarding the importance of pacemaker neurons to rhythm generation based on the effects of riluzole and FFA alone. Following a complete cessation of rhythmic motor output in the slice preparation induced by riluzole and FFA, application of SP, which depolarises preBötC membrane potentials, restarts respiratory rhythm (Del Negro et al., 2005). From this finding it was suggested that high levels of cellular excitability are required to sustain respiratory rhythmogenesis. A recent study utilising transgenic mice in which neurons expressing the GlyT2 gene co-express enhanced green fluorescent protein, have found inspiratory-modulated glycinergic pacemaker neurons in the preBötC (Morgado-Valle et al., 2010). The precise role that these glycinergic pacemaker neurons play in rhythm generation remains elusive, but this finding challenges the view that preBötC pacemaker neurons are excitatory.

1.5.4.2 Group-pacemaker hypothesis

In contrast to the pacemaker theory, the group-pacemaker theory posits that respiratory rhythm generation is an emergent network property. It is believed that excitatory and inhibitory interactions between preBötC neurons underlie respiratory rhythmogenesis. At present there is limited conclusive data that support this theory. It is hypothesised that rhythmic inspiratory bursts in the preBötC result from excitatory connections between preBötC neurons which induce positive feedback through recurrent excitation (Rekling et al., 1996; Rekling and Feldman, 1998). This theory proposes that a proportion of preBötC neurons exhibit spontaneous activity which synapse with and excite silent neurons. These neurons in return excite more silent neurons as well as re-excite the neurons that are already active. It is therefore believed that pacemaker neurons in the preBötC that rely on I_{NaP} or I_{CAN} , function to stabilise the rhythm and contribute to the general excitability of the whole network of respiratory neurons but are not necessary for respiratory rhythmogenesis *per se*. This theory is supported by the observation that in the presence of riluzole and FFA which abolish pacemaker activity *in vitro*, respiratory rhythm can continue as long as pharmacological excitation is provided e.g. with SP as mentioned in section 1.5.4.1 above (Del Negro et al., 2005). SP depolarises preBötC neurons thereby allowing the network rhythm generation to persist (Morgado-Valle and Feldman, 2004). Taken together these data suggest that respiratory rhythm generation is a function of both synaptic connections and the intrinsic activity of pacemakers.

1.5.5 Prenatal development of the preBötC

In order to sustain life, the mammalian respiratory rhythm generator must be functional by birth. The prenatal development of respiratory rhythmogenesis has thus received considerable attention. Breathing is one of the earliest detectable behaviours in the mammalian fetus. During prenatal life, mammals exhibit episodic rhythmic fetal breathing movements (FBMs) involving respiratory muscular contractions (Jansen and Chernick, 1983; Kobayashi et al., 2001), which are believed to be generated by the respiratory rhythm generator. FBMs are postulated to induce appropriate maturation of the lungs as well as influence the development of respiratory motoneurons and musculature allowing for coordinated breathing at birth (Kitterman, 1988). It is therefore essential that the respiratory rhythm generator becomes active prior to postnatal life.

1.5.5.1 Anatomical development of the preBötC

The anatomical formation of the preBötC during prenatal life has been investigated in the rodent. Given that NK1R is an immunohistochemical marker for the preBötC, examining NK1R expression throughout prenatal development can determine when preBötC neurons are formed. At embryonic day (E) 14 in the mouse and E16 in the rat (analogous developmental time periods taking into account the longer gestational period of the rat), weak NK1R immunostaining is found in the region below the NA, believed to represent the preBötC. Stronger NK1R immunolabeling within the region of the preBötC is then detected at E15 and E17 in the mouse and rat respectively (Pagliardini et al., 2003; Thoby-Brisson et al., 2005). The birth date of neurons can be determined using 5-bromo-2-deoxyuridine (BrdU) injections. BrdU is a structural analogue of thymidine that is incorporated into dividing cells and is therefore used as a marker of cell proliferation. BrdU expression can be detected using fluorescently labelled antibodies. Birth dating of NK1R expressing preBötC neurons in the rat has revealed that these neurons are born at E12.5-E13.5 and migrate to the area of the preBötC by E17-E18 (Pagliardini et al., 2003).

1.5.5.2 Functional development of the preBötC

In the rat, extracellular recordings of population activity within the preBötC in the transverse medullary slice preparation have shown that spontaneous rhythmic activity emerges at E17 (Pagliardini et al., 2003), which corresponds with the first detection of

rhythmic FBMs (Kobayashi et al., 2001). This emergence of rhythmic motor output also corresponds with the developmental time at which strong NK1R expression is first detected within the preBötC in the rat (Pagliardini et al., 2003). Using a combination of electrophysiology and calcium imaging in the brainstem-spinal cord and transverse medullary slice preparations, it has been shown that the preBötC becomes rhythmically active at E15.5 in the mouse. This neural activity can sustain the rhythmic activity of hypoglossal motoneurons. The rhythmic output from the embryonic preBötC relies on glutamatergic neurotransmission, is excited by SP and depressed by the μ opioid receptor agonist DAMGO (Thoby-Brisson et al., 2005). These characteristics are also exhibited by the neonatal preBötC (Smith et al., 1991; Gray et al., 1999; Mellen et al., 2003) suggesting that generation and modulation of respiratory rhythm during embryonic life is comparable with that in early postnatal life. The emergence of rhythmic activity in the embryonic mouse preBötC is concomitant to the anatomical formation of the NK1R-expressing preBötC neurons (Thoby-Brisson et al., 2005). This suggests that in both rats and mice, the anatomical emergence of the preBötC correlates with the inception of preBötC functional activity.

1.5.6 Transgenic mouse models

The understanding of central respiratory control and the role of the preBötC has been greatly facilitated by the development of transgenic mouse models. There are an increasing number of studies where gene targeting techniques have been utilised to understand how gene disruptions impact the development of respiratory control. Genetic ablation of VGLUT2 causes the neural circuits within the preBötC to remain inactive. *In vitro* analysis has demonstrated that respiratory-like rhythmic activity from the preBötC is absent during prenatal development and through to birth. Null mutant mice lacking VGLUT2 die at birth from respiratory failure (Wallen-Mackenzie et al., 2006). This confirms that glutamate is an essential neurotransmitter for preBötC rhythmogenesis during development. Several studies have investigated and ascertained the genes that specify the identity of the preBötC neurons. The transcription factor *v-maf musculoaponeurotic fibrosarcoma oncogene homologue B (MafB)* is expressed in a subpopulation of preBötC neurons. Deletion of *MafB* in mice results in fatal prolonged apnoeas *in vivo*, defective respiratory rhythm generation *in vitro* and an anatomical deformation of the preBötC (Blanchi et al., 2003). This observation establishes an important role of *MafB* for sufficient development of preBötC neurons and highlights the importance of the preBötC for postnatal survival.

Studies utilising transgenic mice lacking the transcription factor *developing brain homeobox protein 1 (Dbx1)* have also revealed important information regarding the developmental origins of the preBötC. A loss of *Dbx1* induces an elimination of all glutamatergic neurons within the ventrolateral medulla including SST and NK1R expressing preBötC neurons. *Dbx1* null mutant mice fail to breathe at birth and inspiratory rhythmic activity is also absent *in vitro* (Bouvier et al., 2010; Gray et al., 2010). These data suggest that *Dbx1* is required for the formation of rhythm generating preBötC neurons. Additionally, in *Dbx1* mutant mice, commissural connectivity in the preBötC is impaired, and a mutation of *Robo3*, a gene essential for commissural axon path finding, results in a loss of bilateral synchrony of the preBötC (Bouvier et al., 2010). In further support of the critical role of *Dbx1* in rhythm generation of the preBötC, *Dbx1*-derived neurons within the preBötC are found to be rhythmically active and exhibit an inspiratory-modulated pattern of firing (Picardo et al., 2013). Furthermore, laser ablation of individual *Dbx1*-derived preBötC neurons in a gradual manner in the neonatal medullary slice preparation induces a continuous depression of respiratory rhythm and eventually a complete cessation of inspiratory motor activity (Wang and Hayes, 2014). Taken together, these data provide strong evidence that rhythm generating preBötC neurons are derived from *Dbx1*-expressing progenitors.

1.5.7 Human preBötC

The recent identification of the presumed preBötC in the human brainstem has confirmed the validity of studying the rodent as a model of central respiratory control. Some of the anatomical markers that delineate the preBötC in the rodent have also been identified in the ventrolateral medulla in human tissue. NK1R expressing and SST expressing cells have been located in the region ventral to the scNA in post-mortem brainstem tissue from fetuses, newborns and infants. These cells are believed to represent the human preBötC. Interestingly, structural alterations within the postulated preBötC are found in a high percentage of brains from fetuses and newborns who suffered from sudden unexplained death (Lavezzi and Maturri, 2008). Additionally, in the adult human brain, an area in the rostral ventrolateral medulla displaying co-localisation of NK1R and SST immunoreactive neurons is believed to represent the preBötC. These neurons exhibit small to medium sized soma which distinguishes them from larger motoneurons. Examination of the putative preBötC in post-mortem brain tissue from individuals who suffered from neurodegenerative diseases associated with pathological breathing has revealed a reduction

in the number of NK1R/SST expressing neurons (Schwarzacher et al., 2011) which could contribute in part to the respiratory disturbances observed in these patients. These studies provide evidence to suggest the human preBötC has a similar anatomical location and histological profile as the experimental rodent.

1.6 The retrotrapezoid nucleus/parafacial respiratory group

The retrotrapezoid nucleus/parafacial respiratory group (RTN/pFRG) consists of a bilateral cluster of interneurons in the ventrolateral medulla and has been implicated in central respiratory control. The exact function of the RTN/pFRG is currently debated. This group of respiratory neurons is located in the VRC, rostral to the preBötC and ventral to the facial motor nucleus, in close proximity to the ventral medullary surface (Onimaru and Homma, 2003; Stornetta et al., 2006; Onimaru et al., 2008). Like preBötC neurons, RTN/pFRG neurons are anatomically defined by their expression of NK1R and VGLUT2 mRNA (Stornetta et al., 2006; Onimaru et al., 2008). However in contrast to preBötC neurons, RTN/pFRG neurons also express the transcription factor, paired-like homeobox 2b (Phox2b) and lack the μ opioid receptor (Stornetta et al., 2006; Kang et al., 2007; Onimaru et al., 2008). There is considerable debate as to whether the RTN/pFRG is one nucleus or if the RTN and pFRG are anatomically and functionally distinct. In the neonatal rodent, the group of neurons located in the parafacial region is often termed the pFRG whereas in the adult rodent they are named the RTN. Given the similarity in the histological profiles (NK1R⁺, Phox2b⁺ and VGLUT2⁺) and anatomical location, it is generally believed that the pFRG and RTN represent the same neural group at different developmental stages i.e. the pFRG develops into the RTN. In this thesis this neural group will be termed RTN/pFRG when referring to it in both neonatal and adult rodents.

1.6.1 RTN/pFRG and respiratory rhythm generation

The exact role the RTN/pFRG plays in respiratory control is not fully understood. There is a current hypothesis that the RTN/pFRG functions as a respiratory rhythm generator in the neonatal rodent (Onimaru and Homma, 2003). Studies utilising the neonatal brainstem-spinal cord preparation, which preserves the RTN/pFRG as well as the preBötC, have provided great insight into the potential role of the RTN/pFRG in respiratory rhythmogenesis (Ballanyi et al., 1999). Onimaru and Homma (2003) employed this preparation from the newborn rat and for the first time demonstrated rhythmic activity in

the region of the brainstem that encompasses the RTN/pFRG using optical imaging and electrophysiology. By using these techniques simultaneously, neurons within the RTN/pFRG were found to fire prior to inspiratory motor output (phrenic nerve activity, recorded from C4 nerve rootlets). These RTN/pFRG neurons have thus been given the name preinspiratory (Pre-I) neurons, and are proposed to control the onset of inspiration (Onimaru and Homma, 2003). Importantly, this rhythmic preinspiratory patterning has not been detected in adult rodent preparations (Mulkey et al., 2004), indicating the RTN/pFRG may not function as a rhythm generator in adulthood. Partial bilateral lesioning of the RTN/pFRG in the brainstem-spinal cord preparation induces a reduction in respiratory frequency together with an altered spatiotemporal pattern of respiratory neuronal firing, suggesting the RTN/pFRG may be vital for respiratory rhythmogenesis in neonates (Onimaru and Homma, 2003). The concept that the RTN/pFRG is coupled to the preBötC in the intact neonatal mammal, whereby the RTN/pFRG functions as the master respiratory oscillator was subsequently proposed.

Studies that utilise pharmacological tools to target only the preBötC have provided evidence to suggest a dual respiratory rhythm generator exists in early postnatal life. Application of DAMGO which depresses neural activity of the preBötC but not the RTN/pFRG (Takeda et al., 2001; Mellen et al., 2003), in neonatal brainstem-spinal cord preparations and anaesthetised juvenile rats, induces quantal slowing of respiratory activity. That is inspiratory output becomes irregular and skips cycles (Mellen et al., 2003; Barnes et al., 2007). It has been postulated that opioid-induced quantal slowing is due to a failure in functional connectivity between the RTN/pFRG Pre-I neurons and preBötC inspiratory neurons. These data suggest that during early life the RTN/pFRG is involved in respiratory rhythmogenesis and becomes functionally coupled to the preBötC.

Studies utilising transgenic mouse models with targeted gene deletions affecting the development of the RTN/pFRG have provided invaluable insight into the possible role the RTN/pFRG plays in early postnatal life. In mammals there is a surge of endogenous opiates at birth (Jansen and Chernick, 1983). This increased level of opiates in the blood could result in a depression of the opiate-sensitive preBötC neurons, whereas the opiate-insensitive RTN/pFRG in theory would remain unperturbed (Feldman and Del Negro, 2006; Janczewski and Feldman, 2006). In this situation, in the absence of a functional preBötC, the RTN/pFRG may provide an alternative source of respiratory rhythm and ensure adequate breathing immediately after birth until opiate levels decrease. Experiments

in *Krox-20* homozygous mutant mice support this hypothesis. The *Krox-20* gene plays a role in controlling the hindbrain segmentation process during embryonic development. A *Krox-20* mutation results in abnormal segmentation of rhombomeres (transient rostrocaudal compartments in the developing hindbrain) 3 and 5. *Krox-20* mutant mice have neuroanatomical defects in the brain region that corresponds to the RTN/pFRG, whereas the anatomy of the preBötC is unaffected. At birth, breathing in the mutant mice is markedly depressed and mice die from prolonged apnoeas. This indicates that the preBötC alone is not sufficient for the generation of a robust respiratory rhythm *in vivo*. The administration of naloxone, a μ opioid receptor antagonist, within the first few hours after birth promotes survival by eliminating apnoeas (Jacquin et al., 1996) (Figure 1-5). In the *Krox-20* mutant mice it is likely that the malformed or deleted RTN/pFRG cannot function as a rhythm generator and since the perinatal opiate surge would also inhibit the preBötC, this would result in a complete failure of respiratory rhythm generation. It is hypothesised that naloxone antagonises the opiate depression of the preBötC thereby allowing normal rhythmic breathing to persist (Feldman and Del Negro, 2006). The results from the *Krox-20* study are in accordance with the hypothesis that the RTN/pFRG has a specialised role in rhythm generation to compensate for the opiate-induced preBötC depression.

Investigating respiratory activity in transgenic mice that lack Phox2b-expressing RTN/pFRG neurons has also revealed the importance of this neural group in respiratory control. Mice that exhibit a human PHOX2B mutation (the Phox2b^{27Ala} allele) show a substantial loss of RTN/pFRG neurons and display fatal central apnoeas at birth (Dubreuil et al., 2008). This provides genetic evidence that the RTN/pFRG is essential for driving breathing at birth in the rodent. Further support of the critical role that the RTN/pFRG plays in rhythm generation in early postnatal life comes from a study conducted in mutant mice lacking the transcription factor, *ladybird homeobox homolog 1* (*Lbx1*). These mice die of respiratory failure in the early postnatal period. Importantly, these mutant mice exhibit a depleted *number* of RTN/pFRG neurons but show no preBötC anatomical abnormalities (Pagliardini et al., 2008). *Lbx1* mutant mice do however exhibit anatomical defects in neuromodulatory respiratory nuclei (e.g. the NTS) which could also contribute to the disordered respiratory phenotype. Furthermore, genetic deletion of the *atonal homolog 1* (*Atoh1*) transcription factor results in abnormal formation of the RTN/pFRG. The *Atoh1* mutation is fatal due to a severely depressed central respiratory rhythm. This finding also reinforces the idea that RTN/pFRG is imperative in driving breathing in early life. It is important to highlight the fact that null mutant mice lacking either the preBötC or the

RTN/pFRG do not generate sufficient breathing for survival (Jacquin et al., 1996; Blanchi et al., 2003; Dubreuil et al., 2008; Pagliardini et al., 2008; Rose et al., 2009; Bouvier et al., 2010; Gray et al., 2010), indicating that sufficient development of both rhythm generators is necessary to sustain breathing rhythm essential to life.

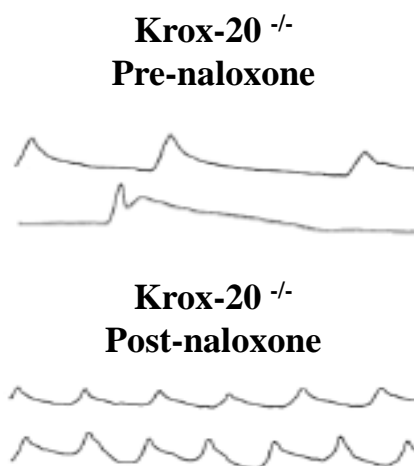


Figure 1-5. Naloxone eliminates apnoeas and increases respiratory frequency in *Krox-20* null mutant mice. Respiratory traces illustrate prolonged apnoeas at birth in *Krox-20*^{-/-} mice which are eliminated after administration of naloxone, a μ opioid receptor antagonist.

1.6.2 Prenatal development of the RTN/pFRG

By employing calcium imaging and neuronal population recording in the isolated embryonic mouse brainstem preparations, rhythmic activity within the parafacial region has been identified (Thoby-Brisson et al., 2009). These intrinsically rhythmogenic neurons border the facial motor nucleus and have been termed the embryonic parafacial oscillator (e-pF). Spontaneous rhythmic activity of the e-pF emerges at E14.5, which is approximately one day prior to the onset of preBötC rhythmic activity at E15.5 (Thoby-Brisson et al., 2005). Application of riluzole abolishes rhythmic bursting of the e-pF, indicating the firing of these neurons is reliant on the I_{NaP} . In contrast to preBötC activity, e-pF rhythmic activity is unaffected by μ opioid receptor agonists. The e-pF neurons are derived from *Krox20*-expressing precursors and are identified anatomically by their expression of NK1R and *Phox2b* (Thoby-Brisson et al., 2009). Given the anatomical overlap and identical expression of histological markers, it is likely that the e-pF represents the embryonic precursor to the RTN/pFRG. Evidence has also revealed that the e-pF and

the preBötC become functionally coupled when both oscillators are active at E15.5. When the e-pF is silenced by riluzole, the frequency of rhythmic bursting from the preBötC is greatly reduced, which suggests the preBötC receives inputs from the e-pF (Thoby-Brisson et al., 2009). These observations demonstrate that analogous with early postnatal life (Mellen et al., 2003), during embryonic development a dual respiratory rhythm generating network forms from two spatially separate neuronal groups.

1.6.3 RTN/pFRG and active expiration

Exploiting the differential sensitivity of the preBötC and RTN/pFRG to μ opioids has revealed that the RTN/pFRG may play an important role in generating active expiration. Under normal resting conditions, expiration is a passive process, caused by the elastic recoil of the inspiratory muscles, lungs and ribcage. Expiration becomes active when there is an increased respiratory drive e.g. during exercise, and is generated by the contraction of expiratory muscles which augment expiratory airflow (Aliverti et al., 1997). Fentanyl administration in juvenile rats induces quantal slowing of inspiratory activity, i.e. occasional skipped inspirations, whereas expiratory modulated abdominal muscle activity, which is believed to represent active expiration, remains unaffected. Furthermore, transection of the brainstem immediately caudal to the RTN/pFRG abolishes abdominal muscle expiratory activity but has little effect on inspiratory motor activity (Janczewski and Feldman, 2006). This observation that inspiration and expiration can be uncoupled has led to the belief that inspiratory and expiratory phases of respiration are not the product of a single oscillator but rather are generated by functionally distinct respiratory oscillators. In support of this theory, a study conducted in adult anaesthetised rats has revealed that stimulating the RTN/pFRG by local disinhibition or optogenetic excitation transforms normally silent RTN/pFRG neurons into rhythmically active neurons that exhibit an expiratory-modulated pattern of firing. This stimulation of RTN/pFRG rhythmic activity generates active expiration i.e. the generation of expiratory-related abdominal muscle activity (Pagliardini et al., 2011). These observations are consistent with the idea that the rhythm generating properties of the RTN/pFRG persist into adulthood, but under resting conditions synaptic inhibition silence these neurons. Taken together, these studies suggest that the RTN/pFRG acts as a conditional expiratory oscillator that generates active expiration.

1.6.4 RTN/pFRG and chemosensitivity

In both neonatal and adult rodents, the RTN/pFRG has been implicated in central chemoreception because 1. RTN/pFRG neurons are located in the parafacial region of the ventrolateral medulla close to the medullary surface which has previously been identified as a site involved in the central respiratory chemoreflex (Loeschcke, 1982) 2. RTN/pFRG neurons are sensitive to increases in CO₂ and acidification (Mulkey et al., 2004; Guyenet et al., 2005; Stornetta et al., 2006; Onimaru et al., 2008) and 3. mutant mice that exhibit a substantial depletion of Phox2b-expressing RTN/pFRG neurons display a reduced respiratory responsiveness to CO₂ at birth (Dubreuil et al., 2008). The proposed chemosensitive role of the RTN/pFRG will be discussed in further detail in the section below (1.7.1.1).

1.7 Chemosensitivity

It is firmly believed that stimulation of breathing by decreases in the partial pressure of O₂ and increases in partial pressure of CO₂ in the blood is fundamental to rhythmic breathing (Loeschcke, 1982). Failure of these processes can be fatal; therefore a sound understanding and identification of the central and peripheral sites involved in the detection of altered blood gases is highly desirable in respiratory research.

1.7.1 Central chemosensitivity

The central chemoreflex is the augmentation of ventilation evoked by an increase in the partial pressure of CO₂ and therefore a reduction in blood pH which is detected within the central nervous system (CNS) (Feldman et al., 2003). Changes in the partial pressure of CO₂ evokes a greater stimulatory effect on breathing compared to equivalent changes in the partial pressure of O₂ (Haldane and Priestley, 1905). Failure of central chemoresponses have been implicated in a number of human genetic conditions including congenital central hypoventilation syndrome (CCHS), whereby patients have an attenuated response to hypercapnia (elevation of blood CO₂ level) and in severe cases respiratory arrest (Spengler et al., 2001; Chen and Keens, 2004).

For neurons to be considered chemosensitive they must possess an intrinsic sensitivity to changes in the partial pressure of arterial CO₂ that is within physiological range and when

stimulated must evoke an appropriate alteration in ventilation (Putnam et al., 2004). It is generally believed that chemosensitive neurons detect pH changes in the blood as a result of increased CO₂.

1.7.1.1 RTN/pFRG

There is substantial evidence to suggest the RTN/pFRG plays a significant role in central chemosensitivity in the rodent. RTN/pFRG neurons are intrinsically sensitive to increases in CO₂ and acidification *in vitro* in neonatal rodents (Mulkey et al., 2004; Onimaru et al., 2008). Furthermore, in the adult rat, RTN/pFRG neurons increase their firing rate in response to decreases in pH in medullary brain slices (Guyenet et al., 2005). CO₂ sensitive RTN/pFRG neurons are found to project directly to the preBötC in adult rats, which further supports their role as central chemoreceptors (Mulkey et al., 2004). In adult rats with denervated peripheral chemoreceptors, CO₂ sensitivity of RTN/pFRG neurons in response to hypercapnia is comparable to rats with intact peripheral chemoreceptors (Mulkey et al., 2004). This suggests that chemoresponses of the RTN/pFRG *in vivo* are not fully reliant on input from the peripheral chemoreceptors and therefore RTN/pFRG neurons may exhibit intrinsic chemosensitive properties. Studies utilising the Phox2b^{27Ala/+} mouse model of CCHS suggest that the RTN/pFRG plays a vital role in central chemoreception at birth. The only anatomical deformation exhibited by these transgenic mice is a substantial loss of Phox2b-expressing RTN/pFRG neurons. Phox2b^{27Ala/+} mice completely lack a ventilatory response to hypercapnia and die soon after birth (Dubreuil et al., 2008), highlighting the importance of the RTN/pFRG neurons in CO₂ sensitivity. An alternative explanation for these respiratory defects is the RTN/pFRG functions to relay chemosensitive information from all central chemoreceptors as opposed to being a chemosensory site *per se* (Guyenet et al., 2009). A study that examined the effects of a RTN/pFRG lesion has provided further support that the RTN/pFRG mediates central chemosensitivity *in vivo*. Destruction of approximately 70% of Phox2b expressing RTN/pFRG neurons using the aforementioned SP-SAP neurotoxin technique, decreases the ventilatory response to hypercapnia in adult rats (Takakura et al., 2008). Furthermore, photostimulation of Phox2b expressing RTN/pFRG neurons in adult rats *in vivo* induces a stimulation of breathing, seen as a long-lasting increase in phrenic nerve activity (Abbott et al., 2009). The ability to evoke a ventilatory increase when activated is a key characteristic expected of a central chemoreceptor *in vivo*. Evidence supports the view that the RTN/pFRG may function as the principal central chemoreceptor in the adult and neonatal rodent.

1.7.1.2 Serotonergic Neurons

Serotonergic neurons have also been proposed to act as central chemoreceptors. These neurons show intrinsic sensitivity to pH/CO₂ changes in cell cultures and brainstem slices *in vitro* (Wang et al., 2001b; Severson et al., 2003) and are found in close proximity to medullary arteries (Bradley et al., 2002). The medullary raphe serotonergic neurons are believed to play a specialised role in the CO₂ chemoreflex. Patch clamp recordings of raphe neurons in rat medullary slice preparations have revealed that these neurons increase their firing rate in response to increasing levels of CO₂ in the bathing solution (Richerson, 1995). Focal acidification of medullary raphe neurons in the anaesthetised rat results in an increase in ventilation as indicated by augmented amplitude of phrenic nerve discharge (Bernard et al., 1996). Furthermore, lesioning of the medullary raphe results in a reduced ventilatory response to hypercapnia *in vivo* in awake goats (Hodges et al., 2004). Studies utilising transgenic mice that lack or have a substantial reduction of serotonergic neurons have provided further evidence that reinforces the concept that serotonergic neurons play a major role in the CO₂ chemoreflex *in vivo*. These mutant mice exhibit normal baseline ventilation but an attenuated respiratory response to hypercapnia (Hodges et al., 2008; Hodges et al., 2011).

1.7.1.3 Locus coeruleus

The locus coeruleus (LC) lies in the dorsal pons (Dahlstrom and Fuxe, 1964) and consists of a cluster of noradrenergic neurons that have been implicated in central chemosensitivity. *In vitro*, LC neurons exhibit chemosensory responses (Filosa et al., 2002; Putnam et al., 2004). Furthermore, focal acidification of the LC noradrenergic induces a significant increase in phrenic nerve activity in cats *in vivo* (Coates et al., 1993). Chemical lesioning studies have demonstrated that bilateral destruction of approximately 80% of noradrenergic neurons of the LC results in a 64% decrease in the ventilatory stimulation to hypercapnia (Biancardi et al., 2008). This data suggests that the LC contributes significantly to the CO₂-induced drive to breathe. However it should be highlighted that chemical lesioning studies can also cause destruction to other neurons other than noradrenergic neurons of the LC, which could also influence the ventilatory effects.

1.7.2 Peripheral chemosensitivity

An increase in ventilation in response to a decrease in the partial pressure of O₂ in the blood is mediated by peripheral chemoreceptors. There is substantial evidence which supports that the principal peripheral chemoreceptors are localised within the carotid bodies. Injection of sodium cyanide into the carotid artery and subsequent stimulation of the carotid bodies results in an augmentation of respiratory activity (Sapru and Krieger, 1977) and exposure to hypoxia in the anaesthetised cat has been shown to increase discharge from the carotid bodies (Lahiri et al., 1981). Furthermore, removal of the carotid body in the adult rat reduces ventilatory stimulation in response to hypoxia (Chiocchio et al., 1984). Adenosine triphosphate (ATP) has been implicated in peripheral chemoreception. *In vitro* studies utilising the carotid body-sinus nerve preparation have found that application of ATP evokes a substantial increase in sinus nerve chemoafferent discharge. Additionally, in P2X₂ receptor (ATP receptor) knockout mice, a blunted ventilatory response to hypoxia is observed. Furthermore, hypoxia-induced increases in the discharge of single chemoafferent fibres of the carotid sinus were attenuated in the knockout mice (Rong et al., 2003). From these studies it has been proposed that O₂ sensitive cells of the carotid body release ATP which activates the carotid sinus nerve via P2X receptors which in return relays these signals to the central respiratory centres to allow for appropriate respiratory responses.

Several studies have also suggested that peripheral and central chemoreception is integrated. In rats it has been shown that the RTN/pFRG receives inputs from peripheral chemoreceptors (Takakura et al., 2006). Further studies in awake dogs have demonstrated that inhibition of the carotid body chemoreflex also depresses the central ventilatory response to hypercapnia, whereas stimulation of the carotid bodies causes an increase in the ventilatory response to central hypercapnia (Blain et al., 2010).

1.8 Developmental plasticity and respiratory activity in early life

Although the respiratory system is ready to function at birth, it is immature and requires a period of postnatal maturation. During early postnatal life in both humans and rodents, breathing patterns are immature and are characterised by a variable and irregular frequency (Fisher et al., 1982; Mortola, 1984; Read and Henderson-Smart, 1984). Whilst the hypercapnic ventilatory response appears to be mature at birth in the rodent (Renolleau et

al., 2001), the ventilatory response to hypoxia undergoes postnatal maturational changes (Robinson et al., 2000; Liu et al., 2006). In both neonatal and mature rodents, the ventilatory response to hypoxia is biphasic, with an initial ventilatory stimulation followed by a secondary decline. In adult mice, the secondary decline in ventilation following hypoxic stimuli tends to fall more slowly and still remains above baseline levels. However in neonatal mice, the ventilatory decline is greater in magnitude and can fall below baseline levels (Robinson et al., 2000). The immaturity and fragility of baseline respiratory patterns during early life means perturbations to the respiratory system during this time period could be detrimental. It is clear that mammals exhibit developmental plasticity, whereby long-term changes in the mature adult respiratory system are induced by experiences that occur during critical developmental time windows in development. Conversely, the same experiences after these critical developmental periods evoke little or no lasting changes (Carroll, 2003; Bavis and Mitchell, 2008). Several studies have demonstrated that exposure to various external stimuli in the neonatal period including hypoxia, hypercapnia, caffeine and stressful events can induce lasting changes in ventilatory control (Okubo and Mortola, 1998, Bavis and Kilgore, 2001; Bavis et al., 2004; Montandon et al., 2006; Gulemetova and Kinkead, 2011). These data are consistent with the idea that disrupting the respiratory system during development when respiratory activity is irregular can induce substantial lasting changes to respiratory activity.

The mechanisms that underlie respiratory rhythm generation during early life are not fully understood. As previously discussed, both the preBötC and the RTN/pFRG are required for postnatal survival, given that an anatomical deformation or deletion of either of these neuronal groups results in respiratory failure at birth in the rodent (Jacquin et al., 1996; Blanche et al., 2003; Dubreuil et al., 2008; Pagliardini et al., 2008; Rose et al., 2009; Bouvier et al., 2010; Gray et al., 2010). At present, how the RTN/pFRG and the preBötC interact *in vivo* to produce rhythmic breathing during early postnatal life remains to be ascertained. Furthermore, their level of involvement in rhythm generation throughout postnatal maturation remains elusive (see Figure 1-6). Determining the mechanisms underlying respiratory rhythm generation during postnatal development will be vital in developing a full understanding of the pathophysiology of many central respiratory disorders that manifest in early life e.g. SIDS.

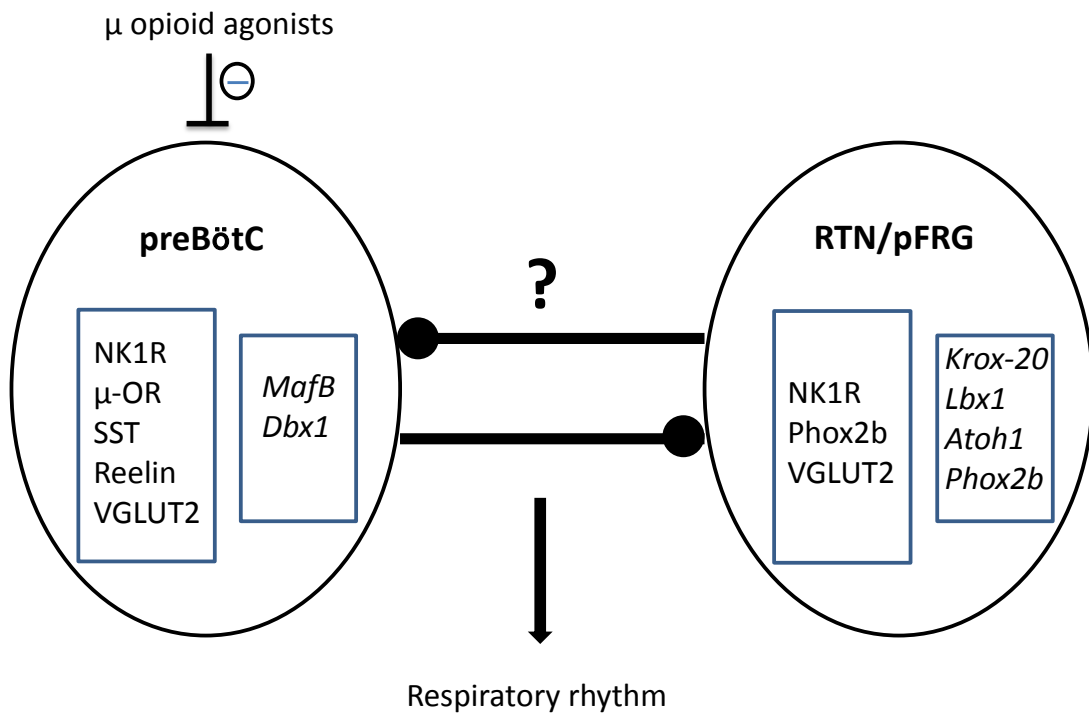


Figure 1-6. Schematic illustration of the two proposed respiratory rhythm generators in early postnatal life. The preBötC is anatomically identified by expression of NK1R, μ-OR, SST, reelin and VGLUT2. The RTN/pFRG differs in that it expresses Phox2b and doesn't express the μ-OR, SST or reelin. Both oscillators have different developmental origins. The development of the preBötC relies on the transcription factors *MafB* and *Dbx1*, whereas transcription factors *Krox-20*, *Lbx1*, *Atoh1* and *Phox2b* are essential for the genetic development of the RTN/pFRG. Only the preBötC is sensitive to opioids. It is currently unknown how the RTN/pFRG interacts with the preBötC *in vivo* to produce rhythmic breathing during early postnatal development.

1.9 Opioids and respiratory depression

In clinical practice, μ opioid receptor agonists such as fentanyl are extensively utilised in pain management, treating both chronic and acute pain (Swarm et al., 2001; Niesters et al., 2013). In addition, they are commonly administered to induce sedation and can be used as adjuncts to general anaesthesia (Anand et al., 1990; Booker, 1999; Tobias, 1999). The most severe and often fatal side effect of opioid treatment is respiratory depression which limits the therapeutic use of these drugs (Pattinson, 2008). Opioids depress respiratory frequency, alter tidal volume, induce rigidity of the chest wall and reduce patency of the upper airways in humans (Leino et al., 1999; Lotsch et al., 2005; Ferguson and Drummond, 2006). Given the extensive use of opioid therapies in a wide range of patient groups, respiratory depression is a major clinical problem. Furthermore, there are subpopulations of patients who exhibit a hypersensitivity to the respiratory depressive effects of opioids including the elderly, obese and patients with pulmonary disease, which further complicates opioid therapeutic application (Desrosiers, 2006). A comprehensive understanding of opioid-induced respiratory depression is required in order to develop suitable therapeutics to overcome this depression thereby enabling more effective and safer treatment for patients. Opioid drugs are often administered for prolonged periods and long-term treatment plans are commonly utilised to provide effective pain relief (Brill, 2013). This repeated exposure to opioids is associated with the development of tolerance to the analgesic effects of the drug (Bailey and Connor, 2005), that is a reduced sensitivity to the analgesic actions. Surprisingly, despite the potent respiratory depressive side effects, the potential long-term respiratory consequences of repeated opioid exposure remain largely unexplored.

μ opioid agonists mediate their effects via the μ opioid receptor. This class of receptor is a member of the family of G-protein coupled receptors (GPCRs), which are made up of seven transmembrane subunits (Figure 1-7). Agonist binding evokes a conformational change in the receptor. The G-protein which is bound to the receptor becomes active and evokes an intracellular signalling cascade. Activation of the μ opioid receptor which is negatively coupled to adenylate cyclase (Law et al., 2000) initiates inhibitory intracellular pathways. This results in closing of voltage sensitive calcium channels, stimulation of potassium efflux, and reduction of cyclic adenosine monophosphate production. As a consequence of these intracellular changes, a reduction of neuronal excitability occurs. The μ opioid receptor is expressed throughout the brain in both respiratory-related and non-

respiratory brain regions (Xia and Haddad, 1991; Lonergan et al., 2003; Kivell et al., 2004), which indicates that μ opioid agonists can exert widespread effects throughout the body. Studies conducted in knockout mice that lack the μ opioid receptor have confirmed that opioids mediate their effects via this receptor. Knockout mice are insensitive to both morphine induced analgesia (Matthes et al., 1996) and respiratory depression (Romberg et al., 2003).

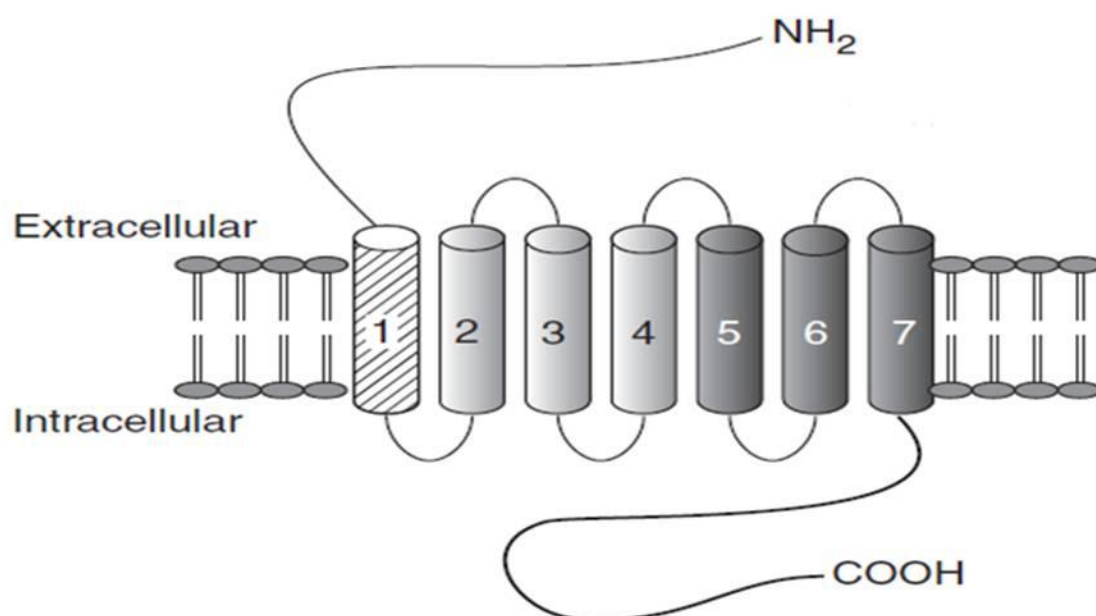


Figure 1-7. Schematic illustration of the structure of the μ opioid receptor. μ opioid receptors are members of the G-protein coupled receptor family, and consist of seven transmembrane subunits. Modified from Davis and Pasternak (2009).

1.9.1 The preBötC and opioid-induced respiratory depression

In vivo, respiratory rhythm generation is more susceptible to depression by opioids when compared to tidal volume (Lalley, 2003). Elucidating the brain sites that are responsible for the depression of respiratory activity by opioids has important clinical benefits which could help to aid the development of new pharmacological approaches to manage pain whilst avoiding respiratory depression. As previously mentioned in this chapter, the preBötC is sensitive to μ opioids *in vitro* (Gray et al., 1999; Takeda et al., 2001; Mellen et al., 2003; Montandon et al., 2011). When DAMGO is directly applied to the preBötC *in vitro*, respiratory-like motor output is depressed (Gray et al., 1999; Takeda et al., 2001; Mellen et al., 2003; Montandon et al., 2011). This opioid sensitivity is attributable to the fact that preBötC neurons express the μ opioid receptor (see Figure 1-3) (Gray et al., 1999; Manzke et al., 2003). An *in vivo* study conducted in the adult rat has identified the preBötC as being the critical brain site that mediates opioid-induced respiratory frequency depression *in vivo*. Injection of μ opioid receptor agonists, including DAMGO and fentanyl, directly into the preBötC via a microdialysis probe induces a sustained slowing of respiratory frequency. Continuous infusion of DAMGO into the preBötC at sufficient concentrations can also cause a complete respiratory arrest. Furthermore, the magnitude of respiratory depression induced by opioids bilaterally applied to the preBötC is greatest under depressed behavioural states when there is a reduction in cortical activation such as sleep and anaesthesia, indicating the effects of opioids at the preBötC are state-dependent. Importantly, it has also been demonstrated that systemically administered fentanyl in the adult rat *in vivo* evokes a depression of respiratory frequency by acting exclusively on preBötC neurons. Bilateral application of naloxone directly into the preBötC alone completely prevents respiratory frequency depression by intravenously administered fentanyl (Figure 1-8). This suggests that μ opioid receptor agonists act solely on preBötC neurons to evoke respiratory frequency depression *in vivo* (Montandon et al., 2011). Given that fentanyl can induce a significant suppression of respiratory rhythm generation through actions at the preBötC alone, this further supports the theory that the preBötC is an essential respiratory rhythm generating site in the adult rodent. This study has also confirmed that μ opioid receptor agonists such as fentanyl can be utilised to selectively target and perturb the rhythmic activity of the preBötC *in vivo*. NK1R-expressing cells of the preBötC can be visualised in the rhythmically active medullary slice preparation by applying SP conjugated to a fluorophore, whereby the fluorescent conjugate is internalised into the NK1R-expressing cells. Targeted whole-cell recordings from NK1R-expressing

rhythmogenic preBötC neurons have revealed that DAMGO induces a slowing of inspiratory activity through postsynaptic membrane hyperpolarisation (Figure 1-9) (Montandon et al., 2011).

Ampakines can alleviate opioid-induced respiratory depression *in vitro* and *in vivo*. Ampakines are a class of molecules that modulate amino-3-hydroxy-5-methyl-4-isoxazolepropionate (AMPA) receptors by increasing the peak and duration of glutamate-induced AMPA receptor-gated inward currents (Arai et al., 2004). Ampakines applied to medullary slice and brainstem-spinal cord preparations counteract the depression of respiratory-like rhythmic activity induced by DAMGO. Furthermore, ampakines can reverse fentanyl-induced respiratory depression in awake adult and neonatal rats (Ren et al., 2006; Greer and Ren, 2009). Glutamatergic neurotransmission is essential to preBötC rhythmogenesis (Greer et al., 1991; Smith et al., 1991; Funk et al., 1993). It has been hypothesised that ampakines increase glutamate-mediated neurotransmission within the preBötC, thereby increasing preBötC neuronal excitability which can overcome the depression induced by opioids. It is also possible that ampakines alleviate opioid-induced respiratory depression by affecting other neuronal populations that rely on AMPA-mediated neurotransmission and have modulatory actions on the preBötC, including the NTS, RTN/pFRG and pontine respiratory nuclei. These findings from studies utilising ampakines also reinforce the idea that the preBötC is the key site at which opioids act to depress respiratory activity.

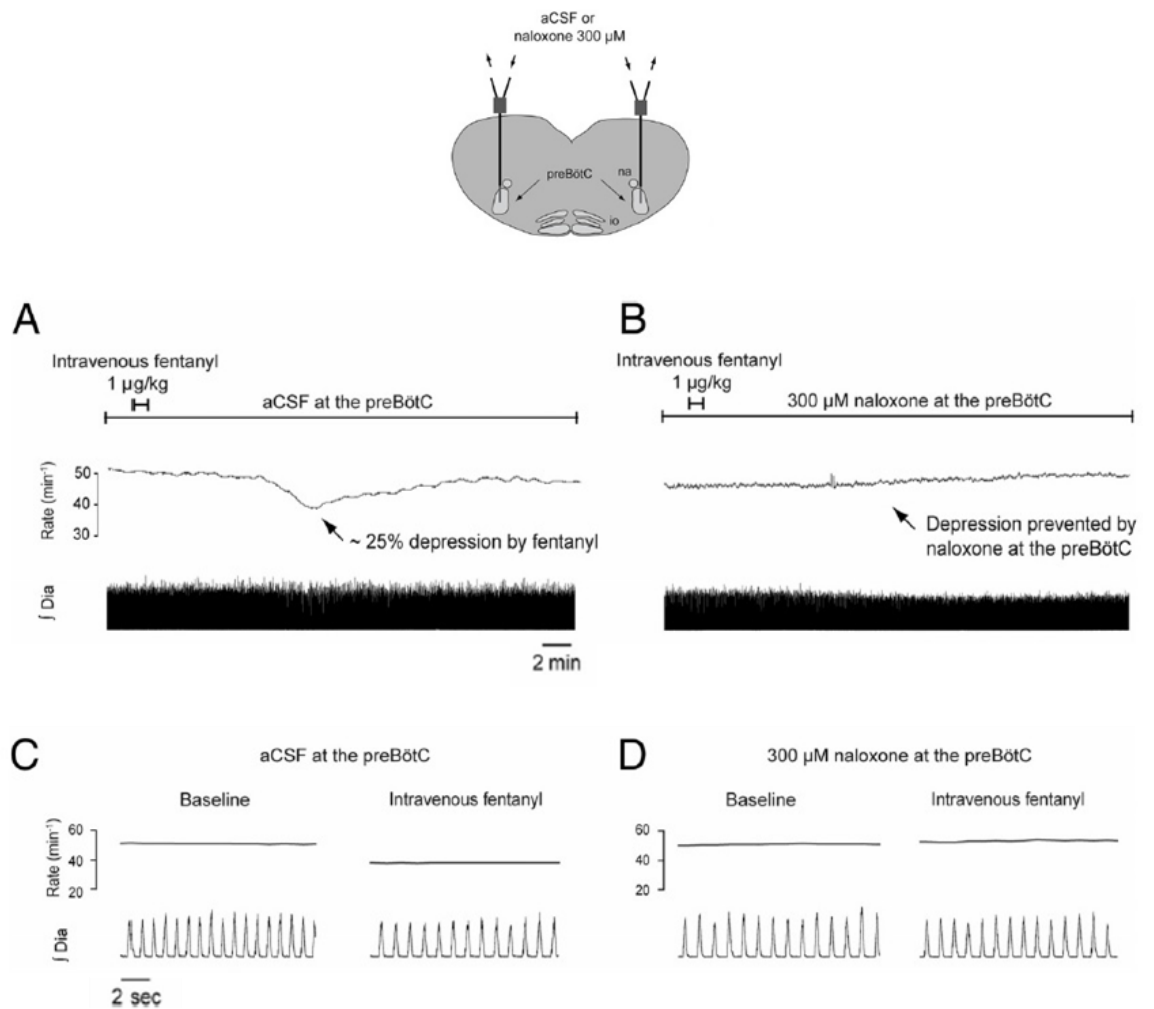


Figure 1-8. Systemically administered fentanyl mediates respiratory frequency depression by directly targeting the preBötC. Top: Schematic illustration of the position of the microdialysis probes in the preBötC allowing bilateral application of naloxone *in vivo*. A: Artificial cerebrospinal fluid (aCSF) injected directly into the preBötC does not prevent depression of respiratory rate or frequency of diaphragm contractions induced by intravenously administered fentanyl. B: Naloxone injected directly into the preBötC fully prevents fentanyl-induced respiratory frequency depression. C+D are traces corresponding to A+B respectively shown in a shorter time scale. Dia: Diaphragm muscle activity recording. Reproduced from Montandon et al. (2011).

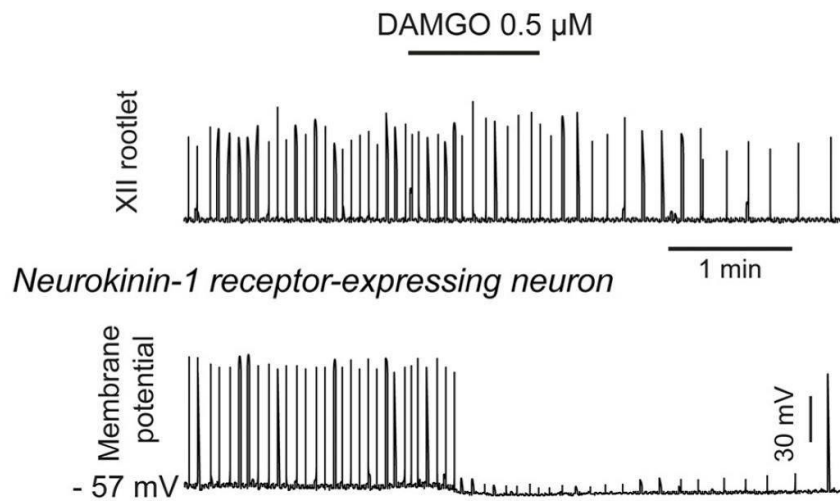


Figure 1-9. μ opioid receptor agonists suppress the activity of NK1R-expressing inspiratory preBötC neurons *in vitro*. Top: Recording of the hypoglossal (XII) nerve rootlet. Bottom: whole-cell intracellular recording of NK1R-expressing preBötC neurons in the medullary slice preparation. Application of DAMGO to the bathing medium decreases the frequency of XII bursting and hyperpolarises NK1R-expressing preBötC neurons. Inspiratory depolarisation was prevented in the NK1R-expressing preBötC neurons, thereby precluding the generation of action potentials. Reproduced from Montandon et al. (2011).

1.10 Thesis aims

The studies presented in this thesis were aimed at investigating central respiratory control in the mouse. Given the fragility of breathing in early postnatal life, it was of particular interest to determine the influence of postnatal maturation on the neural control of breathing. As extensively described in this chapter, μ opioid receptor agonists can be utilised as pharmacological tools to target the preBötC. Furthermore, μ opioid receptor agonists are used widely in clinical practice and are known to induce profound respiratory depressive effects. A large portion of the experimental work detailed in this thesis was aimed at investigating the effects of the μ opioid receptor agonist, fentanyl, on the immature respiratory system of the mouse to not only gain a better understand of central respiratory control during early life but to also gain insight into the potential clinical consequences of repeated opioid exposure during early life.

Study 1

The aim of study 1 was to investigate changes in breathing patterns through early postnatal life and through to early adulthood in order to assess respiratory maturation. It was of specific interest to determine the critical developmental time period by which maturation of respiratory activity occurs.

Study 2 and 3

Studies 2 and 3 were designed to determine the susceptibility of postnatal breathing patterns to fentanyl in order to better understand the influence of postnatal maturation on the central control of breathing. Fentanyl was utilised to pharmacologically manipulate and depress the preBötC *in vivo* throughout early postnatal development. The acute effect of fentanyl on respiratory activity was monitored to investigate the level of involvement of the preBötC in respiratory rhythm generation throughout early postnatal life.

Study 4

The aim of study 4 was to establish if repeated fentanyl exposure during neonatal life (P1-P5) induces long-term alterations in respiratory activity and if it influences the acute respiratory response to subsequent fentanyl exposure in mice *in vivo*.

Study 5

The aim of study 5 was to determine if repeated fentanyl exposure during juvenile life (P9-P13) induces long-term alterations in respiratory activity and if it influences the acute respiratory response to subsequent fentanyl exposure in mice *in vivo*.

Study 6

The aim of study 6 was to ascertain if repeated exposure to fentanyl during neonatal life in the mouse induces long-lasting changes in NK1R and μ opioid receptor expression within a region of the VRC (including the preBötC), using immunohistochemistry.

Chapter 2.

Methods

2.1 Animals

All animal experimental procedures were carried out under licence from the UK Home Office (Personal Licence number 60/11740, working under project Licence number 60/3924) and performed in accordance with the Animals (Scientific Procedures) Act, 1986. All experimental protocols were carried out using ICR mice. Male and female breeder mice were obtained from Harlan Laboratories UK. In house breeding of ICR mice was carried out at the Wellcome Surgical Institute animal research facility. Mouse pups were housed with their mother until weaning age (approximately 21 days old), after which male and female mice were housed separately in groups of no more than six. All mice were maintained on a 12 hour light/dark cycle with food and water available *ad libitum*. In this thesis mice are considered neonates from P0-P7 and juveniles from P8-P21. Mice over the age of P21 are classed as adults. The day of birth is referred to as P0.

2.2 Fentanyl injections

In all studies described in this thesis, fentanyl, a μ opioid receptor agonist was utilised. All neonatal, juvenile and adult mice were administered fentanyl citrate (Janssen-Cilag, UK) via an intraperitoneal (i.p.) injection. Fentanyl was decanted directly from the purchased vial (vial concentration: 50 $\mu\text{g/ml}$), and administered with no preparation required. Neonatal and juvenile mice were administered volumes in the range of 1-15 μl and adult mice were administered volumes in the range of 25-75 μl . Protocols for individual studies will be further discussed in chapters 3-5.

2.3 Whole body plethysmography

Whole body plethysmography is a non-invasive technique that can indirectly record respiration based on pressure deflections caused by a subject breathing within a closed chamber of fixed volume (Chapin, 1954). Whole body plethysmography is highly advantageous for *in vivo* respiratory research as it enables easy measurement of ventilation in unrestrained and freely behaving rodents. This technique is indispensable for recording breathing activity in very small neonatal animals where invasive respiratory measurements or restraint is impractical. In studies detailed in chapters 3 and 4, closed whole body

plethysmography was utilised to record and measure the respiratory behaviour of awake and freely behaving neonatal, juvenile and adult mice.

2.3.1 Neonatal and juvenile plethysmography

The neonatal/juvenile plethysmography set up (apparatus illustrated in Figure 2-1) was utilised for mice up to postnatal day 15. It consisted of a 45 ml recording chamber which housed the animal, and an adjoining reference chamber of equal volume (Buxco Research Systems, USA). This small chamber volume maximised the signal to noise ratio, enabling small neonatal breathing signals to be easily obtained. The recording chamber was fitted with an electrical heated plate designed to maintain the body temperature of the mouse within physiological range (32-34°C when recorded orally). An additional source of heat was supplied by a heat lamp to maintain the chamber temperature at the approximate nest temperature of between 30-32°C. To allow for continuous recording of the chamber temperature, a temperature probe (RET-3, Physitemp Instruments Inc, USA) was securely fitted within a small opening at the top of the chamber. Between respiratory recording sessions, a bias flow regulator (Buxco Research Systems, USA) was connected to and continually supplied the recording chamber with room air (rate of 0.5 l/min) enabling the chamber to be replenished with oxygen to prevent the accumulation of carbon dioxide.

During each recording session, the recording chamber was hermetically sealed to atmospheric air. At the end of every recording session, which lasted approximately 2 minutes, a calibration volume of 10 µl was injected into the recording chamber. Breathing-induced pressure changes within the closed recording chamber, relative to the reference chamber, were recorded by a differential pressure transducer (model DP103-4, Validyne Engineering, Northridge, CA). The analogue signal was passed to an analogue-to-digital converter (CED, Cambridge Instruments, UK) with a sampling frequency of 100 Hz. The resultant respiratory trace was stored on a PC and analysed offline using Spike 2 software (Cambridge Instruments, UK).

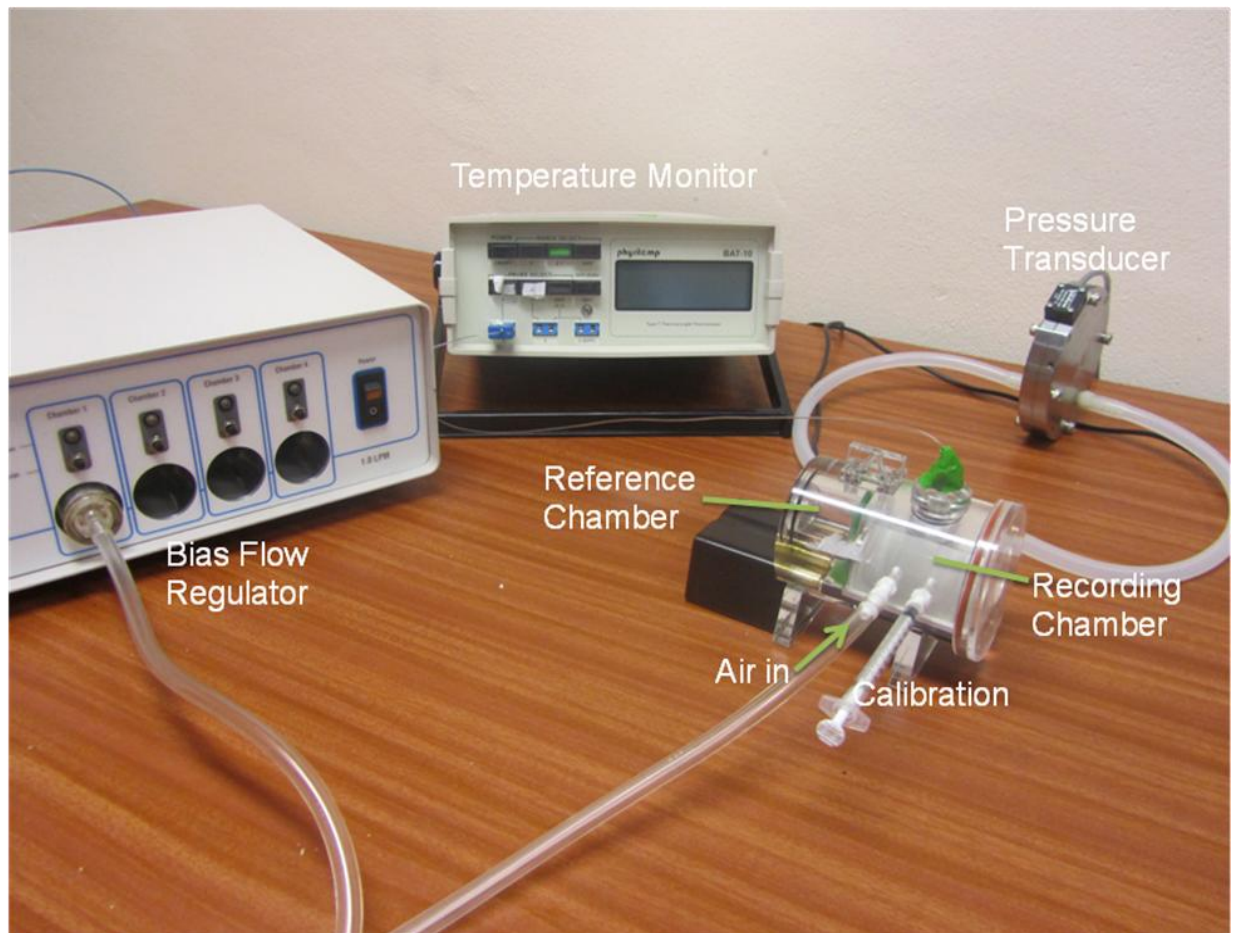


Figure 2-1. Whole body plethysmography apparatus used for neonatal and juvenile mice. The mouse was housed in the recording chamber, and breathing-induced pressure fluctuations relative to the reference chamber were measured by the differential pressure transducer. Between respiratory recordings, the recording chamber was continually flushed with room air (0.5 l/min) using a bias flow regulator. The calibration syringe was removed to allow circulating air to exit the chamber. The chamber temperature was monitored throughout experiments using a temperature monitor.

2.3.2 Adult plethysmography

The adult plethysmography set up (apparatus illustrated in Figure 2-2) was used for mice over 15 days old. The apparatus consisted of a 700ml recording chamber (built in house) that housed the animal and a reference chamber of equal volume. A temperature probe (RET-3, Physitemp Instruments Inc, USA) was securely fitted through a port in the recording chamber to allow continual recording of chamber temperature, which was maintained at 25-26°C. To control for thermal related drifts in the pressure signal, two controlled leaks were integrated into the system by means of 26 gauge needles (Terumo, Exchange Supplies UK). Between recording sessions, the recording chamber was supplied with air or various hypercapnic and hypoxia gas mixtures delivered from gas tanks. Prior to entering the recording chamber the gas passed through a conical flask filled with water in order to humidify the air. The rate of flow was controlled by a flow meter and maintained at 2 l/min.

During each recording session, the recording chamber was fully air tight. At the end of every recording session, which lasted approximately 2 minutes, a calibration volume of 100 µl was injected into the recording chamber. Breathing-induced pressure changes within the closed recording chamber, relative to the reference chamber, were recorded by a differential pressure transducer (model DP103-4, Validyne Engineering, Northridge, CA). The analogue signal was passed to an analogue-to-digital converter (CED, Cambridge Instruments, UK) with a sampling frequency of 100 Hz. The resultant respiratory trace was stored on a PC and analysed offline using Spike 2 software (Cambridge Instruments, UK).

The rectal temperature of the mice was recorded at the start and end of the experiment by means of a rectal temperature probe (IT-18 gauge isolated temperature probe, Linton Instrumentation, Norfolk UK). All adult mice were given a 2 hour habituation session in the recording chamber one day prior to the commencement of experiments.

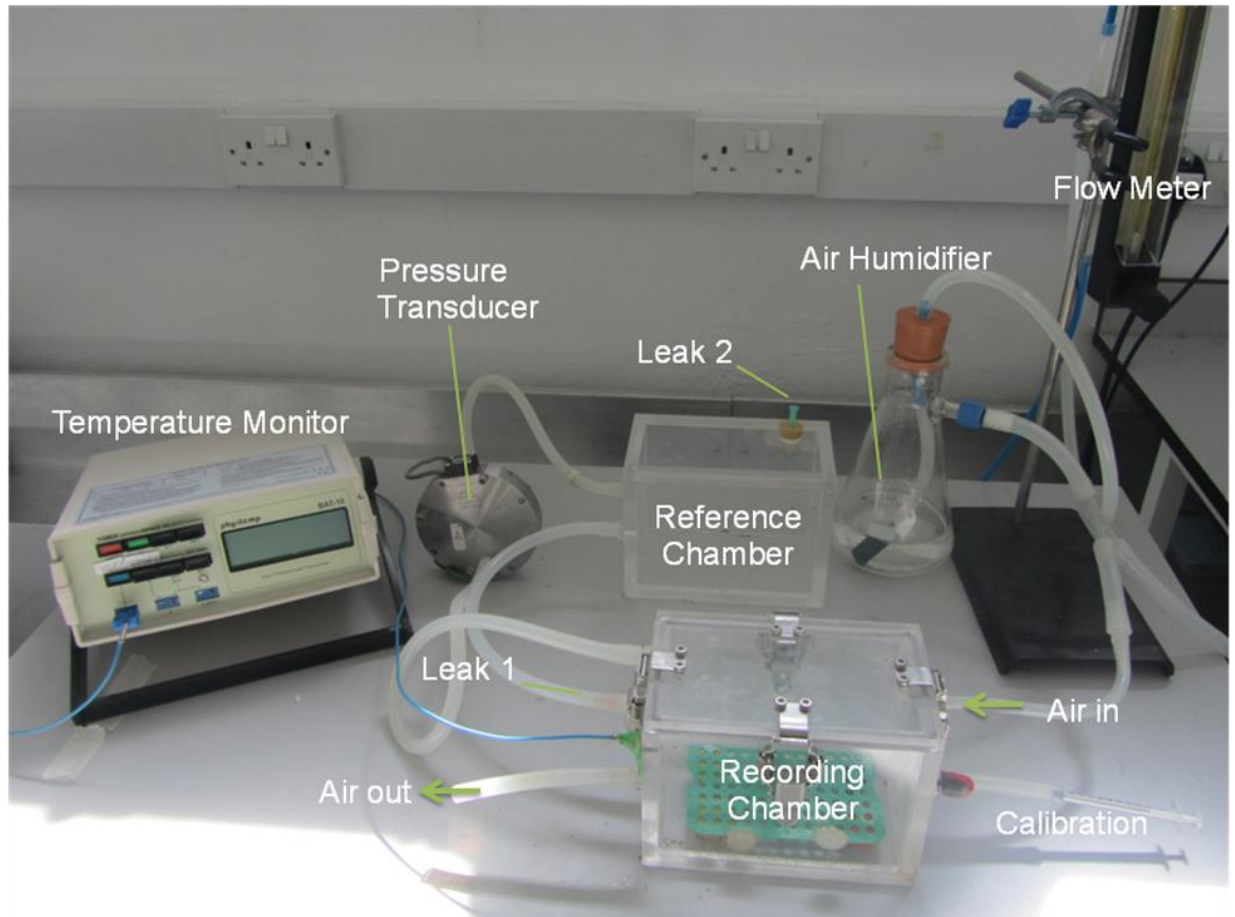


Figure 2-2. Whole body plethysmography apparatus used for adult mice. The mouse was housed in the recording chamber and breathing-induced pressure fluctuations relative to the reference chamber were measured by the differential pressure transducer. Between respiratory recordings, the recording chamber was continually flushed with humidified air or hypercapnic and hypoxic mixtures through the in and out air ports at a rate controlled by the flow meter. The chamber temperature was monitored throughout experiments using a temperature monitor. Two controlled leaks were introduced to compensate for slow thermal pressure changes.

2.4 Neonatal/juvenile behavioural assessments

The overall health status of the neonatal and juvenile mice was evaluated at regular intervals throughout plethysmography procedures, both before and after drug administration (see chapter 3, section 3.2.5 for further details). Mastication rate was measured by placing a small probe at the side of the mouth, and the number of mastication movements made in 10 seconds was counted. The righting reflex was evaluated by placing a mouse on its back and measuring the time taken to reach an upright position. In very young neonatal pups (P1-P3), the presence or absence of the milk sac was noted. In mice aged up to P11, body temperature was measured orally using a thin temperature probe (IT-18 gauge isolated temperature probe, Linton Instrumentation, Norfolk UK) and maintained at 32-34°C.

2.5 Analysis of plethysmograph respiratory traces

To measure respiratory variables, the respiratory recordings were analysed on a breath by breath basis. Movement distorts the plethysmography pressure signal and prevents reliable respiratory measurements, thus only data from periods of quiet, resting breathing were analysed. Prior to analysing the respiratory trace any DC drift in the respiratory signal was digitally removed. For all data analysis, the entire 2 minute respiratory trace was analysed.

2.5.1 Respiratory frequency, tidal volume and minute ventilation

Respiratory frequency, tidal volume (V_t), and minute ventilation (V_e) were calculated for all plethysmography experiments. In adult mouse studies described in chapter 4, inspiratory duration, and expiratory duration were also calculated. The method of calculation of respiratory frequency is illustrated in Figure 2-3. The total breath time (T_{tot}) was measured from the respiratory trace and respiratory frequency was expressed in breaths per minute and calculated as $60/T_{tot}$. V_t , which is defined as the volume of air inspired or expired during each respiratory cycle, was calculated as shown in Figure 2-4. The calculation of V_t from whole-body, closed plethysmography pressure oscillations is based on the principle that the animal is contained within an air-tight recording chamber of constant volume that has a lower temperature and relative humidity compared to the animal's body. Thus, inspiratory and expiratory events will induce cyclic changes in

temperature and water vapour of the air. This in turn will cause the pressure inside the chamber to change by a magnitude proportional to the difference in volume from the chamber to airway conditions i.e. proportional to V_t (Drorbaugh and Fenn, 1955). By taking into account the temperature and humidity of the animal and chamber, as well as barometric pressure, it was therefore possible to derive tidal volume from plethysmography pressure changes by application of an equation proposed in 1955 by Drorbaugh and Fenn (equation detailed in Figure 2-4). An injection of a known calibration volume was also required to calculate V_t . Minute ventilation (V_e), which is defined as the total volume of air inspired or expired each minute, is a product of respiratory frequency and V_t , and is calculated by multiplying the two parameters ($V_e = \text{frequency} \times V_t$). In the neonatal and juvenile mouse studies detailed in chapter 3, V_t is presented as a relative change from baseline following fentanyl administration rather than absolute values (further discussed in chapter 3 section 3.4.3).

2.5.2 Neonatal and juvenile breathing patterns

The prevalence of various breathing patterns was analysed throughout postnatal development in the neonatal and juvenile plethysmography studies described in chapter 3. The entire 2 minute respiratory trace was visually examined and the frequency of apnoeas, hyperpnoeas and hiccups during resting baseline breathing was calculated and expressed as number of breaths per 2 minutes. In this thesis an apnoea is defined as the cessation of breathing for more than two missed breaths following expiration (Jacquin et al., 1996; Renolleau et al., 2001). This was calculated as being at least 2 seconds in length. All apnoeas including post-hyperpnoeic apnoeas were analysed. Hyperpnoeas are defined as hyperventilatory periods of high amplitude breathing characterised by forced inspiratory and expiratory efforts that are often accompanied by a post-hyperpnoea apnoea. Hyperpnoeic episodes were calculated to last at least 2 seconds. Hiccups are defined as very short, high amplitude breaths. A hiccup breath typically lasts approximately 0.12 s and displays a very sharp inspiration and forced expiration. An example of each of these respiratory events is illustrated in Figure 2-5.

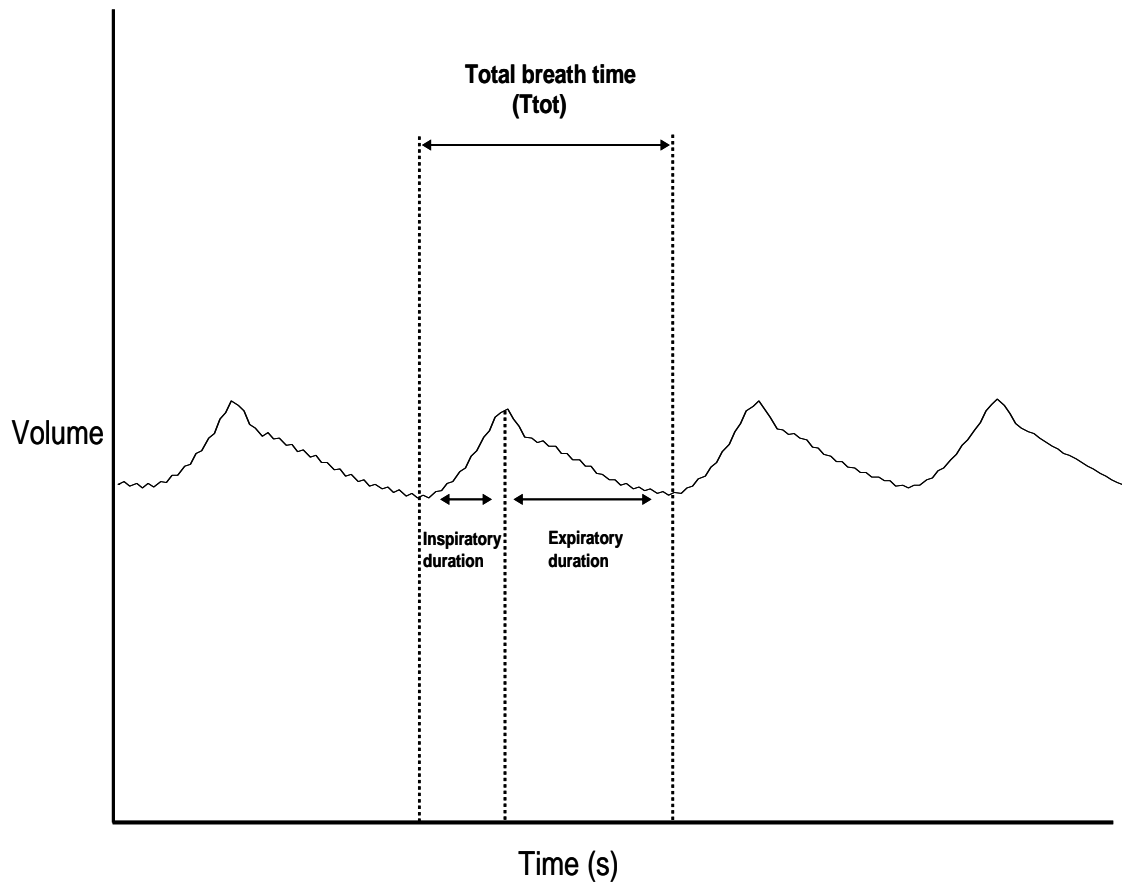
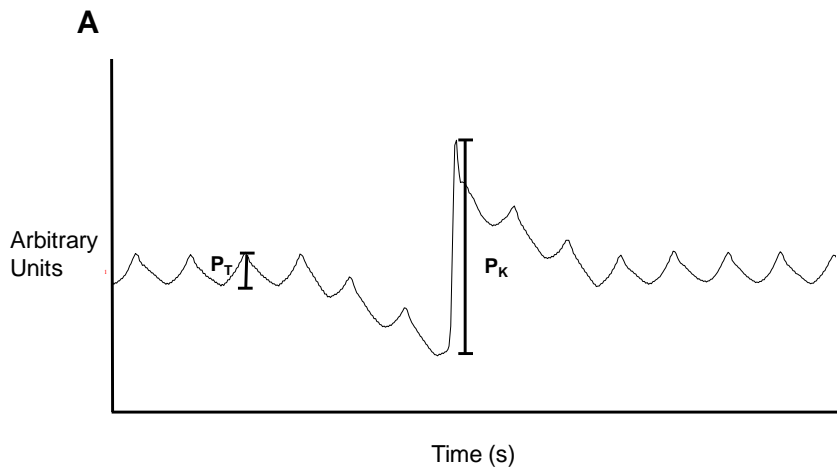


Figure 2-3. Calculation of respiratory frequency from plethysmograph trace.

Upwards pressure deflection of the trace represents inspiration and downwards deflection represents expiration. The duration of inspiration and expiration were calculated as well as the total breath time (T_{tot}) which was measured from the start of inspiration to the end of expiration. The respiratory frequency is expressed in breaths per minute and calculated as $60/T_{tot}$.



B

$$V_t = \frac{P_T}{P_K} \times V_K \times \left(\frac{T_R (P_B - P_C)}{T_R (P_B - P_C) - T_C (P_B - P_R)} \right)$$

Tidal volume was determined on the basis of the above equation, defined as follows:

V_t = tidal volume.

P_T = pressure change associated with each respiratory cycle.

P_K = pressure change associated with injection of the calibration volume.

V_K = calibration volume injected into the recording chamber.

T_R = body temperature of the mouse

T_c = temperature of recording chamber

P_B = barometric pressure

P_R = pressure of water vapour at body temperature (50mmHg)

P_C = pressure of water vapour in the recording chamber (50mmHg)

Figure 2-4. Calculation of tidal volume from plethysmograph trace. Tidal volume was determined from each respiratory trace (A) using the equation (B) derived by Drorbaugh and Fenn (1955). This equation enables pressure changes to be converted to volume changes. Upward deflections in the respiratory trace indicate a rise in pressure. P_T was calculated as the pressure deflection from the start of inspiration to the peak of the breath. P_K was calculated as the sharp pressure deflection induced by injecting the calibration volume.

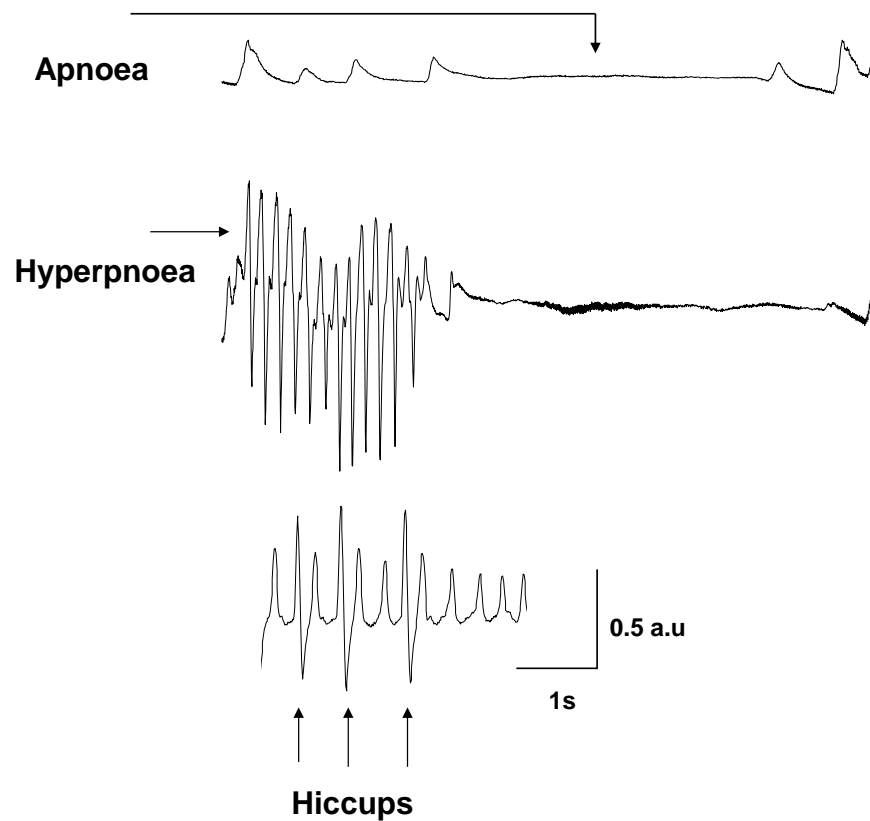


Figure 2-5. Representative respiratory traces illustrating various neonatal breathing patterns. Apnoeas are classified as long expiratory pauses that last for at least 2 missed breaths (approx. ≥ 2 seconds). Hyperpnoeic episodes are defined as periods of hyperventilation with forced inspiratory and expiratory efforts, illustrated by the high amplitude upward and downward deflections respectively. Hiccups are defined as very short breaths displaying sharp, large amplitude inspiratory and expiratory efforts.

2.6 Anaesthetised preparations

2.6.1 General surgical preparation

Animals were first transferred from the animal housing unit to the designated mouse operating theatre. Animals were weighed prior to the induction of anaesthetic. Urethane was used to anaesthetise the mice (see chapter 4, section 4.5.3 for further details on anaesthetic properties). Urethane crystals (Sigma, UK) were dissolved in 0.9% saline solution to prepare an injection solution of 0.1g/ml. Animals were administered an initial intraperitoneal (i.p.) injection of 1.5 g/kg urethane. Once unconscious, 3 supplementary doses of 0.25 g/kg urethane were administered approximately ten minutes apart. This dosing regime allowed for a stable plane of surgical anaesthesia to be maintained from the start and throughout the course of the experiment (approximately 2 hours). To test if animals were adequately anaesthetised prior to commencement of surgery, the hind limb reflex was assessed, whereby a firm pinch of the footpad evokes a withdrawal of the foot. Absence of this reflex is indicative of a sufficient depth of anaesthesia. Once animals were adequately anaesthetised, the muscarinic antagonist, atropine sulphate (Animalcare Ltd, York, UK), was subcutaneously administered (0.05 mg/kg) to reduce excess tracheal and lung secretions that can be detrimental to breathing. Mice were placed in the supine position and fur from the neck and abdominal regions removed using an electric shaver (Wahl, UK). Body temperature was monitored with a rectal probe and maintained between 36.5-37°C using a heat lamp. All anaesthetised experiments were terminal, and on conclusion of the experiment mice were euthanised by cervical dislocation.

2.6.2 Respiratory airflow measurements

To allow respiratory airflow to be measured, mice were transorally intubated. The ventral skin of the neck region was incised to expose the lobes of the thyroid gland which were separated by blunt dissection. The sternohyoid muscles were bluntly split and laterally retracted to expose the underlying larynx and trachea. This allowed for visualisation of the trachea when performing the tracheal intubation. The intubation cannula was made from an intravenous catheter (20 gauge; Vasofix, Braun, Germany) that was shortened to 30 mm in length and tapered distally to facilitate insertion into the trachea. The tongue of the mouse was pulled to one side using forceps and the tracheal cannula was inserted into the mouth and advanced into the trachea. A small animal pneumotachometer (AD Instruments, USA)

was securely connected to the top of the tracheal intubation cannula. Laminar airflow (corresponding to inspiratory and expiratory airflow) across a fine gauze mesh within the pneumotachometer produces a pressure difference which is linearly proportional to the velocity, thereby enabling changes in respiratory airflow to be continually monitored. These pressure differences were measured using a differential pressure transducer (Validyne DP103, USA). The analogue signal was passed to an analogue-to-digital converter (CED, Cambridge Instruments, UK) with a sampling frequency of 100 Hz and the resulting airflow signal was stored on a computer and analysed offline using Spike2 software (Cambridge Instruments, UK). Throughout the experimental period mice spontaneously breathed room air without ventilatory aid. At the end of every experiment a calibration volume of 0.2 ml was injected across the pneumotachometer.

2.6.3 Respiratory musculature EMG measurements

Genioglossus EMG

Electromyography (EMG) is the study of muscle function through the measurement of electrical activity produced during muscular contraction. EMG activity of the genioglossus (GG) muscle was recorded. The GG is the principal protruder muscle of the tongue which also plays a critical role in maintaining upper airway patency. In the rodent, the GG becomes active during inspiration and has therefore been referred to as an inspiratory muscle (Liu et al., 2003; Hajiha et al., 2009; Pagliardini et al., 2012); thus GG muscle activity can provide a measure of inspiratory function. The ventral surface of the GG was exposed via a submental incision using fine scissors, and blunt dissection of the overlying diaphragmatic and mylohyoid muscles. Two fine monopolar needle electrodes (Linton Instrumentation, Norfolk, UK) with modified hooked tips were inserted into the GG muscle approximately 3-4 mm apart. The muscle was covered with oil throughout experiments to prevent desiccation. The electrical signals were amplified at 5000X gain and filtered between 100 and 5000 Hz using a differential amplifier (model EMG 100C; Bipoac system Inc, USA). The EMG activity was sampled at 1000 Hz via an analogue to digital interface (CED, Cambridge Instruments, UK), stored on a computer and analysed offline using Spike2 software (Cambridge Instruments, UK).

Abdominal muscle EMG

Abdominal muscles (ABD) have been shown to exhibit a rhythmic expiratory-related mode of activity in adult rodents *in vivo* (Pagliardini et al., 2011; Pagliardini et al., 2012; Pagliardini et al., 2013). In an attempt to measure expiratory muscle activity, ABD_{EMG} activity was measured in the anaesthetised preparation. A large incision was made in the abdominal region to expose the underlying musculature. Two monopolar needle electrodes (as described for GG_{EMG} measurement) were inserted approximately 3-4 mm apart into the right external oblique abdominal muscle. Muscle desiccation was prevented by application of oil to the muscle surface. The electrodes were attached to the differential amplifier (model EMG 100C; Bipoac system Inc, USA) and the analogue signal was amplified at 5000X gain and filtered between 1 and 5000 Hz. The signal was sampled at 1000 Hz by an analogue to digital converter (CED, Cambridge Instruments, UK) and analysed offline.

A ground electrode made of multistrand, insulated stainless steel wire with the last 2 mm uninsulated (Cooner wire, Chatsworth, CA, USA) was sutured into the hind paw of the mouse. The uninsulated portion of the electrode was in contact with the bony region of the paw which is an electrically neutral area. The ground electrode was also connected to the differential amplifier. The purpose of the ground electrode was to provide a common reference to the differential input of the GG and ABD muscle EMG signals. The differential amplifier generated the raw GG_{EMG} and ABD_{EMG} muscle activity by subtracting the EMG signals from the ground electrode signal.

2.6.4 Analysis of airflow and GG_{EMG} activity

To determine the respiratory parameters, respiratory recordings were analysed on a breath by breath basis. Respiratory frequency, V_t, V_e and GG_{EMG} activity were analysed and quantified for all the anaesthetised preparations before and after fentanyl application. The number of augmented breaths, defined as a breath with a V_t 50% greater than the previous breath, was quantified during baseline breathing. ABD_{EMG} activity was not quantified because on recording, the muscle bursting was not synchronised with the expiratory phase and appeared to be sporadic in nature. Consequently this tonic muscle activity was not analysed as it did not represent expiratory activity. Occasionally, expiratory-related abdominal activity did appear intermittently in a small number of mice, but this was not sufficient for quantification purposes (discussed further in chapter 4, section 4.3.5). The

respiratory frequency was determined from the respiratory airflow signal as shown in Figure 2-6. V_t for each inspiratory cycle was calculated by integrating the area under the inspiratory signal and the area under the calibration signal. To determine V_t the following calculation was applied: (calibration volume/area under calibration signal) x area under inspiratory signal. V_e was subsequently calculated ($V_e = \text{frequency} \times V_t$). V_t and V_e values were always standardised to the weight of the mouse. A digital low pass filter was applied to the GG_{EMG} signal to remove high frequency noise. The filtered signal was then rectified and smoothed with a time constant (τ) of 0.05s. The peak amplitude of the integrated signal was used as a measure of GG_{EMG} activity.

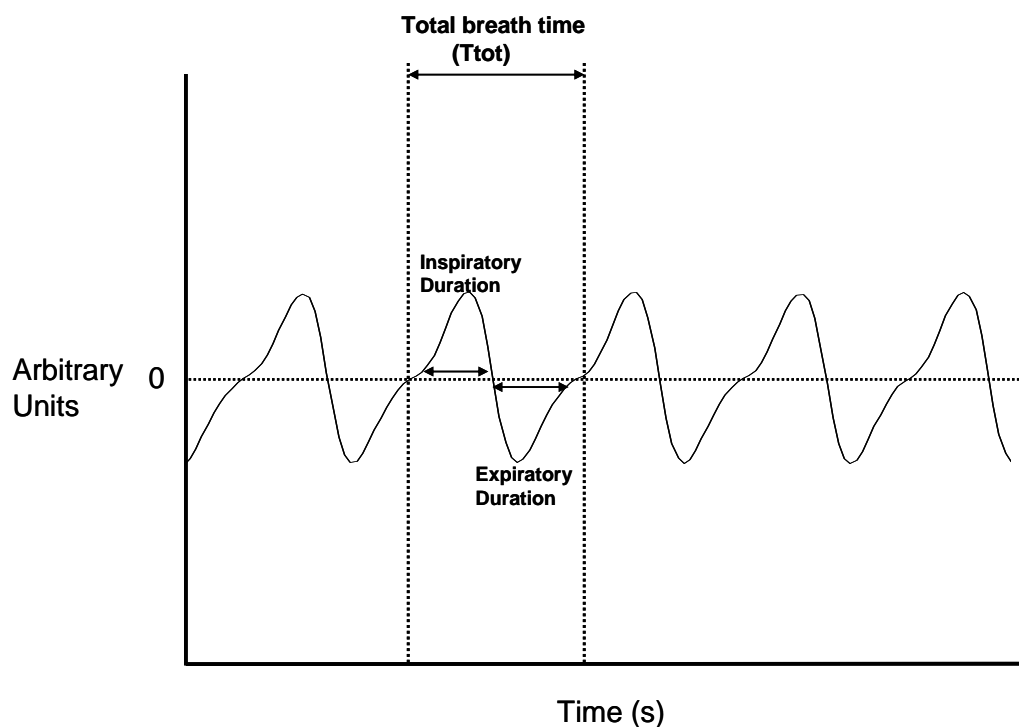


Figure 2-6. Calculation of respiratory frequency from airflow trace. The airflow signal above the dotted zero baseline represents inspiration and the signal below the line represents expiration. The duration of inspiration and expiration were measured. T_{tot} was measured as the time from start of inspiration to end of expiration. Respiratory frequency in breaths per minute was calculated by: $60/T_{tot}$.

2.7 Perfusion fixation

Animals repeatedly exposed to fentanyl or saline in neonatal life were transcardially perfused once they reached adulthood (6 weeks old), to allow for detailed histological analyses of brainstem respiratory areas. Mice were i.p administered an overdose of pentobarbital (0.1 ml) and on abolition of the hind limb withdrawal reflex the procedure commenced. The ventral skin was superficially cut to expose the thoracic and peritoneal membranes. An incision was made in the peritoneal membrane below the sternum to expose the diaphragm. In order to open up the chest cavity and expose the underlying viscera, the diaphragm was incised and the lateral aspects of the rib cage were cut. The rib cage was then reflected towards the head of the mouse and secured in place, allowing full access to the beating heart. A butterfly needle (Butterfly-23 INT, Venisystems) connected to the perfusion apparatus was inserted into the apex of the heart until it entered the left ventricle. The right atrium was cut and heparinised saline (10 ml heparin/1 litre 0.9% saline solution) was pumped through the circulation at a constant pressure of 80 mmHg for approximately 30 seconds or until the perfusate ran clear and the liver turned pale, indicating the blood had been sufficiently cleared from the body. The animal was then immediately perfused with 250 ml of 4% paraformaldehyde at the same pressure. Twitching of the limbs and rigidity of the mouse tissue indicated a successful perfusion. On completion of perfusion fixation, the brain and rostral portion of the spinal cord were carefully excised from the skull and vertebrae. Tissue was post-fixed in 4% paraformaldehyde for 4 hours and then transferred to a 30% sucrose solution. Sucrose functions as a cryoprotectant to remove excess water from the tissue, preventing ice crystals forming when brain tissue is frozen. Brains were stored in sucrose for up to one week or stored long-term in liquid nitrogen prior to tissue processing.

2.8 Cryostat sectioning

Prior to sectioning, the forebrain and excess spinal cord were removed. The brain was then mounted on a chuck using cryomatrix compound (Thermo Scientific, Cheshire, UK) and frozen with dry ice. Forty micrometer coronal, medullary sections were cut at -21°C using a cryostat. Sections were collected sequentially into 48 well plates containing 0.3M phosphate buffered saline (PBS).

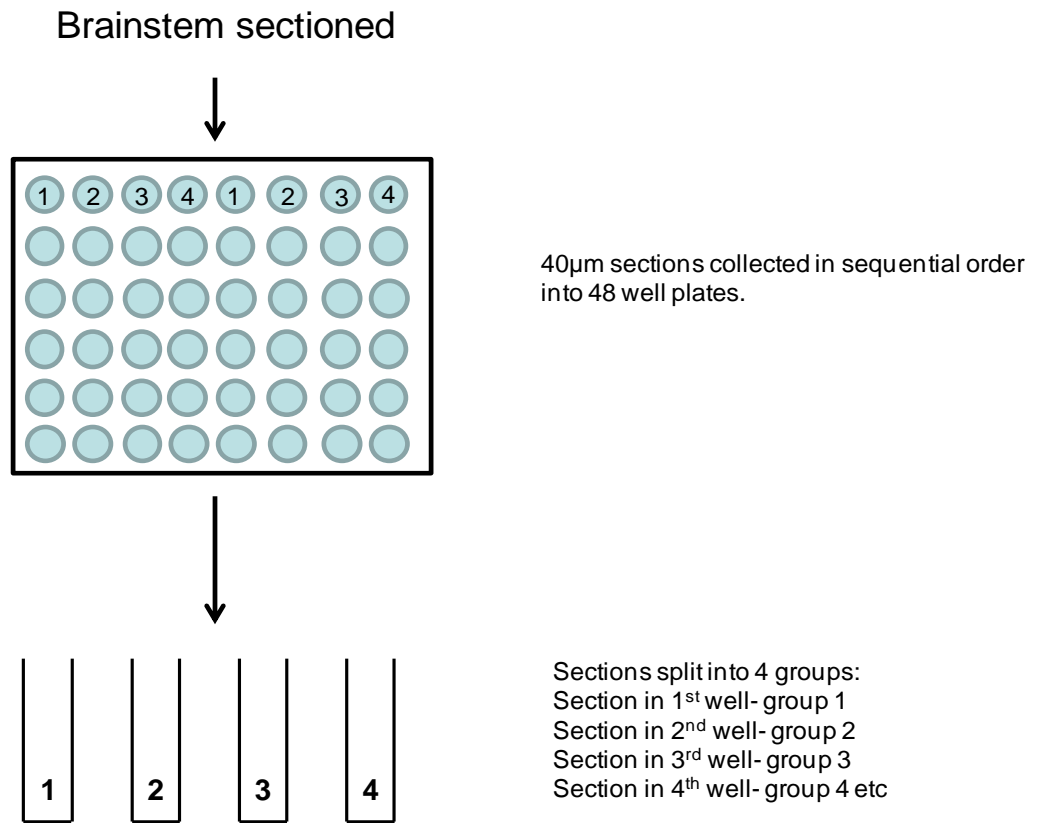
2.9 Fluorescent immunohistochemistry

2.9.1 Staining protocol

In chapter 5, immunohistochemical fluorescent staining was performed to detect and quantify the expression of various anatomical markers of the principal respiratory nuclei located in the ventral respiratory column (VRC). This was carried out on adult brainstems from control mice repeatedly exposed to saline and mice repeatedly exposed to fentanyl in early life. Prior to the immunohistochemistry procedures, the brainstem sections were split into 4 groups (see Figure 2-7 for illustration). This enabled the staining of different neuronal markers to be carried out within each group.

All immunohistochemistry protocols were carried out on free floating brainstem sections. For details of all solution preparation, see Appendix I. The sections were bathed in 50% ethanol for 30 mins to aid with tissue penetration of antibodies. The sections then underwent three 10 min washes in 0.3M PBS followed by a 15 min incubation in 3% hydrogen peroxide (H_2O_2) diluted in 0.3M PBS. The purpose of the H_2O_2 step was to quench endogenous peroxidase activity, which can be a source of background staining if amplification techniques are being utilised. Three 10 min washes in 0.3M PBS followed. Sections were then incubated in primary antibodies diluted in a solution of 1% normal donkey serum (NDS; blocks non-specific binding sites) and 0.3M PBS with 0.3% Triton X-100 (PBST) for 24 hours at 4°C. After a further 3 x 10 min washes in PBST, sections were exposed to species-specific fluorescent or biotinylated secondary antibodies also made up in 1% NDS and PBST. Secondary antibody incubation lasted 12 hours at room temperature. When no amplification of the fluorescent signal was required, a final 3 x 10 min washes in 0.3M PBS took place before sections were mounted in sequential rostrocaudal order on uncoated slides using Vectashield hard set anti-fade mounting medium (Vector Laboratories). When a fluorescent signal required amplification, this was achieved by the tyramide signal amplification (TSA) protocol described in Figure 2-8. Three 10min washes in PBST followed secondary antibody incubation. Sections were then incubated for 4 hours at room temperature in Streptavidin horseradish peroxidase complex (PerkinElmer Inc, UK) diluted in PBST, followed by 3 x 10 min washes in PBST. Sections were then incubated with fluorophore-conjugated tyramide (PerkinElmer Inc, UK) made up in amplification diluent (containing H_2O_2) for 7 mins at room temperature. Following a

final three 10 min washes in 0.3M PBS, sections were mounted on slides as described above. All sections were stored at -20°C.



Different antibody combinations added to each group of sections

Figure 2-7. Schematic diagram illustrating how brainstem sections were split into 4 groups. Different combinations of primary and secondary antibodies were added to each group.

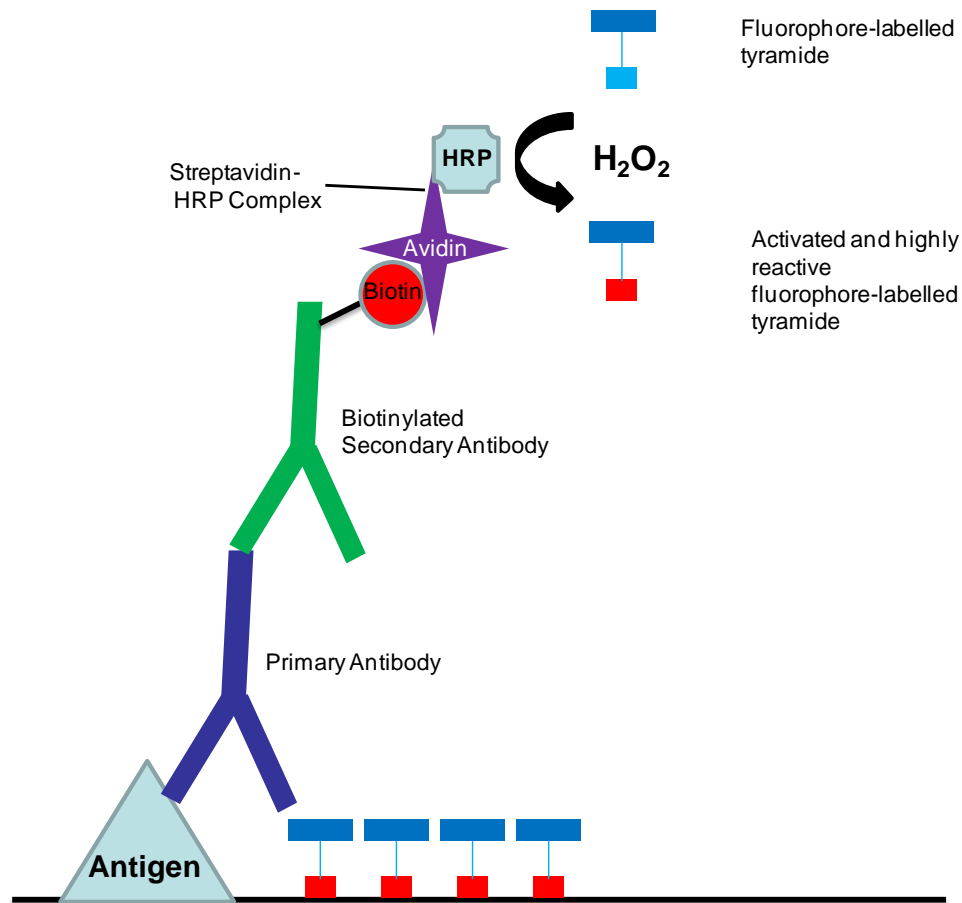


Figure 2-8. Schematic diagram illustrating the principle of tyramide signal amplification (TSA) in immunohistochemistry. TSA is an enzyme-mediated detection method that can amplify fluorescent labelling of a target protein by utilising the catalytic activity of horseradish peroxidase (HRP) enzyme. The target antigen is detected by the primary antibody which is subsequently bound by a biotinylated secondary antibody. Streptavidin conjugated to HRP binds to the biotin molecules on the secondary antibody. In the presence of H₂O₂, the immobilised HRP catalyses the conversion of fluorophore-labelled tyramide, a phenolic compound, into a highly reactive, short-lived intermediate that covalently binds to electron-rich regions of adjacent proteins. Multiple deposition of the labelled tyramide occurs very quickly, thereby amplifying the signal of the target protein.

Chapter 3.
Postnatal Maturation of Central Respiratory Control

3.1 Introduction

The neural circuitry underlying respiratory rhythmogenesis must be fully functional at birth to allow postnatal survival in mammals. However, in spite of its fundamental role for survival, the respiratory system is immature at birth. The immature respiratory system generates a dysrhythmic and fragile breathing pattern during early life in both rodents and humans (Fisher et al., 1982; Mortola, 1984; Read and Henderson-Smart, 1984), thereby potentially making this period of life vulnerable to external perturbations. At birth mice are immature and their irregular breathing is comparable to that of preterm infants (Matrot et al., 2005). It is widely accepted that the mammalian respiratory system undergoes significant postnatal maturation (Hilaire and Duron, 1999). In the mouse there is a proposed respiratory maturational step believed to occur early in postnatal life, after which breathing increases in frequency and follows a more regular and robust pattern (Mortola, 2001). The central mechanisms underlying this step in maturity remain to be elucidated as does the exact time-frame by which it occurs. Any disruptions or alterations to this postnatal respiratory maturation could be detrimental to survival and it is therefore an important time period to investigate. There is a paucity of studies that have thoroughly examined early postnatal changes in the respiratory patterns of mice. In particular the immature respiratory phenotype of neonatal mice has yet to be fully characterised. To better understand the mechanisms of respiratory rhythm generation during early postnatal life, ascertaining the changes in the respiratory phenotype as the respiratory system matures postnatally is fundamental. Furthermore, unravelling the mechanisms of respiratory rhythmogenesis will be vital in understanding the pathophysiology of many central respiratory disorders that manifest in early life e.g. sudden infant death syndrome (SIDS).

As described in chapter 1, there is compelling evidence and a general consensus that a small bilateral region of the ventrolateral medulla, known as the preBötzinger complex (preBötC), is involved in respiratory rhythmogenesis (Smith et al., 1991). The preBötC is postulated to function as an inspiratory oscillator driving rhythmic inspiratory muscular activity in the rodent (Smith et al., 1991; Janczewski and Feldman, 2006). Recent advances in respiratory neurobiology have revealed that a second group of bilateral respiratory neurons known as the retrotrapezoid nucleus/parafacial respiratory group (RTN/pFRG) may function as a respiratory rhythm generator in the neonatal rodent (Onimaru and Homma, 2003; Onimaru et al., 2008). Also located in the ventrolateral medulla, this group

of neurons exhibit endogenous rhythmic activity with a pre-inspiratory mode of firing which can be recorded from neonatal rodent brainstem-spinal cord preparations (Onimaru and Homma, 2003). These Pre-I neurons have been proposed to control the onset of inspiration in the neonatal rodent (Ballanyi et al., 1999; Onimaru and Homma, 2003). Importantly, this pre-inspiratory rhythmic discharge has not been observed in adult rodent preparations (Mulkey et al., 2004; Stornetta et al., 2006), suggesting the RTN/pFRG may not exhibit a rhythm generating role in adulthood. As thoroughly discussed in chapter 1, there is evidence to suggest that an absent or malformed RTN/pFRG results in disordered respiratory rhythm at birth in the rodent, further suggesting its key role in respiratory rhythm generation (Jacquin et al., 1996; Dubreuil et al., 2008; Pagliardini et al., 2008). There is emerging evidence that the preBötC and RTN/pFRG become functionally coupled during embryonic development and form a dual respiratory rhythm generator (Thoby-Brisson et al., 2009). The precise interaction between the preBötC and RTN/pFRG and their functional significance throughout postnatal maturation *in vivo* remains an open issue. Elucidating this interaction and the level of involvement each plays in generating the respiratory rhythm will be essential in understanding the central mechanisms that can lead to respiratory disorders and failure in early life.

Riluzole, a I_{NaP} blocker, has been demonstrated to selectively abolish rhythmic activity of embryonic parafacial neurons (e-pF neurones, proposed embryonic forerunner of the RTN/pFRG) in brainstem-spinal cord preparations of embryonic mice (Thoby-Brisson et al., 2009), and can therefore be postulated to also selectively target the neonatal RTN/pFRG. Conversely, when applied to medullary slice preparations containing the preBötC from neonatal and embryonic rodents, riluzole does not affect the frequency of respiratory motor output (Del Negro et al., 2005; Thoby-Brisson et al., 2009), suggesting the preBötC activity is insensitive to riluzole. Further support of the theory that the RTN/pFRG functions as a respiratory rhythm generator in early postnatal development comes from a study investigating the susceptibility of postnatal breathing patterns to riluzole in the mouse (Dr Leanne McKay, personal communication, SFN abstract 2009). Riluzole was proposed to selectively perturb the functioning of the RTN/pFRG *in vivo* throughout postnatal development in the mouse and induce minimal depression of preBötC activity. The acute effects of this RTN/pFRG perturbation on respiratory activity were measured to determine if respiratory sensitivity to riluzole changes with age. Preliminary findings have shown that systemic riluzole administration from P1-P3 reduces respiratory frequency but evokes no respiratory depression or alteration in respiratory patterns beyond

P3. These data further supports the hypothesis that the riluzole-sensitive RTN/pFRG is involved in respiratory rhythmogenesis, but only in early postnatal life i.e. pre-maturation. Based on these findings we have hypothesised that the RTN/pFRG may function as a respiratory rhythm generating oscillator during development and early postnatal life when the respiratory system is immature, after which the preBötC becomes the dominant respiratory oscillator driving breathing when the respiratory system is mature (Gray et al., 2001; McKay et al., 2005; McKay and Feldman, 2008).

Several *in vitro* and *in vivo* studies have revealed that preBötC neurones are sensitive to the depressive actions of μ opioid receptor agonists, When applied to rodent medullary slice and *en bloc* preparations, μ opioid receptor agonists depress the firing of preBötC neurons and slow respiratory-related motor output (Gray et al., 1999; Takeda et al., 2001; Mellen et al., 2003; Montandon et al., 2011). This opioid sensitivity is attributable to the fact that preBötC neurons express the μ opioid receptor (Gray et al., 1999). Fentanyl is a highly selective μ opioid receptor agonist with respiratory depressive actions. Importantly, when administered systemically in rats, fentanyl has been demonstrated to induce respiratory frequency depression *in vivo* by exclusively targeting and depressing NK1R-expressing preBötC neurons (Montandon et al., 2011). Conversely, RTN/pFRG neurons do not express the μ opioid receptor, thus μ opioids do not alter or depress their rhythmic neural output *in vitro* (Takeda et al., 2001; Janczewski et al., 2002; Mellen et al., 2003). Taken together, these findings suggest that fentanyl can be utilised as an effective tool to pharmacologically perturb the rhythm generating properties of the preBötC *in vivo*, whilst leaving the RTN/pFRG unperturbed. By exploiting their differential opioid sensitivity, fentanyl should allow for a dissociation of the functioning of these two postulated respiratory oscillators.

3.1.1 Study aims and rationale

Study 1: Investigation of postnatal changes in respiratory patterns of mice.

Given that neonatal breathing patterns have not been fully characterised in the mouse, the aim of study 1 was to investigate changes in breathing patterns during early postnatal life and through to early adulthood in order to assess postnatal respiratory maturation. It was of particular interest to determine the critical developmental time period by which maturation of respiratory activity occurs.

Study 2: Susceptibility of postnatal breathing patterns to fentanyl: A longitudinal study.

The aim of study 2 was to determine the influence of postnatal maturation on the central control of breathing. Fentanyl was utilised to pharmacologically manipulate the respiratory system of mice *in vivo* throughout early postnatal development. The acute respiratory effects of fentanyl were measured in order to investigate the level of involvement of the preBötC in respiratory rhythm generation throughout this time period.

Study 3: Susceptibility of postnatal breathing patterns to fentanyl: A single exposure study.

Similar to study 2, the aim of study 3 was also to investigate the influence of postnatal maturation on the central control of breathing. Fentanyl was utilised as a pharmacological tool to manipulate the respiratory system of mice *in vivo* throughout postnatal development and through to early adulthood. The acute respiratory effects of fentanyl were measured in order to establish the level of involvement of the preBötC in respiratory rhythm generation throughout this time period.

Studies 2 and 3 were designed to follow on from and compliment the *in vivo* work by Dr Leanne McKay who investigated the susceptibility of postnatal breathing patterns to riluzole (Dr Leanne McKay, personal communication). It was proposed that fentanyl would selectively depress the activity of the preBötC, but leave the opioid-insensitive RTN/pFRG unperturbed, thereby allowing for the dissociation of the functioning of these two postulated respiratory oscillators throughout the maturation period of breathing. Study 2 was longitudinal in nature and mice were repeatedly exposed to fentanyl throughout early postnatal life. In study 3 different mice were studied on each postnatal day i.e. each mouse was only exposed once. The rationale for conducting both studies will be discussed further within this chapter.

Hypothesis for study 2 and 3: If the preBötC functions as the dominant respiratory rhythm generator when the respiratory system is mature then mice should be more susceptible to the respiratory depressive effects of fentanyl after the maturation step has occurred i.e. the respiratory sensitivity to fentanyl will be age-dependent.

3.2 Methods

3.2.1 Animals

All experimental procedures were carried out under licence from the UK Home Office and performed in accordance with the Animals (Scientific Procedures) Act, 1986. Experiments detailed in this chapter were performed on both male and female ICR mice with ages ranging from P1-P30. A total of 79 mice were utilised in study 1, 84 mice in study 2 and 79 mice in study 3. All mouse pups were housed with their mother until postnatal day (P) 21. Adult mice (P21 and older) were housed according to their gender in groups of no more than six.

3.2.2 Study design

Study 1

Changes in respiratory patterns were assessed throughout postnatal development through to adulthood. Mice were studied from P1-P5 (n=54), P7 (n=6), P10 (n=9) and P30 (n=10). P30 mice were classed as adults. Different mice were studied on each of the postnatal days.

Study 2

The respiratory depressive effects of fentanyl were assessed throughout postnatal development. Mice were studied from P1-P5 (n=60), P9 (n=12) and P11 (n=12). In the fentanyl experiments, the acute respiratory response to a single dose of 0.04 mg/kg fentanyl was measured on each postnatal day. In the control experiments, the acute respiratory response to a saline vehicle was measured on each postnatal day. The study design was longitudinal so mice were continually studied throughout early postnatal life i.e. they were repeatedly exposed to fentanyl or saline.

Study 3

The respiratory depressive effects of fentanyl were assessed throughout postnatal development. Mice were studied from P1-P5 (n=54), P7 (n=6), P10 (n=9) and on P30 (n=10). In the fentanyl experiments, the acute respiratory response to a single dose of 0.04

mg/kg fentanyl was measured on each postnatal day. In the control experiments, the acute respiratory response to a saline vehicle was measured on each postnatal day. In this study, different mice were studied on each postnatal day thus mice were never exposed to fentanyl or saline on more than one occasion.

In both study 2 and 3, fentanyl was administered at a dose of 0.04 mg/kg as previous *in vivo* studies, including studies within our lab have found that this dose induces a significant respiratory depression in neonatal rodents without having significant side effects (Greer et al., 1995; Laferriere et al., 2005).

3.2.3 Respiratory measurements

Respiratory activity was measured in freely behaving, awake mice using the non-invasive technique of whole body plethysmography (see chapter 2, section 2.3). Respiratory monitoring of the neonatal and juvenile pups (P1-P11) took place in the neonatal plethysmograph set up, whereas the larger adult set up was utilised for P30 mice. Respiration was recorded under eupneic conditions. Before experimental sessions began, animals were given 45 minutes to habituate to the recording chamber. Between respiratory recordings the recording chamber was continually supplied with room air using a bias flow regulator (neonatal set up; flow rate of 0.5 l/min) or humidified air supplied from a gas tank (adult set up; 21% O₂, balanced N₂, supplied at 2l/min) to prevent CO₂ accumulation. In study 1, only resting breathing was recorded. Three baseline respiratory recordings that were 2 minutes in length were taken approximately 15 minutes apart. In studies 2 and 3, in addition to baseline respiratory measurements, the acute respiratory response to fentanyl or a saline vehicle was also measured. Following baseline measurements, mice were removed from the recording chamber and given an i.p injection of 0.04 mg/kg fentanyl. Control mice were administered an equivalent volume of physiological saline. Mice were then immediately returned to the recording chamber and their ensuing respiratory activity was recorded at 5, 15, 30 and 45 minutes post drug application. Each respiratory recording lasted 2 minutes. At the end of every recording, a calibration volume of 10 µl (neonatal chamber) or 100 µl (adult chamber) was injected into the recording chamber. Control and fentanyl experiments were run simultaneously. On conclusion of experiments, all mice were transcardially perfused and their brain tissue was removed for studies unrelated to this thesis.

3.2.4 Respiratory analysis

To measure respiratory variables, the plethysmography recordings were analysed using Spike 2 software (see section 2.5). Only periods of quiet resting breathing were analysed given that movement distorts the respiratory signal.

In study 1, respiratory variables under resting conditions were assessed throughout postnatal development. All three baseline respiratory recordings were analysed. Respiratory frequency was analysed on a breath by breath basis (see section 2.5.1 for further details of measurement). In order to measure respiratory variability, the coefficient of variation (CV) of respiratory frequency was measured for each respiratory trace and is calculated by: $[\text{SD}/\text{mean respiratory frequency}] \times 100$. The higher the CV value is, the greater the level of breathing instability. Additionally, individual respiratory patterns e.g. apnoeas, hyperpnoeas, and hiccups, were identified and their frequency was quantified for each 2 minute respiratory trace (see chapter 2, section 2.5.2 for definition of each respiratory characteristic). The frequency of each respiratory pattern was expressed as number of episodes/2 mins.

In study 2 and 3, respiratory frequency and V_t were measured during the baseline period and at 5, 15, 30 and 45 minutes post-fentanyl or saline administration. V_t is presented as a relative change from baseline as opposed to an absolute change (discussed in section 3.4.3 of this chapter).

3.2.5 Behavioural assessments

To evaluate potential side effects of drug administration that could have an indirect impact on respiratory activity, various behavioural assessments were performed on the neonatal and juvenile mice in studies 2 and 3 before and after injection of fentanyl or saline vehicle. Given that fentanyl has sedative properties (Bell and Ellis, 1987; Walsh et al., 1991; Chevillard et al., 2009), righting reflex and mastication rate (see section 2.4 for description of measurements), which can both be altered if an animal is sedated, were assessed in animals up to P11. Since fentanyl is also known to induce hypothermia, particularly in young rodents (Colman and Miller, 2002), body temperature was regularly monitored throughout experiments. Body temperature was measured orally in mice aged between P1-P11 (rectal measurements are not feasible in small pups) and rectally in adult P30 mice. All

behavioural measurements were recorded immediately after removal from the nest, 5 minutes and 60 minutes post drug administration.

3.2.6 Statistical analysis

All statistical analyses were performed using GraphPad Prism4 software. All data are presented as mean \pm SD. The level of statistical significance was set at $p < 0.05$.

Study 1

A one way Analysis of Variance (ANOVA) with Bonferroni's post test was carried out to analyse the change in number of apnoeas, hyperpnoeas, hiccups, respiratory frequency and CV of respiratory frequency throughout the postnatal development period.

Study 2 and Study 3

To compare body temperature, righting reflex and mastication rate before and after saline or fentanyl administration throughout the study period, a 1-way ANOVA was performed. To analyse the acute effects of both saline and fentanyl on respiratory frequency and V_t at each postnatal day, a 2-way ANOVA with Bonferroni's post test was performed. To directly compare the magnitude of the fentanyl-induced change in respiratory parameters across all the age groups, a 2-way ANOVA with Bonferroni's post test was performed.

3.3 Results of Study 1: Investigation of postnatal changes in respiratory activity of mice

Results from study 1 are presented in section 3.3

3.3.1 Respiratory traces

As mentioned previously, the main aim of study 1 was to monitor and characterise the evolution of breathing patterns throughout postnatal life in the mouse to better understand respiratory maturation.

It was evident that mice exhibited an immature respiratory phenotype during early life, particularly from P1-P2, with a striking feature being a rapidly changing and unstable respiratory pattern. Figure 3-1 displays respiratory traces recorded from two P1 mice, a P2, P3, P5 and an adult P30 mouse under resting eupneic conditions. The P1 and P2 mice displayed dysrhythmic, unstable breathing. The respiratory pattern was often interspersed with hyperpnoeic episodes as well as apnoeas. Respiratory frequency was therefore highly variable, owing to the periods of very slow breathing coupled with the transient hyperventilatory episodes. Hyperpnoeas were observed with and without a post-hyperpnoea apnoea and commonly occurred in an episodic manner throughout the respiratory recordings. A defining feature of hyperpnoeic breaths was forced expiration (an increased expiratory airflow), clearly illustrated in Figure 3-1 as pronounced downward deflections from baseline. The most profound change in the respiratory patterns occurred in the period between P2 and P3 in the majority of mice. By P3, most mice exhibited a rhythmic and robust breathing pattern devoid of respiratory abnormalities indicating a maturation of respiratory activity. The exact time window by which this transition of breathing activity occurred did vary between animals, however it was generally between P2-P4. Figure 3-1 illustrates stable, eupneic respiration recorded from a P3 and a P5 mouse. At these postnatal ages apnoeas were virtually absent and hyperpnoeas were rare. Respiratory frequency had increased and was less variable, and the respiratory pattern was comparable to that of the mature P30 mice (oldest mice studied).

Hiccup breathing patterns were observed from P1-P5 only and are illustrated in Figure 3-2, which shows example respiratory traces from a P1 and a P5 mouse. The number of hiccups exhibited by individual mice varied considerably. Hiccups often occurred intermittently and in bursts. Furthermore, hiccups were always interspersed with regular breaths i.e. they never appeared consecutively. A distinctive feature of hiccups was forced sharp inspiration and expiration. Figure 3-2 shows representative plethysmography traces illustrating rhythmic breathing in a P1 and a P2 mouse that was disturbed by intermittent bursts of hiccup breathing patterns.

From the outset of study 1 the aim was to also quantify the frequency of sighs throughout postnatal development as they are prevalent in neonates and young infants (Cross et al, 1960), thus are proposed to signify an immature respiratory system. Sighs are generally defined as spontaneous large amplitude breaths followed by a post-sigh apnoea. These particular breaths were however not observed at any age and therefore no data is shown.

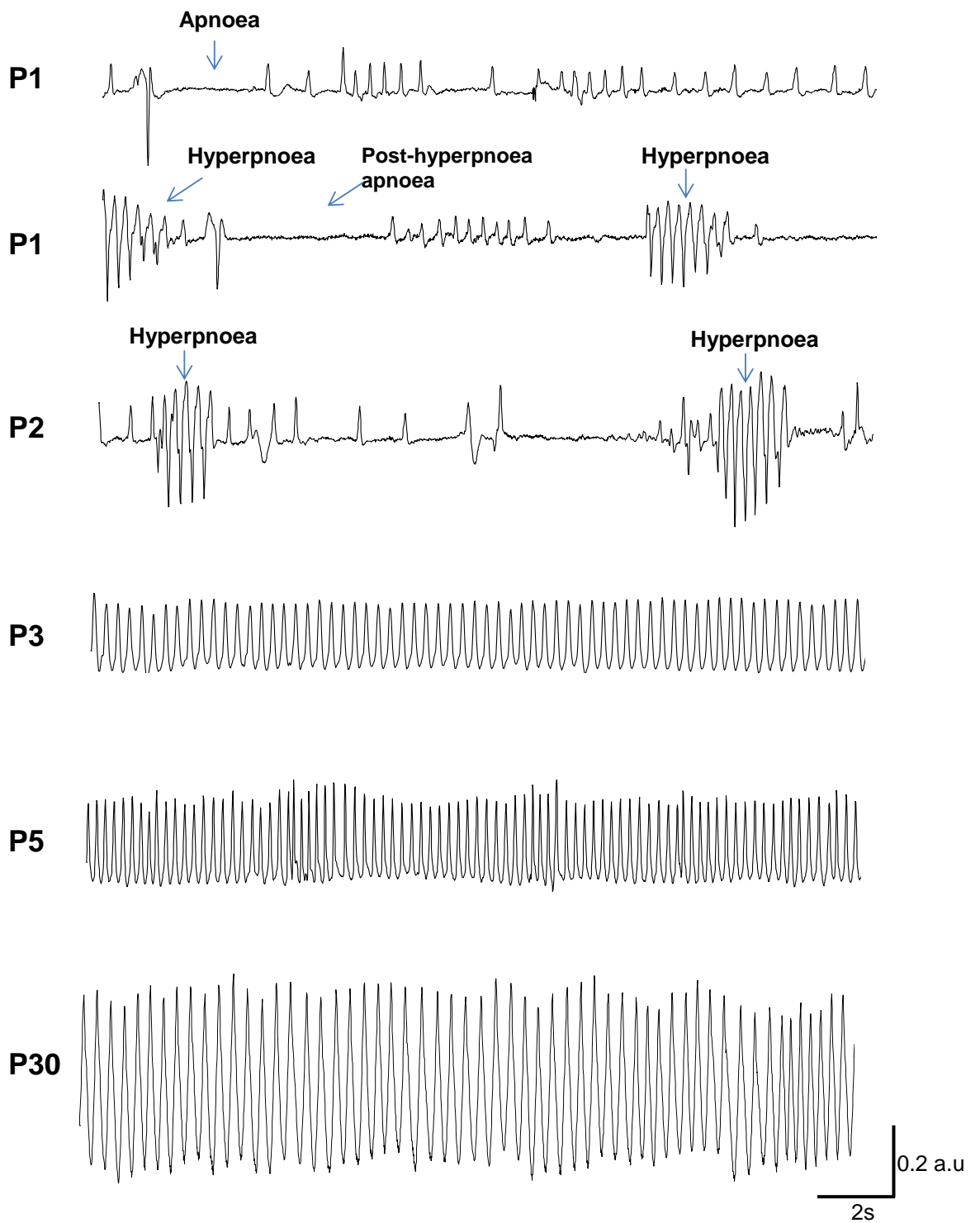


Figure 3-1. Representative respiratory traces illustrating postnatal maturation of breathing patterns. Representative whole-body plethysmography traces recorded from two P1 mice, a P2, P3, P5 and P30 (adult) mouse. Breathing was irregular from P1-P2, characterised by periods of hyperpnoea and apnoea and thus a highly variable respiratory frequency. By P3, breathing exhibited a stable and rhythmic pattern and was similar to adult, P30 respiratory patterns.

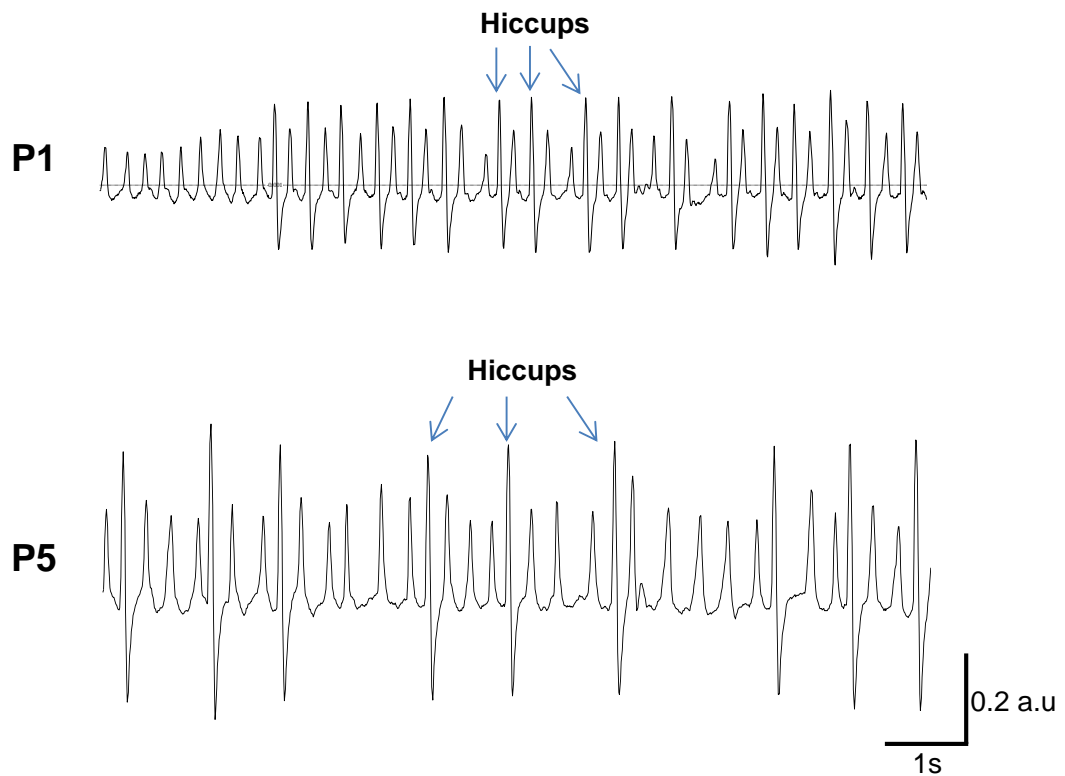


Figure 3-2. Representative respiratory traces illustrating hiccup breathing patterns in a P1 and P5 mouse. Hiccups occurred sporadically and when present were interspersed with regular breaths. Hiccups commonly occurred in bursts and were only observed from P1-P5. Hiccups were characterised by high amplitude inspiration and forced expiration.

3.3.2 Quantification of postnatal changes in respiratory activity

3.3.2.1 Apnoeas

The average number of apnoeas observed per 2 minutes was quantified throughout postnatal development (Figure 3-3). P1 and P2 mice displayed a high number of apnoeas; however there was high degree of variability between individual animals. P1 mice displayed a significantly greater number of apnoeas compared with P2 mice (P1: 7.1 ± 8.5 apnoeas/2 mins vs P2: 4.0 ± 5.4 apnoeas/2 mins, $p < 0.05$). By P3-P4, the frequency of apnoeas was significantly lower than P1 and P2 (P3: 0.7 ± 2.1 apnoeas/2 mins; P4: 0.7 ± 2.1 apnoeas/2 mins, $p < 0.05$). Apnoeas were no longer observed after P4. Given the high variability in the data, only calculating the average frequency of apnoeas for each age group does not fully represent their occurrence. Thus it is important to also calculate the proportion of mice that actually exhibited apnoeas at each postnatal age in order to provide a more comprehensive representation of their occurrence throughout development. Table 3-1 shows the percentage of mice in each age group that exhibited at least one apnoeic episode during the three, 2 minute respiratory recordings that were taken. All of the P1 mice and 82% of the P2 mice displayed apnoeas. The proportion of mice exhibiting apnoeas at P3 decreased to 27% and by P5 mice no longer exhibited apnoeic periods.

3.3.2.2 Hyperpnoeas

The average number of hyperpnoeic episodes observed per 2 minutes was quantified throughout postnatal development (Figure 3-4). Hyperpnoeas were most frequently observed in P1 and P2 mice (P1: 2.6 ± 2.6 hyperpnoeas/2 mins; P2: 4.0 ± 3.7 hyperpnoeas/2 mins). All of the P1 mice and 91% of P2 mice studied exhibited at least one hyperpnoeic episode (Table 3-1). The number of hyperpnoeas observed significantly decreased by P3 (1.2 ± 2.0 hyperpnoeas/2 mins) and remained infrequent until P7 (0.2 ± 0.9 hyperpnoeas/2 mins), with only 17% of mice displaying them (Table 3-1). Hyperpnoeas were no longer exhibited at P10 or beyond.

3.3.2.3 Hiccups

The average number of hiccup breathing episodes observed per 2 minutes was analysed and quantified throughout postnatal life (Figure 3-5). Hiccups were only observed from P1-P5. At P1, P2 and P5 an average of 1.9 ± 4.2 , 1.9 ± 6.3 and 1.9 ± 9.0 hiccups/2 mins was observed respectively. At P3 and P4 the average frequency of hiccup episodes was very low at 0.2 ± 1.0 and 0.4 ± 2.0 hiccups/2 mins, respectively. There was no statistical difference in the occurrence of hiccups between any of the age groups due to the high degree of variability in the data. It is imperative to highlight the fact that the proportion of mice that exhibited hiccups at each postnatal age was also highly variable. At P1, 50% of mice exhibited hiccups whereas 27% of P2 mice displayed hiccup episodes (Table 3-1). At P3, P4 and P5, 20%, 10% and 30% of mice exhibited hiccups respectively (Table 3-1). Whenever hiccups were present they occurred in large bursts and periodically interrupted eupneic breathing (see Figure 3-2 for illustration).

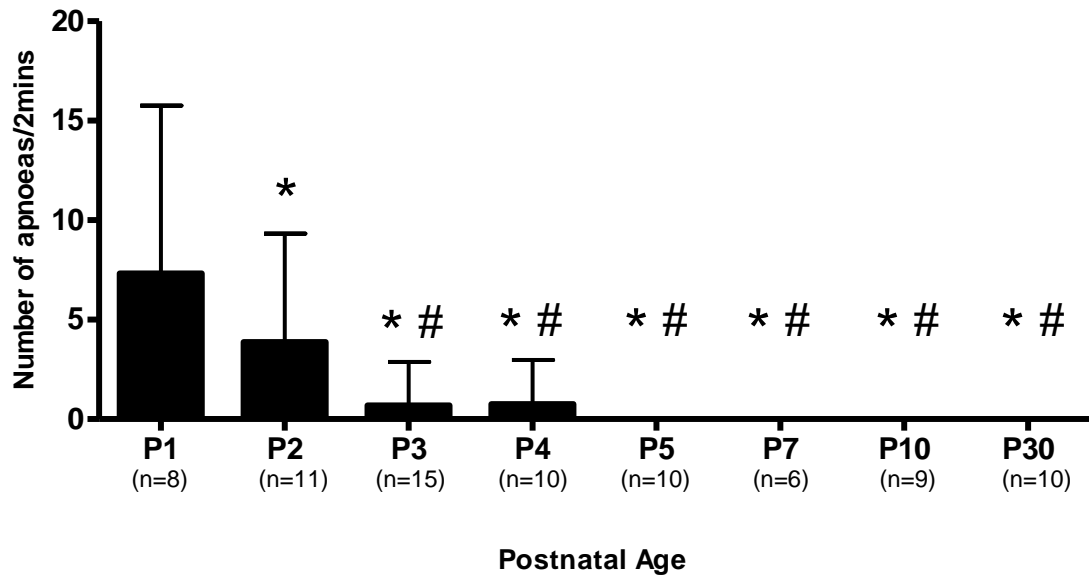


Figure 3-3. Number of apnoeas exhibited throughout postnatal development. The number of apnoeas observed within the 2 minute respiratory traces and under baseline conditions was quantified. Group averages for each postnatal age are shown. Apnoeas were most frequent in P1 and P2 mice and were no longer observed by P5. Data presented as mean±SD. * significantly different ($p < 0.05$) from P1; # significantly different ($p < 0.05$) from P2. One-way ANOVA with Bonferroni's post test performed.

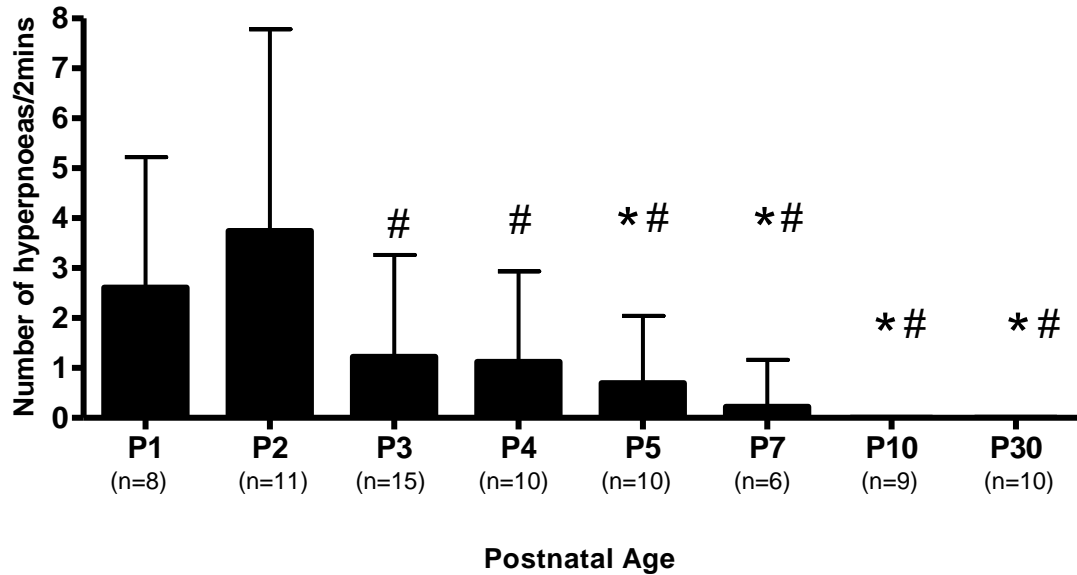


Figure 3-4. Number of hyperpnoeas exhibited throughout postnatal development. The number of hyperpnoeas observed within the 2 minute respiratory traces under baseline conditions was quantified. Group averages for each postnatal age are shown. Hyperpnoeas were most frequent in P1 and P2 mice. Hyperpnoeas were no longer observed from P10 through to adult life. Data presented as mean \pm SD. * significantly different ($p < 0.05$) from P1; # significantly different ($p < 0.05$) from P2. One-way ANOVA with Bonferroni's post test performed.

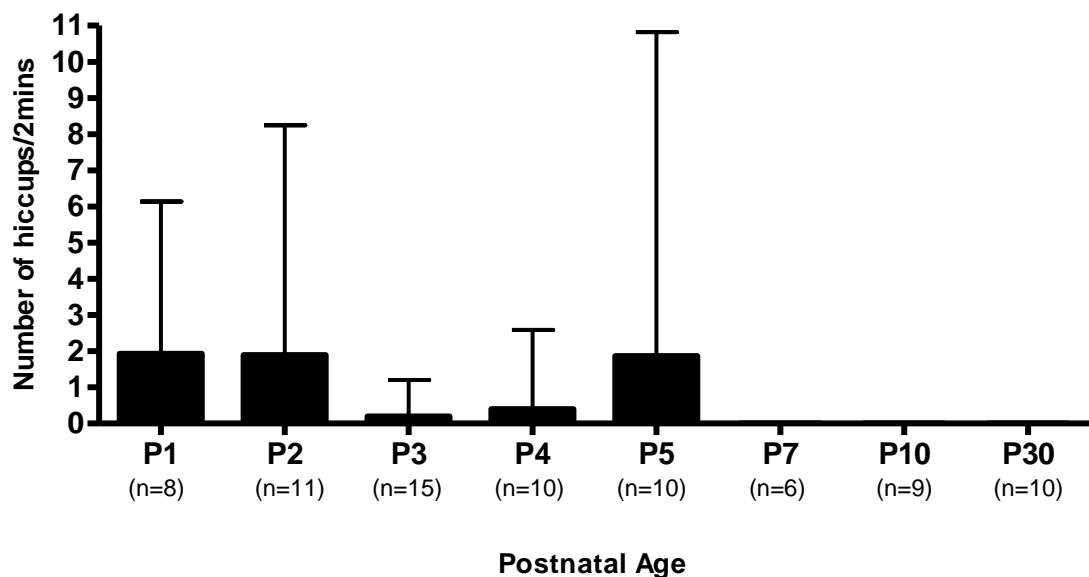


Figure 3-5. Number of hiccups exhibited throughout postnatal development. The number of hiccups observed within the 2 minute respiratory traces and under baseline conditions was quantified. Group averages for each postnatal age are shown. Hiccups were only observed between P1-P5. The number of hiccups observed by individual mice of each age group was highly variable. Data presented as mean \pm SD. No significant difference in the number of hiccups observed across the age groups ($p < 0.05$), one-way ANOVA with Bonferroni's post test.

Breathing Characteristic	% of mice displaying breathing characteristic							
	P1	P2	P3	P4	P5	P7	P10	P30
Apnoea	100	82	27	20	0	0	0	0
Hyperpnoea	100	91	47	60	40	17	0	0
Hiccups	50	27	20	10	30	0	0	0

Table 3-1. Percentage of mice displaying apnoeas, hyperpnoeas and hiccups at each postnatal age. The percentage of mice from each age group that exhibited at least one episode of each of the breathing characteristics was calculated.

3.3.2.4 Respiratory frequency

In addition to analysing individual breathing patterns, postnatal developmental changes in respiratory frequency were also assessed. Respiratory frequency was comparable at P1 and P2 (P1: 154 ± 43 bpm vs P2: 157 ± 43 bpm, $p < 0.05$, Figure 3-6). Mice first displayed a significant increase in respiratory frequency at P3 (219 ± 37 bpm, $p < 0.05$) which continued to increase and reached a peak of 266 ± 42 bpm by P5. This high respiratory frequency was maintained until P10 (256 ± 58 bpm). By adulthood (P30), mice displayed a significantly lower respiratory frequency compared to P5 mice (196 ± 17 bpm, $p < 0.05$).

In addition to measuring the average respiratory frequency for each respiratory recording, the coefficient of variation (CV) of respiratory frequency was also measured to gain an index of how variable and irregular the frequency was within a single respiratory recording. Respiratory frequency showed a high degree of variability at P1 and P2 (P1: 36 ± 21 % CV; P2: 24 ± 10 % CV; Figure 3-7), likely due to the high occurrence of hyperpnoeas and apnoeas and therefore a rapidly changing frequency. By P3, the CV was significantly lower than P1 (P3: 15 ± 6 % CV, $p < 0.05$, Figure 3-7) indicating a more stable respiratory frequency. This reduced variability in respiratory frequency was maintained through to adulthood (P30: 12 ± 5 % CV, Figure 3-7).

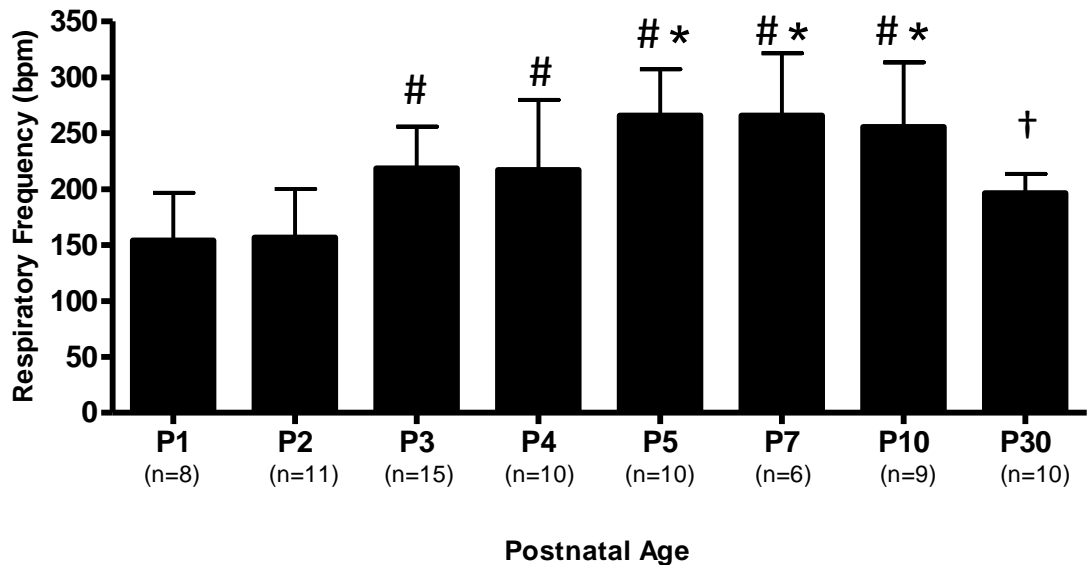


Figure 3-6. Changes in average respiratory frequency (bpm) throughout postnatal development. Respiratory frequency gradually increased from P2-P5 and reached a plateau at P5 and was maintained until P10. Respiratory frequency had declined by adulthood (P30). Data presented as mean±SD. * significantly different ($p < 0.05$) from P1; # significantly different ($p < 0.05$) from P2; † significantly different ($p < 0.05$) from P5. One-way ANOVA with Bonferroni's post test performed.

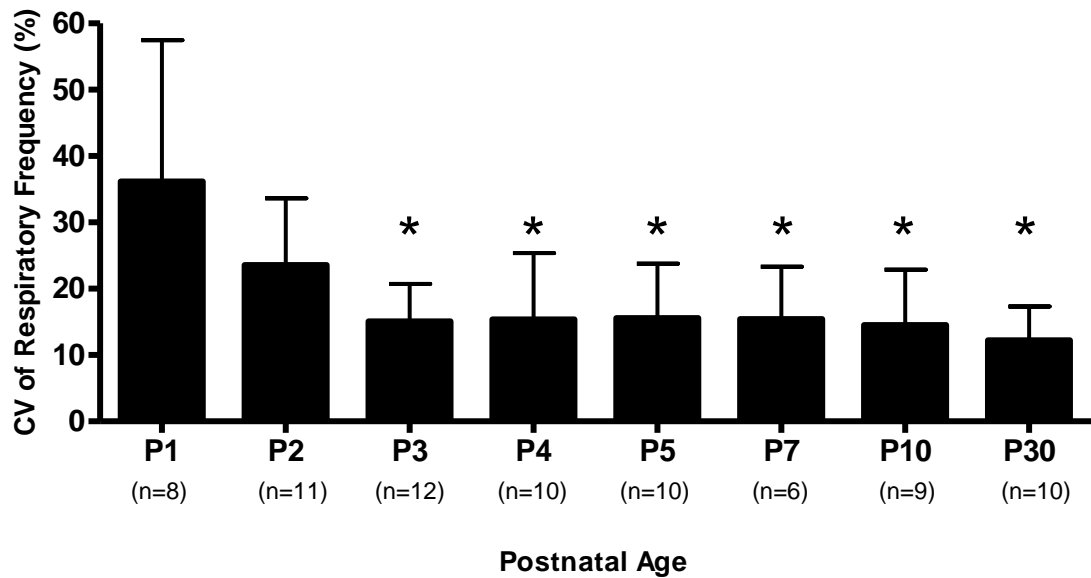


Figure 3-7. Coefficient of variation (CV) of respiratory frequency throughout postnatal development. The variability in respiratory frequency was high at P1 and P2. A significant reduction in variability occurred at P3 and this was maintained through to adulthood. Data presented as mean±SD. * significantly different ($p < 0.05$) from P1. One-way ANOVA with Bonferroni's post test performed.

3.4 Discussion of study 1: Investigation of postnatal changes in respiratory activity of mice

Adequate ventilation at birth is essential for postnatal survival in mammals, thus understanding early postnatal maturation of breathing is of major clinical relevance. Researchers have sought for many years to identify the mechanisms that underlie immature respiratory control. In the mouse, the respiratory system undergoes significant postnatal maturation (Hilaire and Duron, 1999). The rationale of study 1 was to characterise the postnatal evolution of respiratory behaviour in the mouse and determine the critical developmental time period when the respiratory system undergoes a step in maturity. This study was designed to gain further insight into immature respiratory control in early life as well as the subsequent maturation. From this study we have shown that respiratory patterns of ICR mice underwent rapid postnatal developmental changes that were particularly evident between P2 and P3. These postnatal changes manifested as a transition from an unstable and dysrhythmic respiratory pattern to a regular and robust rhythmic respiratory output. To our knowledge, this study is the first to characterise the immature respiratory patterns of the mouse as well as assessing the time-frame of postnatal maturational of respiratory activity.

3.4.1 Respiratory activity undergoes significant postnatal changes

3.4.1.1 Apnoeas

It is well documented that apnoeas are indicators of respiratory instability in mice and humans. Apnoeas are commonly displayed by neonatal rodents (Matrot et al., 2005; Niane and Bairam, 2011; Niane and Bairam, 2012; Niane et al., 2012) and transgenic mice that exhibit respiratory control abnormalities (Jacquin et al., 1996; Dubreuil et al., 2008; Hodges et al., 2009; Abdala et al., 2010; Gray et al., 2010). Our findings show that the prevalence of apnoeas change significantly during early life in the mouse and display a decline in frequency with advancing age which has previously been demonstrated in both rodents and humans (Matrot et al., 2005; Mathew, 2011; Niane and Bairam, 2011; Niane and Bairam, 2012). We have shown that apnoeas were only observed from P1-P4 and importantly were most prevalent at ages P1 and P2. After P2 a sharp decline in apnoea frequency was observed suggesting the occurrence of a respiratory maturational step. In the clinical setting, a high frequency of apnoeic episodes can be used indicator of an

immature respiratory control system, and is a common respiratory feature exhibited by preterm human neonates (Hiatt et al., 1981; Eichenwald et al., 1997). It was not determined if the apnoeas observed in this present study were of central origin (caused by a cessation of inspiratory rhythmogenesis), if they were obstructive (caused by a closure of the upper airways) or if they were a mixture of both types. It is therefore difficult to ascertain the exact source of the apnoeas, but in speculation, apnoeas in neonatal mice could be due to a reduced central respiratory drive reflecting immature central respiratory control. To further examine the potential central origin of this respiratory behaviour, rhythmically active medullary slice or brainstem-spinal cord preparations could be employed to directly record central respiratory motor output throughout postnatal development. Any cessation of respiratory motor activity would indicate a central apnoea. *In vitro* investigations in addition to the *in vivo* studies would give a more comprehensive analysis of the maturation of this respiratory characteristic throughout early life.

3.4.1.2 Hyperpnoeic breathing

In this study, hyperpnoeas are defined as hyperventilatory periods of high amplitude, forced inspiratory and expiratory efforts that are often accompanied by a post-hyperpnoea apnoea. This present study is the first to examine the frequency of hyperpnoeic episodes throughout postnatal development in the rodent under normoxic, resting conditions. Hyperpnoeas were most prevalent at ages P1 and P2 after which they displayed a notable decline in occurrence and were no longer exhibited beyond P10. They occurred spontaneously and resulted in a rapid change in both respiratory frequency and V_t and hence increased respiratory variability. The source of these hyperpnoeas is unknown and the mechanism(s) underlying their generation is also elusive. Hyperpnoeic breathing patterns have been observed in preterm human neonates (Fenner et al., 1973; Razi et al., 2002) and patients with chronic heart failure (Sin et al., 1999; Bradley and Floras, 2003) and are generally believed to be an indicator of respiratory control instability (Khoo et al., 1982). These breathing patterns have been specifically referred to as hyperpnoeic episodic breathing (HEB), which is defined as periods of quiet breathing interspersed with consistent and cyclic periods of hyperpnoes (a cyclic waxing and waning of breathing). Previous investigations by Guimarães and colleagues in 2007 found that administration of retinoic acid (vitamin A metabolite) during the onset of hindbrain segmentation in embryonic development in the mouse disrupts the formation of the rostral pons and induces HEB in postnatal life (Guimaraes et al., 2007). This resultant breathing pattern is

similar to the transient hyperpnoeic episodes observed in the young neonatal mice in this present study. Since the retinoic acid treated mice exhibited anatomical abnormalities in the rostral pons, it is likely that this contributed to the hyperpnoeic breathing. Whether the presence of hyperpnoeas in early life signifies an immaturity of rostral pontine functions cannot be deduced from our study alone, however it is an intriguing speculation. Guimarães and colleagues suggested that hyperpnoeic episodes may be centrally generated but are not due to an abnormality in the rhythm generators *per se* as normal baseline rhythmic respiratory motor output was maintained *in vitro* in mice that displayed HEB *in vivo*. Further *in vitro* analyses using the brainstem-spinal cord preparation from retinoic acid-treated mice demonstrated that excitation of the RTN/pFRG with AMPA induced an increase in the respiratory rhythm followed by a decrease which resembled hyperpnoeic breathing *in vivo*. The authors suggested that the responsiveness of the RTN/pFRG to afferent excitation may be exaggerated, which could cause hyperpnoeic breathing *in vivo* (Guimaraes et al., 2007). It is therefore possible that the hyperpnoeic breathing observed during early life in the present study could be the result of a hypersensitivity of the RTN/pFRG rhythm generator to excitatory inputs. Given that hyperpnoeic episodes appear to represent instability in respiratory control, it is likely that the decline in the hyperpnoea frequency observed after P2 in this study represents respiratory maturation. A prominent feature of hyperpnoeas is the presence of forced inspiratory and expiratory efforts. It is intriguing to speculate that this increased expiratory effort could represent active expiration (i.e. increased expiratory airflow), which is commonly induced when there is an increased respiratory drive. The abdominal muscles are believed to function as the dominant expiratory muscles driving active expiration (Pagliardini et al., 2011). In order to determine if abdominal expiratory-related muscle activity accompanies hyperpnoeic breathing in young immature animals, recordings of muscle activity using surface EMG electrodes placed on the skin could be employed. The RTN/pFRG has been postulated to function as a conditional expiratory oscillator that drives active expiration in the rodent (Janczewski and Feldman, 2006; Pagliardini et al., 2011). Active expiration in early life and potentially hyperpnoeic breathing could therefore be generated by the RTN/pFRG, which would indicate the RTN/pFRG plays a functional role in rhythm generation in early postnatal life.

3.4.1.3 Hiccups

In this study, hiccup breathing patterns were defined as very short, high amplitude breaths displaying a sharp inspiration and expiration. This is the first study to our knowledge that has identified this respiratory behaviour in the neonatal mouse. The occurrence of hiccups was quantified throughout postnatal development, and like both apnoeic and hyperpnoeic episodes, they were only observed during early life. After P5, hiccups were no longer exhibited. Given that these breaths have never been documented before, the mechanism(s) involved in their generation as well as their functional significance are unknown. Similar to hyperpnoeas, hiccups are also characterised by a forced expiratory effort, and as discussed above (section 3.4.1.2) this could signify active expiration. Since the occurrence of hiccups was age dependent, it is possible that hiccups represent a novel marker of immature respiratory control and an immature breathing phenotype. There was a high degree of variability in the frequency of hiccups exhibited by individual animals at each age. Due to the sporadic nature of hiccups, it is likely that these breaths were not always captured in the short recording sessions. It could be beneficial to employ an open flow plethysmography system that delivers a continuous air supply, which would allow for longer recording sessions. This would enable the rapidly changing breathing patterns of young neonatal mice to be fully assessed in real time, thereby providing a more accurate representation of respiratory activity.

3.4.1.4 Respiratory frequency

Baseline respiratory frequency was assessed throughout postnatal development under normoxic conditions. After P2, respiratory frequency displayed a gradual increase with advancing age and reached a peak by P5 which was maintained until P10. Additionally, respiratory frequency instability was high at P1 and P2 after which a notable decline in variability was observed by P3. The reduction in the number of apnoeic episodes would have partly accounted for the increased respiratory frequency during the first week of life. Furthermore, the substantial decline in respiratory pattern abnormalities after P2 would have contributed to the increase in respiratory stability. These findings strongly indicate the presence of significant maturation of respiratory control between P2 and P3. In agreement with our findings from the whole animal, *in vitro* studies utilising brainstem-spinal cord preparations have demonstrated an increase in the frequency of rhythmic respiratory motor output at approximately P3-P4 in the rat and the mouse (Balkowiec and

Katz, 1998; Shvarev and Lagercrantz, 2006), indicating a similar time frame of maturation of respiratory motor output. Our study also demonstrated that by P30, respiratory frequency had declined. This is congruent with the findings from previous *in vivo* studies investigating postnatal changes in respiratory frequency in the rat, where frequency was found to gradually decline from approximately P10 through to adulthood (Huang et al., 2004; Liu et al., 2006). Similarly, a study utilising the tilted-sagittal brainstem slice from the mouse has demonstrated an age-dependent change in respiratory motor output. The frequency of the rhythmic hypoglossal motor output was found to decrease in preparations from mice aged 15 days or older (Paton and Richter, 1995). The reason for this frequency decline observed in both the *in vitro* setting and the intact animal remains elusive, but could denote a second maturational process that occurs before the final mature respiratory pattern is achieved.

3.4.2 Critical developmental time window between P2 and P3

The data from study 1 have clearly demonstrated developmental changes in respiratory activity during early postnatal ontogenesis. Analysis of both respiratory patterns and respiratory frequency has indicated that the time period between P2 and P3 is developmentally distinct. At P1 and P2, changes in respiratory activity were rapid and unpredictable. Apnoeas and hyperpnoeas appear to be the hallmark of an immature respiratory system and hiccups may also represent a novel indicator of immature respiratory control. Importantly, a striking transformation in the respiratory activity from an unstable pattern to a regular and rhythmic pattern occurred between P2 and P3, signifying a critical developmental time window during which a maturational step occurs. The mechanisms that underlie this postulated step in maturity remain to be elucidated. The identification of a critical developmental period could mean respiratory insults during this time induce long-term respiratory defects, which would have significant clinical implications.

3.4.3 Study limitations and future directions

Postnatal changes in V_t were not analysed in the present study and therefore maturation of the overall ventilatory profile of mice could not be assessed. There are a number of reasons for this. Firstly there was a problem with the calibration method used to determine V_t in the commercially designed neonatal and juvenile plethysmography chambers (Buxco

Research Systems, USA). A rapid injection of a known volume of air into the chamber induced a distinctly different pressure change compared to the injection induced pressure change in the adult plethysmography chamber. As illustrated in Figure 2-4 in chapter 2, an injection of air into the recording chamber should evoke a rapid increase in pressure and hence a sharp upward deflection of the signal, followed by a slow decline back to baseline. However this was not seen in the neonatal/juvenile plethysmography system. Instead the calibration injection induced a rapid increase in the pressure signal which was of a lower magnitude, followed by a rapid decline. As a consequence of this, V_t could not be accurately calculated. The reason for this technical issue is not known but it could indicate that there was a small air leak in the system. Another reason for the exclusion of V_t calculations in this study is the fact that V_t measurements derived from plethysmography recordings in neonatal mice have not been validated against pneumotachography (direct recording of respiratory airflow). As a consequence, the accuracy of absolute V_t values based on the small plethysmography pressure signals is questionable (Mortola and Frappell, 1998; Szewczak and Powell, 2003), and are therefore not presented in this study.

In terms of future directions of the study, it would be beneficial to increase the range of postnatal ages that were studied, particularly from P5 through to adulthood. This would allow a more detailed assessment of potential respiratory changes that occur later in postnatal life. Given the high level of variability in the data from the young mice, particularly at P1 and P2, increasing the sample size in these age groups would also help to increase the validity of the data. The genetic background of mice is known to influence maturation of respiratory control (Arata et al., 2010). It would therefore be advantageous to repeat the study using a variety of mouse strains, which would provide a more generalised description of postnatal respiratory maturation. This knowledge could also aid in the understanding of early life respiratory abnormalities exhibited by transgenic mouse models of respiratory control, which would have an important clinical benefit.

3.5 Results of Study 2. Susceptibility of postnatal breathing patterns to fentanyl: A longitudinal study

Results from study 2 are presented in section 3.5

The design of study 2 was longitudinal and mice were repeatedly studied from P1-P5, on P9 and finally on P11. Based on the results from study 1, we have proposed that the time period between P2 and P3 represents a critical developmental window when breathing undergoes a step in maturity and exhibits a transition from an immature, irregular state to a stable, eupneic pattern. To determine if respiratory sensitivity to fentanyl was influenced by postnatal age, the acute respiratory depressive effects of fentanyl were assessed on each postnatal day. It was hypothesised that fentanyl would induce a more pronounced respiratory depression after the respiratory maturation step had occurred.

3.5.1 Behavioural assessments

The acute effects of the saline vehicle (control experiments) and fentanyl on body temperature, righting reflex and mastication rate were assessed. Neither saline nor fentanyl induced any significant changes from baseline in any of the variables which were recorded at both 5 and 60 minutes following administration (Tables 3-2 to 3-4). Body temperature was always maintained within physiological range between 32-34°C throughout control and fentanyl experiments (Table 3-2).

Age	Body Temperature (°C)					
	Saline			Fentanyl		
	Baseline	5 mins post-saline	60 mins post-saline	Baseline	5 mins post-fentanyl	60 mins post-fentanyl
P1	32.4±0.1	32.5±0.1	32.7±0.4	32.6±0.3	32.8±0.2	33.0±0.1
P2	33.1±0.3	33.2±0.3	33.2±0.2	33.0±0.3	33.0±0.3	32.9±0.3
P3	33.0±0.5	32.9±0.4	32.9±0.4	33.1±0.3	33.1±0.3	33.1±0.3
P4	33.4±0.5	33.6±0.4	33.3±0.2	33.3±0.4	33.1±0.6	33.3±0.5
P5	33.4±0.4	33.6±0.3	33.3±0.3	33.2±0.2	33.4±0.6	33.3±0.3
P9	33.4±0.6	33.3±0.4	33.5±0.5	33.5±0.4	33.3±0.5	33.4±0.4
P11	33.8±0.2	33.7±0.4	33.5±0.2	33.6±0.6	33.7±0.5	33.6±0.6

Table 3-2. Assessment of body temperature before and after saline or fentanyl administration. Body temperature was measured orally. Population data for each age group is shown. Data presented as mean±SD. No significant change in body temperature found after saline or fentanyl administration at any age ($p>0.05$), 2-way ANOVA.

Age	Time to upright position (s)					
	Saline			Fentanyl		
	Baseline	5 mins post-saline	60 mins post-saline	Baseline	5 mins post-fentanyl	60 mins post-fentanyl
P1	9±1	8±3	10±0	8±2	7±2	9±2
P2	6±2	7±3	7±2	9±1	9±2	7±4
P3	7±3	8±2	7±2	7±3	6±1	6±2
P4	5±3	4±3	4±2	5±2	5±3	5±3
P5	3±1	3±1	2±1	2±1	3±2	3±2
P9	1±0	1±0	1±1	1±0	2±1	1±1
P11	1±0	1±0	1±0	1±0	1±0	1±0

Table 3-3. Assessment of righting reflex before and after saline or fentanyl administration. The time taken to move from supine to an upright position was measured. Population data for each age group is shown. Data presented as mean±SD. There was no significant change in time to upright position after saline or fentanyl administration at any age ($p>0.05$), 2-way ANOVA.

Age	Mastications/10 seconds					
	Saline			Fentanyl		
	Baseline	5 mins post-saline	60 mins post-saline	Baseline	5 mins post-fentanyl	60 mins post-fentanyl
P1	11±2	10±2	12±3	11±4	11±3	11±5
P2	11±3	11±2	10±2	12±5	12±4	12±4
P3	12±3	14±5	12±4	13±3	13±3	12±2
P4	12±3	13±4	12±5	12±4	12±6	13±8
P5	12±3	13±5	11±5	10±4	10±4	11±4
P9	12±2	12±3	11±3	12±4	12±4	12±6
P11	11±3	10±6	12±5	9±4	11±6	10±4

Table 3-4. Mastication rate before and after saline or fentanyl administration.

The number of mastication movements made in 10 seconds was counted.

Population data for each age group is shown. Data presented as mean±SD. There was no significant change in mastication rate after saline or fentanyl administration at any age ($p>0.05$), 2-way ANOVA.

3.5.2 Respiratory traces

Figure 3-8 illustrates the acute effects of both saline and fentanyl on respiratory activity in P1, P2, P5 and P11 mice. In the control experiments, administration of a saline vehicle did not induce any apparent change in respiratory activity at any age. There was however an augmentation in V_t at 15 minutes post-saline at P1. Respiratory frequency and V_t following saline injection was comparable with baseline values. From the respiratory traces, it is apparent that respiratory activity of P1 and P2 mice was immature, characterised by apnoeic episodes and slow respiratory frequency. Fentanyl failed to induce a substantial respiratory depression at all ages. Respiratory frequency and V_t remained unaltered. It is apparent that the respiratory effects of fentanyl and the saline vehicle were indistinguishable at all ages studied.

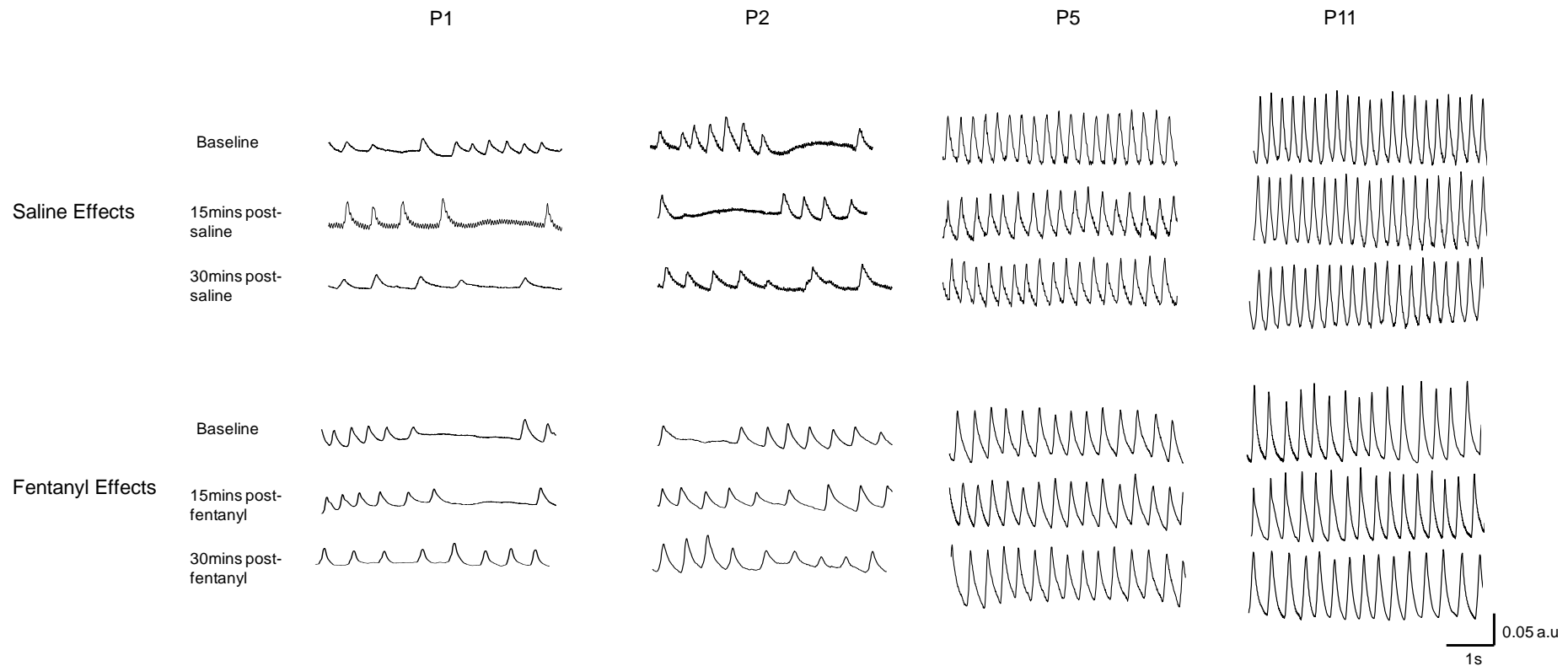


Figure 3-8. Representative plethysmography respiratory traces illustrating the effects of saline and fentanyl in P1, P2, P5 and P11 mice. Saline administration induced no apparent change in respiratory activity at any age. Fentanyl also failed to evoke a respiratory depression in all age groups. Respiratory frequency and V_t was comparable before and after fentanyl administration. Note the immature breathing patterns in the P1 and P2 age groups.

3.5.3 Respiratory frequency

In the control experiments, saline did not evoke any significant changes in respiratory frequency at any of the postnatal ages studied (P1-P5, P9 and P11, Figure 3-9A). Respiratory frequency was comparable with baseline values at all time points following administration. At P1, there was a trend towards a reduction in respiratory frequency from baseline at 15, 30 and 45 minutes following saline administration, however it should be noted that there was a high degree of variability in respiratory frequency between individual animals at all time points.

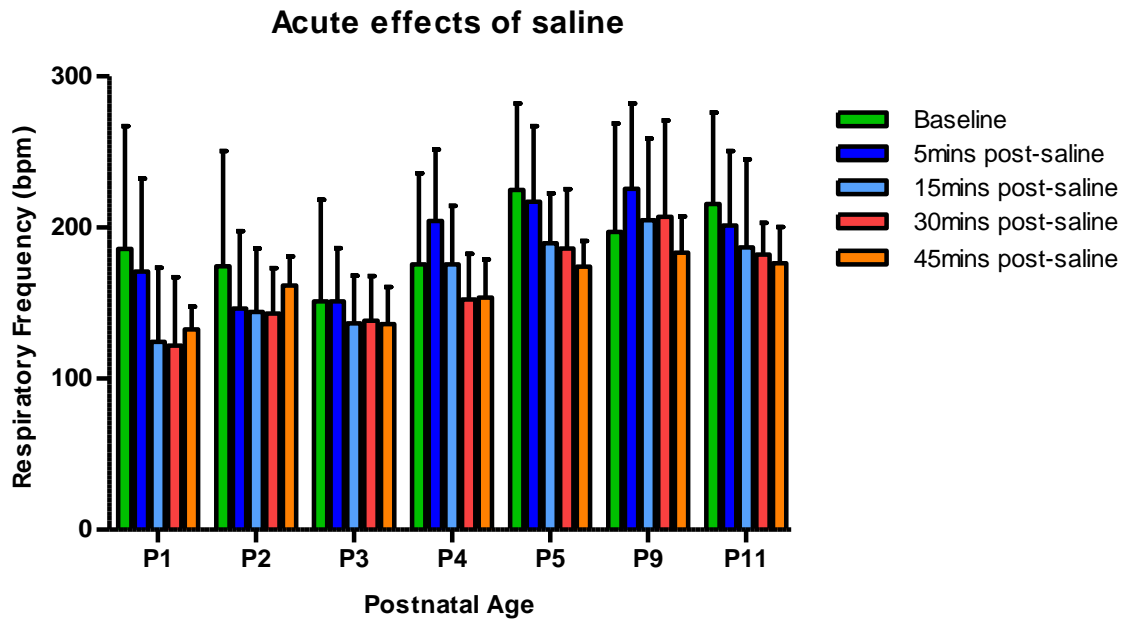
Interestingly, fentanyl also failed to induce a significant change in respiratory frequency at all postnatal ages (P1-P5, P9 and P11, Figure 3-9B). Fentanyl did not evoke a significant depression in respiratory frequency at any postnatal age. On the first exposure to fentanyl at P1, respiratory frequency remained unaltered (baseline: 133 ± 40 bpm; 5 minutes post-fentanyl: 114 ± 10 bpm; 15 minutes post-fentanyl: 128 ± 25 bpm; 30 minutes post-fentanyl: 111 ± 34 bpm; 45 minutes post-fentanyl: 145 ± 49 bpm, $p>0.05$). There was a small but insignificant reduction in respiratory frequency post fentanyl application at P2-P5; however the changes in respiratory frequency are congruent with those seen in response to saline administration and could therefore represent natural variation in the respiratory activity throughout the experimental procedure as opposed to the depressive actions of fentanyl itself. From these data there was no trend towards a more pronounced fentanyl-induced depression in respiratory frequency after the maturation step (i.e. after P2). Mice appeared to be insensitive to fentanyl's respiratory depressive actions at all ages.

3.5.4 Tidal volume

V_t response to saline or fentanyl is presented as a relative change from baseline (Figure 3-10) In the control experiments, saline did not induce a significant change in V_t at any age (P1-P5, P9 and P11, Figure 3-10A). At P1 there was an increase in V_t from baseline values at 5 and 15 minutes following saline administration but this was not significant (5 minutes: $39\pm 49\%$ increase; 15 minutes: $44\pm 55\%$ increase). The variability in baseline V_t as well as the percentage change in response to saline administration was high at all ages. Similarly, fentanyl did not evoke a significant alteration in V_t at any postnatal age (Figure 3-10B), indicating the effects of fentanyl on V_t were not age-dependent. It should be noted that there was also a high level of variability in the data in all of the age groups. The V_t

changes in response to saline and fentanyl throughout postnatal development were indistinguishable.

A



B

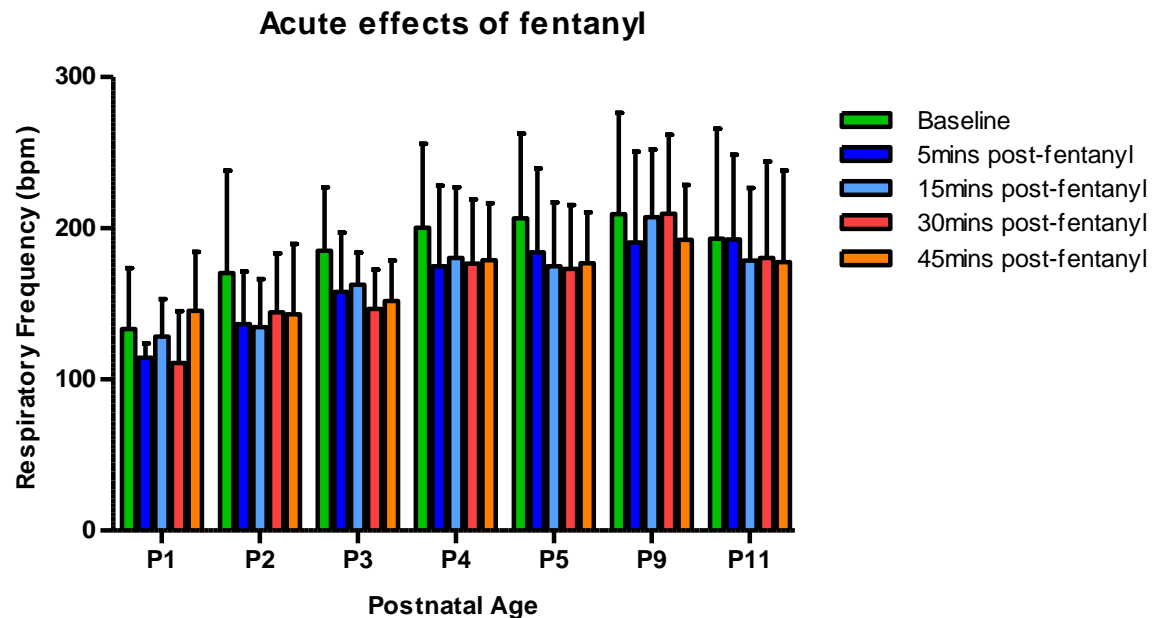


Figure 3-9. Acute changes in respiratory frequency in response to saline or fentanyl throughout postnatal life. Mice were repeatedly exposed to either saline (A) or fentanyl (B) from P1-P5, P9 and P11. Population data for each age group shown. Control mice: n=5; fentanyl-exposed mice: n=7. Data presented as mean \pm SD. Neither saline nor fentanyl evoked a significant reduction in respiratory frequency at any of the postnatal ages studied. 2-way ANOVA performed.

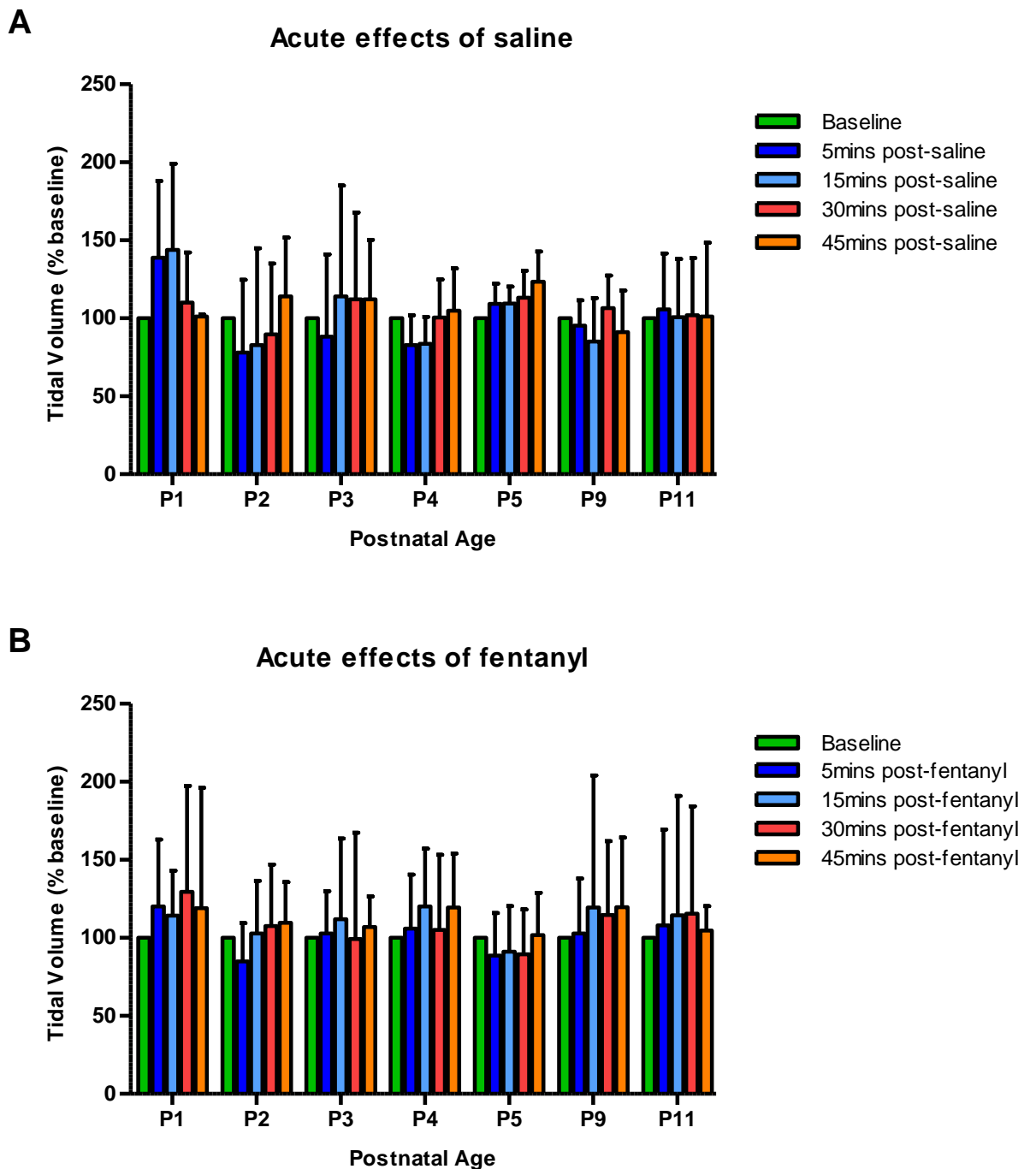


Figure 3-10. Acute changes in tidal volume (Vt) in response to saline or fentanyl throughout postnatal life. Mice were repeatedly exposed to either saline (A) or fentanyl (B) from P1-P5, P9 and P11. Population data for each age group shown. Data shows the percentage change in Vt from baseline values in each age group, where baseline represents 100%. Control mice: n=5; fentanyl-exposed mice: n=7. Data presented as mean±SD. Neither saline nor fentanyl evoked a significant change in Vt at any of the postnatal ages studied. 2-way ANOVA performed.

3.6 Results of Study 3. Susceptibility of postnatal breathing patterns to fentanyl: A single exposure study

The failure of fentanyl to evoke a respiratory depression throughout postnatal life in study 2 may have been due to the mice becoming desensitised to fentanyl's actions (fully discussed in section 3.7.1). Mice were continually studied throughout postnatal development and therefore were subjected to multiple fentanyl exposures throughout the study period, which could have in turn evoked the desensitisation. The study design was consequently altered and different mice were studied at each postnatal age, thereby preventing multiple fentanyl exposures. The change in the study design allowed the proposed hypothesis to be sufficiently tested.

3.6.1 Behavioural assessments

The acute effects of the saline vehicle (control experiments) and fentanyl on righting reflex and mastication rate were assessed in mice up to P10. Neither saline nor fentanyl induced any significant changes from baseline in either of the variables which were recorded at both 5 minutes and 60 minutes following administration (Tables 3-6 and 3-7). In the adult P30 mice, only body temperature was assessed, and was recorded rectally. In the mice aged P1-P10, body temperature was recorded orally and was therefore always underestimated. No significant change in body temperature was seen after saline or fentanyl administration in any of the age groups. Body temperature was always maintained within physiological range of between 32.0-34.0°C (oral) or 36.5-37.0°C (rectal) throughout control and fentanyl experiments (Table 3-5).

Age	Body Temperature (°C)					
	Saline			Fentanyl		
	Baseline	5 mins post-saline	60 mins post-saline	Baseline	5 mins post-fentanyl	60 mins post-fentanyl
P1	32.6±1.2	33.1±0.8	32.8±0.8	32.4±1.7	32.4±1.7	32.2±1.3
P2	32.3±0.8	32.2±0.2	32.5±0.4	32.6±0.8	32.8±0.8	32.8±0.7
P3	32.0±1.4	32.5±1.4	31.9±1.7	32.6±1.0	32.0±1.2	32.2±1.6
P4	32.4±1.4	31.6±1.4	32.1±0.2	32.6±0.4	32.2±0.4	32.3±0.7
P5	32.6±1.2	32.7±1.2	32.8±1.9	32.8±0.9	32.6±1.9	32.3±1.7
P7	33.7±0.7	33.7±0.9	33.6±0.7	33.4±0.6	33.7±1.0	33.7±0.9
P10	32.6±0.6	32.5±0.6	33.1±0.6	32.7±1.0	32.6±0.6	32.9±0.6
P30	36.9±0.2	36.7±0.3	36.8±0.1	36.8±0.3	36.7±0.4	36.8±0.2

Table 3-5. Assessment of body temperature before and after saline or fentanyl administration. Body temperature was measured orally in mice aged P1-P10 and rectally in the P30 mice. Population data for each age group is shown. Data presented as mean±SD. No significant change in body temperature was found after saline or fentanyl administration in all of the age groups ($p>0.05$), 1-way ANOVA.

Age	Time to upright position (s)					
	Saline			Fentanyl		
	Baseline	5 mins post-saline	60 mins post-saline	Baseline	5 mins post-fentanyl	60 mins post-fentanyl
P1	8±3	8±3	7±2	9±3	9±3	8±2
P2	8±3	8±2	9±1	6±3	8±3	8±3
P3	7±4	6±3	7±3	6±3	7±3	8±3
P4	3±2	3±1	5±3	6±3	8±3	5±4
P5	1±0	2±1	1±1	2±2	2±1	3±2
P7	1±0	1±1	2±2	1±0	2±1	2±1
P10	1±0	1±0	1±0	1±0	1±0	1±0

Table 3-6. Assessment of righting reflex before and after saline or fentanyl administration. The time taken to move from supine to an upright position was measured. Population data for each age group is shown. Data presented as mean±SD. There was no significant change in time to upright position after saline or fentanyl administration in all of the age groups ($p>0.05$), 1-way ANOVA.

Age	Mastications/10 seconds					
	Saline			Fentanyl		
	Baseline	5 mins post-saline	60 mins post-saline	Baseline	5 mins post-fentanyl	60 mins post-fentanyl
P1	13±6	11±9	12±8	12±5	11±7	11±7
P2	9±3	9±3	10±2	9±3	8±2	10±1
P3	17±5	16±6	15±8	16±6	13±8	15±8
P4	10±4	10±3	10±3	11±4	8±6	9±5
P5	11±7	11±7	10±8	12±5	9±8	9±7
P7	14±10	10±4	11±5	11±4	8±4	10±7
P10	10±4	9±5	8±4	11±4	10±3	9±5

Table 3-7. Mastication rate before and after saline or fentanyl administration.

The number of mastication movements made in 10 seconds was counted.

Population data for each age group is shown. Data presented as mean±SD. There was no significant change in mastication rate after saline or fentanyl administration in all of the age groups ($p>0.05$), 1-way ANOVA.

3.6.2 Plethysmography respiratory traces

Figure 3-11 illustrates the acute effects of both saline and fentanyl on respiratory activity in P1-P3 mice and in mature adult, P30 mice. In the control experiments, administration of saline vehicle did not evoke any alteration in respiratory output in the P1 and P2 mice. Both respiratory frequency and V_t were similar before and after injection. It is evident from the respiratory traces that respiratory activity of P1 and P2 mice was irregular with periods of apnoeas and hyperpnoeas throughout the experimental procedure. In some P3 mice there was a depression in respiratory frequency at 15 minutes following saline administration, highlighting the high degree of variability in respiratory activity even in the absence of pharmacological intervention. The respiratory activity of the P30 mice was followed a stable pattern before and at all time points following saline administration with no change in respiratory frequency or V_t evident. Fentanyl failed to induce a depression of respiratory activity in both the P1 and P2 mice. Respiratory frequency and V_t remained unaltered and it is apparent that breathing displayed an irregular rhythm before and after fentanyl injection. It is evident that the respiratory effects of fentanyl and the saline vehicle at P1 and P2 were indistinguishable. Conversely, fentanyl did induce a clear depression in respiratory frequency and V_t in the P3 mice. The adult, P30 animals also displayed a reduction in respiratory frequency as well as a contrasting increase in V_t in response to fentanyl.

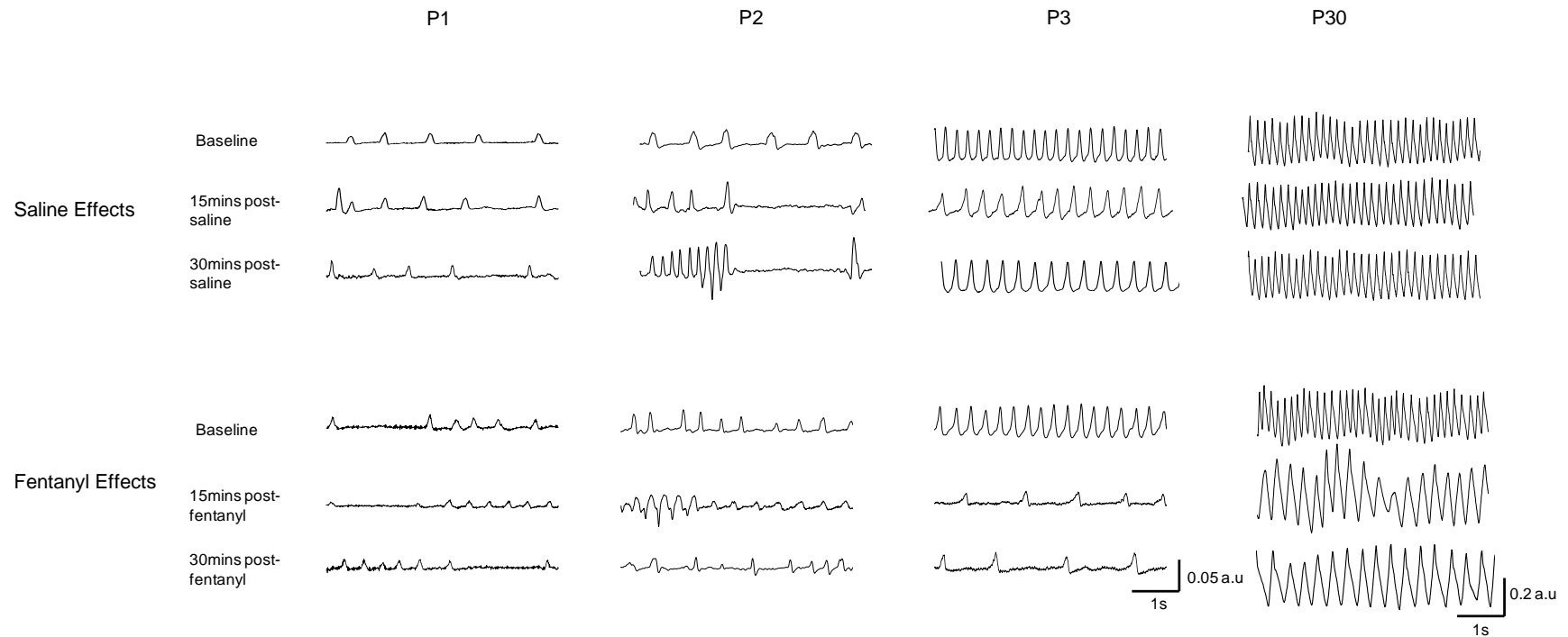


Figure 3-11. Representative plethysmography respiratory traces illustrating the effects of saline and fentanyl in P1, P2, P3 and P30 mice. Saline administration induced no change in respiratory activity in the P1, P2 and P30 mice however a reduction in respiratory frequency was seen following saline injection in the P3 mice. Fentanyl did not induce any respiratory depression in P1 or P2 mice, but induced a clear reduction in respiratory frequency and V_t in the P3 mice. In the adult, P30 mice, fentanyl evoked a decrease in frequency but an increase in V_t . Note the different scale for the P30 traces.

3.6.3 Respiratory frequency

Interestingly, when observing only the baseline respiratory frequency data in each postnatal age group (Figure 3-12), an increase in respiratory frequency throughout postnatal development (P1-P10) and a subsequent decline by P30 is evident in both the control and fentanyl experiments, which reiterates the data from study 1 where the postnatal evolution of breathing frequency was investigated (Figure 3-6).

In the control experiments, respiratory frequency was generally comparable before and after the saline vehicle administration as expected (Figure 3-12A). There was however a significant reduction in respiratory frequency from baseline seen at 15 minutes following saline injection in the P3 mice (baseline: 219 ± 36 bpm vs 15 minutes: 155 ± 26 bpm, $p < 0.05$) and at 30 minutes post saline injection in the P4 mice (baseline: 230 ± 41 bpm vs 30 minutes: 157 ± 36 bpm, $p < 0.05$). Additionally, there was a trend towards a reduced respiratory frequency from baseline at 30 minutes post saline administration at P5 (baseline: 266 ± 55 bpm vs 30 minutes: 197 ± 44 bpm, $p > 0.05$). When observing the data as a percentage change in respiratory frequency from baseline (Figure 3-13A), the reduction in respiratory frequency at P3 and P4 is evident. However, when comparing the magnitude of the respiratory frequency change post saline injection between the age groups, there was no significant difference (2 way ANOVA, $p > 0.05$). It is important to note that the decreases in breathing frequency observed in the control experiments must be taken into consideration when interpreting the respiratory effects of fentanyl.

Fentanyl did not evoke a significant reduction in respiratory frequency at P1 and P2. When observing the absolute respiratory frequency changes of the P1 and P2 mice (Figure 3-12B), respiratory frequency was comparable before and at all time points following injection of fentanyl. It is apparent that this data parallels that of the control experiments. In contrast, fentanyl did induce a significant decrease in respiratory frequency at P3 and P5, seen at 5, 15 and 30 minutes following administration. In addition, fentanyl also evoked a significant reduction in respiratory frequency in the P10 and P30 mice, evident at 30 minutes post administration. There was also a clear trend towards a reduction in respiratory frequency at 30 minutes post fentanyl in the P4 (baseline: 204 ± 82 bpm vs 30 minutes: 154 ± 65 bpm, $p > 0.05$) and P7 mice (baseline: 295 ± 5 bpm vs 30 minutes: 207 ± 48 bpm, $p > 0.05$). From Figure 3-12B, it is clear that a gradual decline in the frequency of breathing occurred from 5 minutes to 30 minutes post fentanyl injection, observed in all

mice from P3 through to P30. By 45 minutes following fentanyl application, respiratory frequency had returned to baseline levels. When studying the absolute changes in respiratory frequency at each postnatal age (Figure 3-12B), the magnitude of the fentanyl-induced respiratory frequency depression appeared to be greatest from P3 onwards i.e. after the proposed respiratory maturation process. It is however important to highlight the high variability in the data, particularly in the younger age groups of P1-P10. Figure 3-13B illustrates the fentanyl-induced alteration in respiratory frequency as a percentage change from baseline in each age group. This set of data allows for a direct comparison of the magnitude of the fentanyl-induced respiratory frequency depression across the age groups. The respiratory frequency depression from P3 through to P30 is evident, reiterating the absolute respiratory changes (Figure 3-12B). The depression of respiratory frequency induced at 5, 15 and 30 minutes following fentanyl was significantly greater in the P3 mice compared to the P2 mice (5 mins: $36\pm 16\%$ vs $4\pm 35\%$ reduction; 15 mins: $46\pm 18\%$ vs $16\pm 27\%$ reduction; 30 mins: $43\pm 18\%$ vs $3\pm 21\%$ reduction, $p<0.05$). In addition, compared with the P2 mice, fentanyl induced a significantly greater respiratory depression from baseline at 15 and 30 minutes in the P5 mice (15 mins: $46\pm 11\%$ vs $16\pm 27\%$ reduction; 30 mins: $40\pm 11\%$ vs $3\pm 21\%$ reduction, $p<0.05$) and at 30 minutes in the P10 mice ($33\pm 5\%$ vs $3\pm 21\%$ reduction, $p<0.05$) and P30 mice ($21\pm 21\%$ vs $3\pm 21\%$ reduction, $p<0.05$). There was also a trend towards a greater depression of respiratory frequency at 30 minutes in the P4 and P7 mice compared to the P2 mice. The magnitude of fentanyl-induced respiratory frequency change was similar between the P1 and P2 groups. There was no significant difference in the degree of fentanyl-induced respiratory frequency depression between the P1 mice and the other age groups; however there was a distinct trend towards the P1 mice exhibiting a smaller frequency depression in response to fentanyl when compared with the P3-P30 mice. Furthermore, there was no significant difference in the magnitude of fentanyl-induced respiratory depression between the P3-P30 age groups. It is important to highlight that at P4 the percentage change in respiratory frequency from baseline observed at 30 minutes following fentanyl is comparable with the relative change seen after saline injection (30 mins post saline: $30\pm 19\%$ reduction; 30 mins post fentanyl: $23\pm 35\%$ reduction).

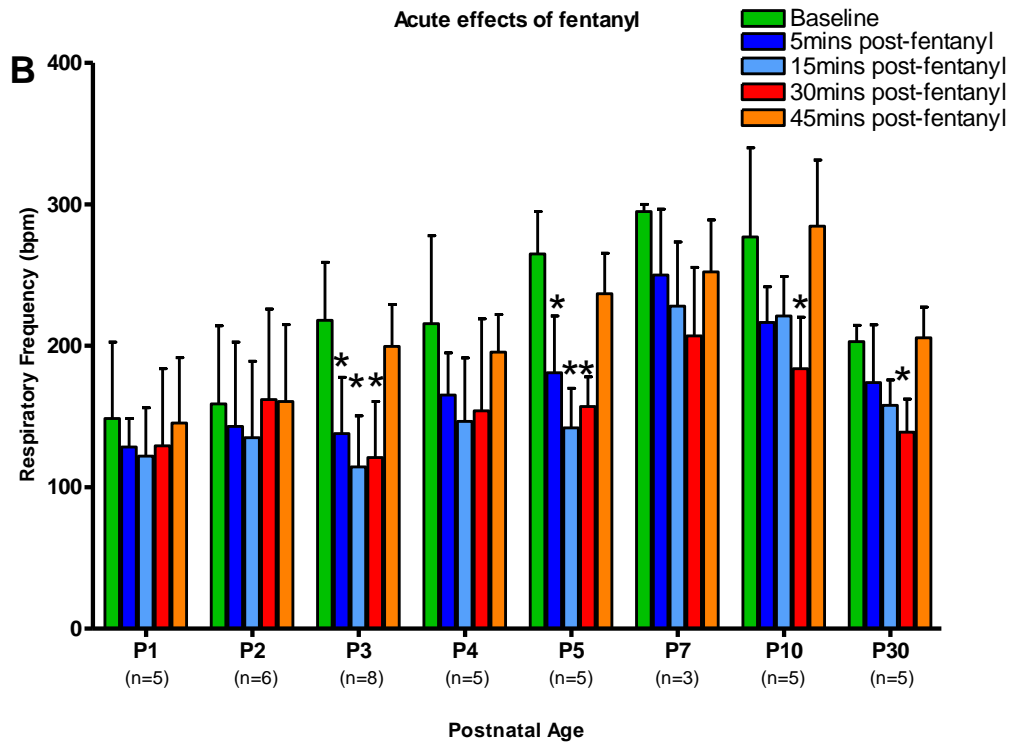
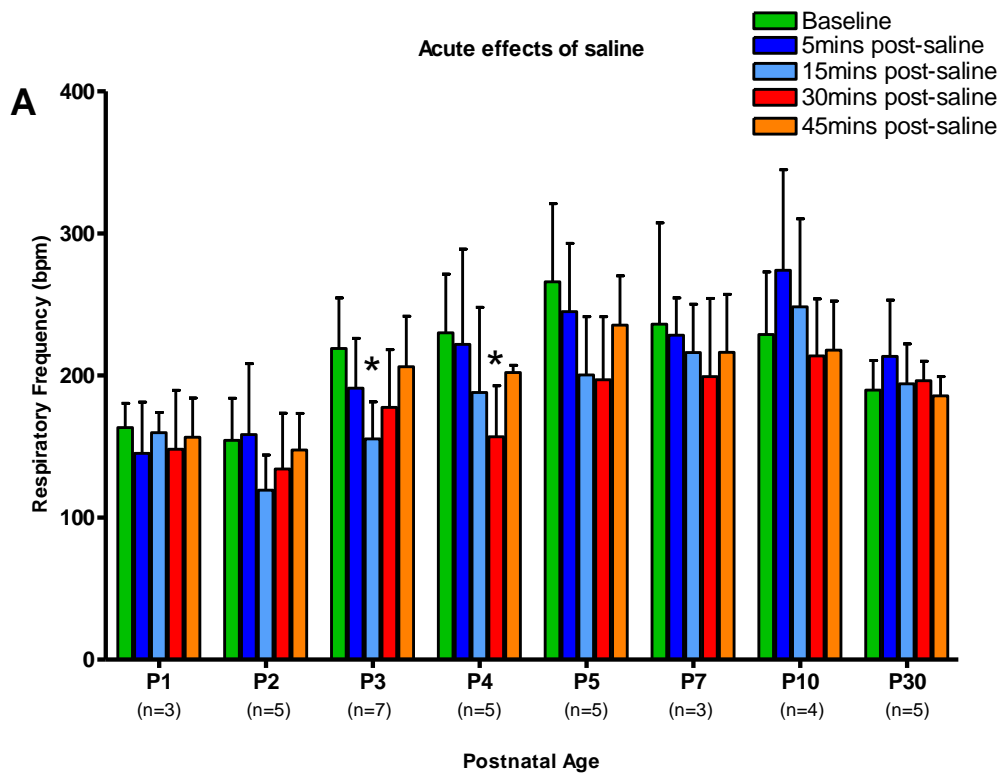


Figure 3-12. Absolute changes in respiratory frequency in response to saline or fentanyl throughout postnatal life. The influence of postnatal age on the acute respiratory frequency effects of saline (A) or fentanyl (B) were assessed. Mice were studied from P1-P5, P7, P10 and P30. Different mice were studied on each postnatal day. Data presented as mean±SD. * denotes a significant reduction ($p < 0.05$) in respiratory frequency from corresponding baseline value, 2-way ANOVA with Bonferroni's post test.

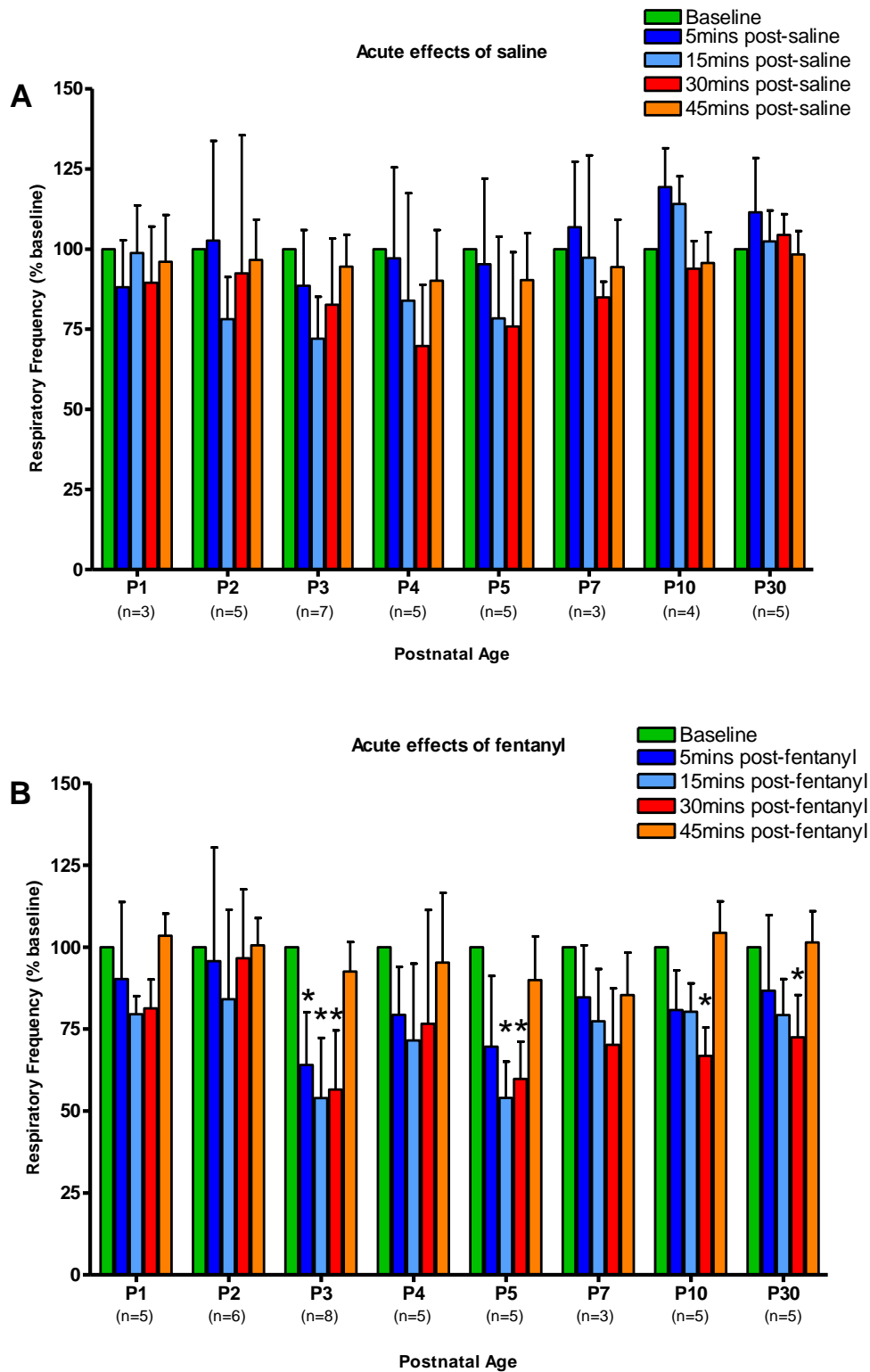


Figure 3-13. Relative change in respiratory frequency in response to saline or fentanyl throughout postnatal life. The influence of postnatal age on the acute respiratory frequency effects of saline (A) or fentanyl (B) were assessed. Data shows the percentage change in respiratory frequency from baseline in each age group, where baseline represents 100%. Mice were studied from P1-P5, P7, P10 and P30. Different mice were studied on each postnatal day. Data presented as mean±SD. * denotes a significant difference ($p < 0.05$) from the corresponding P2 time point, 2-way ANOVA with Bonferroni's post test.

3.6.4 Tidal volume

Figure 3-14 illustrates the relative change in V_t from baseline levels after saline and fentanyl administration (baseline represents 100%). In the control experiments, saline administration did not evoke any significant change in V_t in any of the age groups (Figure 3-14A). V_t remained stable and was always comparable before and at all time points after saline injection. Fentanyl induced a reduction in V_t from P1 to P7 and the magnitude of this depression was not significantly different between these age groups (Figure 3-14B, $p > 0.05$, 2- way ANOVA). In the P1-P7 mice, the percentage reduction in V_t from baseline ranged from 26-44% at 5 minutes post-fentanyl administration and between 20-41% at 15 minutes following fentanyl administration. V_t always returned to baseline levels by 45 minutes post-fentanyl. There was a high degree of variability in the data in all the age groups. In the P10 mice, fentanyl did not appear to induce a substantial reduction in V_t (5 minutes post-fentanyl: $15 \pm 29\%$ reduction; 15 minutes post-fentanyl: $18 \pm 5\%$ reduction), however the magnitude of depression was not significantly different from the younger age groups. The degree of variability in the data was notably high. The V_t response evoked by fentanyl differed significantly in the adult P30 mice compared with the younger age groups. At P30, fentanyl produced an average increase in V_t from baseline at all time point studied (5 minutes post-fentanyl: $24 \pm 69\%$ increase; 15 minutes post-fentanyl: $16 \pm 79\%$ increase; 30 minutes post-fentanyl: $10 \pm 62\%$ increase, 45 minutes post-fentanyl: $19 \pm 55\%$ increase). There was however a high level of variability in the V_t response to fentanyl between individual P30 animals, which should be taken into account when interpreting the data.

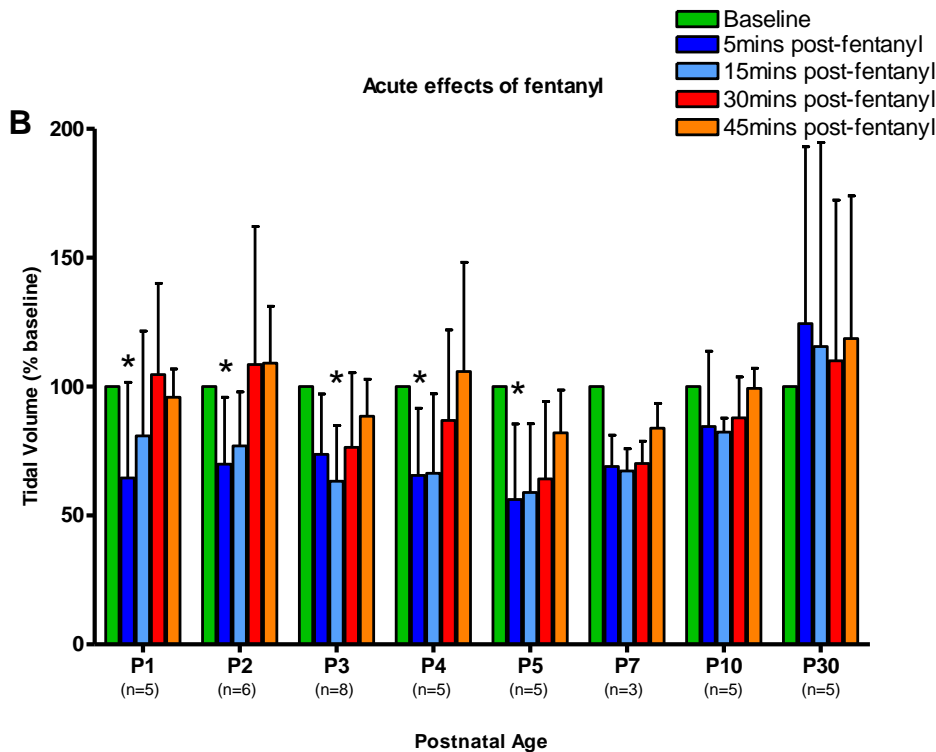
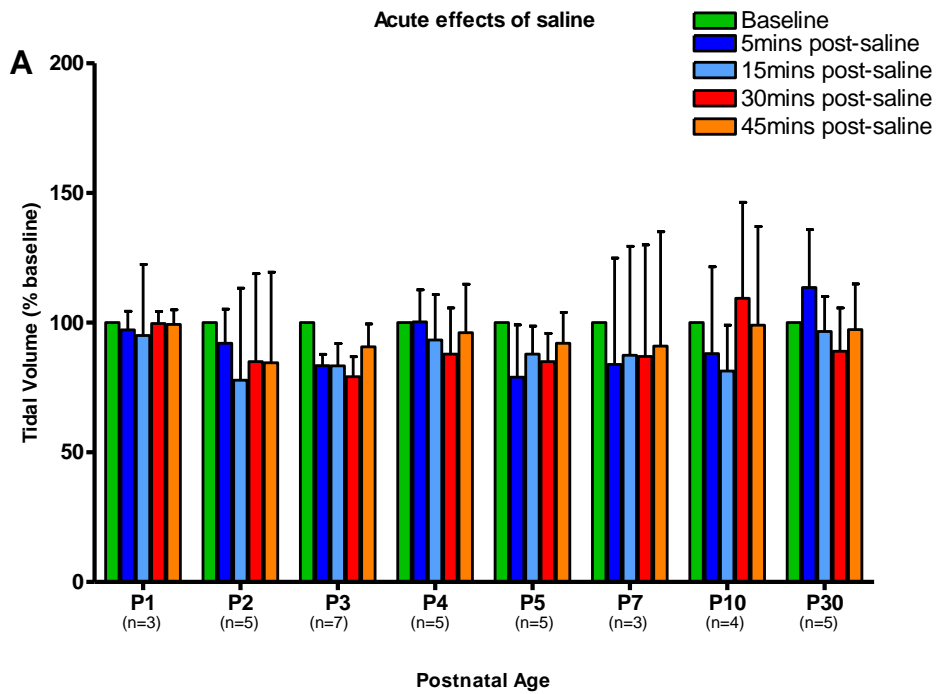


Figure 3-14. Relative change in tidal volume in response to saline or fentanyl throughout postnatal life. The influence of age on the tidal volume effects of saline (A) or fentanyl (B) are shown. Data shows the percentage change in tidal volume from baseline in each age group, where baseline represents 100%. Mice were studied from P1-P5, P7, P10 and P30. Different mice were studied on each postnatal day. Data presented as mean \pm SD. * denotes a significant difference from the corresponding time point in the P30 group, 2-way ANOVA with Bonferroni's post test.

3.7 Discussion of studies 2 and 3

In studies 2 and 3, fentanyl was utilised to pharmacologically manipulate the respiratory system of mice throughout postnatal development. The aim of these studies was to investigate the level of involvement of the preBötC in respiratory rhythm generation throughout early life and test the hypothesis that the preBötC only functions as the dominant respiratory oscillator when the respiratory system has matured. Study 2 was longitudinal in nature and mice were repeatedly exposed to fentanyl throughout life. This repeated exposure induced a rapid desensitisation to the respiratory effects of the drug and therefore our proposed hypothesis could not be tested using this particular study design. The study was therefore repeated with an altered design where mice were only studied once (different mice utilised at each postnatal age), thereby avoiding repeated exposure to the drug (study 3). This study revealed there was a trend towards an age-dependent increase in respiratory sensitivity to fentanyl, where mice displayed a heightened respiratory depression in response to fentanyl from P3 onwards.

3.7.1 Repeated exposure induced an acute respiratory tolerance to fentanyl

From study 1 we found that repeated exposure to fentanyl in early postnatal life evoked a rapid reduction in the sensitivity to the respiratory depressive effects of subsequent applications of the drug. Fentanyl did not induce a depression in either respiratory frequency or V_t at any postnatal age and therefore did not alter overall ventilation. Importantly, the respiratory effects of fentanyl were indistinguishable from the saline control at all ages. This is consistent with previous work indicating that analgesic tolerance to fentanyl occurs rapidly following continuous exposure in neonatal rats (Thornton and Smith, 1997; Choe and Smith, 2000). It is important to note however, that at P1, all mice were naïve to fentanyl. Even so, fentanyl did not elicit a depression in respiratory activity at this age, which lends support to our hypothesis that mice are less susceptible to the depressive actions of fentanyl in early life suggesting the RTN/pFRG may be functioning as the dominant respiratory oscillator driving the breathing rhythm at this time. However given that mice continued to be unresponsive to the depressive actions of fentanyl at all ages, it is likely that the multiple exposures to fentanyl influenced the acute respiratory response to the drug and therefore our hypothesis could not be fully tested.

It is probable that the repeated fentanyl administration induced a tolerance to the respiratory actions of the drug. In this study, tolerance is defined as an attenuated physiological response to a pharmacological agent given at a dose that is known to induce an effect. Given that the dose of fentanyl administered in this study (0.04 mg/kg) has previously been shown to induce acute respiratory depression in neonatal rodents (Greer et al., 1995; Laferriere et al., 2005), we concluded that repeated exposure to fentanyl had evoked a respiratory tolerance. Congruent with this finding, previous clinical and pre-clinical investigations have demonstrated reduced responsiveness to the analgesic effects of fentanyl after repeated exposure (Thornton and Smith, 1997, 1998; Bailey and Connor, 2005). There are however few studies that have examined tolerance to fentanyl's respiratory effects. The mechanisms that underlie the respiratory tolerance to fentanyl reported in this present study are unknown. A number of pre-clinical studies have explored the development of analgesic tolerance which is a significant clinical problem associated with repeated or prolonged opioid exposure, and various mechanisms that may evoke such tolerance have been proposed. The mechanisms underlying the development of tolerance to μ opioid receptor agonists including fentanyl are thought to occur at the level of the receptor. The μ opioid receptors belong to the family of G-protein coupled receptors (GPCRs) and are negatively coupled to adenylate cyclase (Law et al., 2000). Alterations in μ opioid receptor regulation throughout the brain have been implicated in the development of tolerance in the rodent. Several radioligand binding studies have shown that repeated exposure to μ opioid receptor agonists in rodents elicit downregulation of the μ opioid receptor within the brain (Bhargava and Gulati, 1990; Bernstein and Welch, 1998; Stafford et al., 2001) through receptor internalisation, thereby reducing the number of functional receptors and evoking tolerance. Conversely, a study in mice using radioligand binding has demonstrated that changes in the regulation of μ opioid receptors in response to repeated fentanyl administration occurs independently of the development of tolerance and is related to the dose itself (Yoburn et al., 1993). Repeated exposure to a low dose of fentanyl (0.03-0.1 mg/kg/day for 7 days) induced upregulation of μ opioid receptors whereas exposure to a high dose (0.5 mg/kg/day for 7 days) evoked a downregulation. However, irrespective of the fentanyl dose and corresponding change in receptor density, tolerance always developed. More recent studies have proposed an alternative relationship between μ opioid receptor regulation and tolerance. It has been suggested that receptor internalisation and downregulation actually prevents or delays tolerance. An *in vitro* study has shown that morphine is ineffective at producing μ opioid receptor internalisation but rapidly induces tolerance, whereas DAMGO can effectively produce internalisation of μ

opioid receptors but does not readily evoke tolerance (Koch et al., 2005). Additionally, μ opioid receptor phosphorylation and desensitisation has been implicated in the development of opioid tolerance (Pitcher et al., 1998; Liu and Anand, 2001). Repeated exposure to μ opioid receptor agonists has been found to induce phosphorylation of the receptor by G protein-coupled receptor kinases (GRKs). The phosphorylated receptor is then bound by β -arrestin, a protein that is a member of the arrestin family, which subsequently leads to the uncoupling of the μ opioid receptor from G proteins. This induces a desensitisation of the receptor's responsiveness to agonists (Ferguson et al., 1996) and may be responsible for the appearance of tolerance. Protein kinase A (PKA) and protein kinase C (PKC), which are involved in the signal transduction pathways following μ opioid receptor activation, have also been linked to the appearance of analgesic tolerance. PKA and PKC inhibitors are found to prevent the development of tolerance to morphine in mice *in vivo* (Javed et al., 2004). In the present study, it would be interesting to assess the ability of these inhibitors to prevent the development of respiratory tolerance to fentanyl.

From the extensive research, it is evident that there is still considerable uncertainty regarding the exact mechanisms responsible for the development of tolerance. It is likely that a complex set of cellular and molecular processes are involved. It is difficult to directly compare the findings from previous work with the results of the present study, given that there are many discrepancies including the type of opioid agonist administered, the dose administered, method of administration, duration of exposure, species and age of animals assessed. Moreover, most studies have investigated analgesic tolerance to μ opioid receptor agonists which might have a distinct mechanistic profile compared to respiratory tolerance development. These incongruities should therefore be taken into consideration when evaluating potential mechanisms of tolerance in the present study. In order to ascertain the mechanisms directly related to respiratory tolerance, investigations of μ opioid receptor regulation within respiratory-related brain areas e.g. the ventrolateral medulla could be assessed before and after fentanyl exposure. Since fentanyl is believed to induce respiratory frequency depression via direct actions on the preBötC (Gray et al., 1999; Takeda et al., 2001; Mellen et al., 2003; Montandon et al., 2011), it is of particular interest to explore the effects of repeated exposure on the expression of μ opioid receptors within the preBötC. Radioligand binding or immunohistochemistry analyses of the μ opioid receptor could be undertaken. This would help to determine if the lack of fentanyl-

induced respiratory depression is due to changes within the preBötC at the level of the receptor.

The unforeseen development of tolerance to fentanyl-evoked respiratory depression has sparked new interest in the respiratory effects of repeated fentanyl exposure, particularly as a result of exposure during early postnatal life when the respiratory system undergoes significant maturational changes. Given the widespread use of opioid analgesic therapeutics in clinical practice, understanding the respiratory consequences of repeated exposure has an important clinical relevance and certainly warrants further investigation.

3.7.2 Respiratory sensitivity to fentanyl was age-dependent

Study 3 also investigated the respiratory depressive effects of fentanyl throughout postnatal development. To prevent the confounding respiratory effects of repeated fentanyl exposure, and thus allowing our hypothesis to be tested, each mouse was only studied on one postnatal day. As previously discussed, μ opioids including fentanyl are believed to induce respiratory frequency depression *in vivo* by direct actions on the preBötC (Gray et al., 1999; Takeda et al., 2001; Mellen et al., 2003; Montandon et al., 2011). It was therefore proposed that fentanyl could be utilised as a pharmacological tool to selectively depress the activity of the preBötC, but leave the opioid-insensitive RTN/pFRG unperturbed, thereby allowing for the dissociation of the functioning of these two postulated respiratory oscillators throughout postnatal life. Importantly, in all experiments, fentanyl did not induce hypothermia or sedation, indicating that the fentanyl dose administered (0.04 mg/kg) was sufficient to study the desired respiratory actions of the drug with minimal side effects. The acute respiratory effects of fentanyl were investigated from P1-P5, which represents a critical developmental time window that encompasses significant postnatal respiratory maturation (see study 1, section 3.3). Additionally, respiratory modulation by fentanyl was also assessed at P7, P10 and in adulthood (P30).

When examining the effects of fentanyl on respiratory frequency, the data reveals that there was a trend towards an age-dependent increase in respiratory sensitivity to fentanyl after the postulated maturation step, as hypothesised. At P1 and P2 when respiratory patterns still exhibited significant immaturity, fentanyl did not elicit a depression of respiratory frequency. Conversely, when breathing exhibited a mature pattern from P3 onwards, a respiratory frequency reduction was observed in response to fentanyl. Since a

significant postnatal maturation of respiratory activity occurs by approximately P3, it appears the increased respiratory susceptibility to fentanyl was related to postnatal maturation. This heightened respiratory sensitivity to the depressive actions of fentanyl post-maturation supports our hypothesis that the preBötC only functions as the dominant respiratory rhythm generator after the respiratory has undergone a step in maturity. A previous *in vivo* study investigating the effects of fentanyl on breathing patterns of rats during early life has also reported an increase in the magnitude of the respiratory frequency depressant actions of fentanyl with advancing postnatal age (Greer et al., 1995). However this study only investigated fentanyl's respiratory actions at 3 postnatal ages (P1, P4 and P10), thus the age-dependent effects were not as thoroughly assessed compared with the present study. The results from study 3 are also congruent with the findings from previous *in vivo* studies that have explored the acute respiratory effects of riluzole throughout postnatal life in mice (Dr Leanne McKay, personal communication, SFN abstract 2009). Riluzole, which depresses the activity of the RTN/pFRG, was also found to have age-dependent respiratory depressive actions. Riluzole was reported to induce the greatest magnitude of respiratory depression in early life (P1-P3) when the respiratory system is still immature, which is in direct contrast to the age-dependent respiratory effects of fentanyl. Taken together, the fentanyl and riluzole experiments suggest that the level of involvement of the RTN/pFRG and the preBötC in respiratory rhythm generation change with postnatal development, with the RTN/pFRG functioning as the dominant respiratory oscillator in early life when the respiratory system is immature, and the preBötC functioning as the principal respiratory oscillator driving breathing rhythm after the respiratory system has matured. To complement the work carried out in the whole animal, it would be advantageous to also examine the age-dependent changes in fentanyl mediated depression of respiratory frequency *in vitro* by utilising the brainstem-spinal cord preparation, which retains the activity of both the preBötC and the RTN/pFRG. Activity of the preBötC and the RTN/pFRG in addition to respiratory motor output could be recorded in response to fentanyl.

Fentanyl-induced changes in V_t throughout postnatal development and through to adulthood were less clear and did not follow the same age-dependent pattern as seen with fentanyl-induced changes in respiratory frequency. Mice did not exhibit an enhanced susceptibility to fentanyl-induced V_t depression after the proposed maturation step. In this study, V_t was presented as a relative change from baseline given that the accuracy of absolute V_t values calculated from neonatal plethysmography is disputed (see section 3.4.3

for full discussion). Fentanyl induced a reduction in V_t from P1-P7, but the magnitude of depression was not affected by postnatal age during this time window and therefore was also not influenced by respiratory maturation. Surprisingly, at P10, fentanyl did not induce a notable V_t depression. In contrast to the young mice, fentanyl elicited an increase in V_t in the adult (P30) mice. At present, there is no detailed explanation for these differential V_t responses. Furthermore, the reason(s) why fentanyl's age-dependent modulation of respiratory frequency differs from the modulation of V_t also remains to be elucidated. It is likely that the fentanyl-mediated neural mechanisms that account for changes in V_t are distinct from those responsible for respiratory frequency changes. It has been reported that systemically administered fentanyl acutely reduces the excitability of phrenic premotor neurons as well as depressing the intensity of phrenic nerve discharge in the anaesthetised cat (Lalley, 2003). This suggests that fentanyl may act to depress V_t by direct actions at the level of the phrenic spinal nerves. Similar to the effects of fentanyl in the young mice (P1-P7) there are numerous studies that have reported a depression of V_t after μ opioid administration in awake rats (van den Hoogen and Colpaert, 1986; Greer et al., 1995; Manzke et al., 2003; Moss et al., 2006; Ren et al., 2006; Greer and Ren, 2009; Montandon et al., 2011). However comparable to the fentanyl-induced increase in V_t observed in the adult mice in the present study, an augmentation in V_t in response to fentanyl has been previously reported by Colman and Miller (2001) who studied both neonatal and adult mice. These authors did however report a gasping breathing pattern in response to fentanyl, which was not observed in the present study. Additionally in contrast to our findings they did not report a difference in V_t response between neonatal and adult rats. A fentanyl-induced increase in V_t is reported to be mediated via actions at the μ_1 -opioid receptor subtype, whereas a fentanyl-induced depression of V_t is believed to be mediated through the μ_2 -opioid receptor (Colman and Miller, 2001). It is interesting to consider the possibility that the age-dependent V_t effects seen in this present study were due to fentanyl exhibiting differential actions on the μ opioid receptor subtypes, however this has never to our knowledge been investigated. Opioid-induced changes in V_t in the awake rodent have been reported as highly complex (van den Hoogen and Colpaert, 1986), which is in agreement with our data. The mechanisms underlying the V_t responses to fentanyl throughout postnatal development cannot be deduced from this study alone, but certainly warrants further investigation. It is imperative to highlight the high degree of variability observed in the V_t response between individual animals in each age group, particularly the adults (P30). This high variability in the data adds to the difficulty in interpreting the

results and suggests the sample size should be increased to allow more definitive conclusions to be drawn.

Given that we were interested in the direct effects of fentanyl on the preBötC and therefore on respiratory rhythm, the respiratory frequency changes which are an *in vivo* measure of central respiratory rhythm generation, were the most important measure. Although the fentanyl modulation of V_t throughout postnatal life is difficult to interpret, we found a trend towards an increased susceptibility to respiratory frequency depression after respiratory maturation, which supports our hypothesis.

3.7.3 Study limitations and points to consider

When interpreting the respiratory effects of fentanyl in relation to postnatal age in study 3 it is imperative that the control data is also acknowledged. At P3 and P4, respiratory frequency displayed a significant decrease following administration of the saline vehicle. The reason for this unexpected depression in respiratory frequency could be due to natural fluctuations in baseline respiratory activity throughout the experimental procedure. Mice were contained within the plethysmograph chamber for a considerable period of time following drug administration and it is therefore likely that the arousal state (i.e. wakefulness, REM and non-REM sleep) varied throughout the duration of the experiment. Given that arousal state significantly influences respiratory activity (Aserinsky, 1965; Remmers et al., 1978; Horner, 2008; Pagliardini et al., 2012; Pagliardini et al., 2013), fluctuations in arousal state could explain the changes in respiratory frequency observed in the control experiments. While it is difficult to accurately monitor the behavioural state of neonatal mice using typical electroencephalogram (EEG) techniques (Karlsson and Blumberg, 2002), future experiments could measure nuchal muscle EMG activity, where a reduction in activity indicates the presence of sleep (Durand et al., 2005). The invasive nature of this technique could however influence baseline breathing. Another factor that could affect respiratory patterns and should be taken into consideration when interpreting the respiratory frequency changes in the control data is the impact of maternal separation. Neonatal mice were separated from their mother for approximately 2 hours during the experimental protocol. It has been reported that neonatal maternal separation (NMS) induces a stress-related increase in respiratory instability in the rat (Gulemetova and Kinkead, 2011). It is possible that NMS evoked stress responses that could have contributed somewhat to the fluctuations in respiratory frequency throughout the

experiment in the P3 and P4 control mice. These potentially confounding variables do not however explain why a significant change in respiratory frequency in the control experiments was not observed at all ages. Nonetheless, the fact that respiratory frequency reductions were observed in the absence of a respiratory depressant drug should be considered when interpreting the respiratory effects of fentanyl throughout postnatal development. This is particularly important when assessing respiratory modulation by fentanyl at P4, where the magnitude of respiratory frequency depression was comparable to that observed after saline administration. Furthermore, given the high degree of variability in the data from both the control and fentanyl experiments, increasing the number of mice studied at each postnatal age is essential and would help to reveal clearer data trends and increase the validity of the data. It would also be advantageous to increase the range of postnatal ages studied, particularly from P6 onwards, which would allow a more comprehensive analysis of fentanyl-induced respiratory modulation throughout postnatal life.

It is important to consider other possible explanations for the enhanced fentanyl-induced respiratory frequency depression seen post-maturation that might not be related to a switch in the dominant neuronal group generating the respiratory rhythm. It is unlikely that age-dependent differences in enzyme degradation and therefore metabolism of fentanyl could account for the differential respiratory sensitivity to fentanyl, given that this process appears to be fully functional by birth (Thornton et al., 1998). Furthermore, penetration of fentanyl across the blood brain barrier is also comparable between neonatal and juvenile mice (Thornton et al., 1998), so differences in the level of drug reaching the preBötC would not account for differential respiratory responses to fentanyl. Changes in the number of functional μ opioid receptors within the brainstem throughout the maturation period could account for changes in respiratory sensitivity to fentanyl. However, the effects of postnatal development on the density of μ opioid receptors in the brainstem of the mouse have received very little attention, and there are no reports on changes specifically within the preBötC. Autoradiography studies using radioligand binding have revealed that the number of μ opioid receptors in the whole mouse brain increase with age and show the greatest increase within the first few weeks after birth (Tavani et al., 1985). Furthermore the number of μ opioid receptors expressed throughout the medulla is also found to display an age-dependent increase in the rat, with a low level of expression found in early postnatal life (Xia and Haddad, 1991; Kivell et al., 2004). It has therefore been concluded that μ opioid receptors are developmentally regulated in the brainstem. Importantly however, if

this age related increase in μ opioid receptors numbers is observed at the level of the preBötC is unknown. If there is a change in the density of μ opioid receptors within the preBötC then this could contribute in part to the age-related alteration in respiratory sensitivity to fentanyl observed in this present study and should be considered. Immunohistochemical analyses of μ opioid receptors expression within the preBötC throughout postnatal life could be undertaken to provide further insight into the influence of postnatal maturation on μ opioid receptor regulation.

One caveat of using fentanyl to investigate the effects of perturbing the rhythmic activity of the preBötC is the fact that this drug induces global actions throughout the body. Fentanyl likely also targeted other respiratory and non-respiratory central and peripheral sites which may have impacted on the change in respiratory activity. Furthermore, fentanyl was administered via an i.p injection; therefore the level of drug that reached the preBötC could not be controlled for and may have differed between individual animals. This could partly account for the high level of variability in the data. These study limitations should be taken into consideration when interpreting the data.

3.7.4 Summary

Study 2 has provided invaluable insight into the development of respiratory tolerance induced by repeated fentanyl exposure during early postnatal life. These findings have generated interest in the potential long-term respiratory consequences of such repeated opioid exposure. By utilising fentanyl as a pharmacological tool to target the preBötC *in vivo* in study 3, we have increased the understanding of age-dependent effects of fentanyl induced respiratory modulation. The data lends support to the hypothesis that the preBötC acts as the dominant respiratory oscillator driving breathing rhythm after the respiratory system has undergone a significant maturation step. In order to determine if the RTN/pFRG functions as the dominant rhythm generator at birth and during the first few days of life, further investigation is required. Moreover, the data from study 3 has helped to shed some light on the influence of postnatal maturation on central respiratory control.

Chapter 4.
**Long-term respiratory effects of repeated fentanyl
exposure in neonatal and juvenile mice**

4.1 Introduction

In the clinical setting, including the paediatric population, opioids are the most widely used and effective pharmacological agents for treating chronic and acute pain (Swarm et al., 2001; Niesters et al., 2013). In addition, opioids are utilised extensively as sedatives and anaesthetics (Anand et al., 1990; Booker, 1999; Tobias, 1999). The μ opioid receptor agonist, fentanyl, is currently one of the most frequently utilised opioid drugs owing to its high potency, fast onset of action, relatively short-acting nature as well as the fact it is metabolised to a number of pharmacologically inert metabolites (Fitzgerald and Teitler, 1993; Booker, 1999; Saarenmaa et al., 1999). Fentanyl treatment is often administered for continuous and prolonged time periods to provide effective pain relief or sedation (Arnold et al., 1991; DelleMijn et al., 1998; Tobias, 1999; Kornick et al., 2003; Brill, 2013). The most widely acknowledged and potentially fatal side effect of fentanyl, as well as other opioid therapeutics, is respiratory depression (Pattinson, 2008). In clinical practice, respiratory function is routinely monitored during the acute period following opioid administration (Niesters et al., 2013); however despite the profound respiratory depressive actions of this class of drug, the long-term respiratory consequences of repeated opioid treatment, particularly during neonatal and infant life, has never to our knowledge been investigated clinically or in pre-clinical animal studies. To date, most pre-clinical rodent studies investigating the long-term effects of repeated opioid exposure in early life have focused on the development of tolerance and reduced sensitivity to the analgesic properties of the drugs (Thornton and Smith, 1998). There are, however, no detailed investigations into long-term changes in the sensitivity to the respiratory depressive actions of opioids after repeated exposure in early life.

Rhythmic breathing is a fundamental physiological process essential to mammalian life. As thoroughly detailed in chapter 3, at birth and during early postnatal life, respiratory patterns generated by the respiratory system in rodents are irregular and display a variable frequency (Mortola, 2001). Furthermore, breathing is also irregular in newborn humans (Fisher et al., 1982; Mortola, 1984). This immaturity of the respiratory system and consequential fragile breathing phenotype could make early postnatal life a vulnerable time period for mammals, in particular to the lasting effects of opioid respiratory manipulation. In mice, the respiratory system is hypothesised to undergo a maturational change between postnatal days 2 and 3, after which breathing increases in frequency, becomes less variable and exhibits a more robust rhythmic pattern (see study 1, chapter 3). The mechanism(s)

underlying this step in maturity and in particular the level of involvement of the preBötC remain to be ascertained.

As extensively discussed in chapters 1 and 3, there is a wealth of evidence to suggest the preBötC is a critical site for respiratory rhythmogenesis in mammals and is necessary for driving the rhythmic contractions of the inspiratory musculature (Smith et al., 1991; Gray et al., 2001; Janczewski et al., 2002; Mellen et al., 2003; McKay et al., 2005; Janczewski and Feldman, 2006; McKay and Feldman, 2008; Tan et al., 2008). *In vitro* and *in vivo* studies have highlighted the critical role of the preBötC in mediating respiratory frequency depression induced by opioids (Gray et al., 1999; Takeda et al., 2001; Mellen et al., 2003; Montandon et al., 2011). As discussed in chapter 3, it is believed that fentanyl can be used as a pharmacological tool to target the preBötC *in vivo*. Previous studies have investigated the lasting respiratory effects of preBötC neuronal destruction in adult rats to gain a better understanding of its role in respiratory rhythm generation *in vivo* (Gray et al., 2001; McKay et al., 2005; McKay and Feldman, 2008). Fentanyl can be utilised to ascertain the long-term effects of a milder pharmacological depression of the preBötC to help further elucidate its role in respiratory rhythmogenesis *in vivo*.

4.1.1 Study aims and rationale

Study 2 detailed in chapter 3 revealed that repeated fentanyl exposure throughout early postnatal development induced an acute respiratory desensitisation to the drug. The aim of the studies described in this chapter was to expand on these findings and further investigate the long-term respiratory effects of repeated fentanyl exposure in the mouse. Owing to the immaturity of the respiratory system and the corresponding fragile nature of breathing patterns during neonatal life in mammals, it was of interest to investigate the long-term effects of fentanyl exposure during this vulnerable respiratory time period, which also encompasses the critical respiratory maturation step. To determine if the postnatal age of fentanyl-exposure influences long-term respiratory effects, fentanyl exposure during juvenile life which is regarded as being post-respiratory maturation, was also investigated. These studies were designed to give invaluable insight into the susceptibility of the respiratory system including that of the preBötC, to the effects of repeated opioid depression at various time periods in early life. From a clinical rationale, the studies detailed in this chapter may also provide novel insight into the potential long-term respiratory consequences of repeated or prolonged fentanyl exposure in human neonates

and infants, and to ascertain if there is a time period in early life that may be particularly vulnerable to respiratory depression. Given that long-term tolerance to the antinociceptive properties of fentanyl have been observed in juvenile rats chronically exposed to the drug (Thornton and Smith, 1998), it was of particular interest to determine if neonatal and juvenile repeated fentanyl exposure induces long-term changes in sensitivity to the acute respiratory depressive actions of fentanyl that can be seen later in life.

Study 4: Investigation of the long-term respiratory effects of repeated fentanyl exposure in the neonatal mouse

Aim: To determine if repeated fentanyl exposure during neonatal life induces long-term alterations in respiratory activity as well as the acute respiratory response to subsequent fentanyl exposure in mice *in vivo*. When mice reached adulthood their respiratory activity was assessed when they were awake and then when anaesthetised. The anaesthetised state not only allowed more detailed *in vivo* respiratory measurements to be obtained, but also permitted the examination of breathing in a depressed brain state.

Study 5: Investigation of the long-term respiratory effects of repeated fentanyl exposure in the juvenile mouse

Aim: To determine if repeated fentanyl exposure during juvenile life induces long-term changes in respiratory activity as well as the acute respiratory response to subsequent fentanyl exposure in mice *in vivo*. When the mice reached adulthood their respiratory activity was assessed when they were awake and then when anaesthetised.

4.1.2 Hypotheses

Study 4

Owing to the fragility of breathing patterns in neonatal life, it was hypothesised that neonatal fentanyl exposure would induce long-term changes in respiratory activity. Furthermore, given that repeated fentanyl exposure in neonatal life induces an acute desensitisation to the respiratory depressive actions of the drug (study 2, chapter 3) it was hypothesised that this desensitisation would continue into adulthood.

Study 5

Since breathing follows a more stable and rhythmic pattern in juvenile life, it was hypothesised that juvenile fentanyl exposure would induce less pronounced long-term changes in respiratory activity compared to neonatal exposure. It was also hypothesised that repeated juvenile fentanyl exposure would induce a long-term desensitisation to the respiratory depressive actions of fentanyl observed in adulthood.

4.2 Methods

4.2.1 Animals

All experimental procedures were carried out under licence from the UK Home Office and performed in accordance with the Animals (Scientific Procedures) Act, 1986. Experiments detailed in this chapter were performed on male ICR mice. Female mice were not studied as they displayed a variable and unpredictable reaction to the urethane anaesthesia. All mice were bred at the Wellcome Surgical Institute animal research facility. A total of 42 mice were used in study 4 and 32 mice in study 5. All mouse pups were housed with their mother until they reached weaning age (21 days old), after which they were housed according to their sex in groups of no more than six. Mice were maintained on a 12 hour light/dark cycle with food and water available *ad libitum*.

4.2.2 Study design

Both study 4 and study 5 were longitudinal in nature. Repeated exposure to fentanyl or a saline vehicle took place during neonatal life (P1-P5, study 4) or juvenile life (P9-P13, study 5). Repeated exposure was defined as a single i.p. injection of 0.04 mg/kg fentanyl per day for 5 consecutive days. In both study 4 and 5, monitoring of respiratory activity did not take place until mice reached adulthood (6 weeks old). Baseline respiratory activity was measured as well as the ventilatory response to an acute fentanyl challenge when mice were awake and then repeated under anaesthesia. A range of fentanyl doses were studied in adulthood to determine if pre-exposure to fentanyl influences future respiratory responses to the drug, and if these responses are dose dependent. A subgroup of mice from study 4 followed a protocol designed to investigate chemosensory responses in the wakeful state and determine if repeated fentanyl exposure evokes lasting changes in chemosensory

functions. These chemosensory experiments were the only experiments undertaken in this group of mice. Schematic illustrations of the design of study 4 and study 5 are shown in Figure 4-1 and Figure 4-2, respectively. Full details of all experimental protocols are described in the subsequent method sections of this chapter.

4.2.3 Repeated fentanyl exposure

Study 4: Neonatal fentanyl exposure

Neonatal mice were repeatedly administered fentanyl citrate (Janssen-Cilag, UK) from P1-P5 (n=21). Each mouse pup received a single intraperitoneal (i.p) dose of 0.04 mg/kg (same dose as administered in study 2, detailed in chapter 3) on each postnatal day. Control mice (n=21) were administered an equivalent volume of physiological saline the vehicle used for fentanyl, throughout the same postnatal period.

Study 5: Juvenile fentanyl exposure

Juvenile mice were repeatedly administered fentanyl citrate (Janssen-Cilag, UK) from P9-P13 (n=16). Each mouse pup received a single i.p dose of 0.04 mg/kg on each postnatal day. Control mice (n=16) were administered an equivalent volume of physiological saline the vehicle used for fentanyl, throughout the same postnatal period.

4.2.4 Definition of experimental groups

Mice repeatedly exposed to fentanyl in neonatal life (P1-P5, study 4) are defined in this thesis as **neonatal-exposed**. The corresponding saline-exposed mice are referred to as controls.

Mice repeatedly exposed to fentanyl in juvenile life (P9-P13, study 5) are defined in this thesis as **juvenile-exposed**. The corresponding saline-exposed mice are referred to as controls.

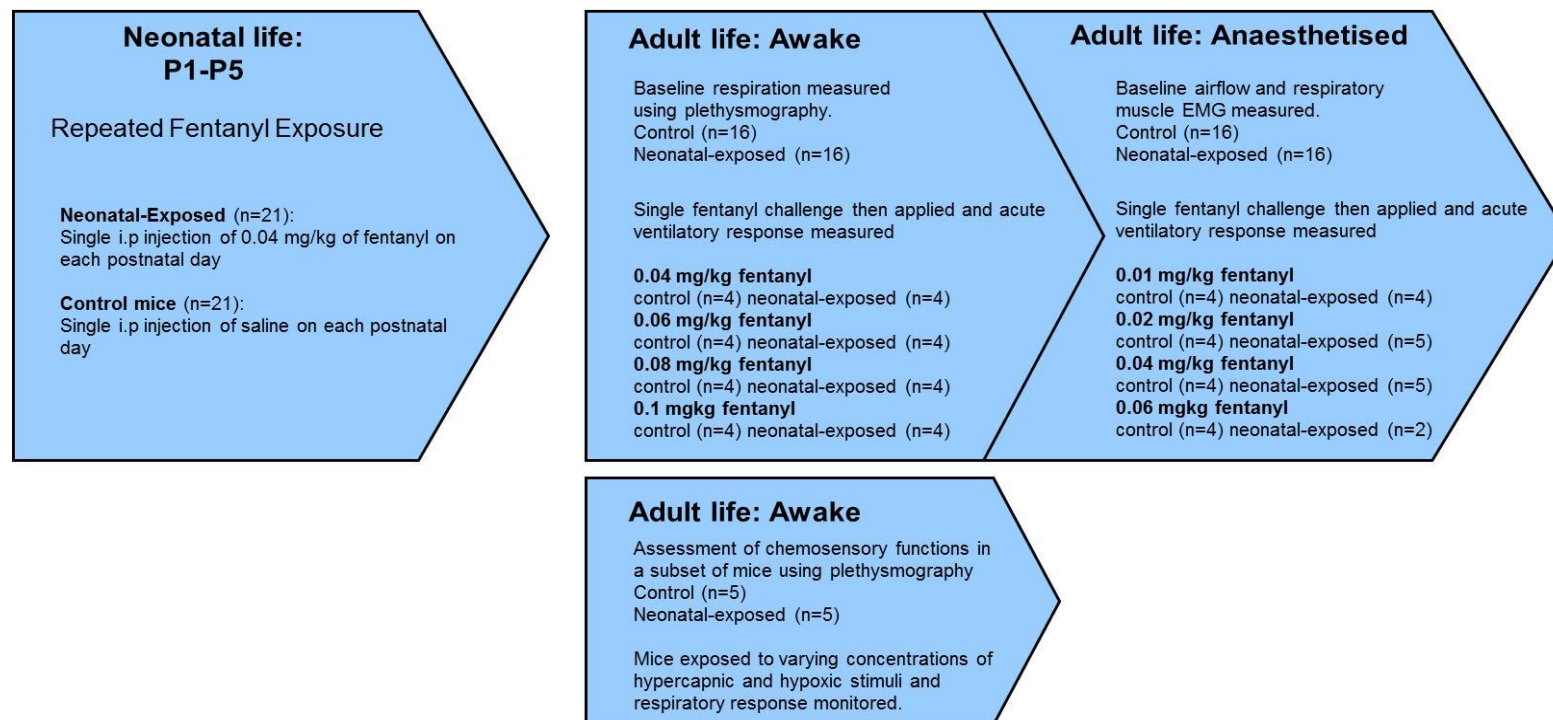


Figure 4-1. Experimental protocols undertaken in study 4. Mice repeated exposed to fentanyl in neonatal life are referred to as neonatal-exposed. Respiratory monitoring began when mice reached adulthood (6 weeks). Baseline respiratory measurements and an acute respiratory response to a single fentanyl challenge were measured when mice were awake and also when anaesthetised. A range of fentanyl doses were studied. Mice were assigned to one of 4 fentanyl doses in the plethysmography experiments (0.04, 0.06, 0.08 or 0.1 mg/kg) as well as the anaesthetised experiments (0.01, 0.02, 0.04 or 0.06 mg/kg). In a subgroup of control and neonatal-exposed mice, only chemosensitivity experiments were carried out in adult life.

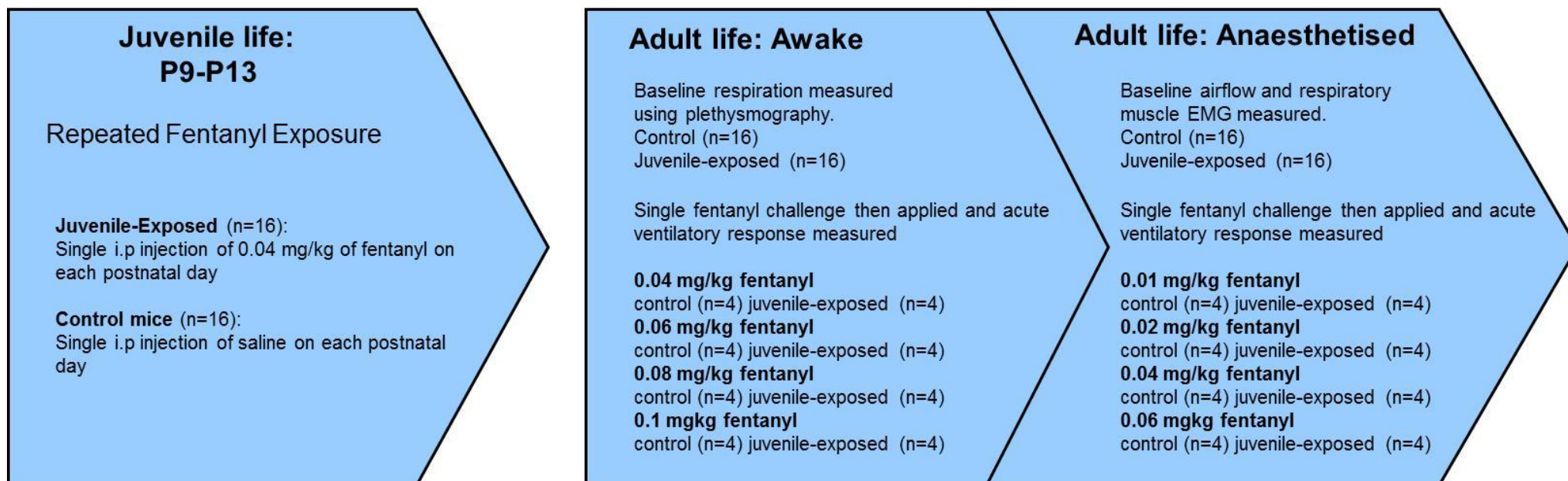


Figure 4-2. Experimental protocols undertaken in study 5. Mice repeatedly exposed to fentanyl in juvenile life are referred to as juvenile-exposed. Respiratory monitoring began when mice reached adulthood (6 weeks). Baseline respiratory activity and the acute respiratory response to a single fentanyl challenge were measured when mice were awake and also when anaesthetised. A range of fentanyl doses were studied. Mice were assigned to one of 4 fentanyl doses in plethysmography (0.04, 0.06, 0.08 or 0.1 mg/kg) and in anaesthetised experiments (0.01, 0.02, 0.04 or 0.06 mg/kg).

4.2.5 Respiratory recording in awake adult mice

4.2.5.1 Baseline breathing and acute respiratory response to fentanyl challenge

In both studies 4 and 5, when mice reached adulthood their resting respiratory activity (under normoxic conditions) as well as the acute respiratory response to fentanyl was examined. Resting breathing parameters were first recorded when mice were in a conscious state and freely behaving, using the non-invasive technique of whole-body plethysmography (see section 2.3). Before experimental sessions began, animals were given 45 minutes to habituate to the recording chamber. Between respiratory recordings, the recording chamber was supplied with humidified air (21% O₂, balanced N₂) at a rate of 2 l/min. Three baseline respiratory recordings were taken (each recording was 2 minutes in duration), approximately 15 minutes apart. After measurement of resting, baseline respiration, the acute ventilatory response to a single fentanyl challenge was recorded. A range of fentanyl doses were examined, and each mouse was assigned to receive only one dose. Mice were removed from the recording chamber and injected (i.p) with a single fentanyl dose of 0.04, 0.06, 0.08 or 0.1 mg/kg, and after placement back into the chamber, their ensuing respiratory output was recorded at 5, 15, 30 and 45 minutes post-injection. Recording of respiration at each time point lasted 2 minutes. At the end of every respiratory recording, a calibration volume of 0.1 ml was injected into the recording chamber.

4.2.5.2 Chemosensitivity experiments

In study 4, the chemosensory responses of a subgroup of control (n=5) and neonatal-exposed mice (n=5) were tested when they reached adulthood. This was the only experimental procedure undertaken on this group of mice. Respiratory parameters were measured under normoxic (21% O₂), hypercapnic (3%, 5% and 8% CO₂) and hypoxic (10% O₂) conditions using whole-body plethysmography. Before experimental sessions began, animals were given 45 minutes to habituate to the recording chamber. Three baseline respiratory recordings were then taken approximately 15 minutes apart under normoxic conditions (air, 21% O₂, balanced N₂). The recording chamber was then filled with a 3% CO₂ gas mixture (3% CO₂, 21% O₂, balanced N₂) for 10 minutes at a rate of 2 l/min. At the end of the 10 minute period, a 2 minute respiratory recording was taken. This protocol was then repeated for 5% CO₂ (5% CO₂, 21% O₂, balanced N₂) and 8% CO₂ (8%

CO₂, 21% O₂, balanced N₂). Following exposure to the final hypercapnic stimuli, the recording chamber was flushed with air (2 l/min) and respiratory recordings were taken at 2 minutes, 15 minutes and 30 minutes to assess post-hypercapnic recovery. The recording chamber was then filled with a hypoxic gas mixture (10% O₂, balanced N₂; 2 l/min) and respiratory recordings were taken at 5 minutes and 10 minutes during hypoxic exposure. The recording chamber was then flushed with air (2 l/min) and respiratory recordings were taken at 2 minutes, 15 minutes and 30 minutes post-hypoxia to measure respiratory recovery. At the end of every respiratory recording, which lasted 2 minutes, a calibration volume of 0.1 ml was injected into the recording chamber.

4.2.6 Respiratory analysis in awake adult mice

To measure respiratory variables, the plethysmography recordings were analysed using Spike 2 software (see section 2.5). Only periods of quiet resting breathing were analysed given that movement distorts the respiratory signal. Blinding to the identity of the experimental group was carried out during analysis.

4.2.6.1 Baseline breathing and acute respiratory response to fentanyl challenge

Baseline respiratory frequency, inspiratory duration, expiratory duration, V_t and V_e were analysed on a breath by breath basis (see chapter 2, section 2.5.1 for further details). All three baseline respiratory recordings were analysed and the data was compiled to generate a baseline value for each respiratory parameter. Respiratory frequency, V_t and V_e were also calculated at 5 minutes, 15 minutes, 30 minutes and 45 minutes post-fentanyl exposure to determine the acute effects of the challenge. Absolute changes in these parameters as well as relative changes (percentage change) from baseline are presented.

4.2.6.2 Chemoresponses

In the experiments assessing chemosensory responses in study 4, changes in respiratory frequency, V_t and V_e in response to hypercapnia and hypoxia as well as respiratory recovery from the stimuli were analysed using Spike 2 software (Cambridge Instruments, UK).

4.2.7 Statistical analysis of respiratory variables in awake adult mice

All statistical analyses were performed using GraphPad Prism4 software. The following statistical analyses were carried out for both studies 4 and 5.

- Unpaired t-tests were performed to compare baseline respiratory frequency, inspiratory duration, expiratory duration, V_t and V_e between control and repeatedly exposed mice.
- For control and repeatedly-exposed mice, fentanyl-induced acute changes in respiratory frequency, V_t , and V_e across time were analysed using a 2-way ANOVA with Bonferroni's post test.

The following statistical analyses were carried out for the chemosensitivity experiments in study 4.

- A comparison of respiratory variables (respiratory frequency, V_t , and V_e) between control and neonatal-exposed mice under each of the respiratory stimuli was performed using a 2-way ANOVA with Bonferroni's post test.

Differences were regarded as significant if $p < 0.05$. All data are presented as mean \pm SD.

4.2.8 Respiratory recording in anaesthetised adult mice

In addition to plethysmographic breathing measurements, baseline respiratory activity and the acute respiratory response to a fentanyl challenge was also examined under anaesthesia. Mice were anaesthetised with an i.p. injection of urethane (initial injection of 1.5 g/kg followed by three 0.25 g/kg supplementary injections administered 5 minutes apart), transorally intubated and allowed to spontaneously breathe room air without ventilatory aid for the duration of the experimental procedure. Body temperature was monitored via a rectal probe and maintained between 36.5 and 37°C using a heat lamp. Respiratory airflow, genioglossus EMG activity (GG_{EMG}) and abdominal muscle EMG activity (ABD_{EMG}) were continually recorded for the duration of each experiment as previously described (chapter 2, section 2.6). It would have been desirable to obtain diaphragm EMG activity as this is the principal inspiratory muscle; however due to unforeseen technical issues, it was not possible to make this measurement (see discussion section 4.5.7 for further information). Animals were given 30 minutes to stabilise before

baseline respiratory activity was recorded continuously for 10 minutes. Following this control period, mice were injected i.p with a single dose of 0.01, 0.02, 0.04 or 0.06 mg/kg of fentanyl. Respiratory airflow and respiratory muscle EMG activity were monitored and recorded for 60 minutes post-fentanyl injection.

4.2.9 Respiratory analysis in anaesthetised adult mice

All respiratory variables were analysed on a breath by breath basis using Spike 2 software (Cambridge Instruments). Respiratory frequency, inspiratory duration, expiratory duration, V_t , V_e and GG_{EMG} activity were analysed throughout the 10 minute baseline period (see chapter 2, section 2.6.4 for further details on calculation of these respiratory variables). The number of augmented breaths observed during the 10 minute period of baseline breathing was also quantified. An augmented breath is defined as an increased respiratory effort with a tidal volume $>50\%$ of a regular breath. Respiratory frequency, V_t , V_e and GG_{EMG} activity were also analysed at 5 minute time points post-fentanyl injection until 30 minutes, then at 45 minutes and 60 minutes post-injection. At each time point, a total of 30 seconds of continuous recording was analysed. Blinding to the identity of the experimental group was carried out during analysis.

4.2.10 Statistical analysis of respiratory variables in anaesthetised adult mice

All statistical analyses were performed using GraphPad Prism4 software. All statistical tests described were performed for both studies 4 and 5.

- Unpaired t-tests were performed to compare baseline respiratory frequency, inspiratory duration, expiratory duration, V_t , V_e and GG_{EMG} activity between control and repeatedly exposed mice. A Mann Whitney test was performed to compare the number of augmented breaths observed during baseline breathing between control and repeatedly exposed mice.
- To compare fentanyl-induced acute changes in respiratory frequency, V_t , V_e and GG_{EMG} activity across time between control and repeatedly exposed mice, a 2-way ANOVA with Bonferroni's post test was used.

Differences were regarded as significant if $p < 0.05$. All data are presented as mean \pm SD.

4.3 Results of study 4: Investigation of the long-term respiratory effects of repeated fentanyl exposure in the neonatal mouse

Results from study 4 are presented in section 4.3

4.3.1 Animal body weights

There was no significant difference in the average body weights of neonatal-exposed and control mice during the drug exposure period from P1-P5 or when they reached adulthood ($p>0.05$, 2-way ANOVA, Table 4-1).

Postnatal Age	Weight (g)	
	Control	Neonatal-Exposed
P1	1.6±0.3	1.8±0.3
P2	2.0±0.5	2.2±0.2
P3	2.8±0.4	2.7±0.3
P4	3.3±0.4	3.1±0.5
P5	3.9±0.3	3.7±0.7
Adult	36.4±4.7	38.9±3.2

Table 4-1. Average body weights of control and neonatal-exposed mice.

Body weight was measured throughout the repeated drug exposure period (P1-P5) and on reaching adulthood. Data presented as mean±SD. No significant difference in body weight between the two experimental groups at all ages, 2-way ANOVA.

4.3.2 Baseline respiratory parameters of awake adult mice

In the wakeful state, adult mice (6 weeks old) which were neonatal-exposed had a significantly lower baseline respiratory frequency compared to control mice (150 ± 8 bpm vs 180 ± 6 bpm, $p<0.05$, Figure 4-3A), owing to the fact that neonatal-exposed mice exhibited a significantly longer inspiratory duration (0.16 ± 0.01 s vs 0.12 ± 0.01 s, $p<0.05$, Figure 4-3B). Expiratory duration was comparable between the two experimental groups (neonatal-exposed: 0.26 ± 0.02 s; control: 0.23 ± 0.01 s $p>0.05$, Figure 4-3C), as was V_t (neonatal-exposed: 12 ± 1 $\mu\text{l/g}$; control: 13 ± 1 $\mu\text{l/g}$, $p>0.05$, Figure 4-3D). Due to the significantly lower respiratory frequency, neonatal-exposed mice also displayed a significantly lower baseline V_e compared to control mice (1797 ± 149 $\mu\text{l/g/min}$ vs 2223 ± 98 $\mu\text{l/g/min}$, $p<0.05$, Figure 4-3E). It should be noted that no obvious respiratory abnormalities or ataxic breathing patterns were observed in any of the control or neonatal-exposed mice. The changes in the respiratory phenotype appeared to be mild.

4.3.3 Acute fentanyl challenge in awake mice

Both control and neonatal-exposed mice were subjected to a fentanyl challenge in adulthood. The acute respiratory response to the fentanyl challenge was first measured in the wakeful state. A range of fentanyl doses (0.04 mg/kg-0.1 mg/kg) were investigated and mice were assigned to receive only one dose.

4.3.3.1 Respiratory Frequency

In the control groups, all 4 fentanyl doses evoked a continual reduction in respiratory frequency from baseline, with the greatest reduction evident at 30 minutes post-injection (Figure 4-4). Respiratory frequency was significantly lower at 30 minutes post 0.04, 0.06 and 0.1 mg/kg fentanyl challenge compared to baseline (0.04 mg/kg: 147 ± 17 bpm vs baseline: 193 ± 27 bpm, $p < 0.05$, Figure 4-4A; 0.06 mg/kg: 137 ± 10 bpm vs baseline: 174 ± 11 bpm, $p < 0.05$, Figure 4-4B; 0.1 mg/kg: 136 ± 18 bpm vs baseline: 171 ± 18 bpm, $p < 0.05$, Figure 4-4D). Respiratory frequency showed a clear trend towards a reduction from baseline at 30 minutes post 0.08 mg/kg fentanyl in the control group (baseline: 181 ± 32 bpm vs 30 mins post-fentanyl: 134 ± 50 bpm, $p > 0.05$, Figure 4-4C). For all doses of fentanyl, respiratory frequency returned to baseline values by 45 minutes post injection in the control groups (Figure 4-4A-D).

In contrast to the control mice, even at the highest dose, a fentanyl challenge failed to induce a depression of respiratory frequency in neonatal-exposed mice. No significant reduction in respiratory frequency from baseline was found at any of the time points examined for any of the fentanyl doses injected ($p > 0.05$, Figure 4-4A-D). Interestingly, at 5 minutes post-fentanyl insult, the neonatal-exposed mice displayed an unexpected increase in respiratory frequency. This was found to be statistically significant after 0.06 mg/kg and 0.01 mg/kg fentanyl challenge ($p < 0.05$, Figure 4-4B and D). This augmented respiratory frequency was not exhibited by the control mice. When looking at the percentage change in respiratory frequency from baseline in response to fentanyl (Figure 4-5), it is evident that the neonatal-exposed mice displayed marked differences in their acute respiratory response to all doses of fentanyl compared to control mice. These data reiterate the changes in absolute respiratory frequency values shown in Figure 4-4 and clearly illustrates the differential frequency response to fentanyl between control and neonatal-exposed mice. At 30 minutes post-fentanyl, control mice showed a clear reduction in

respiratory frequency from baseline (0.04 mg/kg: 23±2% reduction, 0.06 mg/kg: 21±4% reduction, 0.08 mg/kg: 27±16% reduction, 0.1 mg/kg: 20±10% reduction, Figure 4-5), which was not seen in the neonatal-exposed mice (0.04 mg/kg: 8±9% reduction, 0.06 mg/kg: 5±13% reduction, 0.08 mg/kg: 1±1% increase, 0.1 mg/kg: 10±18% increase, Figure 4-5). At 5 minutes post fentanyl injection, the increase in respiratory frequency exhibited by the neonatal-exposed mice ranged from 14±11% to 49±30% depending on the dose of fentanyl administered (Figure 4-5). This increase was not dose related.

4.3.3.2 Tidal volume

In the control group, fentanyl at all doses did not induce any significant changes in Vt at any of the time points post-injection ($p>0.05$ Figure 4-6). At 5 minutes post 0.04 and 0.06 mg/kg fentanyl, there was a trend towards an increase in Vt from baseline (0.04 mg/kg: 15±2 µl/g vs baseline: 13±2 µl/g, $p>0.05$ Figure 4-6A; 0.06 mg/kg: 17±3 µl/g vs baseline: 13±3 µl/g, $p>0.05$, Figure 4-6B). At 15 minutes post injection of 0.1 mg/kg fentanyl there was also a trend towards an increase in Vt from baseline (17±2 µl/g vs baseline: 14±5 µl/g, $p>0.05$ Figure 4-6D). Administration of 0.04 mg/kg and 0.1 mg/kg fentanyl to the neonatal-exposed mice evoked a significant increase in Vt at 5 minutes and 15 minutes post-injection ($p<0.05$, Figure 4-6A and D). Administration of 0.06 mg/kg fentanyl to the neonatal-exposed mice induced a significant increase in Vt from baseline seen at 5 minutes post-fentanyl ($p<0.05$, Figure 4-6B). There was a trend towards an increase in Vt at 5 minutes after 0.08 mg/kg fentanyl administration in the neonatal-exposed mice ($p>0.05$, Figure 4-6C). Figure 4-7 illustrates the Vt response to fentanyl as a percentage change from baseline. From this figure, it is apparent that the neonatal-exposed mice exhibited a large percentage increase in Vt from baseline in response to fentanyl, particularly at the 5 minute time point following the fentanyl challenge (0.04 mg/kg: 57±30% increase, 0.06 mg/kg: 77±34% increase, 0.1 mg/kg: 74±20% increase, Figure 4-7A, B and D). The Vt increase was not as pronounced following 0.08 mg/kg fentanyl (Figure 4-7C). Whilst Vt increases in response to fentanyl were seen in the control mice at 5, 15 and 30 minutes after injection, the magnitude was smaller than that displayed by the neonatal-exposed mice (Figure 4-7A-D).

4.3.3.3 Minute ventilation

Fentanyl given at a dose of 0.04 mg/kg and 0.06 mg/kg, induced a significant increase in V_e observed at 5 minutes post-administration in the control mice (0.04 mg/kg: 2358 ± 1453 $\mu\text{l/g/min}$ vs 3185 ± 183 $\mu\text{l/g/min}$; 0.06 mg/kg: 2134 ± 485 $\mu\text{l/g/min}$ vs 3207 ± 1070 $\mu\text{l/g/min}$ for baseline vs 5 mins post-fentanyl respectively, $p < 0.05$, Figure 4-8A and B). This increase is likely due to the trend towards the increased V_t at this time point (Figure 4-6). There was no significant change in V_e at any of the other time points studied ($p > 0.05$, Figure 4-8A and B). In the control mice, V_e remained unchanged at all time points following 0.08 mg/kg and 0.1 mg/kg fentanyl challenge (Figure 4-8C and D). Owing to the increases in both respiratory frequency and V_t in response to fentanyl, the V_e of the neonatal-exposed mice showed a significant increase 5 minutes after injection of 0.04 mg/kg, 0.06 mg/kg and 0.1 mg/kg fentanyl ($p < 0.05$, Figure 4-8A,B and D). There was a trend toward an increase in V_e in response to 0.08 mg/kg fentanyl at 5 minutes post-injection ($p > 0.05$, Figure 4-8C). In the neonatal-exposed group, V_e was comparable with baseline values at 10, 15 and 45 minutes post-injection, except in the group administered 0.1 mg/kg, where V_e remained significantly elevated up to 15 minutes post-fentanyl. When observing the percentage changes in V_e in response to all doses of fentanyl, it is evident that when compared to the control group, neonatal-exposed mice exhibited a greater fentanyl-induced increase in V_e at 5 minutes following administration (Figure 4-9).

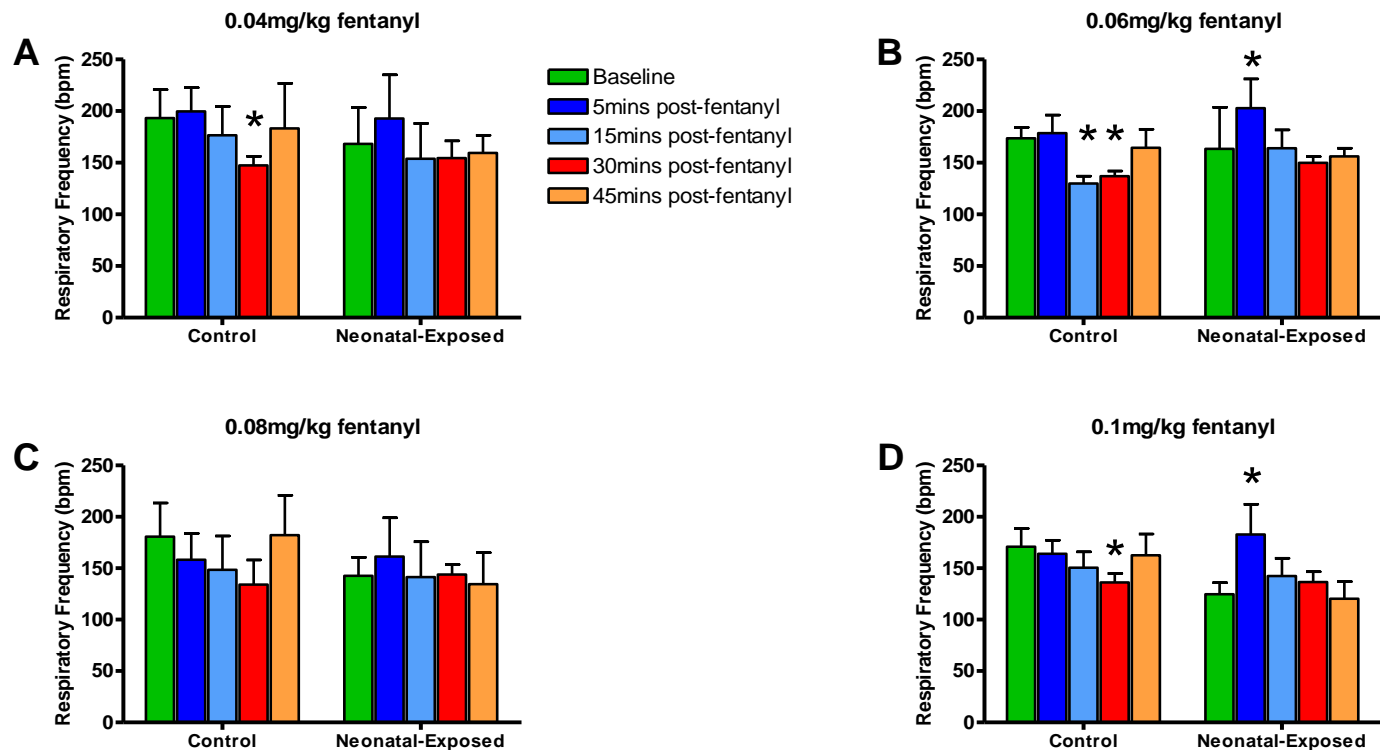


Figure 4-4. Changes in respiratory frequency in response to a single fentanyl challenge in control and neonatal-exposed mice when awake. Acute response to 0.04 mg/kg fentanyl (A), 0.06 mg/kg fentanyl (B), 0.08 mg/kg fentanyl (C) and 0.1 mg/kg fentanyl (D). Control mice; n=4, neonatal-exposed; n=4 for all 4 fentanyl groups. Data presented as mean±SD. * denotes a significant difference (p<0.05) from baseline, 2-way ANOVA with Bonferroni's post test.

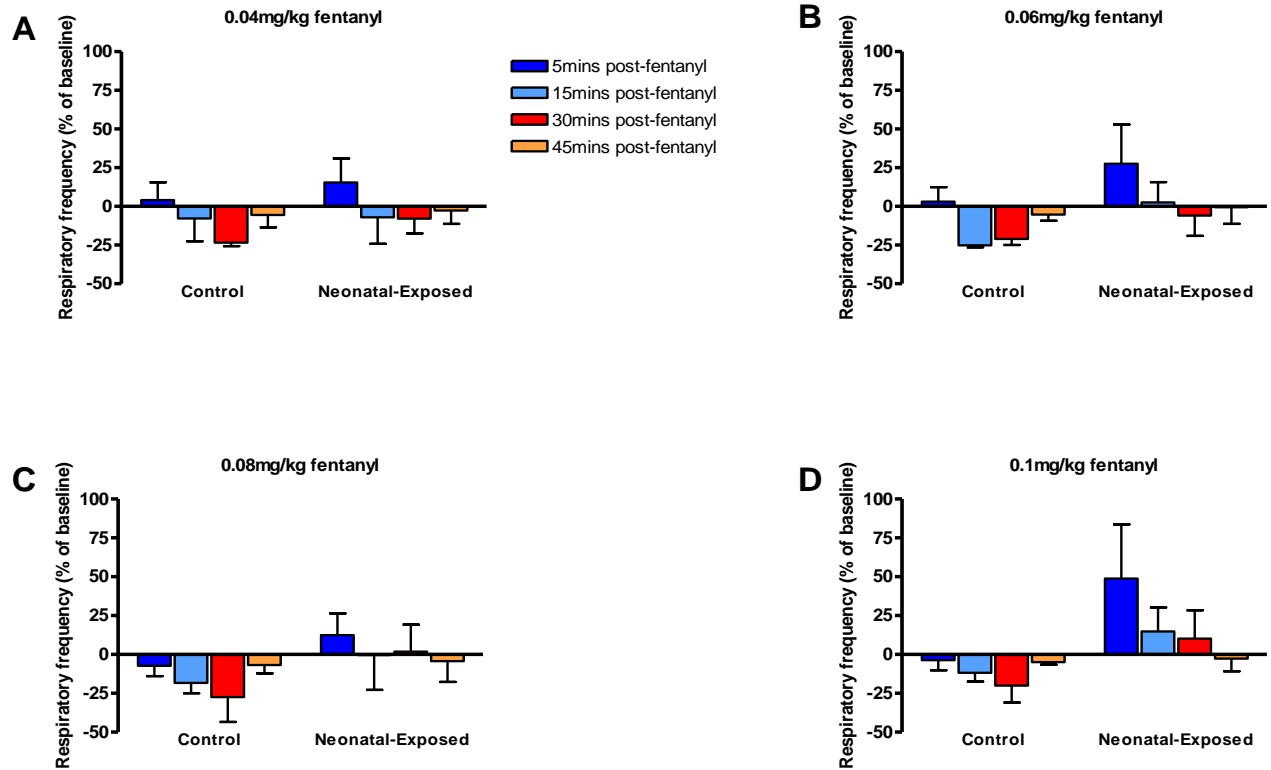


Figure 4-5. Percentage change in respiratory frequency in response to a single fentanyl challenge in control and neonatal-exposed mice when awake. Data shown as a percentage change from baseline. Acute response to 0.04 mg/kg fentanyl (A), 0.06 mg/kg fentanyl (B), 0.08 mg/kg fentanyl (C) and 0.1 mg/kg fentanyl (D). Control mice; n=4, neonatal-exposed; n=4 for all 4 fentanyl groups. Data presented as mean±SD.

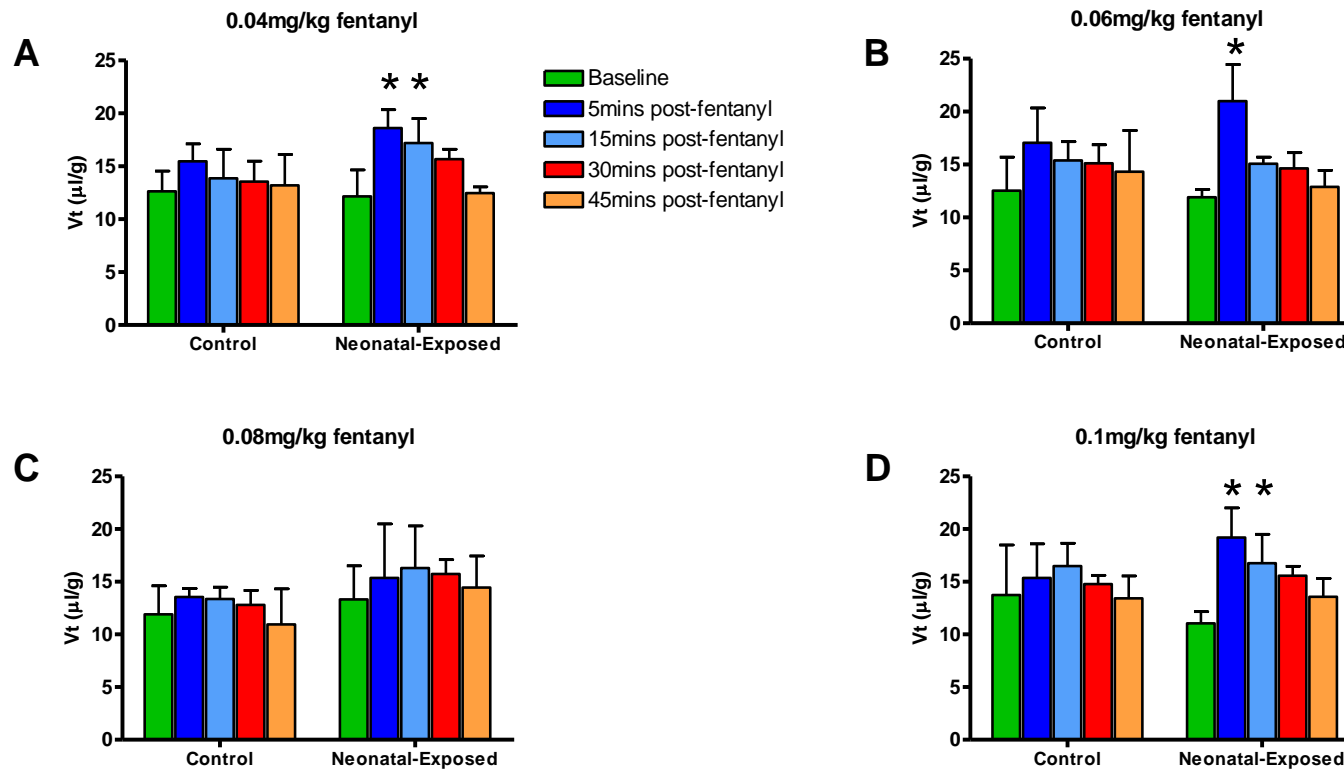


Figure 4-6. Changes in tidal volume (Vt) in response to a single fentanyl challenge in control and neonatal-exposed mice when awake. Acute Vt response to 0.04 mg/kg fentanyl (A), 0.06 mg/kg fentanyl (B), 0.08 mg/kg fentanyl (C) and 0.1 mg/kg fentanyl (D). Control mice; n=4, neonatal-exposed; n=4 for all 4 fentanyl groups. Data presented as mean±SD. * denotes a significant difference (p<0.05) from baseline, 2-way ANOVA with Bonferroni's post test.

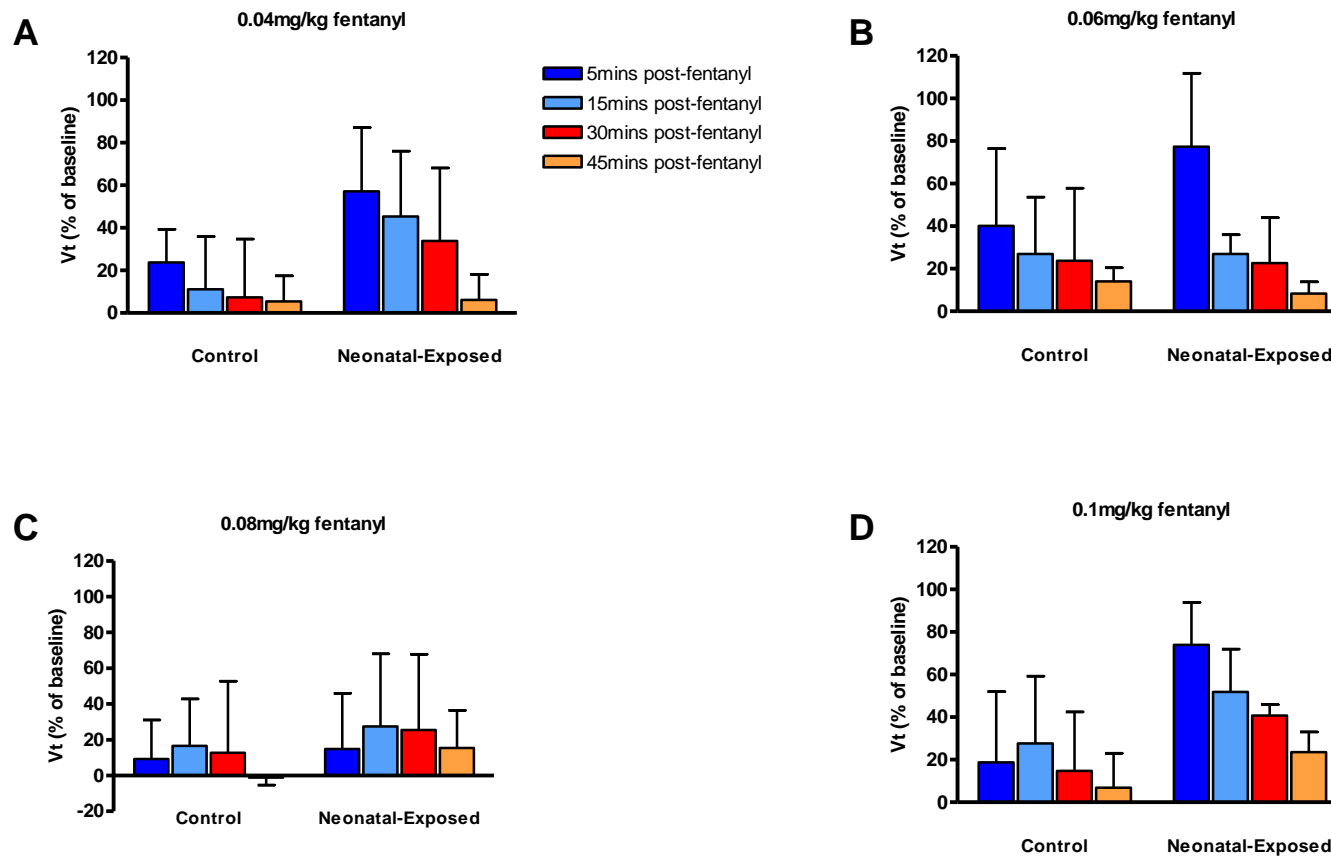


Figure 4-7. Percentage change in tidal volume (Vt) in response to a single fentanyl challenge in control and neonatal-exposed mice when awake. Data shown as a percentage change from baseline. Acute response to 0.04 mg/kg fentanyl (A), 0.06 mg/kg fentanyl (B), 0.08 mg/kg fentanyl (C) and 0.1 mg/kg fentanyl (D). Control mice; n=4, neonatal-exposed; n=4 for all 4 fentanyl groups. Data presented as mean±SD.

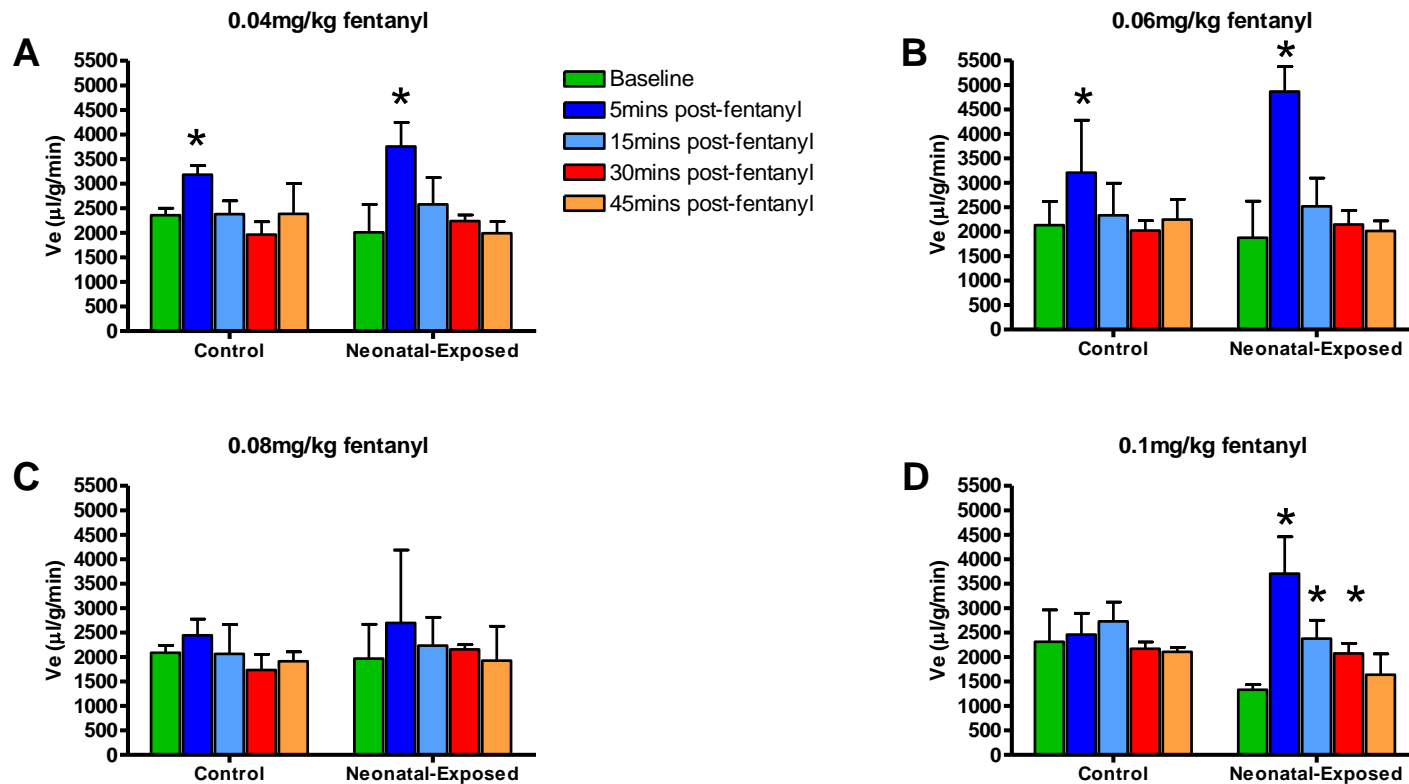


Figure 4-8. Changes in minute ventilation (V_e) in response to a single fentanyl challenge in control and neonatal-exposed mice when awake. Acute V_e response to 0.04 mg/kg fentanyl (A), 0.06 mg/kg fentanyl (B), 0.08 mg/kg fentanyl (C) and 0.1 mg/kg fentanyl (D). Control mice; $n=4$, neonatal-exposed; $n=4$ for all 4 fentanyl groups. Data presented as mean \pm SD. * denotes a significant difference ($p<0.05$) from baseline, 2-way ANOVA with Bonferroni's post test.

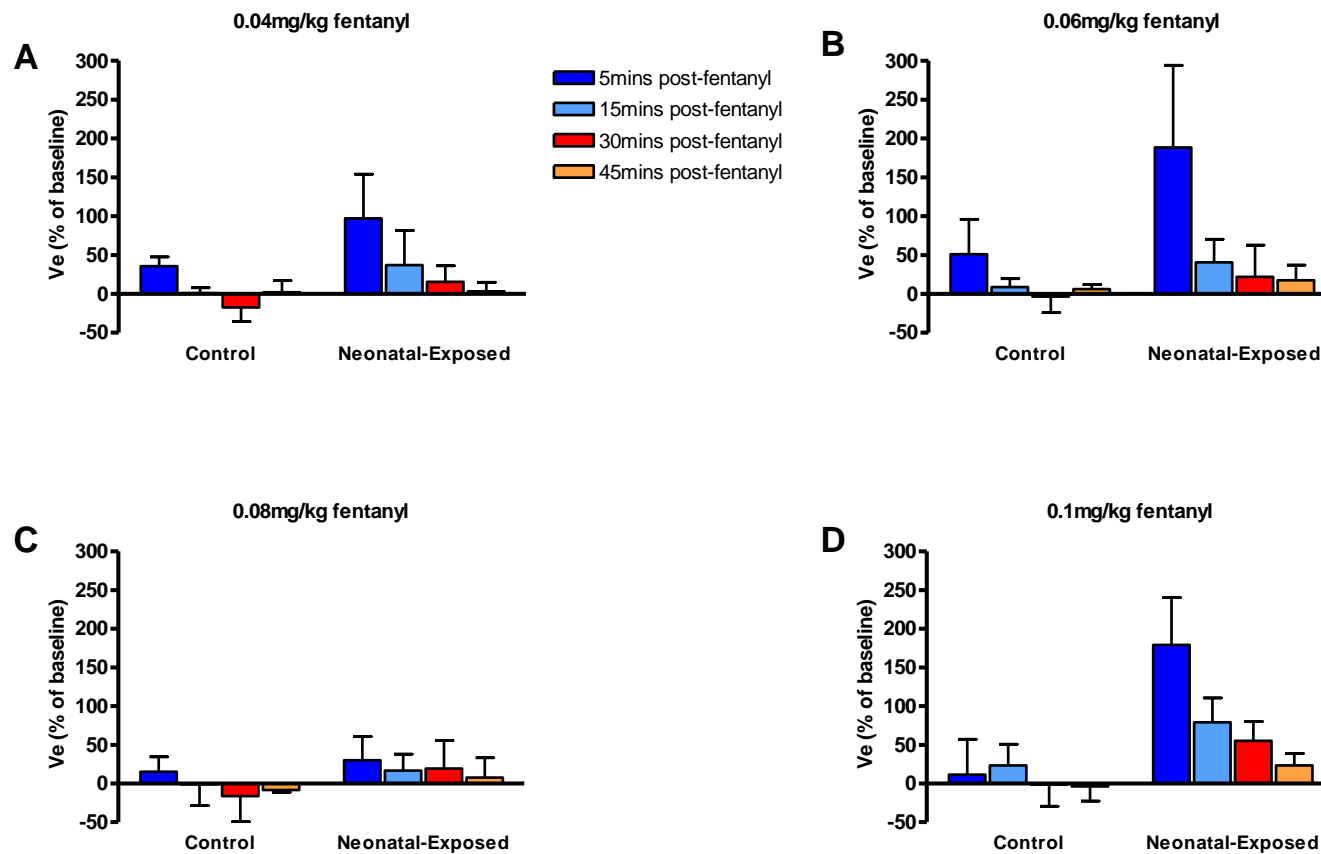


Figure 4-9. Percentage change in minute ventilation (Ve) in response to a single fentanyl challenge in control and neonatal-exposed mice when awake. Data shown as a percentage change from baseline. Acute Ve response to 0.04 mg/kg fentanyl (A), 0.06 mg/kg fentanyl (B), 0.08 mg/kg fentanyl (C) and 0.1 mg/kg fentanyl (D). Control mice; n=4, neonatal-exposed; n=4 for all 4 fentanyl groups. Data presented as mean±SD.

4.3.3.4 Plethysmography respiratory traces

Baseline breathing and the differential acute respiratory response to a fentanyl challenge exhibited between the control and neonatal-exposed mice can be clearly seen from Figure 4-10, which shows example plethysmography respiratory traces before and after administration of the lowest dose of 0.04 mg/kg fentanyl (A) and the highest dose of 0.1 mg/kg fentanyl (B). It is clear that both groups of mice displayed rhythmic baseline breathing with no respiratory disturbances or irregularities. From the respiratory traces it is also apparent that the neonatal-exposed mice had a lower baseline respiratory frequency compared to the control mice (Figure 4-10A and B). It is evident that fentanyl, at both doses, induced a reduction in respiratory frequency and caused an increase in V_t at 30 minutes following administration in the control mice. However, the traces taken from the neonatal-exposed mice show that in contrast to the control mice, fentanyl at both doses failed to induce a respiratory depression from baseline, but rather evoked an increase in both respiratory frequency and V_t at 5 minutes after the challenge.

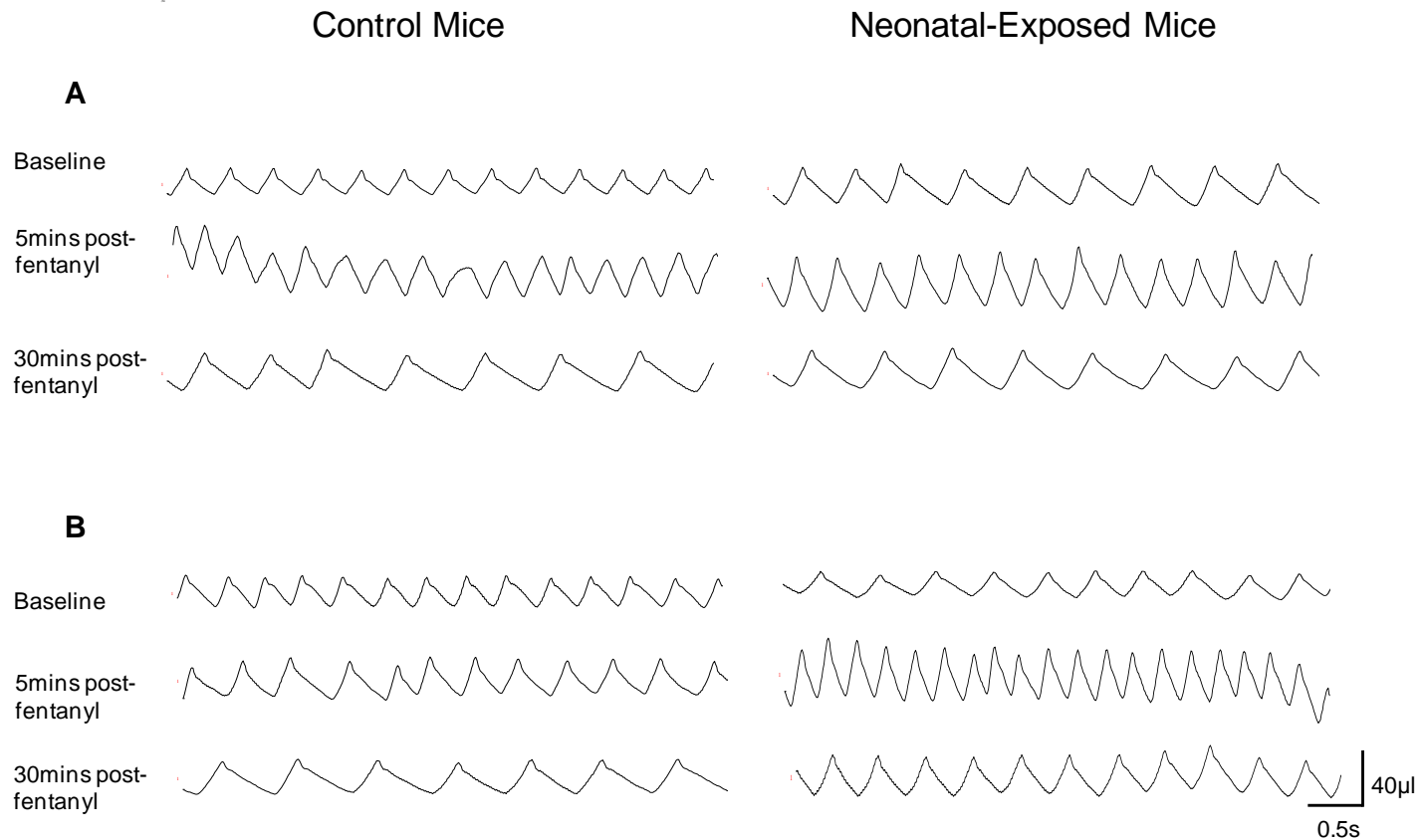


Figure 4-10. Representative respiratory traces before and after fentanyl challenge in control and neonatal-exposed mice. The effects of 0.04 mg/kg (A) and 0.1 mg/kg fentanyl (B) are shown. It is evident that fentanyl at both doses did not induce respiratory depression in the neonatal-exposed mice.

4.3.4 Chemosensitivity

In a subgroup of neonatal-exposed (n=5) and control mice (n=5), chemosensory responses were assessed in adult life when the mice were in the wakeful state. Both groups of mice displayed similar chemosensory responses to hypercapnia and hypoxia and exhibited a comparable respiratory recovery from the stimuli (Figure 4-11). No significant difference in the respiratory parameters under each of the chemosensory stimuli was found between the experimental groups ($p>0.05$, Figure 4-11 A-C). Both groups of mice displayed an increase in respiratory frequency, V_t , and therefore V_e in response to the increasing intensity of hypercapnic stimuli (3%, 5% and 8% CO_2). When normoxia was re-established, respiratory frequency, V_t and V_e returned to baseline values by 15 minutes and were still maintained within baseline levels 30 minutes following hypercapnia. After 5 minutes exposure to hypoxia (10% O_2), respiratory frequency of both control and neonatal-exposed mice increased but began to show a trend towards a decrease by 10 minutes of exposure. V_t did not change in response to either 5 minutes or 10 minutes of hypoxia exposure in both experimental groups. V_e increased after 5 minutes exposure to hypoxia and then started to decrease by 10 minutes exposure in both control and neonatal-exposed. These changes in V_e were due to the corresponding hypoxia-induced changes in respiratory frequency. At the 2 minute recovery period (under normoxia) following hypoxia, both groups of mice exhibited a respiratory frequency, V_t and V_e comparable to baseline values, which was maintained up to 30 minutes following hypoxic exposure.

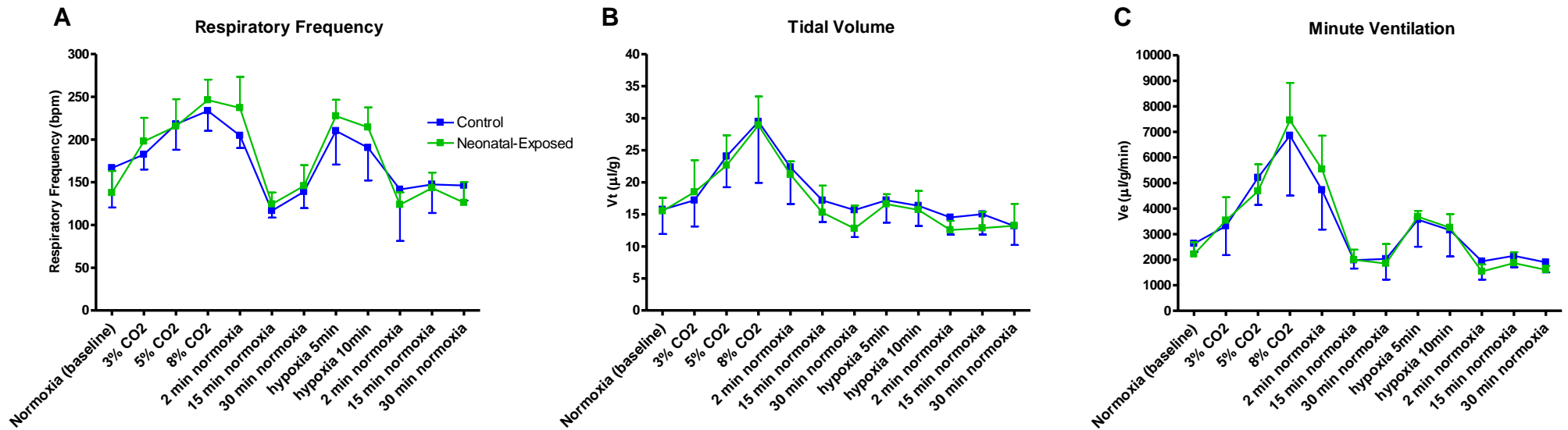


Figure 4-11. Respiratory responses of control and neonatal-exposed mice to hypercapnic and hypoxic stimuli in the wakeful state. Respiratory frequency (A) tidal volume (B) and minute ventilation (C) were measured under each respiratory stimulus. Control: n=5; neonatal-exposed: n=5. No significant difference in the respiratory parameters under each respiratory stimulus was found between the experimental groups, $p > 0.05$, 2-way ANOVA. Data presented as mean \pm SD.

4.3.5 Baseline respiratory parameters of adult mice under anaesthesia

After respiratory monitoring in the conscious state, a more detailed respiratory analysis was carried out in anaesthetised mouse preparations. When under anaesthesia, the baseline respiratory frequency was comparable between the two experimental groups (neonatal-exposed: 165 ± 10 bpm, control: 181 ± 9 bpm, $p > 0.05$, Figure 4-12A). In accordance with this, both groups exhibited a similar inspiratory duration (neonatal-exposed: 0.14 ± 0.001 s; control: 0.15 ± 0.004 s, $p > 0.05$, Figure 4-12B) and expiratory duration (neonatal-exposed: 0.25 ± 0.03 s; control: 0.20 ± 0.02 s, $p > 0.05$, Figure 4-12C). Under anaesthesia, the neonatal-exposed mice had a significantly lower baseline V_t compared to control mice (4 ± 0.2 $\mu\text{l/g}$ vs 5 ± 0.1 $\mu\text{l/g}$, $p < 0.05$, Figure 4-12D). As a result of the significantly lower V_t , the neonatal-exposed mice also displayed a significantly lower V_e than the control group (663 ± 59 $\mu\text{l/g/min}$ vs 863 ± 45 $\mu\text{l/g/min}$, $p < 0.05$, Figure 4-12E). Interestingly, both groups of mice displayed a reduced baseline V_t compared with the values observed during wakefulness (wakefulness; neonatal-exposed: 12 ± 1 $\mu\text{l/g}$, control: 13 ± 1 $\mu\text{l/g}$, Figure 4-3D). No significant difference in baseline GG_{EMG} amplitude was found between the experimental groups (neonatal-exposed: 0.15 ± 0.03 a.u; control: 0.18 ± 0.13 a.u; $p > 0.05$, Figure 4-12F). It is important to highlight that in all experimental mice, the GG muscle displayed a rhythmic, inspiratory-related mode of activity (Figure 4-13).

From the outset of study 4, one of the aims was to gain a measure of baseline expiratory muscle function to determine if this differed between the two experimental groups. The abdominal muscles have been previously reported to exhibit expiratory-related activity in urethane-anaesthetised rats (Pagliardini et al., 2012) thus their activity was recorded in this study. However, rhythmic expiratory ABD_{EMG} activity (i.e. muscle firing concurrently with expiratory airflow in the absence of GG_{EMG} activity) was found in only two of the mice studied (1 control and 1 neonatal-exposed), and in these mice the rhythmic activity appeared suddenly and was of short duration (approximately 2 minutes). In all experimental mice, abdominal muscle activity was predominantly sporadic in nature and did not appear to be respiratory-modulated. For this reason, no quantitative analysis of abdominal muscle activity was performed. Examples of non-respiratory related and expiratory-modulated ABD_{EMG} activity observed in study 4 are illustrated in Figure 4-13.

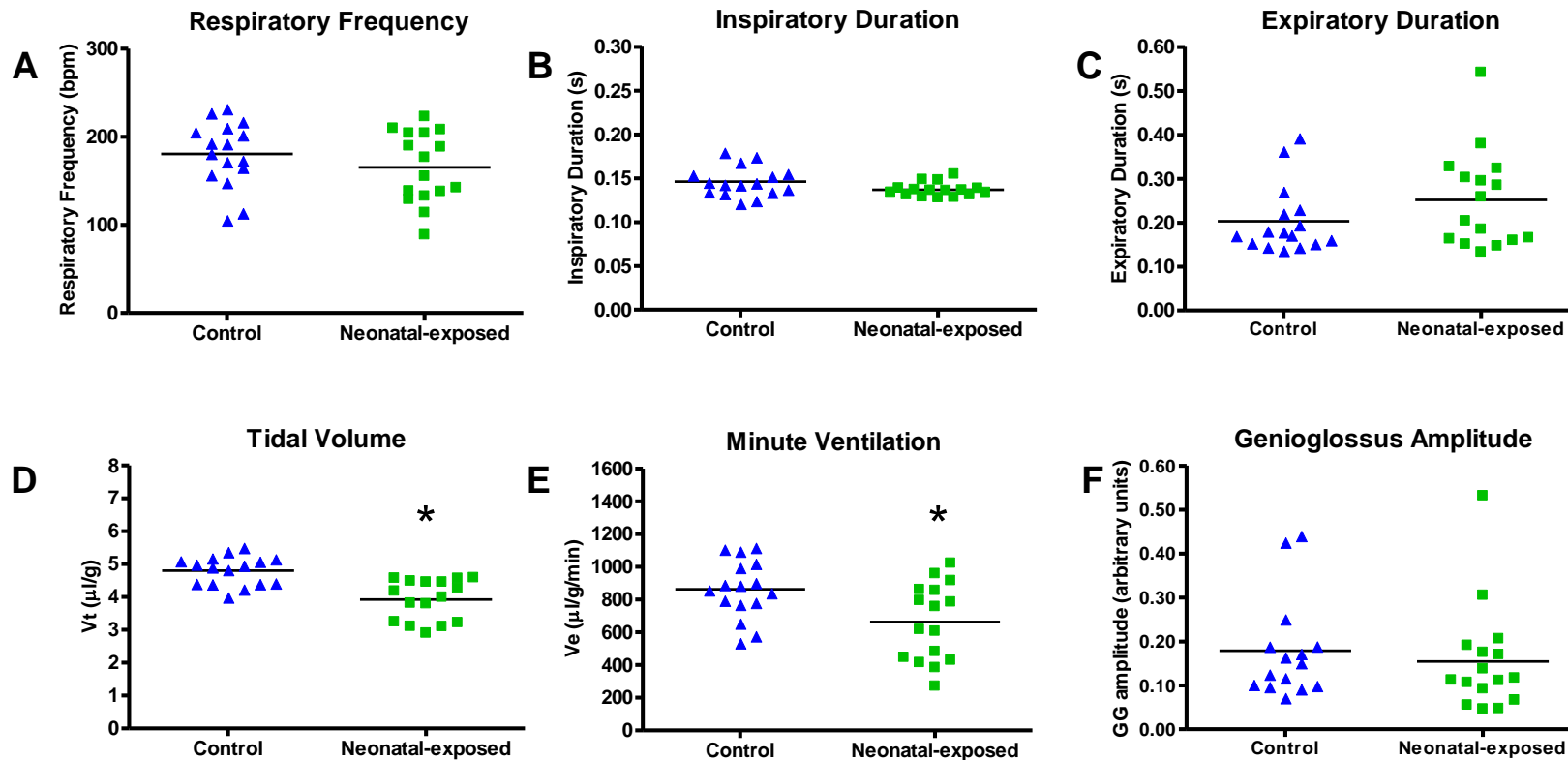


Figure 4-12. Baseline respiratory parameters of adult control and neonatal-exposed mice under anaesthesia. Control mice, n=16; Neonatal-exposed, n=16. Each data point on the scatter plots represents an individual animal. Line denotes the mean. * p<0.05, Student's unpaired t-test.

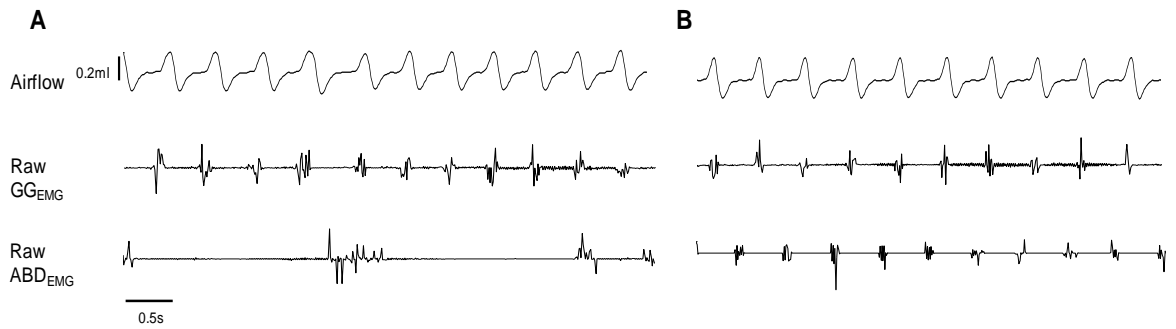


Figure 4-13. Examples of baseline GG_{EMG} and ABD_{EMG} activity. In all experimental mice, the GG showed an inspiratory-modulated pattern of activity (A and B). Sporadic, non-expiratory related ABD muscle activity was exhibited by all urethane-anaesthetised mice (A). Rhythmic, expiratory-modulated abdominal activity was found in only 2 experimental mice (B). This ABD rhythmic EMG bursting was synchronised with the expiratory phase of breathing. It was, however, present for only a short duration.

4.3.6 Augmented breaths

The number of large amplitude, augmented breaths (illustrated in Figure 4-14A) present during 10 minutes of continuous baseline breathing under anaesthesia was quantified for control and neonatal-exposed mice. Neonatal-exposed mice on average exhibited a significantly greater number of augmented breaths compared to the control animals (10.1 ± 12.5 augmented breaths/10 mins vs 0.8 ± 1.4 augmented breaths/10 mins, $p < 0.05$, Figure 4-14B). It is important to note that the number of augmented breaths exhibited by the neonatal-exposed mice was variable. Out of the 16 control mice, 5 mice exhibited augmented breaths (31.3%), whereas 12 out of 16 neonatal-exposed mice displayed augmented breaths (75.0%).

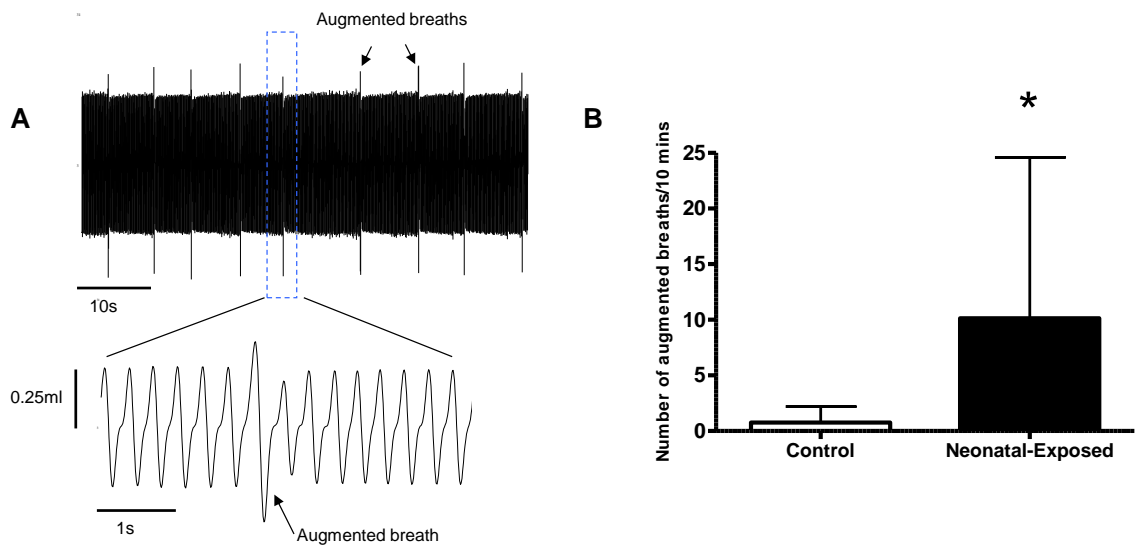


Figure 4-14. Number of augmented breaths exhibited by control and neonatal-exposed mice under anaesthesia. An augmented breath is defined as an increased respiratory effort, with a tidal volume >50% of a regular breath. The number of augmented breaths observed during 10 minutes of baseline breathing was quantified. A: a representative airflow trace from a neonatal-exposed mouse illustrating the presence of augmented breaths during baseline breathing. Augmented breaths appear as spikes in the compressed airflow trace on top. The area demarcated by the blue box is expanded and show in the trace below. B: neonatal-exposed mice (n=16) exhibited a significantly greater number of augmented breaths during baseline breathing (10 minutes) compared to control mice (n=16). * $p < 0.05$, Mann Whitney test. Data presented as mean \pm SD.

4.3.7 Acute fentanyl challenge in anaesthetised mice

When mice were under anaesthesia, fentanyl was found to induce a quicker and more pronounced respiratory depression compared to the effects when awake. For this reason the range of doses investigated was decreased. The doses administered ranged from 0.01 mg/kg-0.06 mg/kg. Mice were assigned only one dose. All neonatal-exposed mice displayed a complete respiratory failure in response to fentanyl that occurred at varying time points post-injection, therefore the absolute values for each of the respiratory parameters were not averaged at each time point as this would result in the data being skewed. Thus the percentage changes from baseline are shown.

4.3.7.1 Respiratory frequency

Fentanyl at all doses induced a depression of respiratory frequency in the control group (Figure 4-15). A reduction in respiratory frequency was seen as early as 5 minutes following fentanyl injection (0.01 mg/kg: $12\pm 2\%$ reduction; 0.02 mg/kg: $18\pm 6\%$ reduction; 0.04 mg/kg: $33\pm 28\%$ reduction; 0.06 mg/kg: $40\pm 27\%$ reduction, Figure 4-15A-D). Although the respiratory frequency never returned to baseline levels, all control mice continued to spontaneously breathe for the duration of the experiment, i.e. up to 60 minutes post-fentanyl challenge. With the neonatal-exposed mice, fentanyl evoked a profound depression of the respiratory frequency that was of a significantly greater magnitude compared with the control mice, and resulted in a respiratory arrest in 100% of the mice (Figure 4-15, $p < 0.05$). This fentanyl-induced respiratory failure was observed at all fentanyl doses. Respiratory arrest was identified as a complete cessation of airflow and genioglossus muscle activity and is indicated on the plots when the data line reaches a value of zero (Figure 4-15A-D). When respiratory arrest was identified, artificial ventilation was provided, however spontaneous breathing never returned in any of the neonatal-exposed mice. The average latency for complete suppression of respiration varied depending on the dose of fentanyl administered, and was variable between individual mice, but by 30 minutes post-injection all of the neonatal-exposed mice exhibited complete respiratory depression. At the highest dose of 0.06 mg/kg, fentanyl induced respiratory failure within 5 minutes following the acute challenge (Figure 4-15D). Given that 0.06 mg/kg fentanyl induced such a rapid respiratory failure, only 2 neonatal-exposed mice were studied in this group. The high variability in the average data from the neonatal-exposed mice, highlighted by the large error bars, is attributed to the fact than mice entered

respiratory failure at varying times post-injection. It is very interesting to highlight the fact that anaesthetised neonatal-exposed mice displayed a striking difference in their response to fentanyl when compared to the wakeful state, where fentanyl did not induce a respiratory frequency depression.

4.3.7.2 Tidal volume and minute ventilation

Fentanyl at all doses induced a reduction in V_t from baseline in the control mice (Figure 4-16), which was evident at 5 minutes post-fentanyl (0.01 mg/kg: $5\pm 4\%$ reduction; 0.02 mg/kg: $11\pm 19\%$ reduction; 0.04 mg/kg: $15\pm 13\%$ reduction; 0.06 mg/kg: $12\pm 7\%$ reduction, Figure 4-16A-D). Post-injection, V_t never reached baseline values except in the group of mice administered 0.02 mg/kg fentanyl, where V_t returned to baseline levels by 60 minutes following administration. Similar to respiratory frequency effects, fentanyl at all doses, evoked a significantly greater depression of V_t in the neonatal-exposed mice (Figure 4-16 $p < 0.05$), inducing a complete suppression. As a result of the combined effects on respiratory frequency and V_t , neonatal-exposed mice also exhibited a complete failure in V_e in response to all doses of fentanyl, which was not observed in the control mice (Figure 4-17).

4.3.7.3 Genioglossus activity

The effect of an acute fentanyl insult on the GG_{EMG} activity was also measured. Fentanyl did not appear to induce a marked depression of the amplitude of the GG activity in the control mice at any of the time points following fentanyl administration. This was observed for all of the doses of fentanyl studied (Figure 4-18A-D). It should be noted that there was a high degree of variability in the response of the GG muscle to fentanyl between individual control mice. Some mice displayed an increase in the amplitude of EMG bursting; others displayed a decrease and most showed no change. In the neonatal-exposed mice, all fentanyl doses induced a complete suppression of the GG_{EMG} (Figure 4-18A-D). The failure in the GG muscle output occurred at the same time as the ventilatory arrest. Not all neonatal-mice displayed a gradual decline in GG muscle function after fentanyl injection; some displayed an increase in activity just prior to ventilatory failure which seemed to be irrespective of the fentanyl dose. The reduction in the amplitude of the GG_{EMG} activity after a 0.01 mg/kg and 0.02 mg/kg fentanyl challenge was significantly greater than the control mice. Due to the high level of variability in the data, no statistically

significant difference was found in the GG_{EMG} response between control and neonatal-exposed animals after injection of 0.04 mg/kg and 0.06 mg/kg fentanyl ($p>0.05$). Considering the fact that complete suppression of the muscle activity was induced in the neonatal-exposed mice and not in the control animals, the findings were evidently biologically significant. In both the control and neonatal-exposed mice, the genioglossus fired simultaneously with the inspiratory phase i.e. it was inspiratory-modulated (Figure 4-19), and thus the rate of muscle bursting was always identical to the respiratory frequency. Fentanyl therefore always depressed the frequency of genioglossus firing to the same extent as the respiratory frequency.

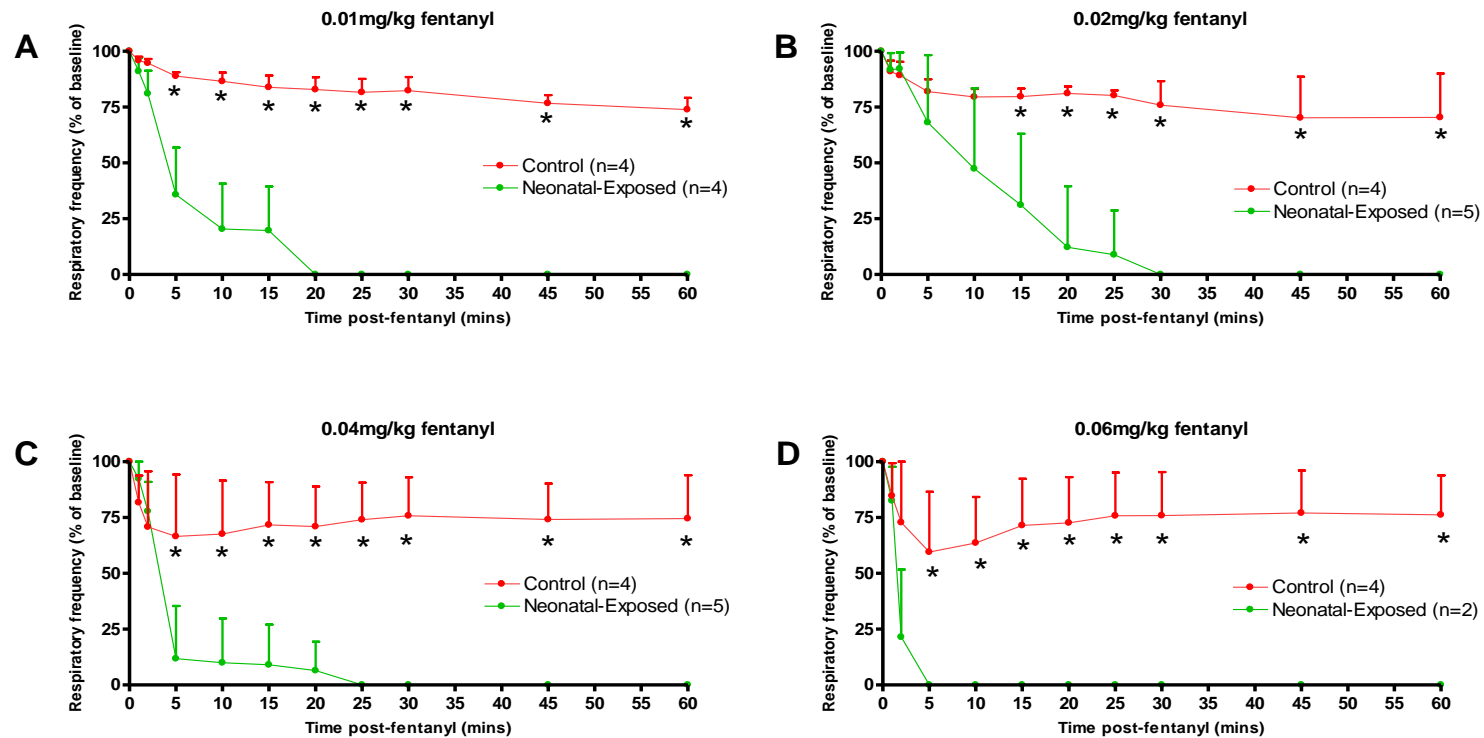


Figure 4-15. Changes in respiratory frequency in response to a fentanyl challenge in control and neonatal-exposed mice under anaesthesia. Data shows the change in respiratory frequency as a percentage of baseline, where baseline represents 100%. Acute effects of 0.01 mg/kg (A) 0.02 mg/kg (B) 0.04 mg/kg (C) and 0.06 mg/kg fentanyl (D). When values reached 0% of baseline this represents respiratory failure, seen in all neonatal-exposed mice in response to all doses of fentanyl. This response was not exhibited by the control animals. Data presented as mean±SD. *denotes a significant difference between the experimental groups ($p < 0.05$), 2-way ANOVA with Bonferroni's post test.

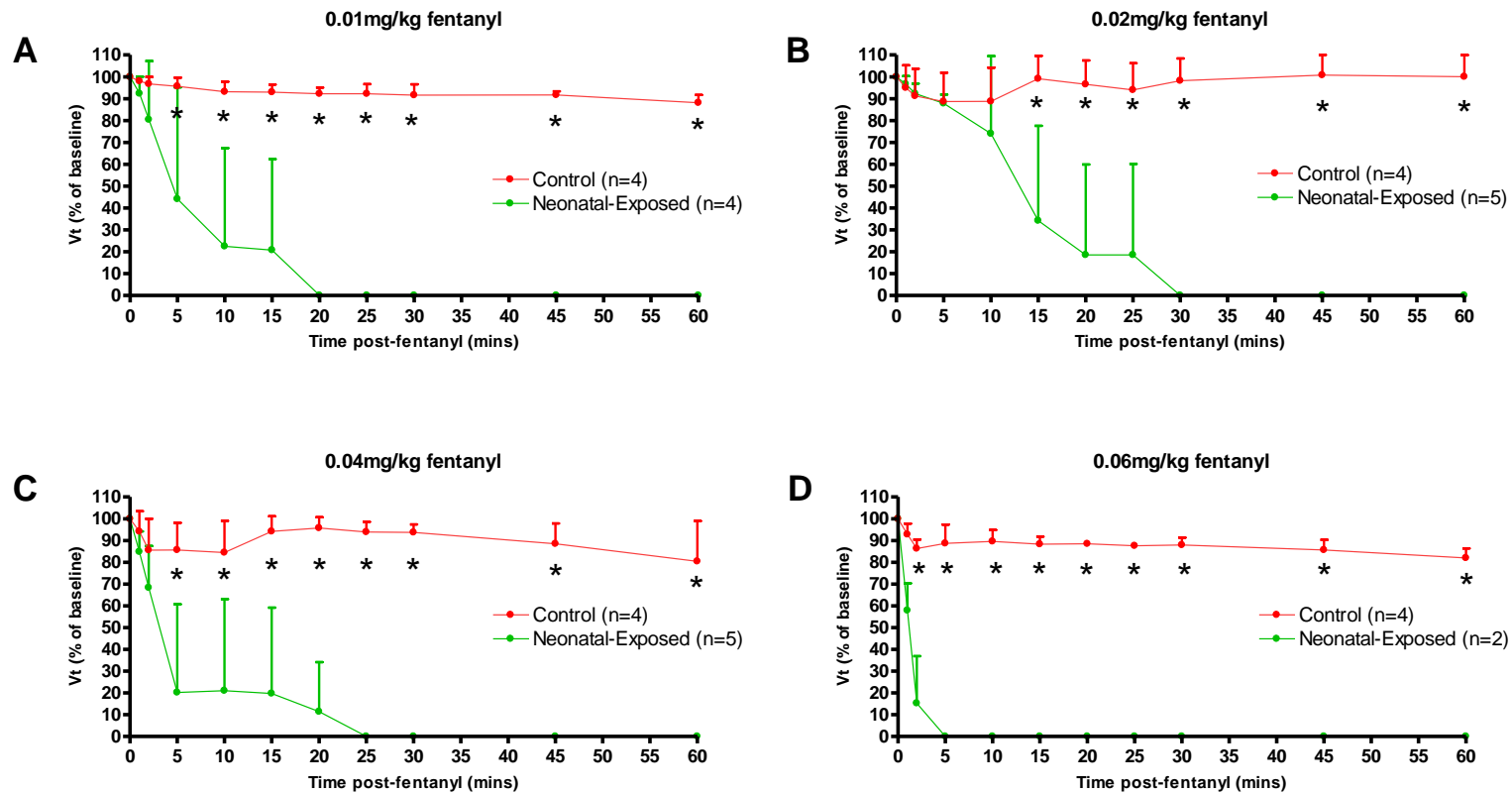


Figure 4-16. Changes in tidal volume (Vt) in response to a fentanyl challenge in control and neonatal-exposed mice under anaesthesia. Data shows the change in Vt as a percentage of baseline, where baseline represents 100%. Acute effects of 0.01 mg/kg (A) 0.02 mg/kg (B) 0.04 mg/kg (C) and 0.06 mg/kg fentanyl (D). When values reached 0% of baseline this represents respiratory failure, seen in all neonatal-exposed mice in response to all doses of fentanyl. This response was not exhibited by the control animals. Data presented as mean±SD. *denotes a significant difference between the experimental groups (p<0.05), 2-way ANOVA with Bonferroni's post test.

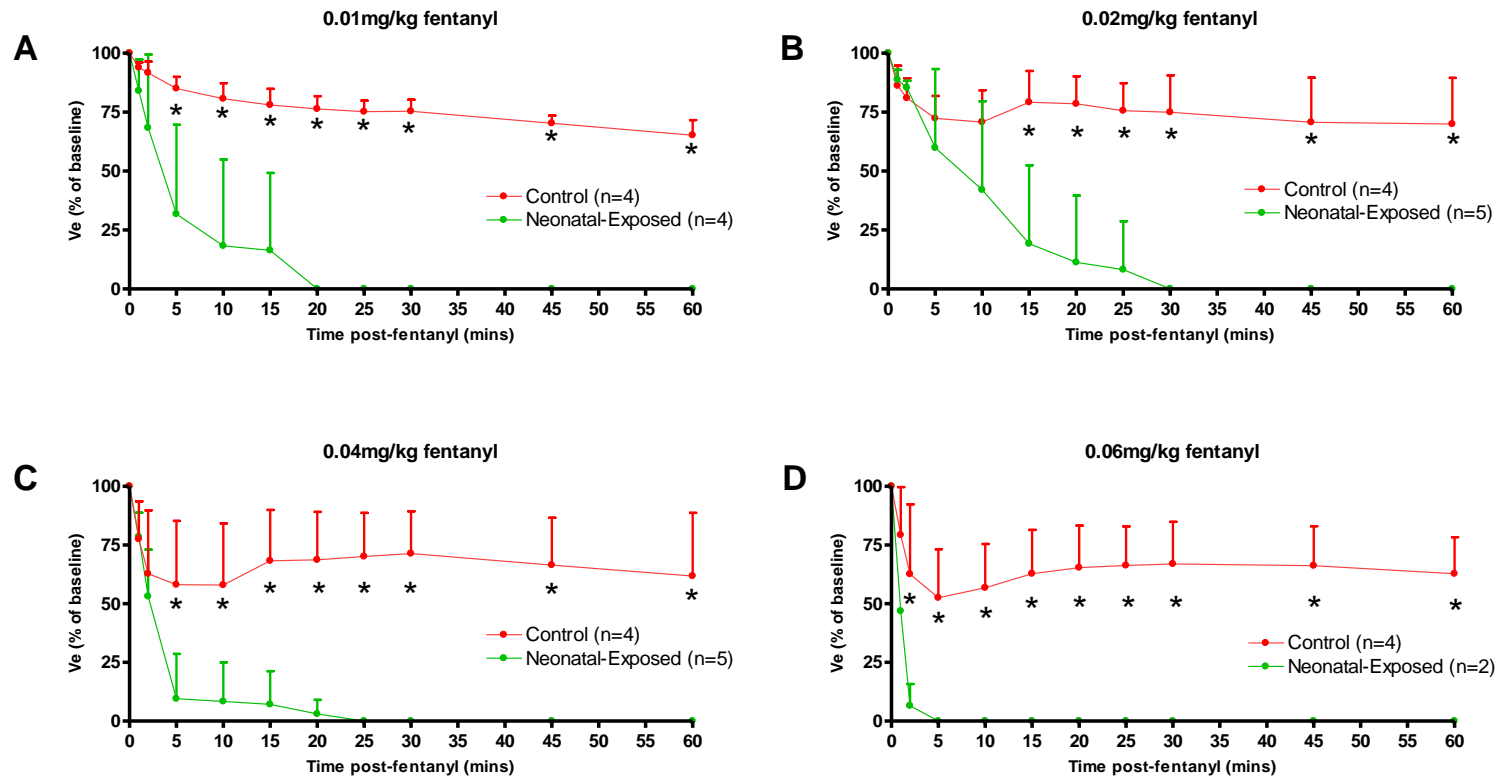


Figure 4-17. Changes in minute ventilation (V_e) in response to a fentanyl challenge in control and neonatal-exposed mice under anaesthesia. Data shows the change in V_e as a percentage of baseline, where baseline represents 100%. Acute effects of 0.01 mg/kg (A) 0.02 mg/kg (B) 0.04 mg/kg (C) and 0.06 mg/kg fentanyl (D). When values reached 0% of baseline this represents respiratory failure, seen in all neonatal-exposed mice in response to all doses of fentanyl. This response was not exhibited by the control animals. Data presented as mean \pm SD. *denotes a significant difference between the experimental groups ($p < 0.05$), 2-way ANOVA with Bonferroni's post test.

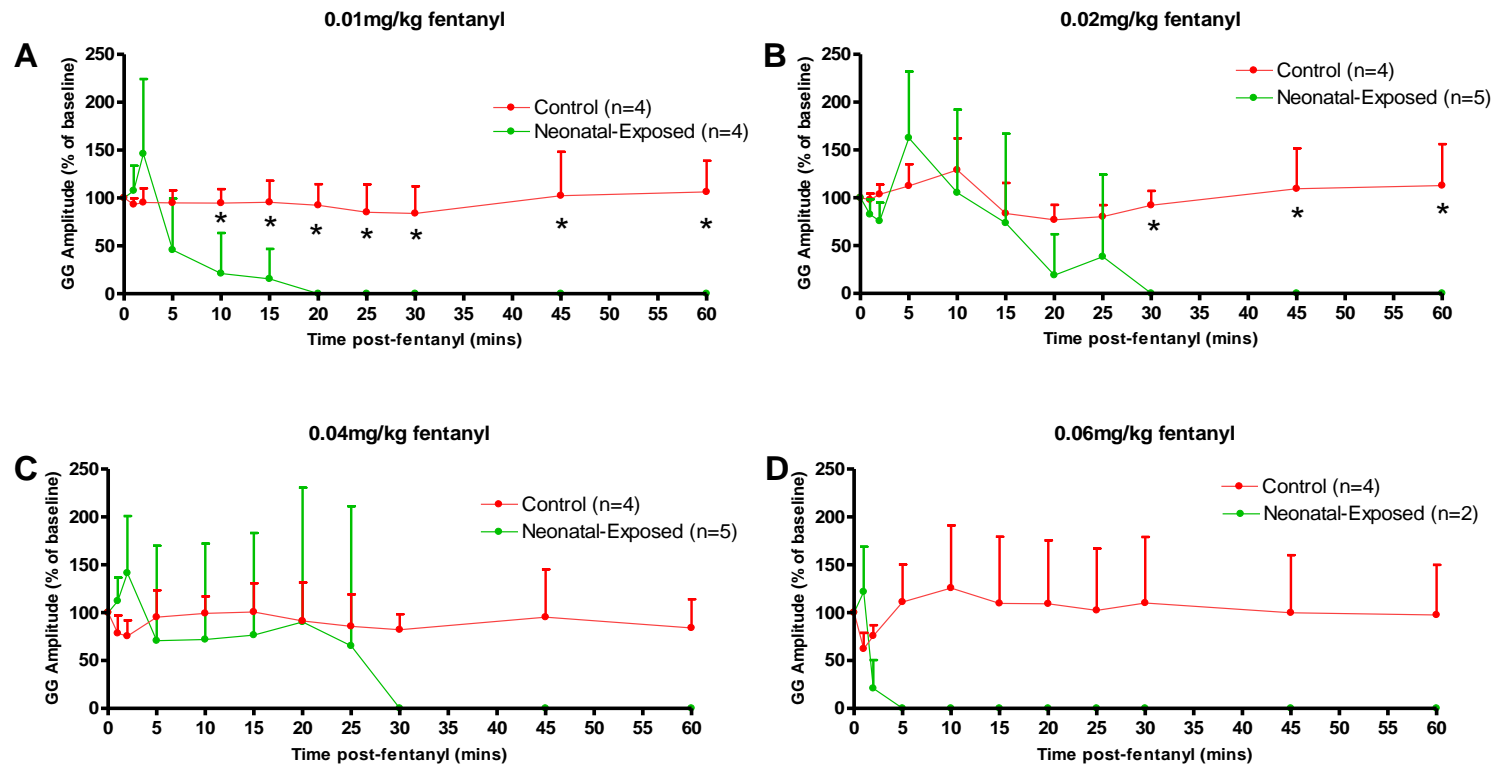


Figure 4-18. Changes in genioglossus amplitude in response to a fentanyl challenge in control and neonatal-exposed mice under anaesthesia. Data shows the change in GG amplitude as a percentage of baseline, where baseline represents 100%. Acute effects of 0.01 mg/kg (A) 0.02 mg/kg (B) 0.04 mg/kg (C) and 0.06 mg/kg fentanyl (D). When values reached 0% of baseline this represents respiratory failure, seen in all neonatal-exposed mice in response to all doses of fentanyl. This response was not exhibited by the control animals. Data presented as mean±SD. *denotes a significant difference between the experimental groups ($p < 0.05$), 2-way ANOVA with Bonferroni's post test.

4.3.7.4 Physiological traces from anaesthetised preparations

The striking difference in the acute respiratory response to a fentanyl challenge between the control and neonatal-exposed mice under anaesthesia is clearly illustrated from Figure 4-19 and Figure 4-20. Representative airflow and GG_{EMG} traces, continually sampled for the duration of the experiment are shown, highlighting the acute respiratory response to 0.02 mg/kg fentanyl in a control mouse (Figure 4-19) and a neonatal-exposed mouse (Figure 4-20). Fentanyl induced a depression of respiratory activity in the control mouse; however despite this depression and the fact that the respiratory frequency and tidal volume never returned to baseline levels, the mouse continued to spontaneously breathe for the full course of the experiment, i.e. up to 60 minutes following the fentanyl challenge (Figure 4-19). Conversely, the neonatal-exposed mouse suffered a complete respiratory arrest, i.e. a failure of respiratory airflow and GG muscle activity, in response to an acute 0.02 mg/kg fentanyl challenge. There was a continual decline in respiratory frequency and tidal volume. By 14 minutes post-fentanyl administration, respiratory activity was very weak and a complete cessation of airflow i.e. a fatal apnoea and respiratory muscular activity quickly followed (Figure 4-20). Artificial ventilation failed to evoke spontaneous breathing. This fentanyl-induced respiratory arrest occurred in all 16 neonatal-exposed mice in response to all four fentanyl doses investigated. The exact time at which the arrest occurred following fentanyl did however differ between experimental mice.

It is evident from both Figures 4-19 and 4-20 that the GG muscle was inspiratory modulated i.e. fired concomitantly with the inspiratory phase of respiration, and the frequency of muscle firing was always identical to the respiratory frequency. While fentanyl induced a variable effect on the amplitude of the GG_{EMG} signal, it always depressed the rate of firing in both control and neonatal-exposed mice (Figure 4-19 and 4-20).

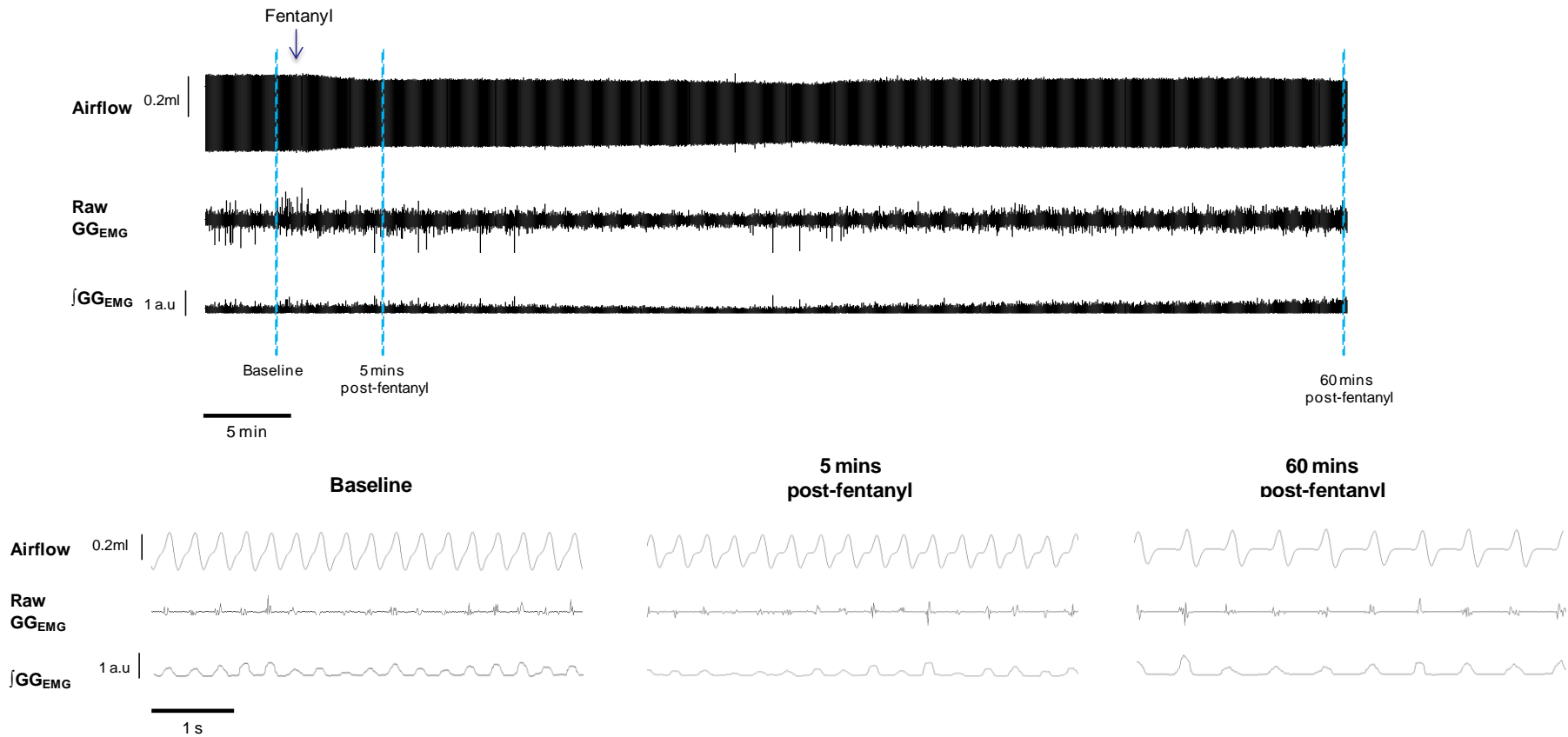


Figure 4-19. Representative airflow and GG_{EMG} trace taken from a control mouse administered 0.02 mg/kg fentanyl under anaesthesia. Airflow, raw and integrated GG_{EMG} traces are shown. The areas demarcated by the blue dashed lines are expanded and shown in the traces below. 0.02 mg/kg fentanyl evoked a depression of respiratory activity, but did not induce a respiratory arrest.

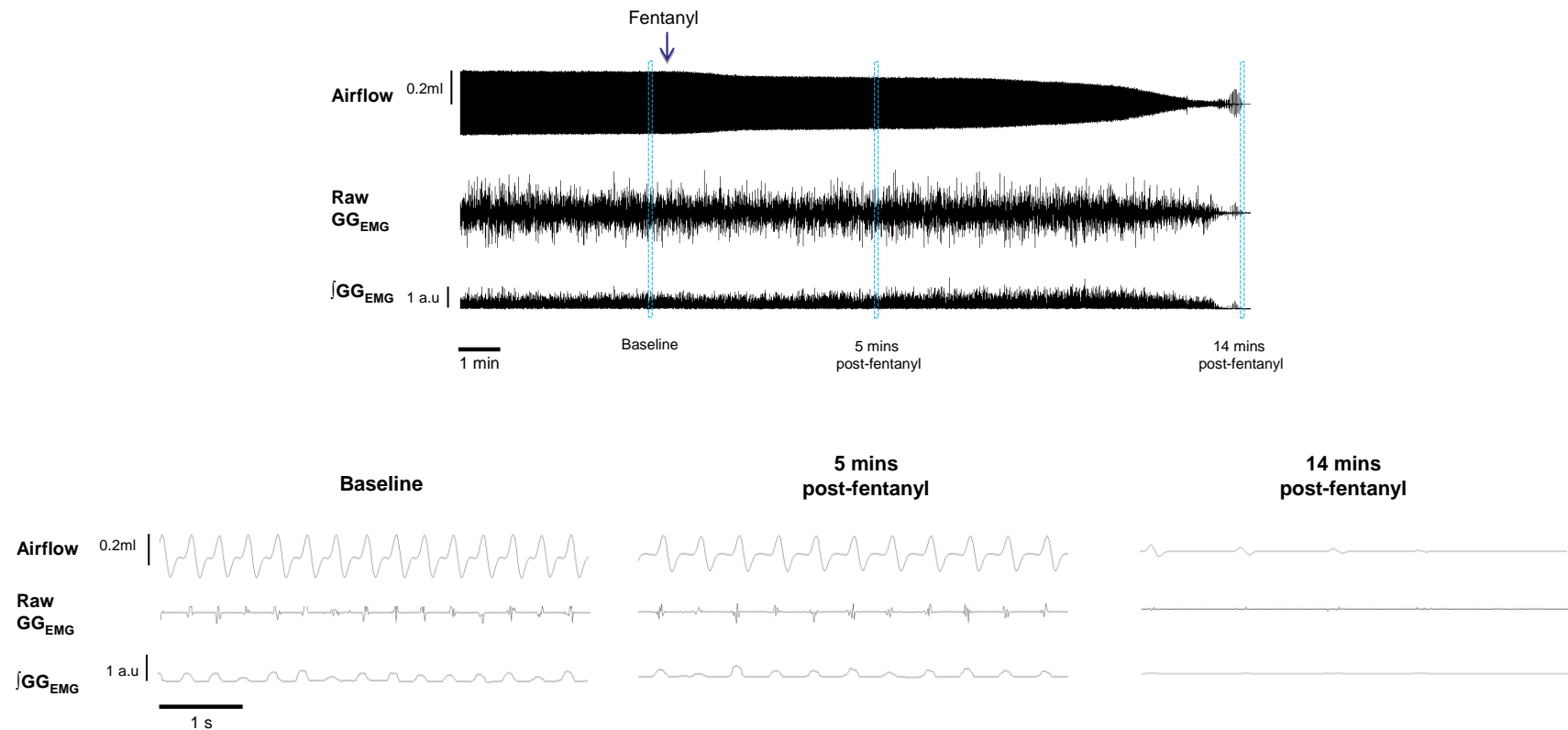


Figure 4-20. Representative airflow and GG_{EMG} trace taken from a neonatal-exposed mouse administered 0.02 mg/kg fentanyl under anaesthesia. Airflow, raw and integrated GG_{EMG} traces are shown. The areas demarcated by the blue dashed lines are expanded and shown in the traces below. 0.02 mg/kg fentanyl evoked a complete suppression of respiratory activity by 14 minutes post-injection.

4.4 Results of study 5: Investigation of the long-term respiratory effects of repeated fentanyl exposure in the juvenile mouse

Study 5 differs for study 4 in that mice were exposed to fentanyl at a later stage in postnatal life, from P9-P13. Results from study 5 are presented in section 4.4

4.4.1 Animal body weights

There was no significant difference in the average body weights of control and juvenile-exposed mice during the repeated drug exposure period from P9-P13 or when they reached adulthood ($p>0.05$, 2-way ANOVA, Table 4-2).

Postnatal Age	Weight (g)	
	Control	Juvenile-Exposed
P9	5.4±1.9	6.0±1.3
P10	5.8±1.9	6.4±1.4
P11	6.2±1.8	6.7±1.4
P12	6.5±1.8	7.0±1.4
P13	6.9±1.8	7.3±1.5
Adult	33.4±2.9	35.2±4.0

Table 4-2. Average body weights of control and juvenile-exposed mice. Body weight was measured throughout the repeated drug exposure period (P9-P13) and on reaching adulthood. Data presented as mean±SD. No significant difference in body weight between the two experimental groups at all ages.

4.4.2 Baseline respiratory parameters of awake adult mice

In the wakeful state, adult mice (6 weeks old) which were juvenile-exposed showed a trend towards a lower baseline respiratory frequency compared to control mice (161 ± 6 bpm *vs* 182 ± 9 bpm, $p > 0.05$, Figure 4-21A). While inspiratory duration was comparable between the two groups (juvenile-exposed: 0.13 ± 0.003 s *vs* control: 0.13 ± 0.01 s, $p > 0.05$, Figure 4-21B), there was a trend towards a longer expiratory duration in the juvenile-exposed mice (juvenile-exposed: 0.25 ± 0.01 s *vs* control: 0.22 ± 0.01 s; $p > 0.05$, Figure 4-21C) which would account for the lower respiratory frequency exhibited. No significant difference in V_t was found between the experimental groups (juvenile-exposed: 11 ± 1 μ l/g *vs* control: 12 ± 1 μ l/g, $p > 0.05$, Figure 4-21D). Due to the trend towards a lower respiratory frequency, juvenile-exposed mice displayed a significantly lower baseline V_e compared to control mice (1829 ± 69 μ l/g/min *vs* 2262 ± 179 μ l/g/min, $p < 0.05$, Figure 4-21E). It is important to highlight that no obvious respiratory anomalies or ataxic breathing patterns were observed in any of the juvenile-exposed mice; all mice displayed a rhythmic and stable respiratory pattern.

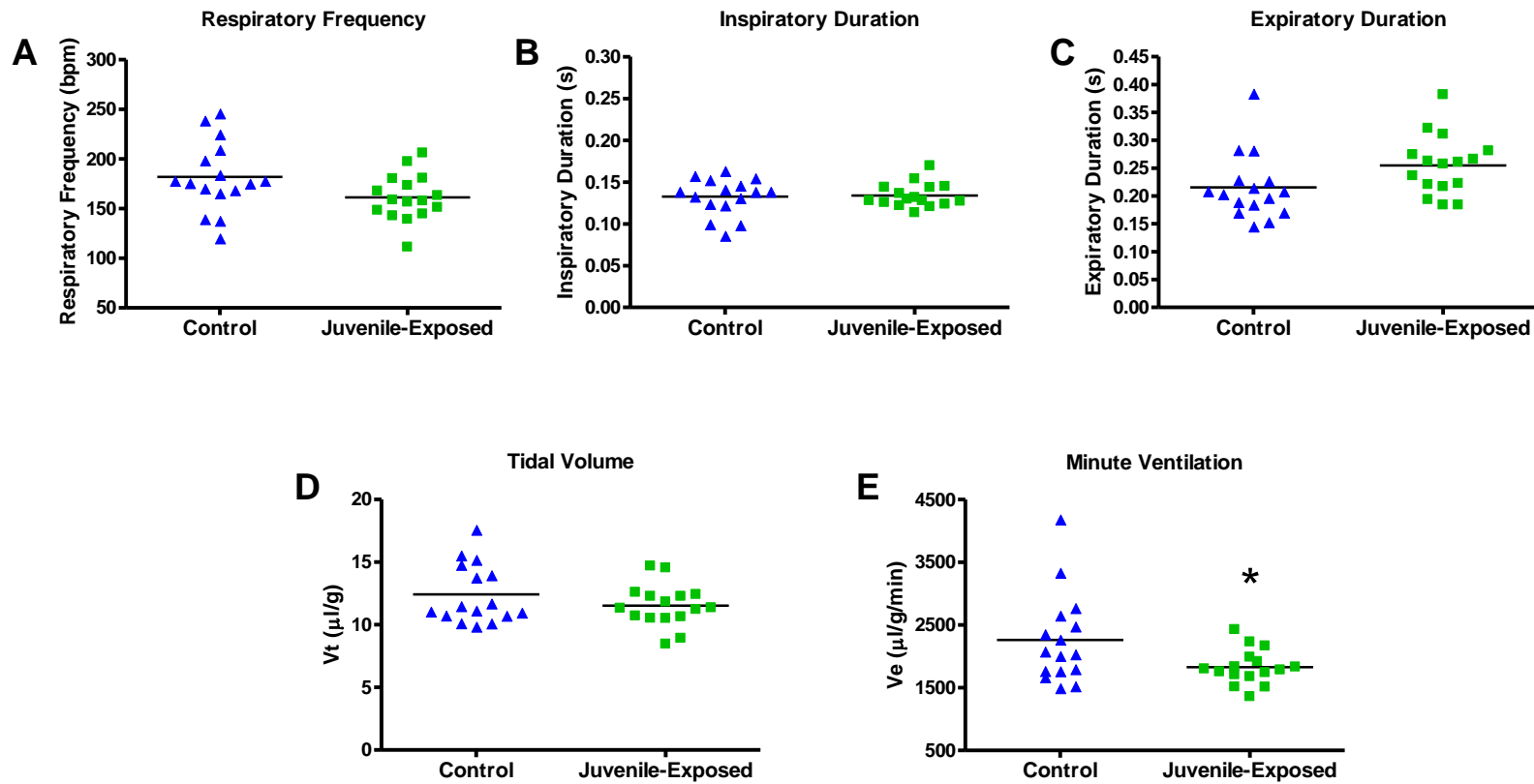


Figure 4-21. Baseline respiratory parameters of adult control and juvenile-exposed mice during wakefulness. Control mice, n=16; juvenile-exposed, n=16. Each data point on the scatter plots represents an individual animal. Line denotes the mean. *p<0.05, Student's unpaired t-test.

4.4.3 Acute fentanyl challenge in awake mice

The same range of fentanyl doses detailed in study 4 (0.04 mg/kg-0.1 mg/kg) were investigated, and each mouse was administered only one dose.

4.4.3.1 Respiratory frequency

In the control groups, all 4 fentanyl doses induced a continual reduction in respiratory frequency from baseline that was greatest at 30 minutes post-injection (Figure 4-22). Respiratory frequency was significantly lower at 30 minutes post 0.04, 0.06 and 0.08 mg/kg fentanyl challenge compared to baseline (0.04 mg/kg: 131 ± 30 bpm vs baseline: 180 ± 13 bpm, $p < 0.05$, Figure 4-22A; 0.06 mg/kg: 112 ± 20 bpm vs baseline: 184 ± 41 bpm, $p < 0.05$, Figure 4-22B; 0.08 mg/kg: 130 ± 14 bpm vs baseline: 180 ± 46 bpm, $p < 0.05$, Figure 4-22C). Respiratory frequency showed a clear trend towards a reduction at 30 minutes post 0.1 mg/kg fentanyl challenge in the control group (30 minutes post-challenge: 153 ± 15 bpm vs baseline: 185 ± 46 bpm, Figure 4-22D). Respiratory frequency had returned to baseline values by 45 minutes post-fentanyl injection in the control mice (Figure 4-22A-D, $p > 0.05$).

Incongruent to the respiratory response observed in the control mice, even at the highest dose, a fentanyl challenge failed to induce a depression of respiratory frequency in juvenile-exposed mice. No significant reduction from baseline respiratory frequency was found at any of the time points examined for any of the fentanyl doses injected ($p > 0.05$, Figure 4-22A-D). Interesting to highlight, at 5 minutes post-fentanyl challenge, juvenile-exposed mice exhibited an unexpected increase in respiratory frequency. This increase was only found to be statistically significant following administration of 0.04 mg/kg and 0.06 mg/kg fentanyl ($p < 0.05$, Figure 4-22A-B); however there was a trend towards an increase post 0.08 mg/kg and 0.1 mg/kg fentanyl challenge ($p > 0.05$, Figure 4-22C+D). This increase in respiratory frequency was not exhibited by the control mice. When looking at the changes in respiratory frequency in response to fentanyl as a percentage change from baseline (Figure 4-23), it is apparent that the control and juvenile-exposed mice displayed a clear disparity in their acute respiratory response. This was seen for all the doses of fentanyl studied. These data reinforce the data illustrated in Figure 4-22 and clearly highlights the discrepancy in the respiratory frequency response to fentanyl between control and juvenile-exposed mice. At 30 minutes post-fentanyl, control mice showed a clear reduction in respiratory frequency from baseline (0.04 mg/kg: $28 \pm 11\%$

reduction, 0.06 mg/kg: 38±7% reduction, 0.08 mg/kg: 27±11% reduction, 0.1 mg/kg: 20±10 reduction, Figure 4-23A-D), which was not seen in the juvenile-exposed mice (0.04 mg/kg: 2±15% increase, 0.06 mg/kg: 12±25% increase, 0.08 mg/kg: 2±25% reduction, 0.1 mg/kg: 8±11% reduction, Figure 4-23A-D). In the juvenile-exposed mice, the increase in respiratory frequency at 5 minutes post-fentanyl ranged from 18±29% to 45±20% from baseline, depending on the dose of fentanyl administered (Figure 4-23A-D). This increase did not appear to be associated with an increase in fentanyl dose.

4.4.3.2 Tidal volume

In the control group, V_t increased following administration of 0.04 mg/kg, seen at 15 minutes, although not significant (baseline: 13±2 µl/g; 15 mins post-fentanyl: 16±3 µl/g, $p>0.05$, Figure 4-24A). V_t significantly increased at 5 minutes, 15 minutes and 30 minutes post 0.06 mg/kg fentanyl challenge (baseline: 14±3 µl/g; 5 mins: 18±2 µl/g, 15 mins: 18±2 µl/g, 30 mins: 18±2 µl/g, $p<0.05$, Figure 4-24B). A slight increase in V_t was seen at 5 minutes and 15 minutes after 0.08 mg/kg fentanyl injection (baseline: 11±2 µl/g; 5 mins: 14±2 µl/g; 15 mins: 15±3 µl/g, $p>0.05$, Figure 4-24C). A dose of 0.1 mg/kg fentanyl did not induce any changes in V_t at any time point ($p>0.05$, Figure 4-24D).

The juvenile-exposed mice exhibited similar V_t increases in response to fentanyl as the control mice. Administration of 0.04 mg/kg fentanyl evoked an increase in V_t at 5 minutes, 15 minutes and 30 minutes post-injection (baseline: 12±1 µl/g; 5 mins: 16±4 µl/g, 15 mins: 17±2 µl/g, 30 mins: 16±2 µl/g, Figure 4-24A). The increase was however only found to be statistically significant at the 15 minute time point. An injection of 0.06 mg/kg fentanyl induced an increase in V_t from baseline seen at 5 minutes and 15 minutes post-fentanyl (baseline: 11±3 µl/g; 5 mins: 14±4 µl/g, 15 mins: 14±1 µl/g, $p>0.05$, Figure 4-24B). A dose of 0.08 mg/kg evoked an increase in V_t , seen at 5, 15 and 30 minutes following administration (baseline: 12±2 µl/g; 5 mins: 17±2 µl/g, 15 mins: 14±1 µl/g, 30 mins: 17±1 µl/g, Figure 4-24D). The highest dose of 0.1 mg/kg fentanyl also caused an increase in V_t at 5 minutes and 15 minutes following injection (baseline: 10±1 µl/g; 5 mins: 15±4 µl/g, 15 mins: 15±3 µl/g, $p>0.05$, Figure 4-24D). Figure 4-25 illustrates the V_t response to fentanyl as a percentage change from baseline. From this figure, it is apparent that both control and juvenile-exposed mice exhibited an increase in V_t in response to fentanyl at 5 minutes, 15 minutes and 30 minutes following the fentanyl challenge at all doses. The changes in V_t induced by fentanyl were variable within both the control and juvenile-

exposed groups. There did not appear to be a dose dependent effect of fentanyl at any of the doses investigated.

4.4.3.3 Minute ventilation

In the control mice, fentanyl at all doses did not evoke any significant changes in V_e from baseline ($p > 0.05$, Figure 4-26A-D). This is due to the combined effect of a lowered respiratory frequency and increased V_t in response to fentanyl, thereby resulting in no overall alteration in V_e . As a result of the increases in both respiratory frequency and V_t in response to fentanyl, V_e was increased post-fentanyl in the juvenile-exposed mice (Figure 4-26A-D). Following 0.04 mg/kg fentanyl injection, there was a significant increase in V_e at 5 minutes and 15 minutes (baseline: 1803 ± 134 $\mu\text{l/g/min}$; 5 mins: 3564 ± 1481 $\mu\text{l/g/min}$, 15 mins: 3010 ± 631 $\mu\text{l/g}$, $p < 0.05$, Figure 4-26A). V_e increased significantly from baseline at 5 minutes post 0.06 mg/kg fentanyl (baseline: 1688 ± 352 $\mu\text{l/g/min}$; 5 mins: 3360 ± 1609 $\mu\text{l/g/min}$, $p < 0.05$, Figure 4-26B) and 0.08 mg/kg fentanyl (baseline: 2084 ± 303 $\mu\text{l/g/min}$; 5 mins: 3606 ± 1140 $\mu\text{l/g/min}$ $p < 0.05$, Figure 4-26C). Juvenile-exposed mice also displayed a trend towards an increase in V_e at 5 minutes and 15 minutes following 0.1 mg/kg fentanyl (baseline: 1741 ± 155 $\mu\text{l/g/min}$; 5 mins: 2964 ± 1265 $\mu\text{l/g/min}$; 15 mins: 2562 ± 531 $\mu\text{l/g/min}$, $p > 0.05$, Figure 4-26D). In the juvenile-exposed mice, V_e returned to baseline values by 45 minutes post-injection of all fentanyl doses. When observing the percentage changes in V_e in response to all doses of fentanyl, it is apparent that, when compared to control mice, juvenile-exposed mice exhibited a greater fentanyl-induced increase in V_e , particularly at 5 and 10 minutes following administration (Figure 4-27A-D).

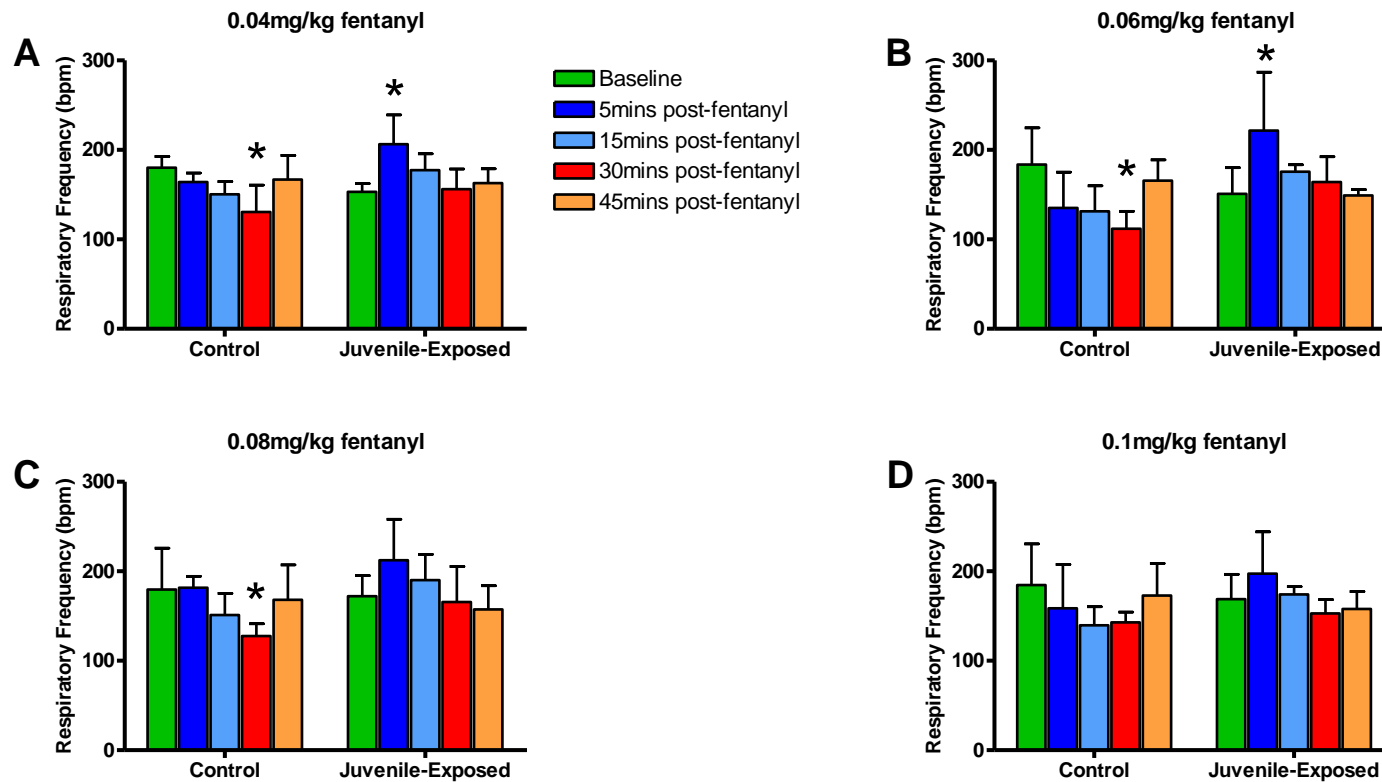


Figure 4-22. Changes in respiratory frequency in response to a single fentanyl challenge in control and juvenile-exposed mice when awake. Acute response to 0.04 mg/kg fentanyl (A), 0.06 mg/kg fentanyl (B), 0.08 mg/kg fentanyl (C) and 0.1 mg/kg fentanyl (D). Control mice; n=4, juvenile-exposed; n=4 for all 4 fentanyl groups. Data presented as mean±SD. * denotes a significant difference ($p < 0.05$) from baseline, 2-way ANOVA with Bonferroni's post test.

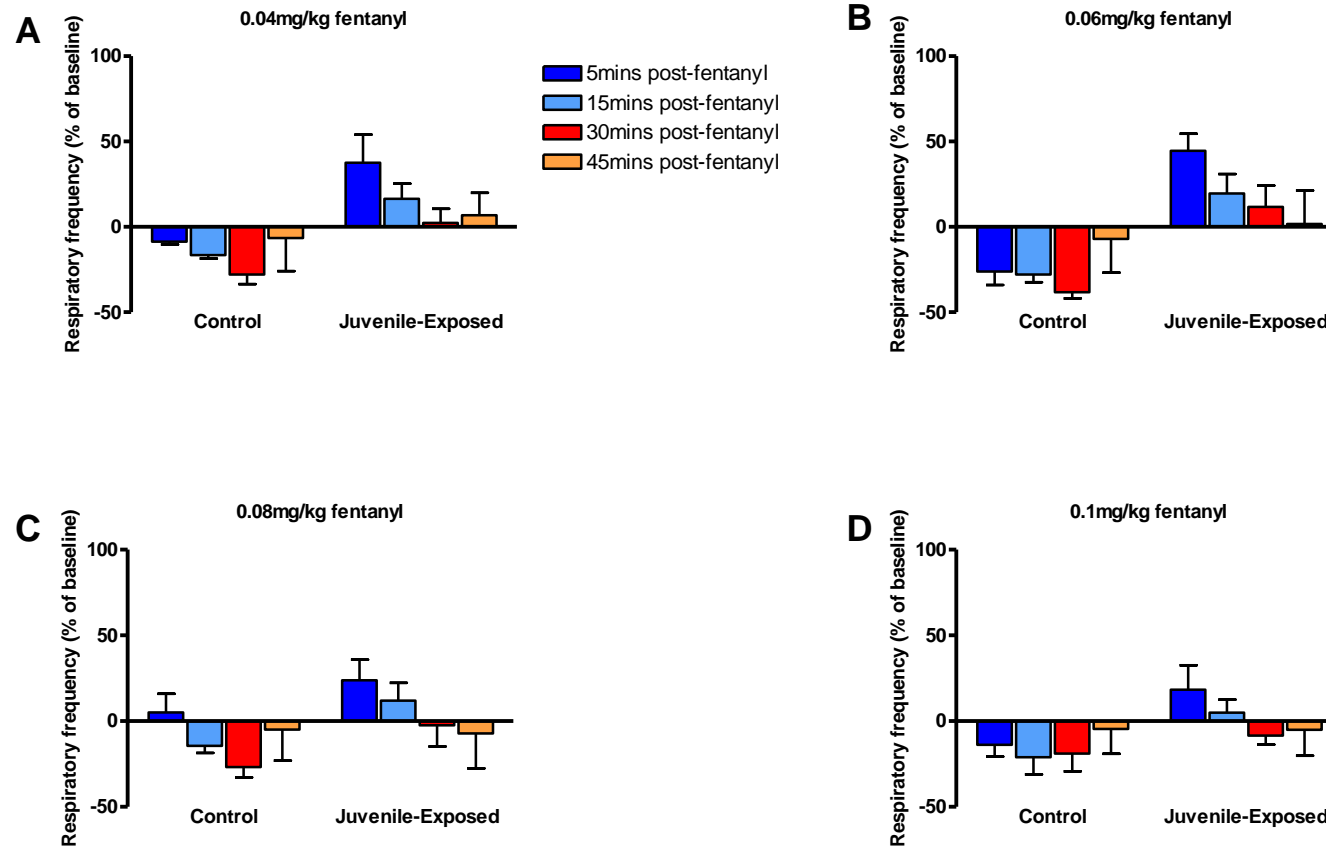


Figure 4-23. Percentage change in respiratory frequency in response to a single fentanyl challenge in control and juvenile-exposed mice when awake. Data shown as a percentage change from baseline. Acute response to 0.04 mg/kg fentanyl (A), 0.06 mg/kg fentanyl (B), 0.08 mg/kg fentanyl (C) and 0.1 mg/kg fentanyl (D). Control mice; n=4, juvenile-exposed; n=4 for all 4 fentanyl groups. Data presented as mean±SD.

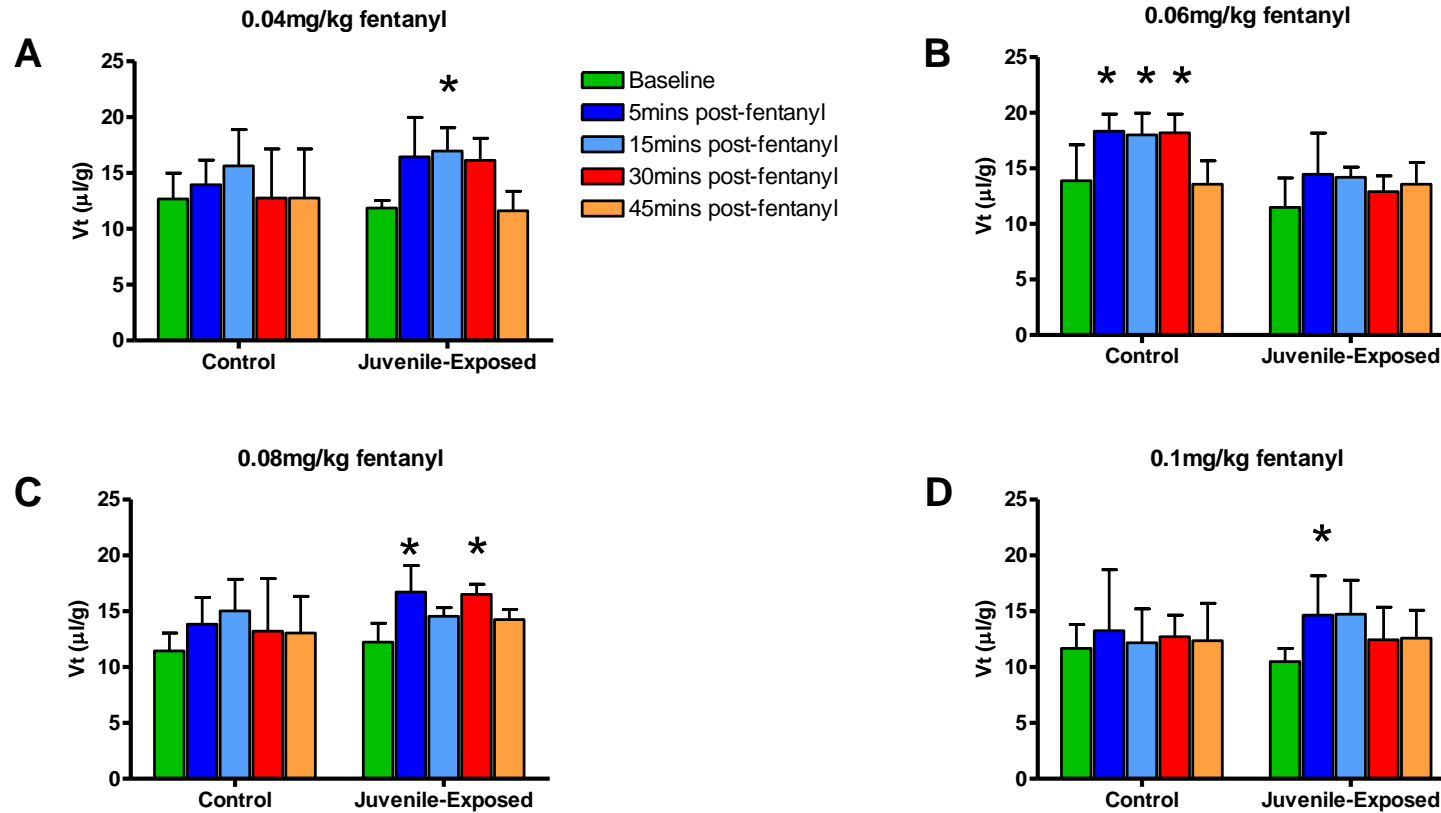


Figure 4-24. Changes in tidal volume (Vt) in response to a single fentanyl challenge in control and juvenile-exposed mice when awake. Acute Vt response to 0.04 mg/kg fentanyl (A), 0.06 mg/kg fentanyl (B), 0.08 mg/kg fentanyl (C) and 0.1 mg/kg fentanyl (D). Control mice; n=4, juvenile-exposed; n=4 for all 4 fentanyl groups. Data presented as mean±SD. * denotes a significant difference (p<0.05) from baseline, 2-way ANOVA with Bonferroni's post test.

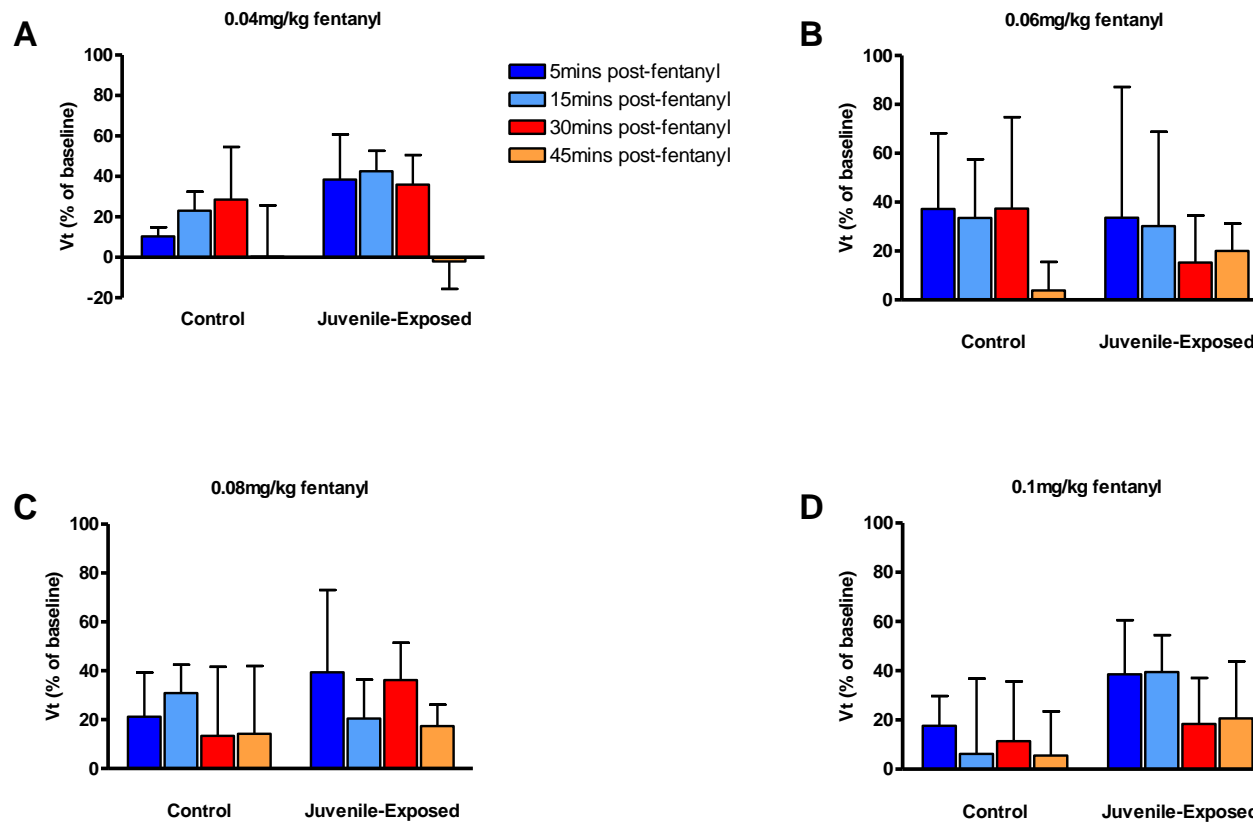


Figure 4-25. Percentage change in tidal volume (Vt) in response to a single fentanyl challenge in control and juvenile-exposed mice when awake. Data shown as a percentage change from baseline. Acute response to 0.04 mg/kg fentanyl (A), 0.06 mg/kg fentanyl (B), 0.08 mg/kg fentanyl (C) and 0.1 mg/kg fentanyl (D). Control mice; n=4, juvenile-exposed; n=4 for all 4 fentanyl groups. Data presented as mean±SD.

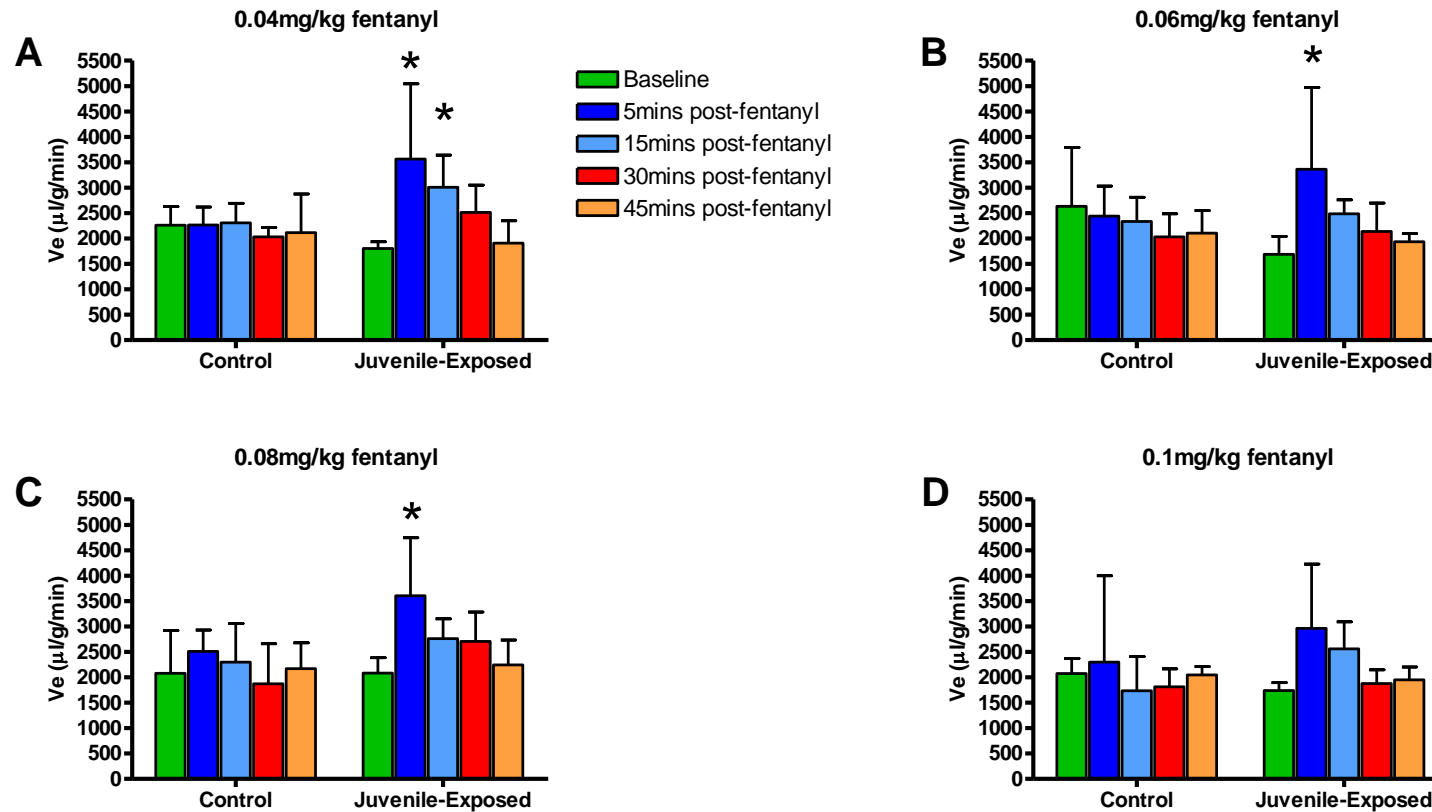


Figure 4-26. Changes in minute ventilation (V_e) in response to a single fentanyl challenge in control and juvenile-exposed mice when awake. Acute V_e response to 0.04 mg/kg fentanyl (A), 0.06 mg/kg fentanyl (B), 0.08 mg/kg fentanyl (C) and 0.1 mg/kg fentanyl (D). Control mice; $n=4$, juvenile-exposed; $n=4$ for all 4 fentanyl groups. Data presented as mean \pm SD. * denotes a significant difference ($p<0.05$) from baseline, 2-way ANOVA with Bonferroni's post test.

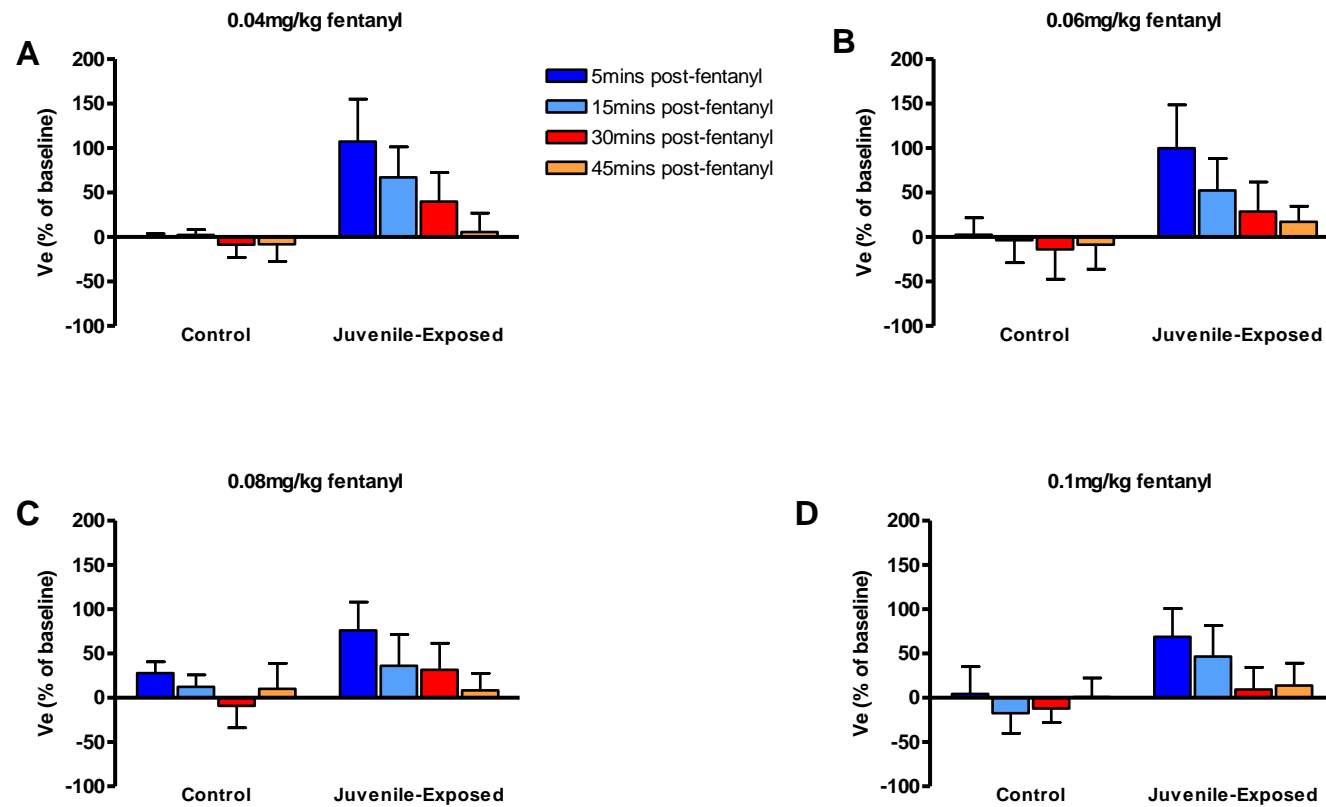


Figure 4-27. Percentage change in minute ventilation (V_e) in response to a single fentanyl challenge in control and juvenile-exposed mice when awake. Data shown as a percentage change from baseline. Acute V_e response to 0.04 mg/kg fentanyl (A), 0.06 mg/kg fentanyl (B), 0.08 mg/kg fentanyl (C) and 0.1 mg/kg fentanyl (D). Control mice; n=4, juvenile-exposed; n=4 for all 4 fentanyl groups. Data presented as mean \pm SD.

4.4.3.4 Plethysmography Respiratory Traces

Baseline breathing and the differences in the acute ventilatory response to a fentanyl challenge between the control and juvenile-exposed mice during wakefulness are clearly illustrated in Figure 4-28, which shows example plethysmographic respiratory traces taken before and after administration of the lowest dose of 0.04 mg/kg fentanyl (A) and the highest dose of 0.1 mg/kg fentanyl (B). In terms of the baseline breathing, it is clear that both groups of mice exhibited rhythmic breathing with no evident respiratory abnormalities. The representative plethysmography traces also show the juvenile-exposed mice had a lower baseline respiratory frequency compared with the control mice (Figure 4-28A and B). It is apparent that fentanyl, at both doses, evoked a depression of respiratory frequency and induced an increase in V_t at 30 minutes following administration, in the control mice. On the contrary, the juvenile-exposed mice did not display any respiratory depression post-fentanyl insult at either dose. The increase in both respiratory frequency and V_t at 5 minutes after both fentanyl doses is also clearly highlighted from the traces.

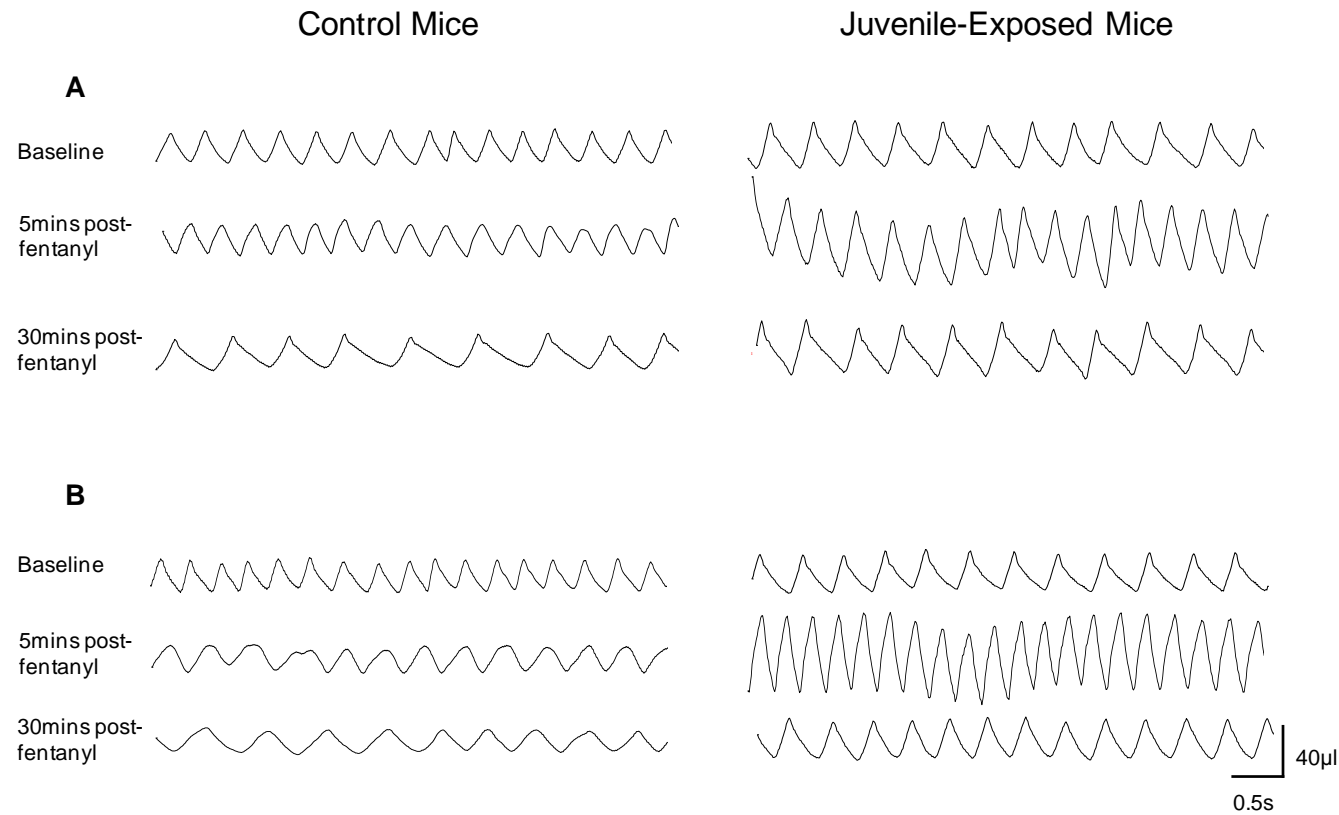


Figure 4-28. Representative respiratory traces before and after a fentanyl challenge taken from control and juvenile-exposed mice. The effects of 0.04 mg/kg (A) and 0.1 mg/kg fentanyl (B) are shown. It is apparent that the control and juvenile-exposed mice exhibited a different respiratory response to fentanyl. Fentanyl did not induce a depression of respiratory activity in the juvenile-exposed mice at either dose.

4.4.4 Baseline respiratory parameters of adult mice under anaesthesia

After recording of respiratory activity when mice were in the conscious state, a more detailed respiratory analysis was carried out in anaesthetised mouse preparations. When under anaesthesia, adult mice (weeks old) that were juvenile-exposed exhibited a significantly higher baseline respiratory frequency compared to control mice (224 ± 32 bpm vs 184 ± 30 bpm, $p < 0.05$, Figure 4-29A). This was due to juvenile-exposed mice having a significantly shorter inspiratory duration (0.13 ± 0.01 s vs 0.15 ± 0.01 s, $p < 0.05$, Figure 4-29B) and expiratory duration (0.14 ± 0.04 s vs 0.19 ± 0.06 s, $p < 0.05$, Figure 4-29C). Under anaesthesia, the juvenile-exposed mice exhibited a significantly lower baseline V_t compared to control mice (4.7 ± 0.7 $\mu\text{l/g}$ vs 5.2 ± 0.6 $\mu\text{l/g}$, $p < 0.05$, Figure 4-29D). The combination of a reduced V_t and increased respiratory frequency resulted in the minute ventilation of the juvenile-exposed mice to remain unchanged and comparable to that of the control mice (1058 ± 205 $\mu\text{l/g/min}$ vs 966 ± 183 $\mu\text{l/g/min}$, $p > 0.05$, Figure 4-29E). As observed in study 4, both control and juvenile-exposed mice had a lower baseline V_t under anaesthesia compared with the wakeful state (awake juvenile-exposed: 11 ± 1 $\mu\text{l/g}$; awake control: 12 ± 1 $\mu\text{l/g}$, Figure 4-21D). No significant difference in GG_{EMG} amplitude was found between the experimental groups (juvenile-exposed: 0.24 ± 0.16 a.u. vs control: 0.22 ± 0.15 a.u., $p > 0.05$, Figure 4-29F). The GG muscle always displayed a rhythmic pattern of activity, and was strongly inspiratory-related in all experimental mice. As also discussed in section 4.3.5, expiratory-modulated ABD muscle activity was not found in any of the experimental mice in study 5 and therefore no analysis of this muscle activity was performed. All abdominal muscle activity recorded was sporadic in nature (Figure 4-13).

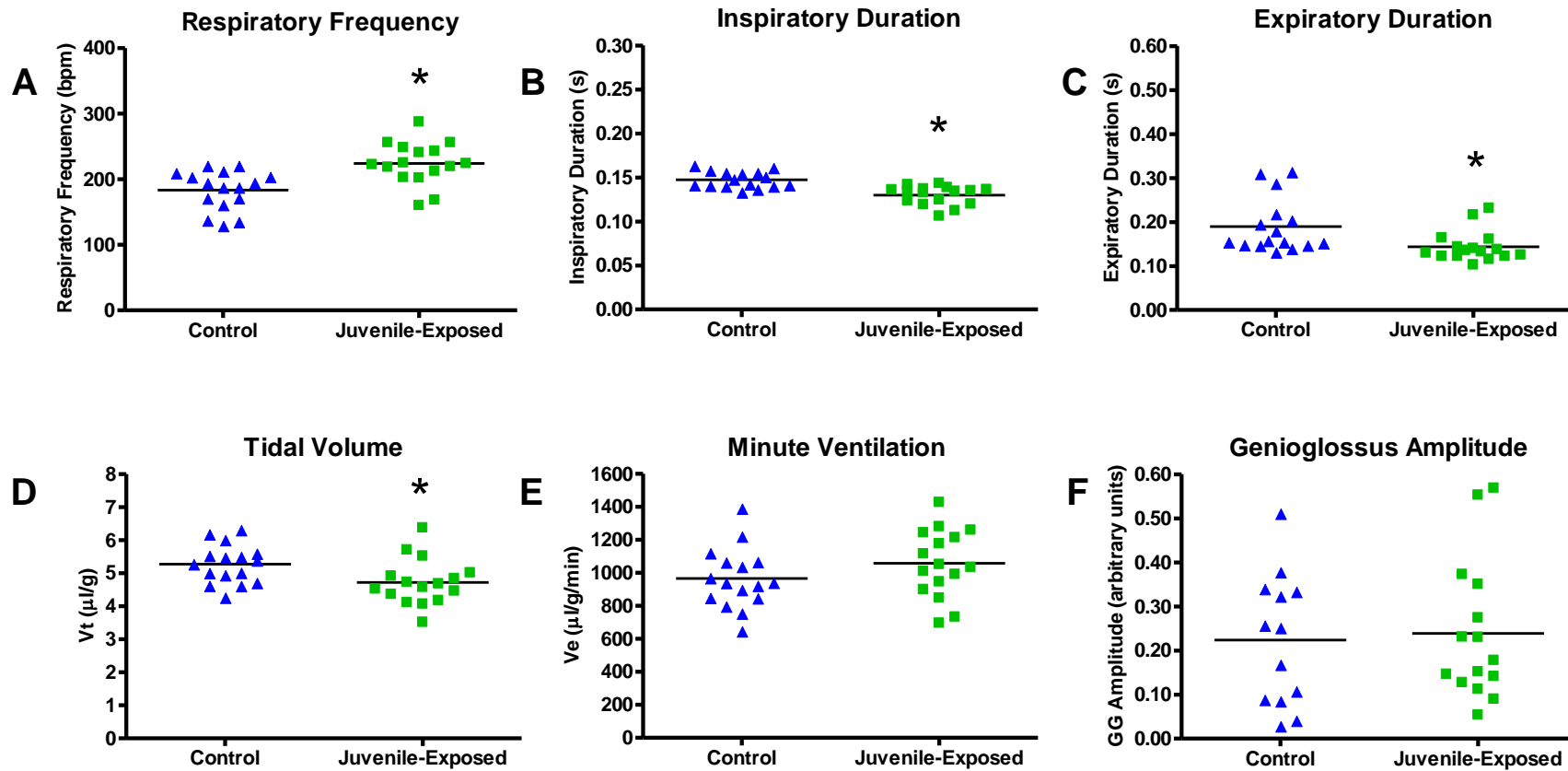


Figure 4-29. Baseline respiratory parameters of adult control and juvenile-exposed mice under anaesthesia. Control mice, n=16; Juvenile-exposed, n=16. Each data point on the scatter plots represents an individual animal. Line denotes the mean. * $p < 0.05$, Student's unpaired t-test.

4.4.5 Augmented breaths

As in study 4, the number of augmented breaths (illustrated in Figure 4-14A) observed during 10 minutes of continuous baseline breathing under anaesthesia was quantified for control and juvenile-exposed mice. Only a small number of mice in each experimental group exhibited augmented breaths. In the control group, 5 out of 16 mice (31.3%) displayed augmented breaths and 2 out of 16 juvenile-exposed mice (12.5%) exhibited them. Both control and juvenile-exposed mice exhibited a low occurrence of augmented breaths per 10 minutes and the average number exhibited was not significantly different between the groups (juvenile-exposed: 0.3 ± 0.9 augmented breaths/10 mins *vs* control: 1.6 ± 4.3 augmented breaths/10 mins, $p > 0.05$, Figure 4-30).

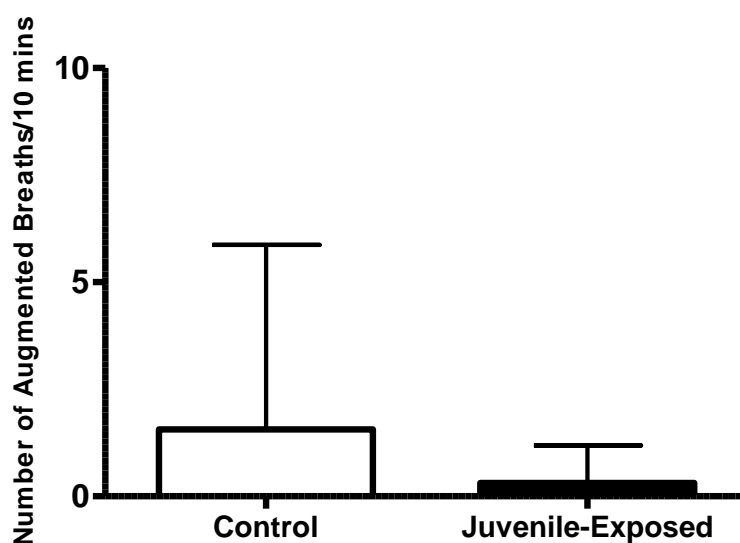


Figure 4-30. Number of augmented breaths exhibited by control and juvenile-exposed mice under anaesthesia. The number of augmented breaths observed during 10 minutes of baseline breathing was quantified. There was no significant difference ($p > 0.05$) in number of augmented breaths exhibited between control ($n=16$) and juvenile-exposed mice ($n=16$), Mann-Whitney test. Data presented as mean \pm SD.

4.4.6 Acute fentanyl challenge in anaesthetised mice

The same range of fentanyl doses investigated in the adult anaesthetised mouse preparations in study 4 were also examined in study 5 i.e. 0.01 mg/kg-0.06 mg/kg fentanyl. Mice were administered only 1 dose.

4.4.6.1 Respiratory frequency

Fentanyl at all doses induced a similar depression of respiratory frequency in both control and juvenile-exposed mice (Figure 4-31). There was no significant difference in the acute respiratory response to fentanyl at any time point following fentanyl administration between the two groups of mice. In both control and juvenile-exposed mice, a reduction in respiratory frequency was seen as early as 5 minutes following fentanyl challenge (all doses, Figure 4-31A-D). Although the respiratory frequency never returned to baseline levels within the 60 minutes following all doses of fentanyl, all control and juvenile-exposed mice continued to spontaneously breathe for the duration of the experiment, with the exception of one juvenile-exposed mouse in the 0.06 mg/kg fentanyl group. With this mouse, an injection of 0.06 mg/kg induced respiratory failure within 20 minutes post-insult. As a result of this loss of respiratory activity, the variability in the data was high for the 0.06 mg/kg fentanyl group (Figure 4-31D). It is important to highlight the fact that when under anaesthesia, the juvenile-exposed mice showed a different respiratory response to fentanyl compared to when they were awake. Fentanyl at the range of doses studied induced a reduction in respiratory frequency which was not observed in the wakeful state.

4.4.6.2 Tidal volume and minute ventilation

Fentanyl at all doses induced a similar reduction in V_t in control and juvenile-exposed mice (Figure 4-32). There was no significant difference in the acute fentanyl-induced V_t depression at any time point following fentanyl administration between the two groups of mice. The suppression of V_t was evident at 5 minutes following all four doses of fentanyl. Within the 60 minutes recording period following fentanyl, V_t never reached baseline levels except in the juvenile-exposed mice administered 0.02 mg/kg fentanyl, where V_t returned to baseline levels by 30 minutes following administration (30 minutes post-fentanyl: $1 \pm 14\%$ reduction from baseline, Figure 4-32B). As a result of the combined reduction in respiratory frequency and V_t following all doses of fentanyl, control and

juvenile-exposed mice also displayed a reduction in V_e (Figure 4-33). There was no significant difference in the fentanyl-induced reduction of V_e at any time point following the fentanyl challenge between the two experimental groups (Figure 4-33A-D).

4.4.6.3 Genioglossus activity

The effect of an acute fentanyl insult on the GG_{EMG} activity was measured. There was no significant difference in the GG_{EMG} response to fentanyl between the control and juvenile-exposed mice at all of doses studied ($p > 0.05$, Figure 4-34A-D). On average, fentanyl did not depress the amplitude of the GG activity in the control mice or the juvenile-exposed mice. This was observed for all four doses of fentanyl studied (Figure 4-34A-D). Both groups of mice did however display a high degree of variability in the GG_{EMG} response to fentanyl. Some mice displayed an increase in the amplitude of EMG bursting whereas others displayed a decrease or no change. The response was not affected by the dose administered. In both groups of mice, the genioglossus displayed an inspiratory-modulated pattern of activity (see Figure 4-35 and 4-36 for illustration), and therefore the frequency of muscle bursting was always identical to the respiratory frequency. The frequency of GG muscle firing was therefore always reduced to the same extent as the respiratory frequency in response to fentanyl (Figure 4-31).

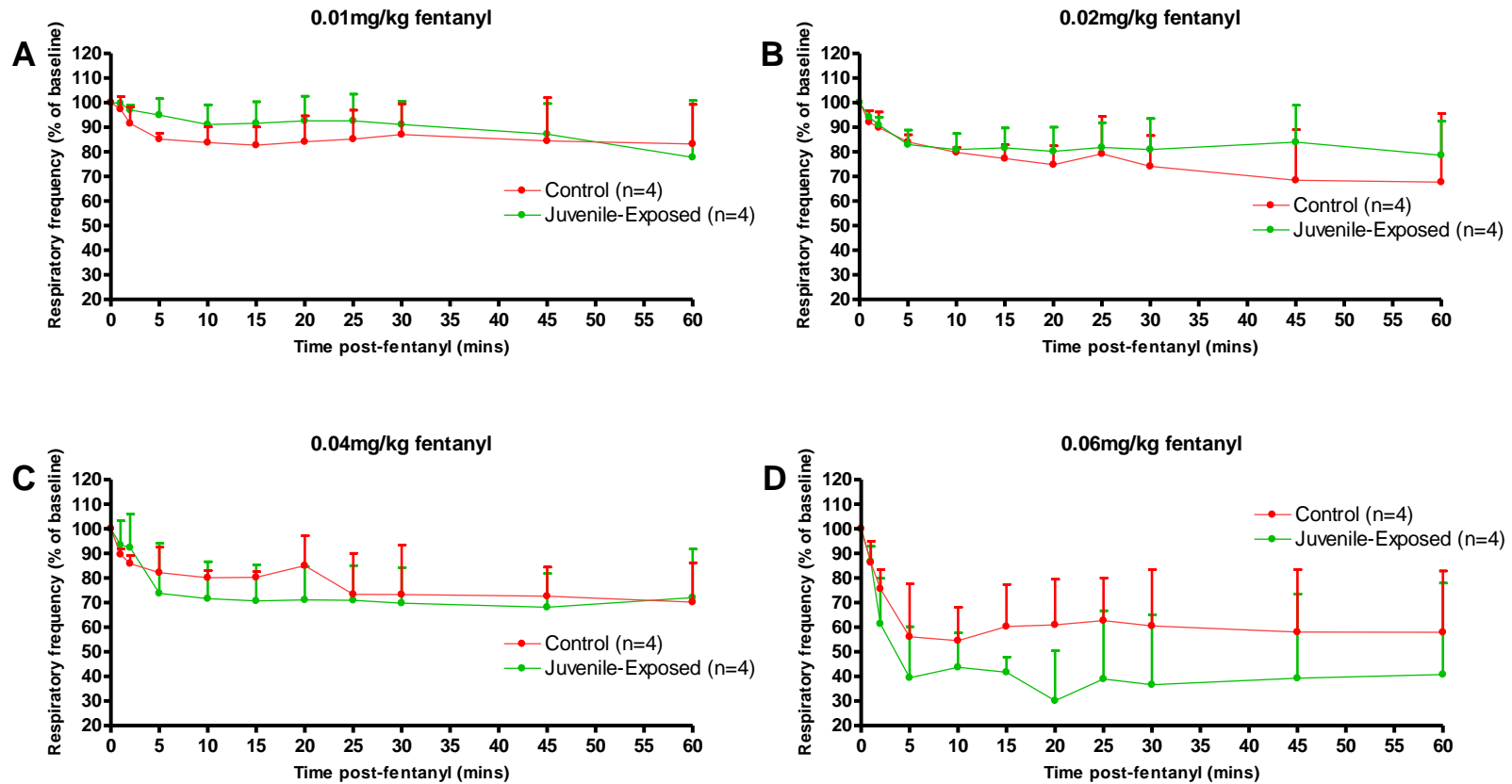


Figure 4-31. Changes in respiratory frequency in response to a fentanyl challenge in control and juvenile-exposed mice under anaesthesia. Changes in respiratory frequency presented as a percentage of baseline, where baseline represents 100%. Acute effects of 0.01 mg/kg (A) 0.02 mg/kg (B) 0.04 mg/kg (C) and 0.06 mg/kg fentanyl (D). Data presented as mean±SD.

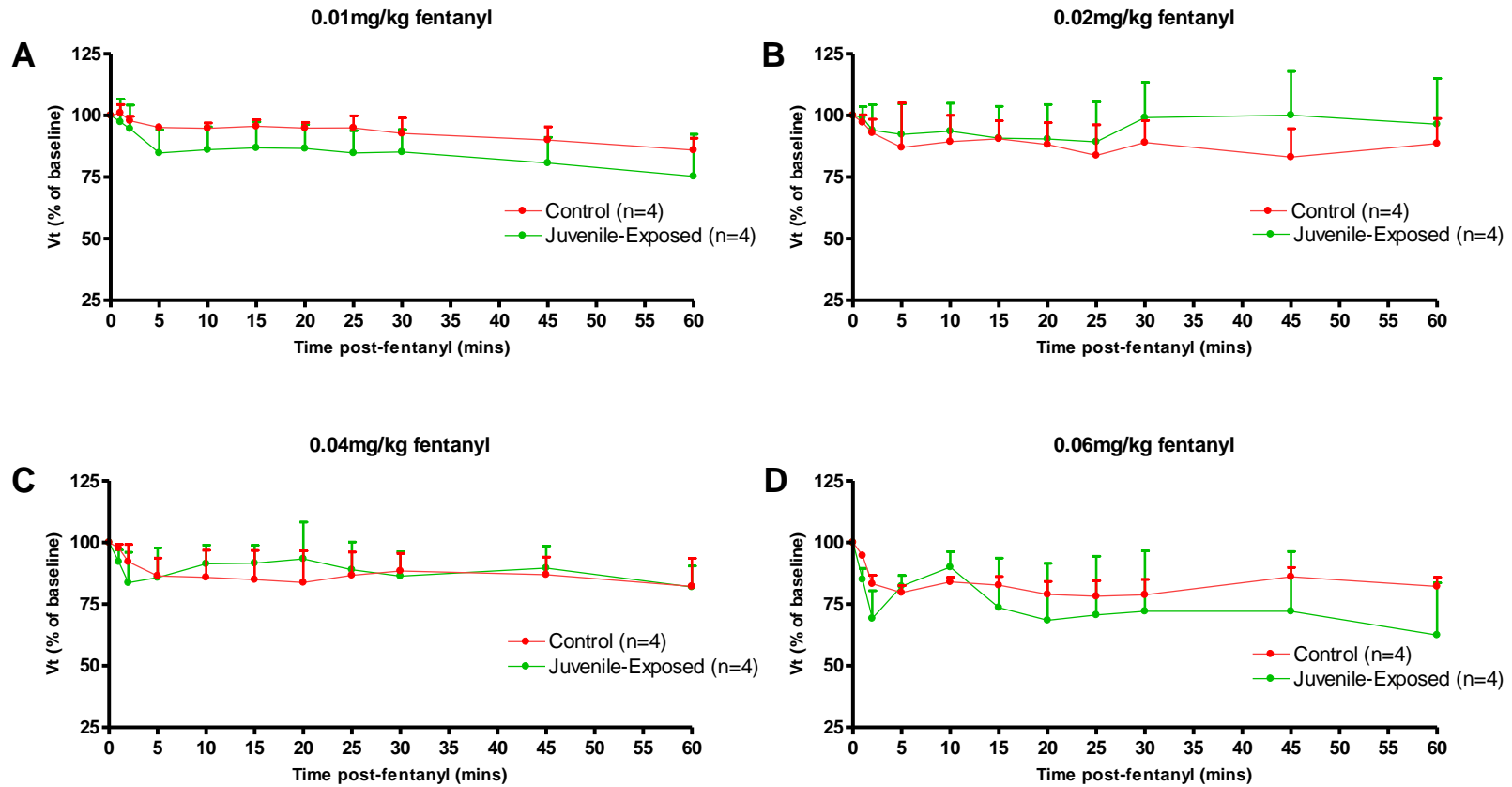


Figure 4-32. Changes in tidal volume (Vt) in response to a fentanyl challenge in control and juvenile-exposed mice under anaesthesia. Changes in Vt presented as a percentage of baseline, where baseline represents 100%. Acute effects of 0.01 mg/kg (A) 0.02 mg/kg (B) 0.04 mg/kg (C) and 0.06 mg/kg fentanyl (D). Data presented as mean±SD..

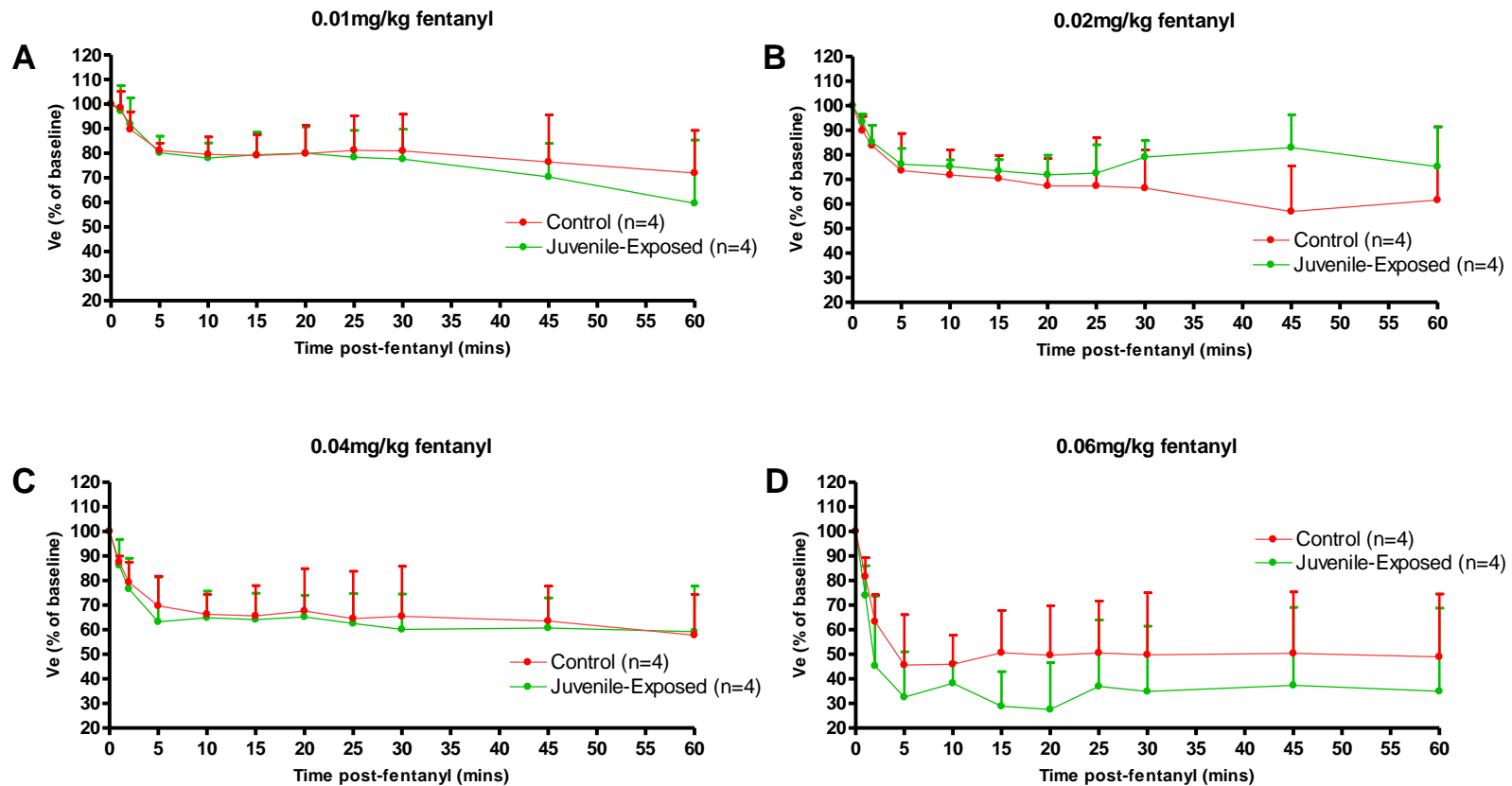


Figure 4-33. Changes in minute ventilation (V_e) in response to a fentanyl challenge in control and juvenile-exposed mice under anaesthesia. Changes in V_e presented as a percentage of baseline, where baseline represents 100%. Acute effects of 0.01 mg/kg (A) 0.02 mg/kg (B) 0.04 mg/kg (C) and 0.06 mg/kg fentanyl (D). Data presented as mean \pm SD.

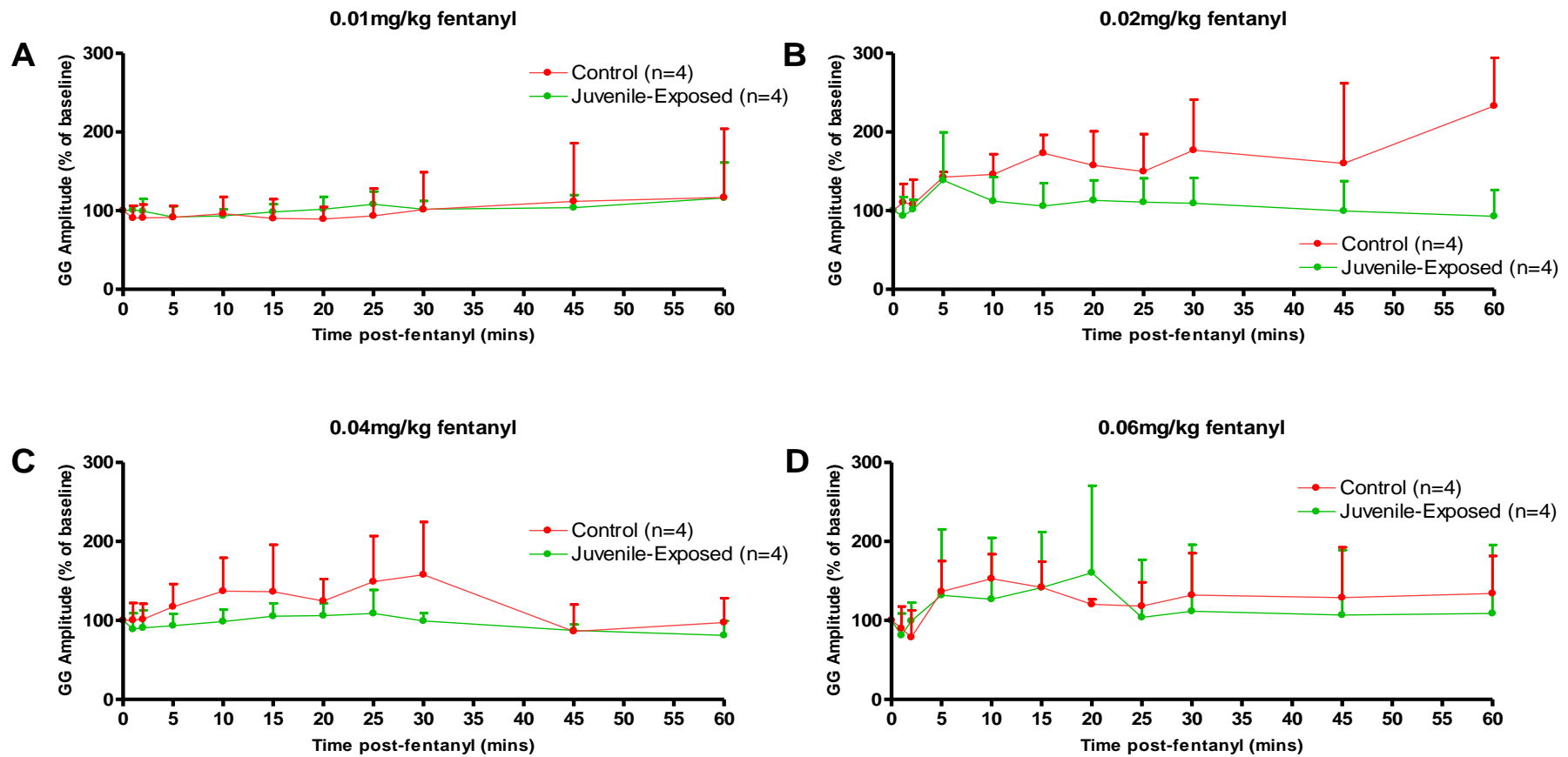


Figure 4-34. Changes in GG amplitude in response to a fentanyl challenge in control and juvenile-exposed mice under anaesthesia. Changes in GG amplitude presented as a percentage of baseline, where baseline represents 100%. Acute effects of 0.01 mg/kg (A) 0.02 mg/kg (B) 0.04 mg/kg (C) and 0.06 mg/kg fentanyl (D). Data presented as mean±SD.

4.4.6.4 Physiological traces from anaesthetised preparations

The acute respiratory response to a fentanyl challenge exhibited by the control and juvenile-exposed mice under anaesthesia is illustrated in Figure 4-35 and 4-36 respectively. Shown are example airflow and GG_{EMG} traces that were continually sampled for the duration of the experiment, highlighting the ventilatory effects of 0.02 mg/kg fentanyl. From the airflow traces it can be seen that the juvenile-exposed mouse had a higher baseline respiratory frequency compared to the control mouse (Figure 4-35 and 4-36). Fentanyl induced a respiratory depression in both mice. A reduction in respiratory frequency, V_t and GG_{EMG} amplitude and frequency was observed and can be clearly seen at 5 minutes following the fentanyl challenge in both groups of mice. At 60 minutes following fentanyl administration, the control mouse still displayed a depressed respiratory activity compared to baseline levels (Figure 4-35), whereas the respiratory parameters had returned to baseline value by 60 minutes in the juvenile-exposed mouse (Figure 4-36). Importantly, both the juvenile-exposed and control mouse maintained spontaneous respiratory output after the fentanyl challenge and throughout the course of the experiment. This finding was consistent for all fentanyl doses studied for both groups of mice.

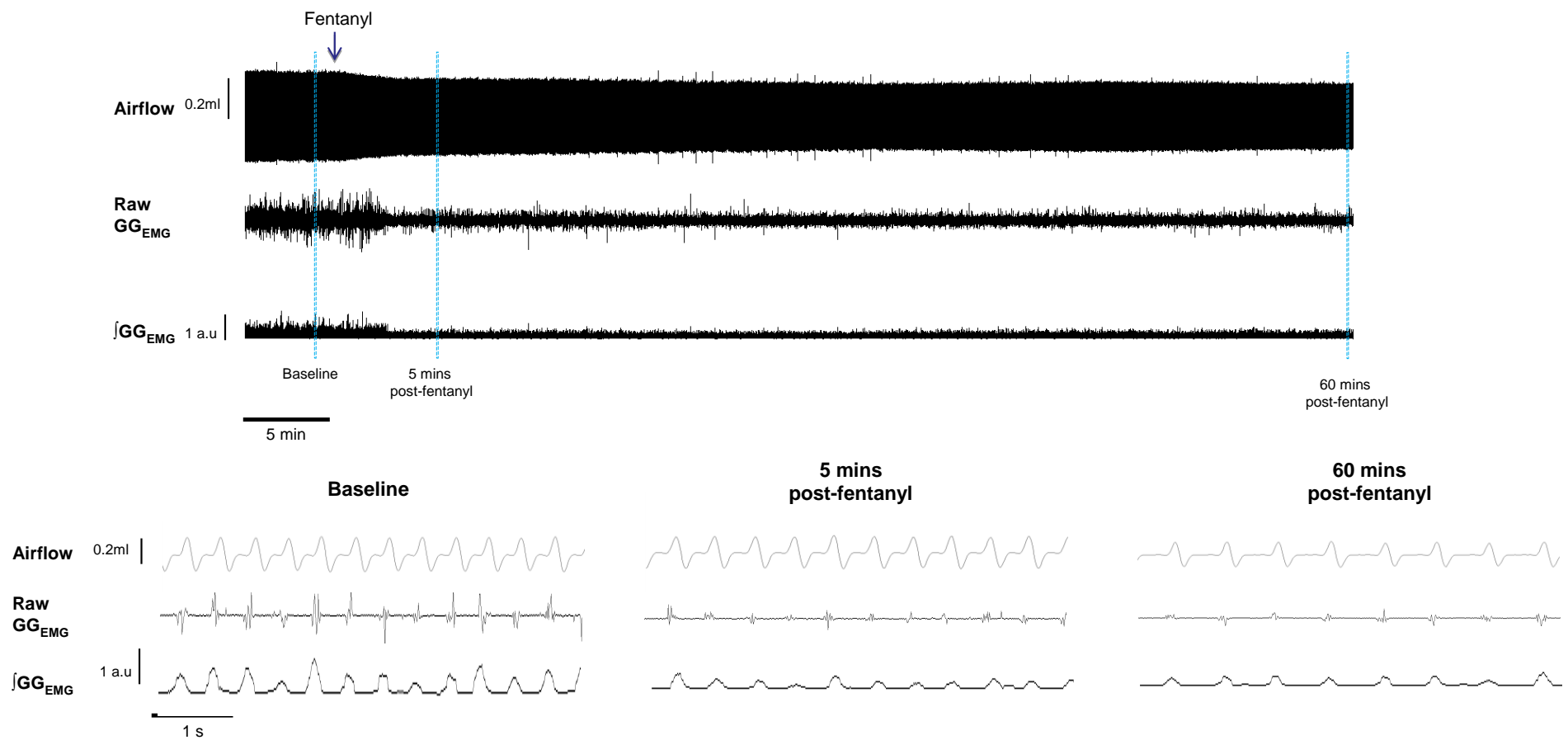


Figure 4-35. Representative airflow and GG_{EMG} trace taken from a control mouse administered 0.02 mg/kg fentanyl under anaesthesia. Airflow, raw and integrated GG_{EMG} traces are shown. The areas demarcated by the blue dashed lines are expanded and shown in the traces below. 0.02 mg/kg fentanyl evoked a depression of respiratory activity, but did not induce a respiratory arrest.

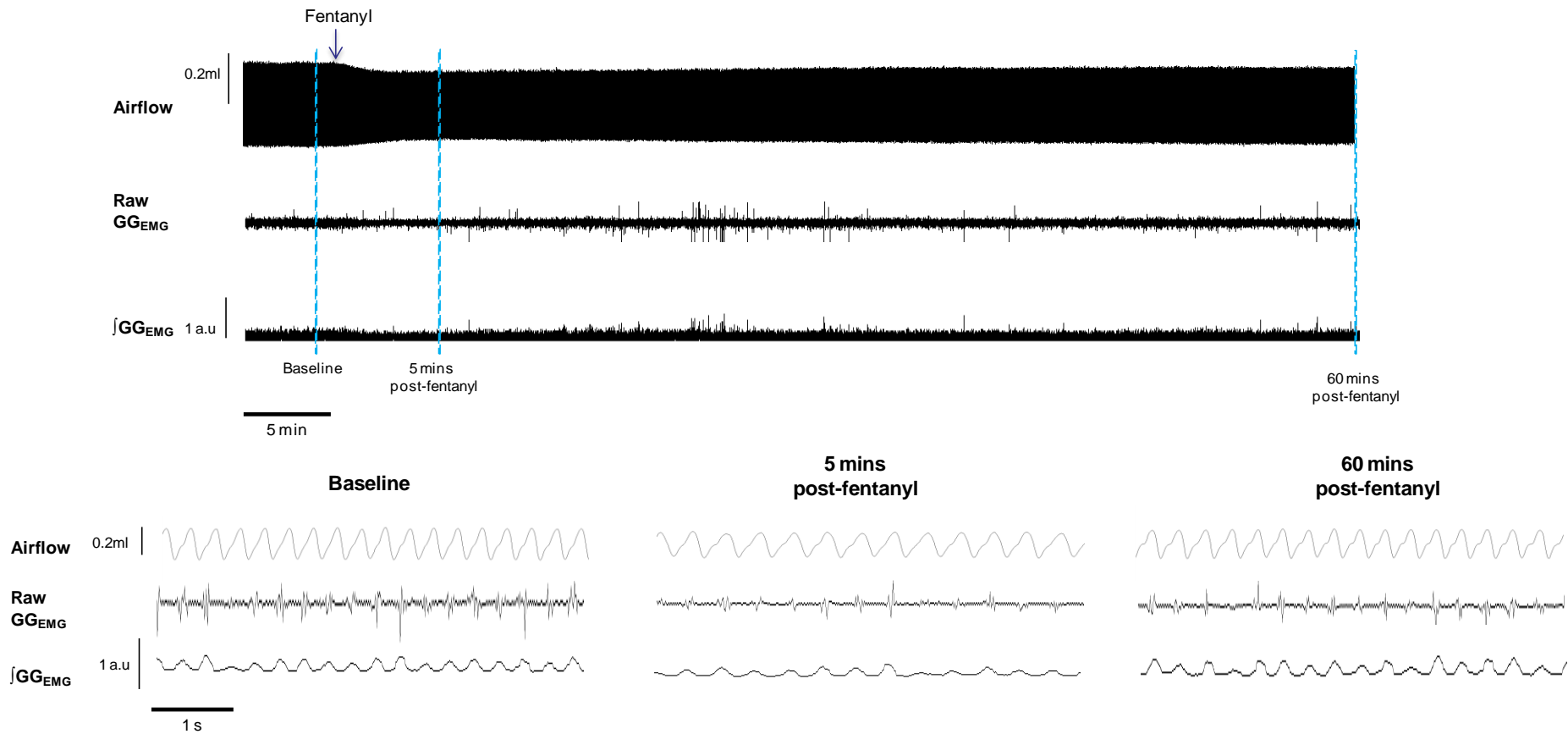


Figure 4-36. Representative airflow and GG_{EMG} trace taken from a juvenile-exposed mouse administered 0.02 mg/kg fentanyl under anaesthesia. Airflow, raw and integrated GG_{EMG} traces are shown. The areas demarcated by the blue dashed lines are expanded and shown in the traces below. 0.02 mg/kg fentanyl evoked a depression of respiratory activity, but did not induce a respiratory arrest.

4.5 Discussion

The studies described in this chapter are the first to assess the long-term respiratory consequences of neonatal and juvenile repeated fentanyl exposure in mice. Neonatal life encompasses a critical maturation of respiratory activity and is therefore an interesting time period to target with the respiratory depressant drug fentanyl. Exposing mice to fentanyl during neonatal life induced long-term respiratory alterations as was hypothesised. In particular this exposure evoked a notable change in the acute respiratory response to future fentanyl challenges, which interestingly was state-dependent. The juvenile exposure studies were complementary experiments to assess if the long-standing respiratory alterations were in fact a developmental phenomenon. Juvenile fentanyl exposure also resulted in a lasting change to respiratory activity; however the striking long-term alteration in the acute respiratory response to fentanyl induced by neonatal exposure was not observed.

4.5.1 Wakeful state: resting breathing

4.5.1.1 Neonatal fentanyl exposure induced lasting changes in resting breathing during wakefulness

When neonatal-exposed mice reached adulthood they exhibited a reduced resting respiratory frequency and therefore an overall reduction in resting ventilation in the wakeful state. The slower respiratory frequency was a result of a longer inspiratory phase. Given that fentanyl was systemically administered and would therefore have widespread effects throughout the body, the mechanism(s) by which fentanyl acts to induce these lasting respiratory changes cannot be elucidated from this study. A previous *in vivo* study in adult rats established that systemically administered fentanyl fully mediates respiratory frequency depression by exclusively depressing NK1R-expressing preBötC neurons (Montandon et al., 2011). In this study, fentanyl-induced slowing of respiratory frequency was completely prevented by local bilateral application of naloxone into the preBötC, therefore it was concluded that the preBötC is the critical brain site where fentanyl acts to suppress respiratory rate (Montandon et al., 2011). Furthermore, systemic application of fentanyl to the decerebrate cat slows the rhythm of phrenic nerve discharge, suggesting a direct effect on the respiratory rhythm generator (Lalley, 2003). Based on these findings, it

is postulated that in this present study, the long-term reduction of baseline respiratory frequency and thus the ventilatory profile could be due fully or in part to the depressive actions of fentanyl on the preBötC during neonatal life. This hypothesised repeated preBötC depression may have induced long-term changes in the rhythm generating properties of the neurons. Since it is widely accepted that inspiratory rhythmogenic drive originates from the preBötC (Smith et al., 1991; Gray et al., 1999), the fact that the neonatal-exposed mice had an altered inspiratory duration also supports our hypothesis that neonatal fentanyl exposure has affected preBötC functioning. However, it is imperative to highlight the fact that the central respiratory system is comprised of a complex network of functionally interacting neurons, and in the behaving animal the preBötC functions as part of a larger network. It is therefore very difficult to determine fentanyl's long-term effects on individual neural groups *in vivo*. Affecting one component of the respiratory network could have an indirect impact on various other components, and in the whole animal system these potential complex network effects cannot be ascertained. In accordance with this theory, it is possible that alterations in respiratory frequency could reflect changes in neural groups that shape or relay the output of the preBötC as opposed to rhythm generation per se. There is evidence that opioids target the Kölliker-Fuse and parabrachial nuclei of the pons to affect respiratory output (Lalley, 2006). These nuclei have connections with the VRG in the ventrolateral medulla (Jiang et al., 2004) and computational modelling studies suggest these areas regulate the output from the pre-Bötzinger complex (Rybak et al., 2004). It is therefore a possibility that long-term changes in the functioning of these respiratory nuclei also contribute to the altered respiratory frequency in neonatal-exposed mice. Despite the depression in the baseline respiratory frequency, repeated neonatal fentanyl exposure did not predispose mice to respiratory pattern disturbances in adult life when in the wakeful state. All neonatal-exposed mice displayed a regular and rhythmic respiratory pattern at rest. This suggests that in the wakeful state, the ability of the preBötC to generate a reliable and robust respiratory output is unaffected by repeated neonatal fentanyl exposure.

4.5.1.2 Neonatal fentanyl exposure does not alter respiratory response to hypercapnia or hypoxia

It is firmly believed that stimulation of breathing by decreases in the partial pressure of O₂ and increases in partial pressure of CO₂ in the blood is fundamental to rhythmic breathing,

and failure of this vital process can lead to disordered breathing (Loeschcke, 1982; Dubreuil et al., 2008; Dubreuil et al., 2009), therefore it was of interest to determine if repeated neonatal fentanyl exposure induced lasting effects on chemosensory responses. Neonatal-exposed mice and control mice exhibited the same ventilatory response to both hypercapnic and hypoxic stimuli, and showed a comparable respiratory recovery following the chemosensory stimuli. Hypercapnia evoked a typical ventilatory stimulation and hypoxia induced the characteristic biphasic response, with an initial increase in ventilation followed by a secondary decline. This suggests that neonatal fentanyl exposure did not elicit lasting changes to central or peripheral chemosensory functions. Congruent with this finding is work by Berkenbosch and colleagues (Berkenbosch et al., 1997), who conducted an *in vivo* study showing that morphine, a μ opioid receptor agonist, does not acutely influence the hypoxic ventilatory response in the cat when administered intravenously which is likely due to the fact that morphine exerts a weak effect on the activity of the carotid body (McQueen and Ribeiro, 1980), which is known to express the μ opioid receptor (Lundberg et al., 1979). It is therefore likely that fentanyl exposure in neonatal life did not elicit long term changes in the O₂ sensitivity of the carotid body or the relaying of chemoafferent information to the CNS. There is a wealth of evidence to suggest that the RTN/pFRG contributes to the central chemoreflex and may function as the principal central chemosensory site in the adult rodent (Mulkey et al., 2004; Guyenet et al., 2005; Takakura et al., 2008; Marina et al., 2010) as well as the neonatal rodent (Dubreuil et al., 2008; Onimaru et al., 2008). Previous studies have shown that μ opioid receptor agonists do not depress the neural activity of the RTN/pFRG *in vitro* (Takeda et al., 2001; Janczewski et al., 2002; Mellen et al., 2003), thus it was hypothesised that fentanyl application would not induce any perturbation to RTN/pFRG function *in vivo*. It is probable that the function of the RTN/pFRG was unaffected by fentanyl exposure in early neonatal life, thus central chemoreception remained unperturbed. In support of this theory, an *in vivo* study using rats has demonstrated that intravenous administration of morphine induces a respiratory depression but does not alter the CO₂ responsiveness of RTN neurons (Mulkey et al., 2004). Serotonergic raphe neurons are also proposed to play a role in mediating CO₂ chemosensitivity (Hodges and Richerson, 2010). From our results, it can therefore be speculated that repeated neonatal fentanyl exposure does not affect the long term functioning of this neuronal group. The presence of normal chemoresponses also suggests that CNS processing of peripheral chemoafferent input as well as neurotransmission of chemosensory signals to the rhythm generator were unaltered in neonatal-exposed mice. Regardless of the sites involved or the mechanisms of central and

peripheral chemoreception, these data indicate that fentanyl exposure in neonatal life does not induce any lasting effects on the function of the chemosensory centres under resting conditions in the wakeful state.

4.5.1.3 Juvenile fentanyl exposure did not induce lasting changes in resting breathing during wakefulness

In the wakeful state, the baseline respiratory activity of the juvenile-exposed mice generally appeared unaltered. Juvenile-exposed mice did exhibit a statistically significant reduction in ventilation due to a trend towards a lowered respiratory frequency, but these changes were very subtle and therefore too much emphasis should not be placed on the biological significance. Furthermore, similar to neonatal exposure, juvenile fentanyl exposure did not induce any long-term respiratory anomalies; all mice displayed a rhythmic respiratory pattern. Taken together, these results highlight that juvenile fentanyl exposure did not evoke any marked lasting changes in resting respiratory activity during wakefulness and when compared to neonatal fentanyl exposure, the changes are more subtle. This suggests that the preBötC was capable of generating a eupneic respiratory rhythm at rest in the wakeful state and therefore was unlikely to exhibit notable alterations in its functioning. Chemosensory functions of juvenile-exposed mice during wakefulness were not tested in the present study. We demonstrated that ventilatory responses to hypercapnia and hypoxia were normal in neonatal-exposed mice and considering juvenile-exposed mice also displayed normal, rhythmic breathing at rest it is unlikely that they would have presented with altered chemosensory functions

4.5.2 Wakeful state: acute respiratory response to fentanyl

4.5.2.1 Neonatal-exposed mice exhibited a reduced sensitivity to fentanyl during wakefulness

In the control mice, first exposure to fentanyl in adulthood induced the expected attenuation of respiratory frequency. Although non-significant, V_t was slightly augmented in response to fentanyl, similar to the response observed in the adult mice of study 3 (investigation of the susceptibility of postnatal breathing patterns to fentanyl: a single exposure study) described in chapter 3 (see section 3.6.4). A fentanyl-induced increase in V_t has been previously reported by Colman and Miller (2001) who studied the effects of

fentanyl on neonatal and adult rats. However they observed a gasping-like breathing pattern in response to fentanyl, which was not observed in this study. Conversely, there are numerous studies that have reported a profound depression of V_t after opioid administration in awake rats (van den Hoogen and Colpaert, 1986; Greer et al., 1995; Manzke et al., 2003; Moss et al., 2006; Ren et al., 2006; Greer and Ren, 2009; Montandon et al., 2011), whereas one study in the awake adult rat found no change in V_t in response to a greater i.p dose of fentanyl than investigated in this present study (Chevillard et al., 2009). The reasons for these differences are not known. Opioid-induced changes in V_t in the awake rodent have been reported as complex and can be highly dependent on the dose administered (van den Hoogen and Colpaert, 1986). A wide range of fentanyl doses have been investigated in the previous studies which could account for the different V_t responses. Furthermore, variations in the route of administration may also explain the divergent results among these studies. It was also apparent that fentanyl did not induce dose-dependent respiratory effects in the control mice as anticipated and as documented in previous studies in the rat (Greer et al., 1995). An increasing fentanyl dose did not alter the magnitude of the respiratory effects. The reason for this remains elusive. Much of the work examining the effects of fentanyl has been conducted in the rat. The lack of dose-dependent fentanyl actions found in this study could be attributable to the species used or more specifically the strain of mouse (ICR). Further studies conducted in various mouse strains would help to determine if this is the case.

In the wakeful state, the respiratory response to fentanyl in adulthood was altered in the neonatal-exposed mice. Repeated neonatal fentanyl exposure appeared to induce a long-term desensitisation to the acute respiratory depressive actions of subsequent fentanyl. It is possible that the mice developed a respiratory tolerance to fentanyl. Tolerance is generally defined as an attenuated physiological response to a pharmacological agent at a dose that should induce an effect. Mice pre-exposed to fentanyl in neonatal life no longer exhibited the typical respiratory frequency depression when they were exposed to fentanyl again in adulthood. Interestingly, this reduced respiratory depression was found in response to a wide range of fentanyl doses (0.04 mg/kg-0.1 mg/kg). This desensitisation to fentanyl occurs rapidly and within days of the repeated exposure as shown from study 2 detailed in chapter 3. The longitudinal study described here confirms that the reduced sensitivity to fentanyl's respiratory depressive actions is maintained into adulthood. The mechanism(s) underlying this long-term respiratory tolerance during wakefulness cannot be determined from this study alone. Repeated or long-term exposure to agonists that act on μ opioid

receptors are known to induce tolerance to the analgesic actions of the drugs; however studies examining the effects on the respiratory actions are scarce. A number of studies have investigated and postulated potential mechanisms of opioid tolerance that involve μ opioid receptor regulation as thoroughly discussed in chapter 3, section 3.7.1. It is possible that these hypothesised mechanisms could also explain this long-term tolerance to respiratory depression observed after neonatal exposure. It is imperative to highlight that this tolerance is no longer observed in the anaesthetised state, suggesting the mechanism(s) of tolerance is not permanent but can be altered or even reversed depending on the state of the animal.

Not only did the neonatal-exposed mice lack respiratory depression during wakefulness they also displayed a surprising increase in ventilation at 5 minutes following the acute fentanyl challenge, which was not observed by the control mice. This ventilatory increase was due to a combined increase in respiratory frequency and V_t . A possible explanation for this observation is repeated exposure to fentanyl during neonatal life may have predisposed the mice to increased anxiety in adulthood thereby augmenting their sensitivity to stressful events. There is evidence to suggest repeated opioid exposure in rats induces glucocorticoid-dependent changes in the expression of Fos transcription factors within stress-related brain areas including the central amygdala and the hypothalamic paraventricular nucleus, which could alter the stress-responsive system (Garcia-Perez et al., 2012). Furthermore, dependence and withdrawal symptoms have been reported in neonatal rats chronically administered fentanyl (Thornton and Smith 1997; Thornton and Smith, 1998), which in turn could alter anxiety levels. To determine if mice exhibited heightened anxiety, baseline and post-injection levels of serum corticosterone, a known stress marker, could be measured (Ren et al., 2012b), where elevated levels would indicate increased anxiety. If the neonatal-exposed mice were in fact more stressed later in adult life, they would be highly sensitive to noxious stimuli including the i.p fentanyl injection. Furthermore, removing the animal from the recording chamber in order to administer the drug would also induce a stress response. The respiratory stimulation after the fentanyl challenge could therefore represent an injection-induced hyperventilation, which could in turn counteract the respiratory depressive effects of fentanyl. This could mean the reduced fentanyl depression does not actually signify tolerance, but rather a masking of the respiratory depression response. Thus, the method of administration utilised in these studies may not be optimal. An osmotic mini pump could represent an alternative method of drug delivery for future studies that would not induce an injection stress response. It is

also possible that if tolerance has in fact developed, fentanyl would not induce the same magnitude of respiratory depression that would otherwise counteract the injection-induced respiratory increase, and hence in the neonatal-exposed mice respiratory stimulation following the injection is evident. We also cannot rule out the possibility that fentanyl itself induced a stimulation in ventilation in the neonatal-exposed mice. A potential method to determine if the increase in ventilation is due to an injection-induced stress response as opposed to a pharmacological effect of fentanyl would be to pre-treat mice with naloxone (μ opioid receptor antagonist) prior to fentanyl administration. If the ventilatory increase is naloxone-insensitive and hence fentanyl-insensitive, then it is likely a result of the injection itself. Additionally an increase in ventilation in response to a vehicle injection would also suggest the injection is responsible.

4.5.2.2 Juvenile-exposed mice exhibited a reduced sensitivity to fentanyl during wakefulness

Repeated juvenile fentanyl exposure also evoked a long-term tolerance to the acute respiratory depressive actions of subsequent fentanyl, which was observed in the wakeful state. Identical to the respiratory response to fentanyl exhibited by neonatal-exposed mice, juvenile-exposed mice did not display the typical respiratory frequency depression when exposed again to fentanyl in adulthood. Again, fentanyl failed to induce respiratory depression at a wide range of doses. Furthermore, juvenile-exposed mice displayed an augmentation in ventilation directly after fentanyl administration that was also exhibited by the neonatal-exposed animals. Considering the similarity in the long-term altered fentanyl responsiveness seen in the wakeful state, it is highly likely that the mechanisms underlying these changes are similar in both the neonatal and juvenile-exposed mice. See section 4.5.2.1 above for discussion on the possible explanations for the altered respiratory response.

Taken together, the neonatal and juvenile exposure studies suggest that repeated fentanyl exposure early in life induces a long-term reduction in the sensitivity to the respiratory depressive actions of the drug observed during wakefulness. Given that the same respiratory response to fentanyl is seen in both neonatal and juvenile-exposed animals, the long-term change in the responsiveness to the drug in the wakeful state appear to occur independently of the age of exposure.

4.5.3 Anaesthetised state: resting breathing

Mice were anaesthetised with urethane to allow more detailed respiratory measurements to be performed as well as enabling respiratory activity to be assessed in a more depressed brain state. Urethane is an atypical general anaesthetic in that it does not potentiate GABAergic neurotransmission or reduce glutamatergic neurotransmission, but rather hyperpolarises cortical neurons by modulating a resting potassium conductance (Antkowiak, 2001; Thompson and Wafford, 2001; Hara and Harris, 2002; Sceniak and Maciver, 2006). Urethane was the anaesthetic of choice owing to its reported long duration of action and minimal depressive effects on the cardiovascular and respiratory system (Maggi and Meli, 1986).

4.5.3.1 Neonatal fentanyl exposure induced lasting changes in resting breathing under anaesthesia

Under anaesthesia, whilst respiratory frequency was unaffected, compared with wakefulness, all control and neonatal-exposed mice displayed a lower tidal volume and therefore lower minute ventilation when anaesthetised, suggesting that urethane induced a selective depressive action on tidal volume resulting in a more depressed and vulnerable breathing state. When under anaesthesia, the neonatal-exposed mice no longer exhibited a lower respiratory frequency compared with the control mice; however they displayed a lower tidal volume and therefore reduced minute ventilation. It has been reported that systemically administered fentanyl acutely reduces the excitability of phrenic premotor neurons as well as depressing the frequency and intensity of phrenic nerve discharge in the adult anaesthetised cat (Lalley, 2003). Accordingly, it can be speculated that repeated neonatal fentanyl exposure may have induced a long-term depression of phrenic nerve activity and hence also reduced the contraction of the diaphragm and depth of breathing that only becomes apparent in the anaesthetised state. This would account for the lasting reduction in tidal volume and consequential lowered ventilatory profile. *In vivo* recording of the phrenic nerve discharge in the anaesthetised adult mice could be investigated in future studies to determine if there are lasting alterations in its motor output.

The activity of the GG, an upper airway muscle with an inspiratory-modulated activity profile, was assessed. The GG is believed to maintain upper airway patency. In humans, a reduction in GG activity during sleep has been implicated in obstructive sleep apnoea

(Sauerland and Harper, 1976; Remmers et al., 1978). Furthermore, fentanyl has been found to evoke inhibitory actions on hypoglossal premotor neurons (Montandon et al., 2011) and hypoglossal motor pools (motoneurons that innervate the GG) thereby inducing a depression of the GG muscle activity (Hajiha et al., 2009). Accordingly, the effects of repeated neonatal fentanyl exposure on the long-term activity of this muscle were investigated in this present study. Under baseline conditions, neonatal-exposed mice did not exhibit any change in the amplitude of GG bursting, nor in the activation profile of the muscle. In all experimental mice in study 4 (control and neonatal-exposed), the GG muscle fired rhythmically and in synchrony with the inspiratory phase, suggesting early neonatal fentanyl exposure does not induce any lasting detrimental effects on the function of this inspiratory muscle. Previous studies have shown that GG activity is depressed during rapid eye movement (REM) and non-REM (nREM) sleep in rats (Pagliardini et al., 2012). It would be advantageous to undertake sleep/wake studies where EEG electrodes are implanted into the cortex to determine the sleep state of the rodent. GG muscle activity could be measured under various sleep states to determine if this previously reported state dependent depression of the GG is altered or augmented by repeated neonatal fentanyl exposure.

ABD muscles have been demonstrated to exhibit an expiratory pattern of firing in rodents, and are defined as the main expiratory muscles in mammals (Pagliardini et al., 2011; Pagliardini et al., 2012). To gain an index of expiratory muscle activity and the effects of repeated fentanyl exposure on the functioning of expiratory muscles, ABD muscle EMG was recorded. It was found however that ABD muscle expiratory-modulated activity was not present in the majority of the experimental mice. Instead, ABD muscle activity was consistently tonic in nature and not synchronised with any phase of respiration. This is congruent with findings from two previous *in vivo* studies where ABD_{EMG} activity was measured in urethane-anaesthetised rats and mice and it was found that approximately half of the animals displayed tonic ABD muscle activity throughout the experiment (Pagliardini et al., 2012; Pagliardini et al., 2013). In our study, 2 mice (one control and one neonatal-exposed) did intermittently display expiratory-related, rhythmic ABD muscle activity, which appeared suddenly but was short-lived. The source of this expiratory activity is not known, nor is its exact function. It is hypothesised that ABD expiratory activity is present during active expiration when there is an increased respiratory drive (e.g. during exercise), and contraction of the abdominal muscles act to force more air out of the lungs thereby aiding ventilation (West, 2007). In rodents, ABD expiratory activity can be evoked or

augmented by chemosensory stimulation (Iizuka and Fregosi, 2007; Marina et al., 2010; Abbott et al., 2011), focal excitation of the RTN/pFRG (Pagliardini et al., 2011) and during REM sleep states (Pagliardini et al., 2012; Pagliardini et al., 2013). It is probable that expiratory activity was predominantly inactive in the current study as mice were under normal resting conditions so expiration was likely in a passive state. Pagliardini and colleagues (Pagliardini et al., 2012; Pagliardini et al., 2013) demonstrated that urethane-anaesthetised rats and mice undergo sleep-like brain state alternations that can influence expiratory-related ABD muscle activity. They found that REM-like brain states induce or potentiate ABD expiratory muscle activation through unknown mechanisms. It is possible that the urethane-anaesthetised mice in the present study underwent similar brain-state changes that could have influenced ABD muscle recruitment and induced the sudden expiratory activation seen in the two mice; however this does not explain why it was completely absent in the majority of the mice. Irrespective of the underlying source or functional significance of respiratory-related ABD muscle activity; these results do suggest that fentanyl exposure in neonatal life does not influence the respiratory activity of this muscle under the conditions assessed.

An interesting respiratory characteristic exhibited by neonatal-exposed mice when under anaesthesia and air breathing was spontaneous augmented breaths. More specifically, augmented breaths in this study are defined as large amplitude inspiratory efforts, where the tidal volume is 50% greater than that of a regular breath. Augmented breaths were not common in the control mice. Conversely, a large proportion of neonatal-exposed mice displayed spontaneous augmented breaths during baseline breathing, and many exhibited a high occurrence of these breaths. The precise physiological function and neural correlates of augmented breaths *in vivo* are not known. Augmented breaths are similar to sighs which have been widely reported in rodent *in vivo* and human studies. Sighs are generally defined as spontaneous large amplitude breaths followed by a post-sigh pause (Bartlett, 1971; Marshall and Metcalfe, 1988; Hoch et al., 1998; Voituron et al., 2010; Pagliardini et al., 2012). The augmented breaths observed in this study were not followed by an expiratory pause and therefore cannot strictly be defined as sighs; however they are sigh-like behaviours. Sighs are believed to be an essential component of the respiratory system that function to increase lung compliance, maintain functional residual capacity, prevent alveolar atelectasis (Glogowska et al., 1972) and improve alveolar oxygenation (Patroniti et al., 2002). Augmented breaths are commonly induced by hypoxic stimuli in rodents (Bell et al., 2011; Pagliardini et al., 2012) and local cyanide stimulation of the carotid

bodies evokes sighing behaviour in cats (Glogowska et al., 1972). Taken together, these data suggest that augmented breaths may be induced by an activation of the peripheral chemoreceptors under hypoxic conditions. It is possible that when under anaesthesia, the neonatal-exposed mice were hypoxaemic (reduced arterial partial pressure of O₂), and consequently exhibited a high frequency of augmented breaths through peripheral chemoreceptor stimulation, in an attempt to increase blood oxygenation. The reduced baseline V_t observed in the anaesthetised neonatal-exposed mice will have contributed to a poorer ventilation and potentially the increased generation of augmented breathing patterns to counteract this. It would have been beneficial to monitor the blood gas status of a subgroup of these mice throughout the experimental procedure via blood sampling, to determine if mice were hypoxaemic. A non-invasive pulse oximeter positioned on the tail to measure blood O₂ saturation levels could also be employed (Ren et al., 2012a). In addition, assessment of chemosensory function under anaesthesia would have helped to ascertain if peripheral and central chemoreception was altered, which would affect blood gas homeostasis and potentially contribute to the frequent appearance of these sigh-like behaviours. Previous *in vivo* studies using a mouse model of Rett Syndrome have demonstrated that Rett mutant mice display a disordered respiratory phenotype that is characterised by an increased occurrence of sighing (Robinson et al., 2012). The frequent occurrence of augmented sigh-like breaths displayed by the neonatal-exposed mice in this present study may therefore be indicative of an unstable and fragile breathing state, and could potentially signify inadequate ventilatory function. *In vitro* studies using reduced brainstem slice preparations from embryonic and neonatal rodents have demonstrated that in addition to eupneic bursting, the preBötC can generate sigh-like respiratory output in the absence of peripheral chemosensory inputs (Lieske et al., 2000; Lieske and Ramirez, 2006b, a; Chapuis et al., 2014). This suggests that the preBötC alone may be sufficient for the generation of augmented breaths and may represent their central origin. It is therefore intriguing to speculate that the high frequency of augmented breaths under anaesthesia could be an indication of an altered preBötC function in the neonatal-exposed mice, which generates an unstable respiratory pattern. Additionally, sighs have been postulated to play an important role in resetting the neurorespiratory control system (Baldwin et al., 2004). It can therefore also be hypothesised that the increased frequency of augmented breaths may be an attempt to reset respiratory rhythm generation, and improve respiratory control. Since no abnormal breathing characteristics, including sighs, were noted during wakefulness, it is conceivable that neonatal fentanyl exposure predisposes mice to respiratory defects that are only observed when mice are in a more depressed and

vulnerable state e.g. under anaesthesia. This finding is supported by a previous clinical study that reported normal respiratory activity during wakefulness but sleep-disordered breathing in adult patients receiving prolonged opioid therapy (Farney et al., 2003).

4.5.3.2 Juvenile fentanyl exposure induced lasting changes in resting breathing under anaesthesia

Similar to the neonatal-exposed mice, when under urethane anaesthesia, juvenile-exposed mice displayed a reduced baseline V_t . However in contrast to the neonatal-exposed animals, juvenile-exposed mice also exhibited an increased respiratory frequency. This in turn maintained their minute ventilation. This increase in respiratory frequency could represent a compensatory mechanism to overcome the lowered V_t , thereby maintaining a normal ventilatory profile. The reason why this heightened baseline respiratory frequency was not observed in the neonatal-exposed mice is unknown. This could signify that exposing mice to fentanyl in neonatal life may induce detrimental changes in respiratory control in the mature system that could prevent compensatory changes in respiratory activity. Juvenile-exposed mice did not exhibit any long-term change in either the amplitude of the GG bursting or the activation profile of the muscle, which consistently showed inspiratory-related activity in all experimental mice. This suggests juvenile fentanyl exposure, akin to neonatal exposure, does not induce any lasting effects on the function of this inspiratory muscle. In terms of ABD muscle activity, this was found to be tonic in nature and did not display an expiratory-modulated mode of activation in either control or juvenile-exposed mice. This is congruent with the findings from the neonatal exposure study (see section 4.5.3.1 for discussion), and suggests juvenile-exposed mice also exhibited passive expiration under anaesthesia and repeated juvenile fentanyl exposure does not alter this.

In contrast to the neonatal-exposed mice, juvenile-exposed mice did not exhibit a high frequency of augmented, sigh-like breaths during baseline breathing under anaesthesia. If these breaths are an indication of hypoxaemia and therefore unstable ventilation as previously discussed, then the data from study 4 and study 5 suggests that repeated fentanyl exposure in neonatal life may induce more pronounced long-term detrimental respiratory effects compared to juvenile exposure. Unlike neonatal-exposed mice, the anaesthetised juvenile-exposed mice did not exhibit a reduced baseline minute ventilation due to their enhanced respiratory frequency and were therefore unlikely to have blood gas

values outside the physiological range. This would suggest that there was no requirement for the high occurrence of augmented breaths to improve blood oxygenation. As discussed with regards to the neonatal exposure study, it would also be advantageous to measure the partial pressure of O₂ and CO₂ in the blood of a subgroup of juvenile-exposed mice to confirm blood gas homeostasis is in fact maintained throughout the experimental procedures. Again, if our speculation that a high occurrence of augmented breaths is indicative of altered function at the level of the preBötC, the low occurrence in the juvenile-exposed mice could imply that juvenile exposure does not induce the same lasting effects on preBötC activity as exposure during the neonatal period.

4.5.4 Anaesthetised state: acute respiratory response to fentanyl

4.5.4.1 Neonatal-exposed mice exhibited a heightened sensitivity to fentanyl under anaesthesia

When neonatal-exposed mice were under anaesthesia they exhibited a strikingly different respiratory response to fentanyl compared with wakefulness. The mice no longer exhibited a reduced respiratory responsiveness to fentanyl, but rather displayed an enhanced sensitivity. Fentanyl, even at the lowest dose studied, induced a complete arrest of respiratory activity in all neonatal-exposed animals. This respiratory failure was not observed in any of the control mice. The loss of coordinated, rhythmic respiratory musculature movements and the development of persistent apnoea would have been fatal if mice were not artificially ventilated. The respiratory depression was so profound that artificial ventilation failed to restore spontaneous breathing. Here we have demonstrated that a non-destructive, pharmacological depression of the respiratory system with fentanyl during the early postnatal period can induce a heightened sensitivity to future respiratory challenges, but only when mice are anaesthetised. The mechanisms underlying these state-dependent fentanyl effects can only be hypothesised at present.

From the outset of the study, the initial aim was to examine the same fentanyl dose when mice were awake and anaesthetised; however it was clear that in both control and neonatal-exposed mice, anaesthesia represented a particularly vulnerable state for fentanyl-induced respiratory depression. The doses examined under anaesthesia were consequently lowered. This finding is in agreement with data reported by Montandon and colleagues (Montandon et al., 2011), who found that the magnitude of opioid-induced respiratory depression after

direct bilateral application to the preBötC in adult rats was correlated with the level of cortical activation as determined by EEG monitoring. Brain states with depressed cortical activity such as those under anaesthesia and non-REM sleep were most vulnerable to the depressive actions of opioids. This finding lends support to our data and fits with the theory that wakefulness can provide ample excitatory drive to the central respiratory system to help overcome depressed respiratory activity (Phillipson and Bowes, 1986). This concept of state-dependent respiratory depression and loss of cortical drive under anaesthesia can help to explain the hypersensitivity to fentanyl. Once again we speculate alterations in the rhythm generating capacity of the preBötC in these neonatal-exposed mice. μ opioid receptor agonists depress the neural activity of the preBötC *in vitro* (Takeda et al., 2001; Mellen et al., 2003; Montandon et al., 2011) and *in vivo* the preBötC is found to be the critical brain site where fentanyl acts to depress respiratory frequency (Montandon et al., 2011). Given that in this current study a subsequent fentanyl challenge caused a failure in the generation of a robust and rhythmic respiratory output under anaesthesia, it can be postulated that these effects are due to alterations at the level of the preBötC. It is possible that repeated fentanyl exposure in early life induces long-term neural alterations in the preBötC, making it more sensitive to the effects of future fentanyl. This proposed dysfunction may only become apparent when there is a loss of cortical drive to the central respiratory system and when the preBötC neural activity is further depressed. It should be noted however that increased preBötC sensitivity to opioids does not necessarily mean the rhythm generating function has been altered. Another point to consider is the reduced V_t and the presence of augmented breaths during baseline breathing, which as previously discussed could indicate respiratory instability in neonatal-exposed mice under anaesthesia. This already vulnerable baseline breathing state may be more sensitive to depressive agents and thus could also be attributable to the respiratory failure evoked by fentanyl. The finding that destruction of NK1R-expressing preBötC neurons induces breathing disturbances that are first observed in sleep in adult rats (McKay et al., 2005) together with the finding that respiratory instability is marked in nREM sleep in CCHS patients (Shea, 1997), is consistent with the idea that respiratory abnormalities and vulnerabilities to perturbations tend to initially manifest in depressed states, and is also congruent with the data reported here. Sleep represents a depressed brain state that significantly influences respiratory activity (Pagliardini et al., 2012). Given that opioids are widely used to manage post-operative pain together with the fact that patients tend to spend a substantial portion of time asleep following surgery (Caplan et al., 1989; Gourlay et al., 1990; Viscusi et al., 2004), it would be beneficial to examine the response to fentanyl

during sleep in the mice, which would provide further translational value to the study. It would be interesting to determine if similar findings are observed under sleep. Since wakefulness can clearly overcome or compensate for defects in components of the respiratory system, studying respiratory activity during wakefulness alone could mask respiratory disturbances. For a comprehensive respiratory analysis, it is imperative that respiration activity is analysed under various brain states.

It is important to highlight that the specific actions of urethane on the central respiratory system and its individual components including the preBötC have not been identified. Further investigation is required to determine if urethane exerts increased depressive actions in the neonatal-exposed mice or induces more adverse effects that could contribute to the increased responsiveness to fentanyl. As discussed above in section 4.5.2.1, the neonatal-exposed mice may have exhibited exaggerated stress-responses when in the wakeful state that could have counteracted the depressive effects of fentanyl. Under anaesthesia stress responses are abolished which could also explain why fentanyl induced a clear respiratory depression and may represent the true response to fentanyl.

Fentanyl has been shown to induce acute hypoxemia in rats (Chen et al., 1996; Chevillard et al., 2009). Furthermore, work by Moss and colleagues (Moss et al., 2006) has revealed that recurrent hypoxic exposure in juvenile rats, which renders them hypoxemic, induces an increased respiratory sensitivity to subsequent fentanyl exposure in adulthood. The authors suggest that this increased sensitivity is due to hypoxemia producing a repeated release of endogenous opiates that could in turn activate μ opioid receptors and sensitise them to subsequent opioid administration. If repeated fentanyl exposure in neonatal life induces recurrent hypoxemia then this mechanism of increased endogenous opiate release and consequential sensitisation of the μ opioid receptors within the preBötC could underlie the increased respiratory responsiveness to future fentanyl application in adult life under anaesthesia. Repeated hypoxemia in early life may therefore induce a detrimental impact on the respiratory system.

4.5.4.2 Juvenile-exposed mice did not exhibit an altered sensitivity to fentanyl under anaesthesia

When juvenile-exposed mice were anaesthetised they exhibited a different respiratory response to fentanyl compared with wakefulness. Fentanyl induced a significant

respiratory depression which was not observed during wakefulness. This once again highlights the concept of state-dependent respiratory depression (see section 4.5.4.1) and suggests the mechanisms of respiratory depression may change depending on the arousal state. The loss of stress-related responses under anaesthesia as discussed above (section 4.5.4.1) could also account for the depressed respiratory activity only observed under anaesthesia. The respiratory depression evoked by fentanyl under anaesthesia was of the same magnitude as that seen in the control mice, suggesting fentanyl exposure in juvenile life does not alter the response to subsequent fentanyl challenges under anaesthesia. Importantly, the profound suppression of respiratory activity and eventual respiratory failure seen in the neonatal-exposed mice in response to fentanyl was not exhibited by the juvenile-exposed mice (with the exception of one mouse). The low occurrence of augmented breaths and the fact they exhibited unaltered minute ventilation suggests the juvenile-exposed mice had a more stable breathing phenotype under anaesthesia compared to the neonatal-exposed mice, therefore making them less susceptible to fentanyl's depressive actions. Whether neonatal and juvenile-exposed mice exhibited differences in central respiratory control including preBötC functioning that could account for this differential fentanyl response remains to be elucidated.

It is clear that the striking difference in the respiratory response to fentanyl between the neonatal and juvenile-exposed mice only became apparent when the mice were in the anaesthetised state. In terms of respiratory function and fentanyl effects during wakefulness, there were only subtle differences between the two groups of mice. Studying breathing in the wakeful state alone would have drawn a different interpretation. This highlights the complexity of opioid respiratory depression and the fact that in order to gain a full analysis of opioid depression and its effects on respiratory control, respiratory activity must be explored under varying behavioural states. Taken together, the neonatal and juvenile exposure studies suggest that the postnatal age of fentanyl-exposure influences long-term respiratory effects. It appears that repeated neonatal fentanyl exposure is more detrimental to respiratory control.

4.5.5 Neonatal life is vulnerable to repeated fentanyl exposure

Only the neonatal-exposed mice displayed a depressed baseline ventilation and high rate of augmented breaths under anaesthesia coupled with an enhanced sensitivity to fentanyl that resulted in respiratory arrest. This strongly suggests that neonatal life represents a time

period that is particularly vulnerable to the lasting effects of opioid depression. The reason(s) behind this age-dependent difference cannot be elucidated at present; however we can offer some speculation.

The increased vulnerability of neonatal mice to the long-term respiratory effects of repeated fentanyl exposure is unlikely due to age-dependent differences in blood brain barrier integrity that could influence the level of drug that reaches and acts on the brain. Previous studies have demonstrated that the degree of fentanyl penetration across the blood brain barrier is similar between neonatal and juvenile rats, given that the concentration of fentanyl in brain tissue following administration was comparable at all ages (Thornton and Smith, 1997). Furthermore, fentanyl is highly lipophilic and readily crosses the blood brain barrier (Bragg et al., 1995), so age is unlikely to affect this. It would however be advantageous to measure fentanyl levels in the brain tissue of the neonatal and juvenile mice of this study to confirm similar drug penetration. It is also unlikely that repeated fentanyl exposure hampered the feeding ability of the neonatal mice, which could have indirectly impacted the respiratory system, given that the body weights of the mice during the exposure period and on reaching adulthood were not affected by fentanyl administration.

Previous studies have investigated the long-term consequences of the perinatal environment on respiratory control in rodents, and in accordance with the data presented in this chapter have found that exposure to various environmental stimuli in the neonatal period including hypoxia, hypercapnia, caffeine and stressful events can induce lasting changes in ventilatory control (Okubo and Mortola, 1988; Bavis and Kilgore, 2001; Bavis et al., 2004; Montandon et al., 2006; Gulemetova and Kinkead, 2011). Together with our findings, this is congruent with the idea that manipulations to the developing respiratory system can have profound, lasting changes in respiratory activity. It is widely acknowledged that the central respiratory system has a large capacity for plasticity, and constantly adapts to the internal and external environment of the organism. Our data suggests that fentanyl exposure in neonatal life induces developmental plasticity, which in terms of respiratory control has been defined as long-term changes in the mature respiratory system that are induced by experiences that occur during a critical developmental time period, whereas the same experiences after this critical time window evoke little or no lasting changes (Carroll, 2003; Bavis and Mitchell, 2008). This theory is strengthened by the fact that juvenile exposure to fentanyl did not elicit the same profound

long-term respiratory changes, suggesting the first five days of life in the mouse represents a critical developmental time period highly susceptible to opioid-induced developmental plasticity. The reasons behind this developmental susceptibility can only be hypothesised. In mammals there is a surge of endogenous opiates at birth (Jansen and Chernick, 1983) that have been proposed to depress preBötC function (Feldman and Del Negro, 2006; Janczewski and Feldman, 2006). The exogenous application of fentanyl coupled with the endogenous perinatal opiate surge could exert a significant depression on the preBötC in the neonatal mice and may be partly or fully accountable for the more pronounced long-term respiratory effects compared with juvenile-exposure. In addition, breathing exhibits an irregular and fragile pattern immediately after birth. Given that a critical postnatal maturation of breathing occurs within the first 3-5 days of life in the mouse (see chapter 3 for full details), it is possible that neonatal fentanyl exposure interferes with this maturation process thereby inducing profound long-term respiratory consequences and altered respiratory responsiveness to future fentanyl challenges that persist into adulthood. This would explain why juvenile exposure did not induce such profound respiratory changes, since juvenile mice would have exhibited a mature breathing pattern at the time of exposure. An immature respiratory system is perhaps highly susceptible to repeated perturbations. From our studies we cannot deduce if fentanyl exposure during all 5 postnatal days (P1-P5) is essential for the lasting respiratory effects, or if there is a more narrow critical time window. Repeating the studies with slight variations in the exposure time frame would help to ascertain the exact critical developmental time period. The results from both neonatal and juvenile exposure studies have highlighted the potential long-term health consequences of developmental plasticity in respiratory control.

4.5.6 Future experimental studies

It is imperative to highlight the fact that the fundamental mechanisms by which repeated fentanyl exposure evokes the long-term respiratory effects can only be speculated at present. The studies described in this chapter have examined the long-term physiological effects at the system level. Whether fentanyl induces its long-term effects by specific actions on single neural groups or via more complex network effects remains elusive. Fentanyl was administered systemically and likely targeted respiratory and non-respiratory brain areas, as well as peripheral sites, which could have contributed directly or indirectly to the respiratory changes seen in adult life. This study design is clinically relevant. However to unravel the underlying mechanisms of repeated opioid exposure and its

respiratory consequences, further studies must be undertaken in more reduced *in vitro* preparations. Whether repeated neonatal fentanyl exposure induces long-term defects or alterations in preBötC functioning that continue into adulthood as postulated based on the studies described in this chapter, certainly warrants further investigation. This hypothesised opioid-induced abnormality in preBötC functioning could be further investigated by directly recording the inspiratory activity of preBötC neurons in medullary slice or *en bloc* hindbrain preparations using electrophysiology or calcium imaging techniques. These preparations are however most viable in young neonatal tissue (Fong et al., 2008). The working heart-brainstem *in situ* preparation could be employed in the adult mouse. This preparation has the advantage of an intact circulatory system as well as having a more intact respiratory network including peripheral chemoreception and cardiorespiratory reflexes (Paton, 1996b, a). From this preparation central respiratory motor output (phrenic and hypoglossal nerve discharge) can be monitored and recorded in addition to extracellular recordings of the preBötC neurons (Paton, 1996b, a). Employing this experimental preparation would enable the lasting central respiratory effects of fentanyl exposure to be more comprehensively investigated in the adult mouse.

Another future research direction could be to establish the brain regions acutely affected by fentanyl in adulthood and determine if neonatal and juvenile repeated fentanyl exposure alters this. A quantitative 2-deoxyglucose (2-DG) autoradiography study could be employed to explore the complex neuropharmacological effects of fentanyl. The 2-DG technique uses a radiolabelled analogue of glucose and works on the principle that cerebral metabolism is closely linked to glucose utilisation (Wree, 1990). Studying the fate of the injected radiolabelled glucose analogue can give indications of the functional activity of individual neural structures and hence can show the functional effect of fentanyl on discrete brain regions. This study would help to delineate the acute effects of fentanyl on the brain and identify if repeated fentanyl exposure in neonatal or juvenile life elicits long-term changes in fentanyl's actions that could explain the physiological changes described in the present studies of this chapter. Furthermore, the influence of anaesthesia on fentanyl's activity in the brain could be investigated, which would further aid in the understanding of state-dependent respiratory depression.

4.5.7 Limitations and technical issues

It was very difficult to design these pre-clinical studies to be fully clinically relevant given the heterogeneous nature of opioid treatment in clinical practice. For one, the route of administration of fentanyl in the studies described in this chapter differs from that seen in the clinical setting. Mice received bolus intraperitoneal fentanyl injections over several days, whereas fentanyl is often given to patients by continuous intravenous infusion or transdermal application (DelleMijn et al., 1998; Kornick et al., 2003). These routes of administration are not feasible in mouse pups. It is therefore very difficult to replicate the doses administered clinically as these vary depending on the route of administration. In addition, the duration of opioid treatment administered in the clinic can differ significantly depending on both its therapeutic purpose and on the individual patient and their physiological response to the treatment. These limitations should be considered when interpreting the clinical relevance of the data.

In addition to recording GG muscle activity, the original objective was to also measure EMG activity of the diaphragm, given that it is the principal inspiratory muscle. There was however technical issues that prevented recording. Initially, wire EMG electrodes were sutured into the diaphragm muscle; however insertion of the electrodes through the thin muscle wall created a small hole that allowed air to enter the pleural cavity consequently inducing a pneumothorax. This in turn had a detrimental impact on respiration. In a further attempt to measure diaphragm activity, hooked needle EMG electrodes were also inserted into the muscle. Although they did not damage the diaphragm, it was difficult to keep them secured in place to allow continual and reliable EMG measurements. The use of smaller gauge EMG wire electrodes that induce less damage to the diaphragm and remain securely in contact with the muscle could overcome the problem. To enable sufficient diaphragm EMG recordings for future respiratory studies in the mouse, it is fundamental that the experimental technique is optimised.

4.5.8 Summary

For the first time we have shown that repeated exposure to fentanyl during early life in the mouse induces lasting respiratory alterations including a remarkable respiratory hypersensitivity to fentanyl under anaesthesia (see Table 4-3 for summary of main findings). Given the widespread application of opioids in clinical practice and their potent

respiratory depressive actions, understanding long-term detrimental respiratory effects of opioid exposure is invaluable. If these findings translate to the clinical setting then long-term neonatal opioid therapy in humans could predispose a patient to respiratory abnormalities later in life that may manifest initially in depressed behavioural states e.g. during sleep. Furthermore, repeated neonatal opioid exposure could induce a dangerous hypersensitivity to the respiratory depressive actions of opioid drugs in depressed behavioural states, thus limiting their therapeutic usefulness. In conclusion these studies have generated novel data yielding invaluable insight into the vulnerabilities of the immature mammalian respiratory system to opioid-induced depression. Moreover these studies have aided in the understanding of state-dependent respiratory modulation and depression, whilst laying a solid foundation for future studies examining the impact of repeated fentanyl exposure on respiratory control.

	Repeated fentanyl exposure in the neonatal mouse	Repeated fentanyl exposure in the juvenile mouse
Long-term changes in baseline breathing during wakefulness	<ul style="list-style-type: none"> •Reduced respiratory frequency •Increased duration of inspiration •Unaltered tidal volume •Reduced minute ventilation 	<ul style="list-style-type: none"> •Unaltered respiratory frequency •Unaltered inspiratory and expiratory duration •Unaltered tidal volume •Subtle reduction in minute ventilation
Long-term changes in respiratory response to fentanyl during wakefulness	<ul style="list-style-type: none"> •Reduced sensitivity to the respiratory depressive effects of fentanyl 	<ul style="list-style-type: none"> •Reduced sensitivity to the respiratory depressive effects of fentanyl
Long-term changes in baseline breathing under anaesthesia	<ul style="list-style-type: none"> •Unaltered respiratory frequency •Unaltered inspiratory and expiratory duration •Reduced tidal volume •Reduced minute ventilation •Unaltered genioglossus activity •Increased frequency of augmented breaths 	<ul style="list-style-type: none"> •Increased respiratory frequency •Reduced inspiratory duration •Reduced tidal volume •Unaltered minute ventilation •Unaltered genioglossus activity
Long-term changes in respiratory response to fentanyl under anaesthesia	<ul style="list-style-type: none"> •Hypersensitivity to the respiratory depressive effects of fentanyl •Fentanyl evoked a respiratory arrest 	<ul style="list-style-type: none"> •No change in the respiratory sensitivity to fentanyl •Fentanyl induced typical respiratory depression but did not evoke a respiratory arrest

Table 4-3. Summary of the long-term respiratory effects of repeated fentanyl exposure in the neonatal and juvenile mouse.

Chapter 5.

Long-term respiratory effects of repeated fentanyl exposure in the neonatal mouse: Immunohistochemical analysis of the ventral respiratory column

5.1 Introduction

From study 4 discussed in chapter 4, it was shown for the first time that repeated exposure to fentanyl during neonatal life in the mouse induces lasting alterations in resting ventilation and evokes a striking change in the response to future administrations of fentanyl, with a reduced sensitivity to fentanyl exhibited when awake but a hypersensitivity displayed when anaesthetised. Understanding the processes underlying these long-term respiratory changes is of clinical significance as opioids are utilised widely in clinical practice (Swarm et al., 2001; Niesters et al., 2013). However, at present, these underlying mechanism(s) remain elusive. Given that fentanyl is known to reduce respiratory frequency *in vivo* by acting on and depressing the activity of NK1R-expressing preBötC neurons (Montandon et al., 2011), it is possible that repeated fentanyl exposure induces a long-term change in preBötC function which may be due to lasting histological changes to the preBötC e.g. changes in NK1R expression. Histological alterations could be responsible for the long-term respiratory effects exhibited by the neonatal-exposed mice. The central respiratory system is comprised of a complex network of functionally interacting neurons, so it is not known if repeated depression of the preBötC by fentanyl induces indirect effects on other respiratory nuclei. Furthermore, fentanyl's actions are widespread and not limited to the preBötC; therefore anatomical alterations in other respiratory and non-respiratory related brain regions could also contribute to the long term respiratory changes exhibited by neonatal-exposed mice. Since fentanyl acts on the μ opioid receptor to induce its pharmacological effects, it is possible that changes at the receptor level within respiratory-related brain areas, including that of the preBötC, are responsible for the long-term change in both resting respiratory activity and the respiratory responsiveness to fentanyl exhibited by the neonatal-exposed mice. In support of this theory, alterations in μ opioid receptor regulation and therefore receptor density throughout the brain have been implicated in the development of tolerance and reduced sensitivity to opioids following repeated exposure (Bhargava and Gulati, 1990; Yoburn et al., 1993; Bernstein and Welch, 1998; Stafford et al., 2001). As discussed in section 3.7.1 in chapter 3, there is considerable debate concerning the exact receptor changes induced by repeated opioid exposure as well as the physiological significance of these changes. From the wide range of *in vivo* studies that have been conducted, there are incongruities in the observed changes in receptor density following repeated opioid exposure, with both upregulation and downregulation of the μ opioid receptor reported (see section 3.7.1 for full discussion). To date there have been no studies carried out which have investigated if repeated opioid

exposure induces long-lasting changes in μ opioid receptor regulation. Additionally, the long-term effect of repeated opioid exposure on the expression of the μ opioid receptor within specific respiratory-related brain regions has never been reported. The ventral respiratory column (VRC) is a region of the ventrolateral medulla containing some of the principal respiratory neurons including the preBötC. Elucidating potential histological changes within the VRC could be vital in understanding the long-lasting and remarkable change in the susceptibility to the respiratory depressive actions of fentanyl observed in the neonatal-exposed mice described in study 4 (chapter 4).

5.1.1 Study 6 aims and rationale

The aim of study 6 described in this chapter was to determine if repeated exposure to fentanyl during neonatal life in the mouse induces long-lasting changes in receptor expression within a region of the VRC, using immunohistochemistry (IHC). The preBötC and the RTN/pFRG are two important respiratory neural groups implicated in respiratory control (Smith et al., 1991; Onimaru and Homma, 2003); therefore examining histological changes within these regions was of greatest interest. Given that fentanyl acts on the μ opioid receptor to evoke its effects, it was of particular interest to determine the effect of repeated fentanyl exposure on μ opioid receptor expression throughout the VRC, particularly within the region of the preBötC, which is reported to express a high level of the μ opioid receptor (Gray et al., 1999). Since both preBötC and RTN/pFRG neurons express the NK1R (Gray et al., 1999; Guyenet and Wang, 2001; Wang et al., 2001a; Guyenet et al., 2002; Onimaru et al., 2008; Pagliardini et al., 2008), the long-term effect of fentanyl exposure on NK1R expression throughout the VRC was also examined. Phox2b is a selective marker for the RTN/pFRG (Stornetta et al., 2006; Kang et al., 2007; Onimaru et al., 2008) therefore its expression within the VRC was also assessed. Study 6 was designed to elucidate some of the potential mechanisms underlying the long-term changes in baseline respiratory behaviour as well as the lasting altered respiratory response to fentanyl displayed by neonatal-exposed mice from study 4. It was hypothesised that neonatal-exposed mice would exhibit long-lasting changes in μ opioid receptor expression within the region of the VRC corresponding to the preBötC.

Given that repeated fentanyl exposure during juvenile life in the mouse also evoked long-term respiratory effects as reported from study 5 (detailed in chapter 4) it was also of interest to determine if juvenile exposure induces long-lasting changes in receptor

expression within the VRC. This work was designed to complement and follow on from study 5. However, due to a number of technical issues no data were generated. This will be discussed in full in section 5.4.5.

5.2 Methods

5.2.1 Animals

All experimental procedures were carried out under licence from the UK Home Office and performed in accordance with the Animals (Scientific Procedures) Act, 1986. Experiments detailed in this chapter were performed on male ICR mice. All mice were bred at the Wellcome Surgical Institute animal research facility and a total of 9 mice were studied. All mouse pups were housed with their mother until they reached weaning age (approximately 21 days old), after which they were housed in groups of no more than six. Mice were maintained on a 12 hour light/dark cycle with food and water available *ad libitum*.

5.2.2 Chronic fentanyl exposure

Neonatal mice were repeatedly administered fentanyl citrate (Janssen-Cilag, UK) from P1-P5 (n=5). They received a single intraperitoneal (i.p) dose of 0.04 mg/kg on each postnatal day. This was the same dose as administered to neonatal mice in study 4, detailed in chapter 4. Control mice (n=4) were administered an equivalent volume of physiological saline from P1-P5. Mice repeatedly exposed to fentanyl in neonatal life are referred to as neonatal-exposed.

5.2.3 Perfusion fixation and cryostat sectioning

When mice reached adulthood (6 weeks old) their brains were perfused to allow for detailed histological analyses of the VRC. Mice were administered a lethal i.p injection of pentobarbital (0.1ml) and on abolition of the hindlimb reflex were transcardially perfused with 4% paraformaldehyde (see chapter 2, section 2.7 for full details of perfusion fixation protocol). The brainstem was removed and post-fixed for 4 hours in the same fixative solution. 40 micrometer coronal medullary sections were cut at -21°C using a cryostat. Sections were collected sequentially into 48 well plates containing 0.3M PBS and then split into 4 groups to allow for different immunostaining within each group (see chapter 2,

Figure 2-7 for illustration). Neurons were immunostained for NK1R in groups 1 and 3, μ opioid receptor in group 2 and Phox2b transcription factor in group 4.

5.2.4 Antibody combinations

All immunohistochemistry protocols were carried out on free floating brainstem sections. Neonatal-exposed and control tissue were always processed simultaneously for direct comparisons. For full details of the immunostaining protocol see chapter 2, section 2.9.1.

5.2.4.1 NK1R immunostaining

NK1R expression was detected using a rabbit anti-NK1R primary antibody (1:5000; Sigma-Aldrich, UK) and a biotinylated donkey anti-rabbit secondary antibody (1:500; Vector Laboratories, UK). A tyramide signal amplification step was carried out using tyramide conjugated to tetramethylrhodamine (1:50, Perkin Elmer Inc, UK).

5.2.4.2 μ opioid receptor immunostaining

Mu opioid receptor expression was detected using a rabbit anti- μ opioid receptor primary antibody (1:5000; Immunostar, UK) and a biotinylated donkey anti-rabbit secondary antibody (1:500; Vector Laboratories, UK). A tyramide signal amplification step was carried out using tyramide conjugated to tetramethylrhodamine (1:50, Perkin Elmer Inc, UK).

5.2.4.3 Phox2b immunostaining

Phox2b expression was detected using a rabbit anti-Phox2b primary antibody (1:500; gift from C.Goridis, ENS, France) and a donkey anti-rabbit secondary antibody conjugated to Alexa-488 (1:500; Stratech-Jackson Immunoresearch). Phox2b staining proved to be variable so quantification was not carried out (discussed in section 5.4.4).

All sections were also stained for VGLUT2 and choline acetyltransferase (ChAT) enzyme. VGLUT2 is a marker for both preBötC and RTN/pFRG neurons and ChAT is expressed in motor neurons and helps to delineate the facial motor nucleus (one of the reference landmarks used in the method of cell counting). However the immunostaining for these

markers did not work and will be discussed in section 5.4.4. To stain for VGLUT2, a guinea pig anti-VGLUT2 primary antibody (1:1000, Millipore, UK) and a donkey anti-guinea pig secondary antibody conjugated to dylight-649 (1:500, Stratech-Jackson Immunoresearch) were used. To stain for ChAT, a goat anti-ChAT primary antibody (1:1000, Sigma-Aldrich, UK) and a donkey anti-goat secondary antibody conjugated to either Alexa-488 or Rhodamine Red (1:500, Stratech-Jackson, Immunoresearch) were used.

5.2.5 Immunofluorescent imaging and quantification

NK1R, μ opioid receptor and Phox2b immunopositive cells were imaged and analysed throughout a section of the VRC extending from the preBötC to the RTN/pFRG, using an epifluorescent microscope (Axioscop, Zeiss, UK). Coronal sections were first examined under the epifluorescent microscope to identify the ones that contained the chosen reference landmarks, between which the cell counts took place. The first caudal landmark was the rostral border of the lateral reticular nucleus (LRN), where this neuronal group no longer exists as a single outline but rather exhibits a medial and lateral portion. This section was identified as the zero reference point and cells counts were performed in the consecutive sections. The second rostral landmark was the rostral portion of the facial motor nucleus and the section containing this landmark was the last to be analysed. Within this rostrocaudal extent of the ventrolateral medulla, NK1R-immunopositive and μ opioid receptor immunopositive cells were counted bilaterally (illustrated in Figure 5-1). Within the VRC, the preBötC is reported to be located ventral to the subcompact formation of the NA (scNA) (Gray et al., 1999). It was however difficult to determine the exact location and boundaries of the preBötC based on the NK1R and the μ opioid receptor staining in the mouse (discussed in section 5.4.4). As a result of this, NK1R and μ opioid receptor immunopositive cells were counted within a box (600 x 400 μ m) that was large enough to encompass an extensive area below the NA to ensure the preBötC was contained. In the first four consecutive sections following the LRN landmark, NK1R and μ opioid receptor immunopositive cells were counted within the box, which was positioned so that the middle of its dorsal portion touched the ventral border of the NA (see Figure 5-2 for illustration). The first three sections are believed to contain the preBötC and the fourth section is believed to contain the Bötzing complex (Franklin and Paxinos, 2008). The RTN/pFRG is reported to extend rostrocaudally along the entire length of the facial motor nucleus (Onimaru and Homma, 2003; Stornetta et al., 2006; Onimaru et al., 2008). In the

next three consecutive sections containing the facial motor nucleus, NK1R and μ opioid receptor expressing cells were also quantified. In these three sections, cells were counted in the area directly ventral to the facial motor nucleus and through to the ventral medullary surface (see Figure 5-3 for illustration) which encompasses the RTN/pFRG neurons. All sections were identified by their distance from the LRN and the last section examined was 1120 μm rostral from the LRN.

All sections examined were 160 μm apart to prevent duplicate counting of cells. The NK1R and μ opioid receptor are membrane bound receptors. A cell was only counted as being NK1R or μ opioid receptor immunopositive if there was clear immunostaining that outlined the somatic membrane i.e. there was a complete cell boundary and the soma was at least 10 μm in diameter. Bilateral cell counts were performed manually using Axiovision software (Carl Zeiss, UK). In addition, Phox2b immunopositive cells were qualitatively assessed throughout the same region of the VRC as described for the NK1R and μ opioid receptor; however no cells counts were performed. A cell was deemed Phox2b immunoreactive if staining clearly outlined the cell nucleus.

5.2.6 Statistical analysis

All statistical analyses were performed using GraphPad Prism 4 software. The number of NK1R and μ opioid receptor immunopositive cells found throughout the VRC was compared between control and neonatal-exposed mice using a 2-way ANOVA with Bonferroni's post test. Differences were regarded as significant if $p < 0.05$. All data are presented as mean \pm SD.

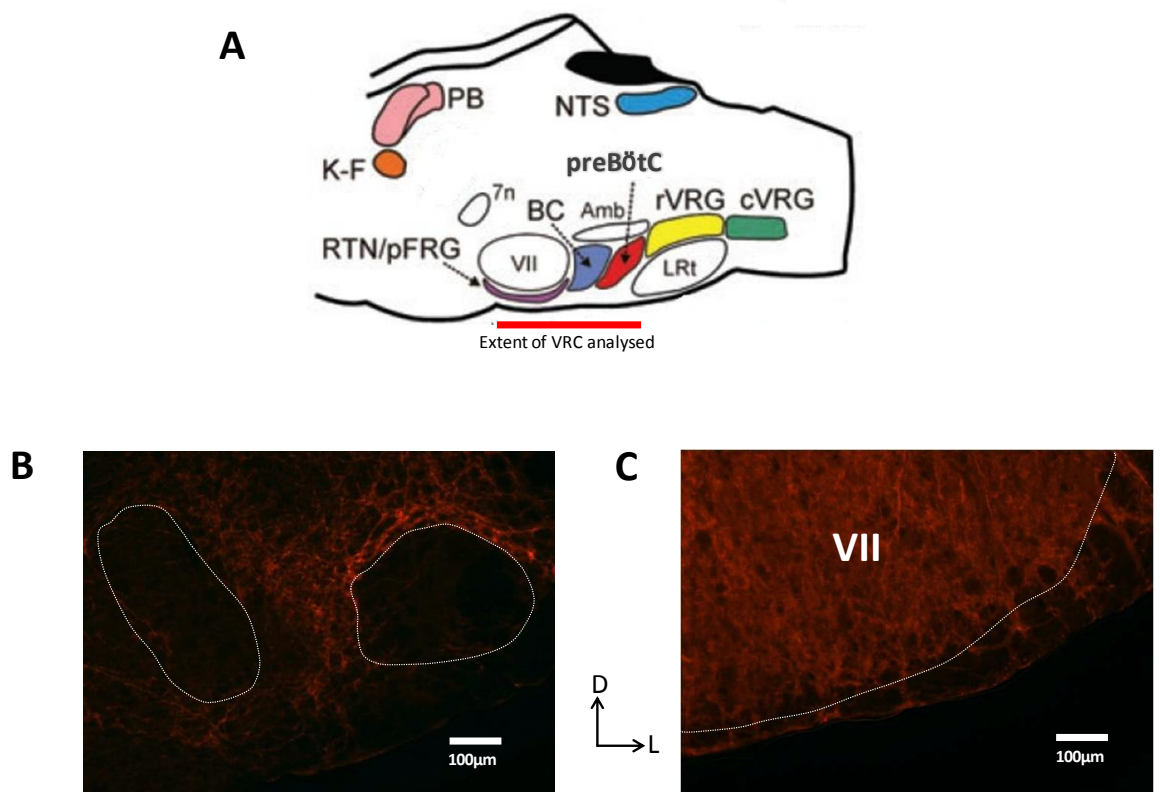


Figure 5-1. The rostrocaudal extent of the ventral respiratory column (VRC) analysed. A: Schematic illustration showing the region of the VRC analysed i.e. between the rostral aspect of the lateral reticular nucleus and the rostral portion of the facial motor nucleus. B: Immunofluorescent image showing NK1R expression in a coronal section that contained the rostral aspect of the lateral reticular nucleus, which was deemed the zero reference point after which cell counts began. Note the lack of NK1R immunostaining which highlights the medial and lateral rostral tips of the lateral reticular nucleus (circled in white). C: Immunofluorescent image showing NK1R expression in a coronal section that contained the rostral end of the facial motor nucleus which was the last section within the VRC analysed. Scale bar=100µm. Abbreviations: Amb, nucleus ambiguus; BC, Bötzinger complex; cVRG, caudal ventral respiratory group, K-F, Kölliker-Fuse nucleus; LRt, lateral reticular nucleus; NTS, nucleus tractus solitarius; PB, parabrachial complex; preBötC, preBötzinger complex; RTN/pFRG, retrotrapezoid nucleus/parafacial respiratory group; rVRG, rostral ventral respiratory group; VII, facial motor nucleus.

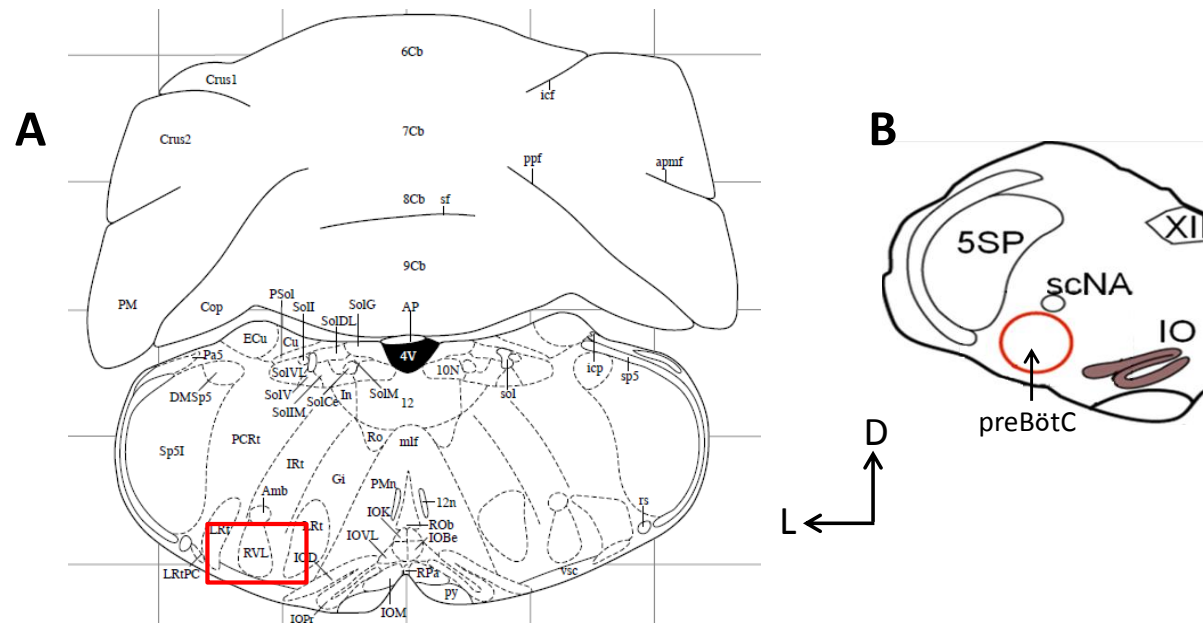


Figure 5-2. Method of cell counting within the region of the VRC containing the preBötC. A: Schematic illustration of a coronal medullary section showing the position of the box (600x400 μ m) within which cell counts took place. The box was positioned so that the middle of its dorsal portion touched the ventral border of the NA. This method of cell counting was applied to the first four consecutive sections following the section that contained the LRN. B: Schematic illustration of a coronal hemisection showing the estimated location of the preBötC, ventral to the subcompact formation of the NA (scNA).

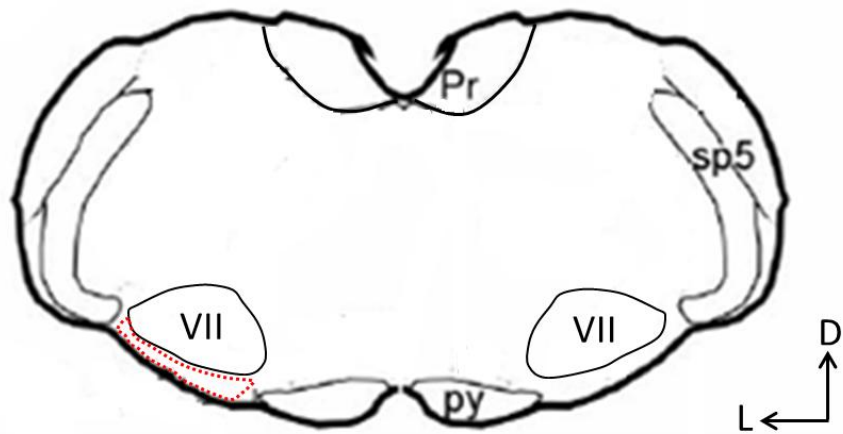


Figure 5-3. Method of cell counting within the region of the RTN/pFRG.

Schematic illustration of a coronal medullary section showing the region below the facial motor nucleus analysed which is believed to encompass the RTN/pFRG. Cells were counted in the region directly ventral to the facial motor nucleus and through to the ventral medullary surface as highlighted by the red outline. This method of cell counting was carried out in all three coronal sections containing the facial motor nucleus. sp5: spinal trigeminal nucleus, Pr: prepositus nucleus, py: pyramidal tract, VII: facial motor nucleus.

5.3 Results

5.3.1 NK1R expression throughout the VRC

The NK1R is a neuronal marker for both the preBötC and the RTN/pFRG (Gray et al., 1999; Guyenet and Wang, 2001; Wang et al., 2001a; Guyenet et al., 2002; Onimaru et al., 2008; Pagliardini et al., 2008). The number of NK1R expressing cells found throughout the VRC of control and neonatal-exposed mice was compared. In both groups of mice, NK1R expressing cells showed a similar rostrocaudal distribution and were present throughout the entire section of the VRC that was analysed i.e. from the section 160 μm rostral to the LRN through to the section 1120 μm rostral to the LRN (Figure 5-6). According to the mouse brain atlas by Franklin and Paxinos, the preBötC extends rostrally from approximately 160 μm to 600 μm from the LRN (Franklin and Paxinos, 2008). NK1R expressing cells were found within this rostrocaudal extent of the VRC in both control and neonatal-exposed mice (Figure 5-6) and were observed in the region below the subcompact formation of the NA, believed to represent the preBötC as illustrated in Figure 5-4. It is evident that NK1R immunoreactivity outlined the somatic membranes of cells (Figure 5-4). With reference to the mouse brain atlas (Franklin and Paxinos, 2008), the RTN/pFRG begins at 800 μm rostral from the LRN and extends rostrally to a distance of 1120 μm from the LRN and is located below the facial motor nucleus. NK1R immunopositive cells of the RTN/pFRG of both control and neonatal-exposed mice are shown in Figure 5-5. NK1R expressing cells were present directly ventral to the facial motor nucleus and in close proximity to the ventral medullary surface. NK1R expression was also found within the facial motor nucleus, which facilitated the anatomical delineation of this landmark nucleus.

Quantification of NK1R immunopositive cells within the region of the preBötC demonstrated a similar distribution pattern in both the control and neonatal-exposed mice (Figure 5-6). The position and size of the counting box (600 x 400 μm) ensured that all of the NK1R immunopositive cells in the region estimated to be the preBötC were covered. In all sections containing the preBötC, NK1R immunopositive cells were present. The greatest number of NK1R immunopositive cells were found in the section located 480 μm rostral to the LRN in both control and neonatal-exposed mice. Neonatal-exposed mice did however exhibit significantly less NK1R expressing cells in this section when compared with control animals (neonatal-exposed: 17.2 ± 6.5 NK1R immunopositive cells vs control:

27.8 ± 3.8 NK1R immunopositive cells, $p < 0.05$, Figure 5-6). Compared to control mice, neonatal-exposed mice also showed a trend towards having less NK1R expressing cells within the other sections that contained the preBötC (160 µm and 320 µm rostral to the LRN), however this was not found to be significant ($p > 0.05$).

In both control and neonatal-exposed mice, NK1R immunopositive cells were present in the region of the BC (estimated to be located in the section 640 µm rostral to the LRN, Figure 5-6). There was a slight trend towards the neonatal-exposed mice exhibiting fewer NK1R immunopositive cells within the BC, but this was not significant (neonatal-exposed: 8.2 ± 1.8 NK1R immunopositive cells vs control: 14.8 ± 8.3 NK1R immunopositive cells, $p > 0.05$, Figure 5-6).

NK1R expressing cells were found within the region of the RTN/pFRG in both control and neonatal-exposed mice (located in sections 800, 960 and 1120 µm rostral to the LRN, Figure 5-6). In these three sections, cells were counted in the area ventral to the facial motor nucleus and through to the ventral medullary surface. There was no significant difference in the number of NK1R expressing cells found within the RTN/pFRG between the two groups of mice.

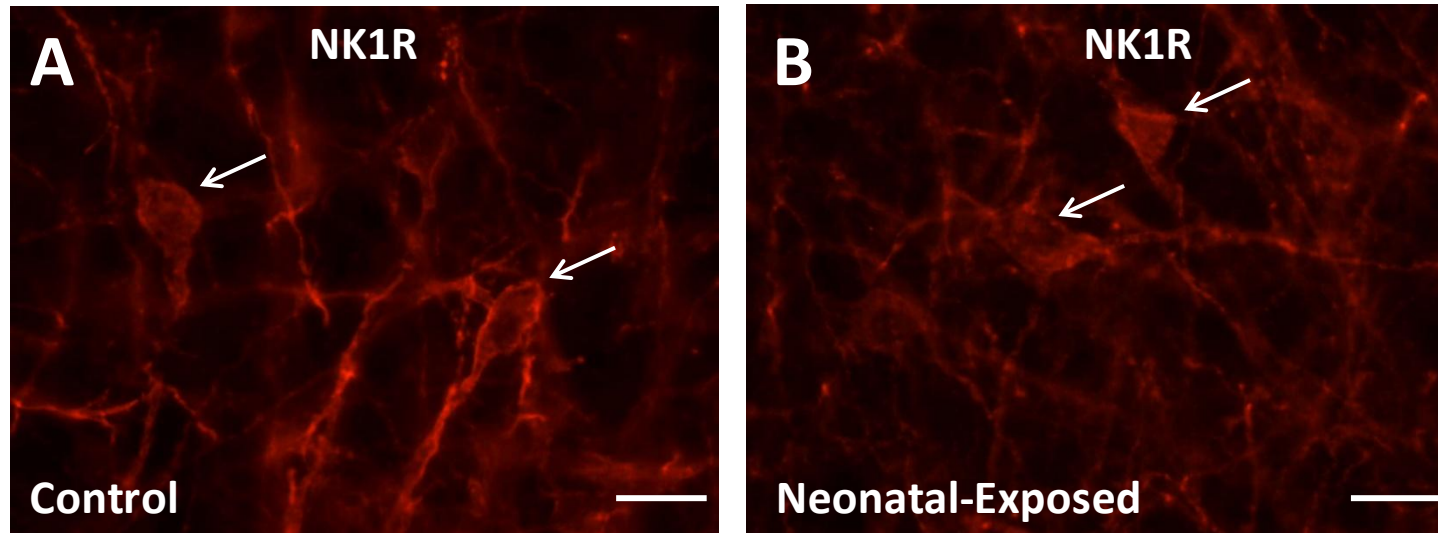


Figure 5-4. Fluorescent images showing NK1R expressing cells within the preBötC of control (A) and neonatal-exposed (B) mice. In both control and neonatal-exposed mice, NK1R expressing cells were found within the preBötC. Arrows show NK1R immunopositive somas. The coronal sections imaged were 480 μm rostral to the LRN and cells shown were located ventral to the subcompact formation of the nucleus ambiguus. Scale bar = 20 μm . Images were acquired using an epifluorescent microscope.

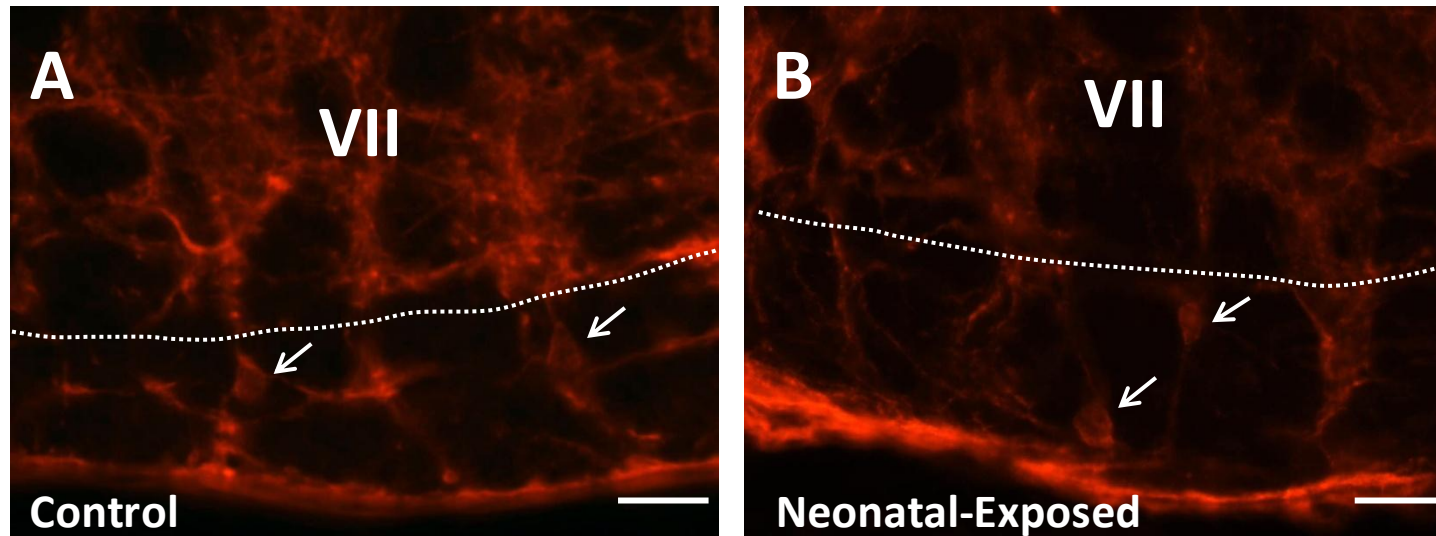


Figure 5-5. Fluorescent images showing NK1R expressing cells within the RTN/pFRG of control (A) and neonatal-exposed (B) mice. In both control and neonatal-exposed mice, NK1R expressing cells were found within the RTN/pFRG. Arrows show NK1R immunopositive cells of the RTN/pFRG. The cells of the facial motor nucleus also expressed the NK1R. The coronal sections imaged were 960 μm rostral to the LRN. Scale bar = 20 μm . Images were acquired using an epifluorescent microscope. VII: facial motor nucleus (delineated by dotted line).

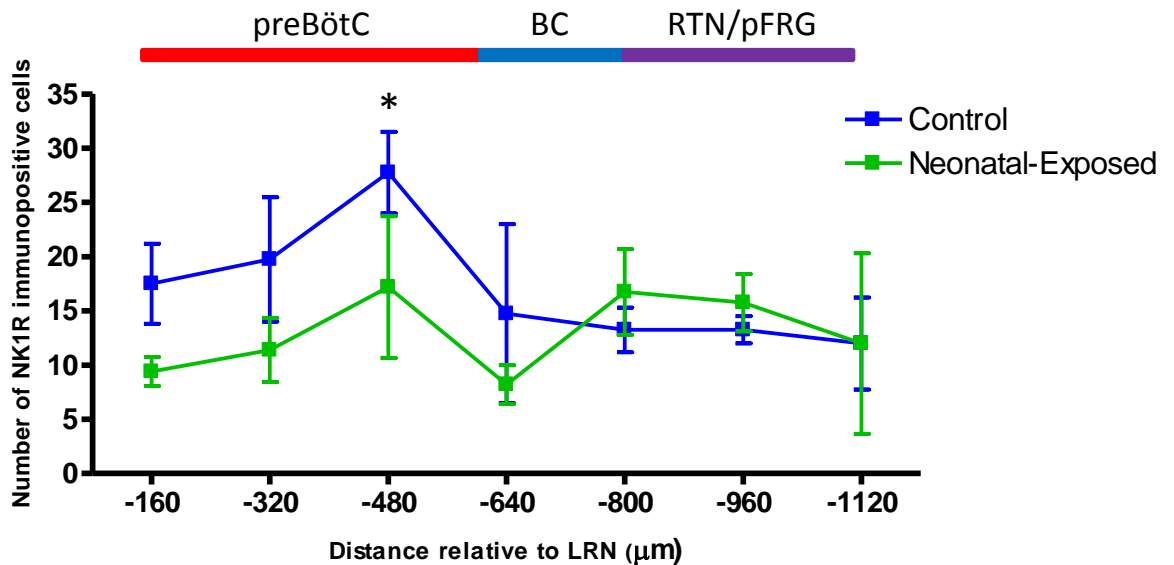


Figure 5-6. Number of NK1R immunopositive cells throughout the VRC in control and neonatal-exposed mice. Bilateral cell counts were performed. Sections were identified by their rostral distance from the LRN. The preBötC is estimated to lie between 160 μm to 600 μm from the LRN, the BC is reported to extend from 600 μm to 800 μm from the LRN and the RTN/pFRG is estimated to lie between 800 μm to 1120 μm rostral to the LRN (with reference to Franklin and Paxinos adult mouse brain atlas). Control mice exhibited a significantly greater number of NK1R immunopositive cells in the section located 480 μm rostral to the LRN, which is believed to contain the preBötC. Control mice, n=4; neonatal-exposed, n=5. Data presented as mean±SD. * denotes a significant difference (p<0.05) between experimental groups, 2-way ANOVA with Bonferroni's post test.

5.3.2 μ opioid receptor expression throughout the VRC

The distribution and number of μ opioid receptor expressing cells found throughout the VRC of control and neonatal-exposed mice was compared. Within the region of the preBötC, a large number of μ opioid receptor expressing cells were present in the control mice (Figure 5-7A). It is evident from the immunofluorescent images that μ opioid receptor immunoreactivity outlined the somatic membranes of cells (Figure 5-7A). Interestingly, in the neonatal-exposed mice there was a striking reduction in the number of cells expressing the μ opioid receptor within the region of the preBötC which is clearly illustrated in Figure 5-7B. In accordance with previous studies (Gray et al., 1999), when examining μ opioid receptor immunostaining within the region of the RTN/pFRG, it is apparent from Figure 5-8 that the cells within this neuronal group did not express the receptor. This was the case for both control and neonatal-exposed mice. Although not quantified, a cluster of μ opioid receptor expressing cells was found within the facial motor nucleus in the control mice (Figure 5-8A+B). However in the neonatal-exposed animals there were very few μ opioid receptor expressing cells found in the facial motor nucleus (Figure 5-8C+D). Interestingly, the few μ opioid receptor immunopositive cells that were present were weakly stained.

Quantification revealed that within the VRC, μ opioid receptor immunopositive cells were present in the highest levels within the preBötC in the control mice (Figure 5-9). The greatest number of μ opioid receptor immunopositive cells were found in the section located 480 μm rostral to the LRN (74.7 ± 26.3 μ opioid receptor immunopositive cells). The cells within the BC also expressed the μ opioid receptor in the control group (67.0 ± 27.1 μ opioid receptor immunopositive cells). Interestingly, the neonatal-exposed mice exhibited significantly less μ opioid receptor immunopositive cells throughout the preBötC (sections 160 μm through to 480 μm rostral to the LRN) and the BC (section 640 μm rostral to LRN) compared to control mice (-160 μm : 4.4 ± 6.6 vs 55.7 ± 10.6 ; -320 μm : 5.8 ± 4.4 vs 57.3 ± 12.7 ; -480 μm : 6.8 ± 12.0 vs 74.7 ± 26.3 ; -640 μm : 1.8 ± 3.0 vs 67.0 ± 27.1 μ opioid receptor immunopositive cells for neonatal-exposed vs control respectively, $p < 0.05$, Figure 5-9). In both experimental groups, μ opioid receptor immunopositive cells were not found within the RTN/pFRG (i.e. no immunopositive cells found in sections 800 μm , 990 μm and 1120 μm from the LRN, Figure 5-9).

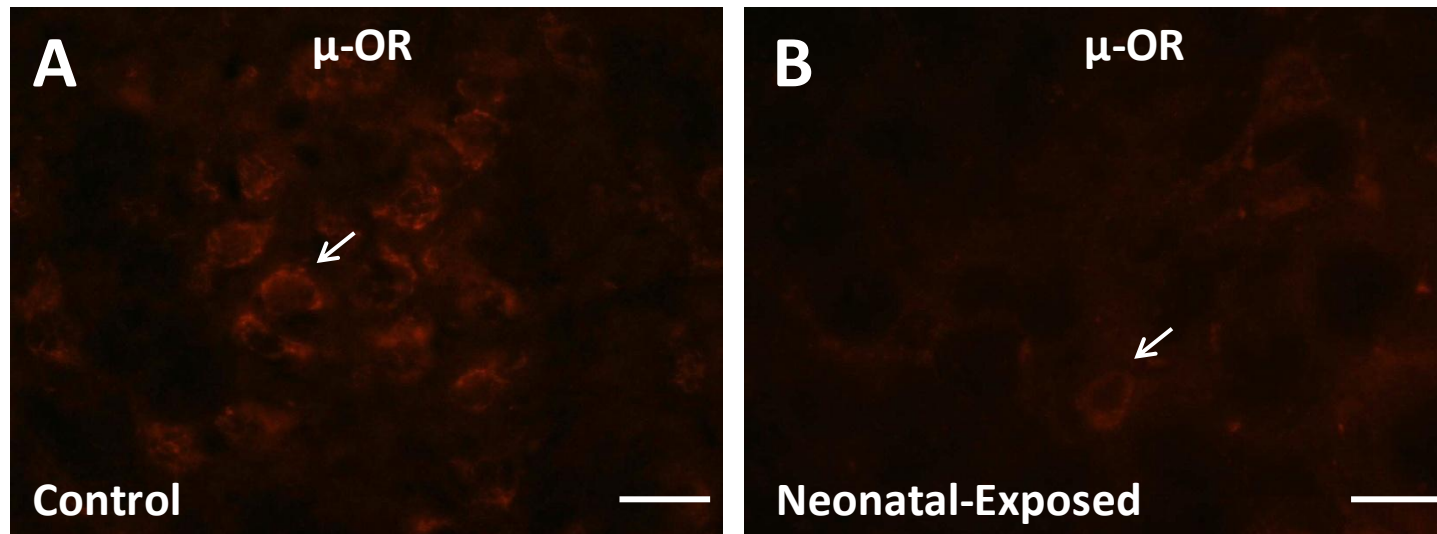


Figure 5-7. Fluorescent images showing μ opioid receptor expressing cells within the preBötC of control (A) and neonatal-exposed (B) mice. A: In control mice, there was a large number of μ -OR expressing cells found within the region of the preBötC. B: Neonatal-exposed mice exhibited a substantial reduction in the number of μ -OR expressing cells within the preBötC. Arrows show example of μ -OR immunopositive cell. The coronal sections imaged were 480 μ m rostral to the LRN and cells shown were located ventral to the subcompact formation of the nucleus ambiguus. Scale bar = 20 μ m. Images were acquired using an epifluorescent microscope. μ -OR: μ opioid receptor.

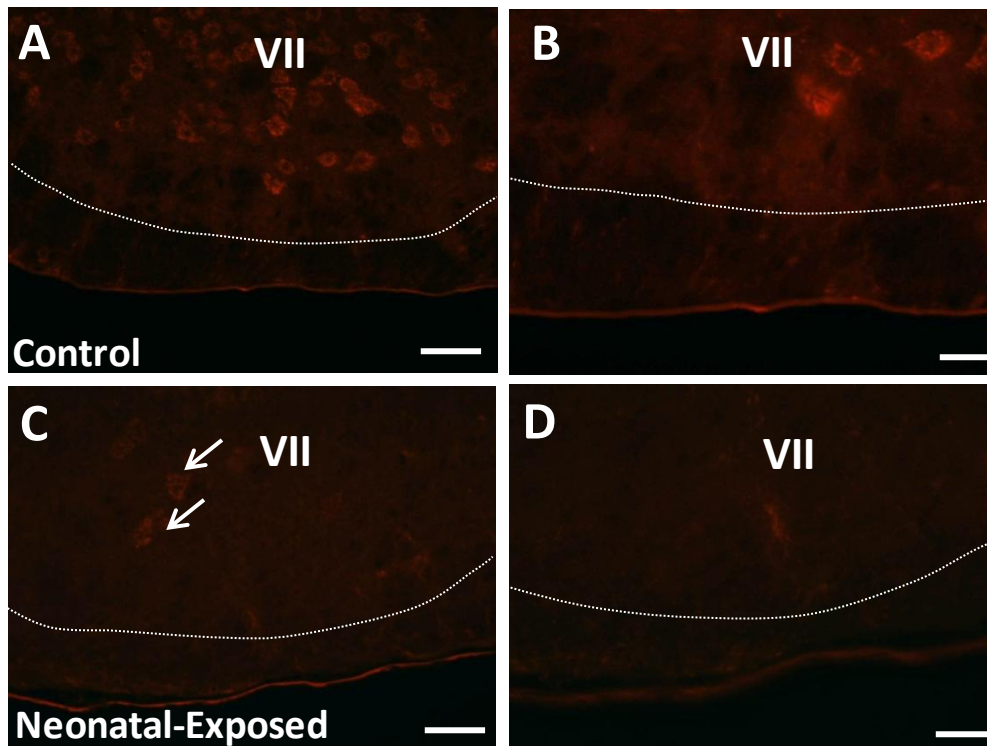


Figure 5-8. Fluorescent images showing a lack of μ opioid receptor expressing cells within the RTN/pFRG of control and neonatal-exposed mice. Higher magnification images of the RTN/pFRG in A and C are shown in B and D respectively. In control and neonatal-exposed mice there were no μ -OR expressing cells found within the region of the RTN/pFRG. The region ventral to the facial motor nucleus (VII) through to the ventral medullary surface contained no staining. In control mice, cells within the VII expressed high levels of the μ -OR (A and B). However the level of μ -OR immunostaining in the VII was greatly reduced in neonatal-exposed mice (C and D). The few μ -OR expressing cells that were present appeared to be weakly stained (shown by arrows). The coronal sections imaged were 960 μ m rostral to the LRN. Scale bar = 50 μ m in images A and C and 20 μ m in images B and D. The area of the VII is delineated by the dotted line. Images were acquired using an epifluorescent microscope. μ -OR: μ opioid receptor.

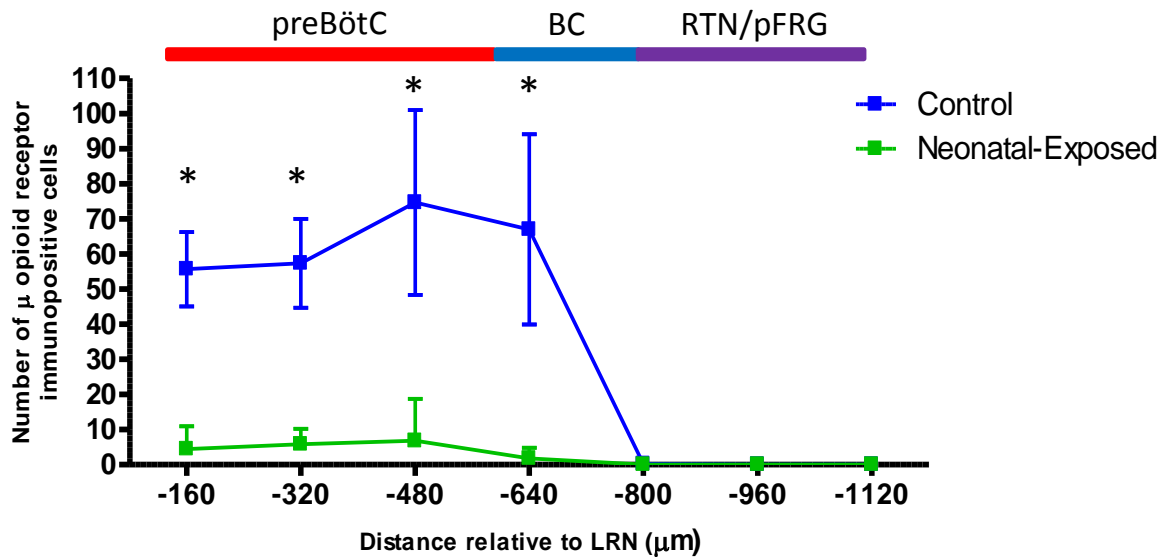


Figure 5-9. Number of μ opioid receptor immunopositive cells throughout the VRC in control and neonatal-exposed mice. Cells were counted bilaterally. Sections were identified by their rostral distance from the LRN. The preBötC is estimated to lie between 160 μm to 600 μm from the LRN, the BC is reported to extend from 600 μm to 800 μm from the LRN and the RTN/pFRG is estimated to lie between 800 μm to 1120 μm rostral to the LRN (with reference to Franklin and Paxinos adult mouse brain atlas). μ opioid receptor immunopositive cells were found throughout the preBötC and BC in high numbers in control mice. Neonatal-exposed mice exhibited a significantly lower number of μ opioid receptor immunopositive cells within both the preBötC and the BC. μ opioid receptor immunopositive cells were not found within the RTN/pFRG in control or neonatal-exposed mice. Control mice, n=4; neonatal-exposed, n=5. Data presented as mean±SD. * denotes a significant difference (p<0.05) between experimental groups, 2-way ANOVA with Bonferroni's post test.

5.3.3 μ opioid receptor expression outside the VRC

Given that neonatal-exposed mice displayed a significantly reduced number of μ opioid receptor immunopositive cells throughout an extensive area of the VRC, it was of interest to determine if this was also found outside the VRC. μ opioid receptor expression levels within the hypoglossal nucleus, a region located in the dorsomedial medulla, close to the ventrolateral portion of the central canal, was qualitatively assessed. The hypoglossal nucleus has been reported to express the μ opioid receptor (Xia and Haddad, 1991; Kivell et al., 2004). Both control and neonatal-exposed mice expressed a high level of μ opioid receptor immunopositive cells within the hypoglossal nucleus (Figure 5-10). This confirmed that the reduction in μ opioid receptor expressing cells exhibited by the neonatal-exposed mice was not a global effect throughout the medulla.

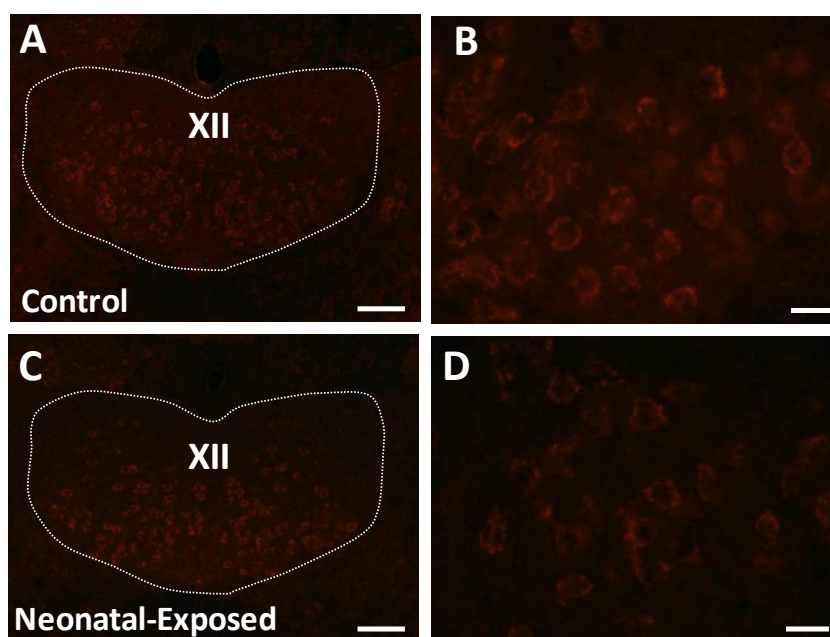


Figure 5-10. Fluorescent images showing μ opioid receptor expressing cells within the hypoglossal nucleus of control and neonatal-exposed mice. The hypoglossal nucleus (XII) is located in the dorsomedial medulla, below the central canal. Higher magnification images of the XII in A and C are shown in B and D respectively. The region of the XII is demarcated by the dotted line. A dense cluster of μ -OR immunopositive cells were found in the XII of control and neonatal-exposed mice. Scale bar = 100 μ m in images A and C and 20 μ m in images B and D. Images were acquired using an epifluorescent microscope. μ -OR: μ opioid receptor.

5.3.4 Phox2b expression throughout the VRC

Phox2b transcription factor is a known marker of RTN/pFRG neurons in both neonatal and adult rodents (Stornetta et al., 2006; Kang et al., 2007; Onimaru et al., 2008). The presence of Phox2b expressing cells throughout the VRC (from the preBötC to the RTN/pFRG) was assessed in control and neonatal-exposed mice, with a particular interest in the expression within the RTN/pFRG. The quality of the Phox2b staining was however variable between individual brains from both experimental groups. As a result, no quantification was carried out. When the VRC was qualitatively assessed, no Phox2b immunoreactive cells were found within the region of the preBötC or the BC in both experimental groups. There was a small number of Phox2b expressing cells found in the region of the RTN/pFRG. These cells were located directly ventral to the facial motor nucleus and on the ventral medullary edge in both control and neonatal-exposed mice (Figure 5-11).

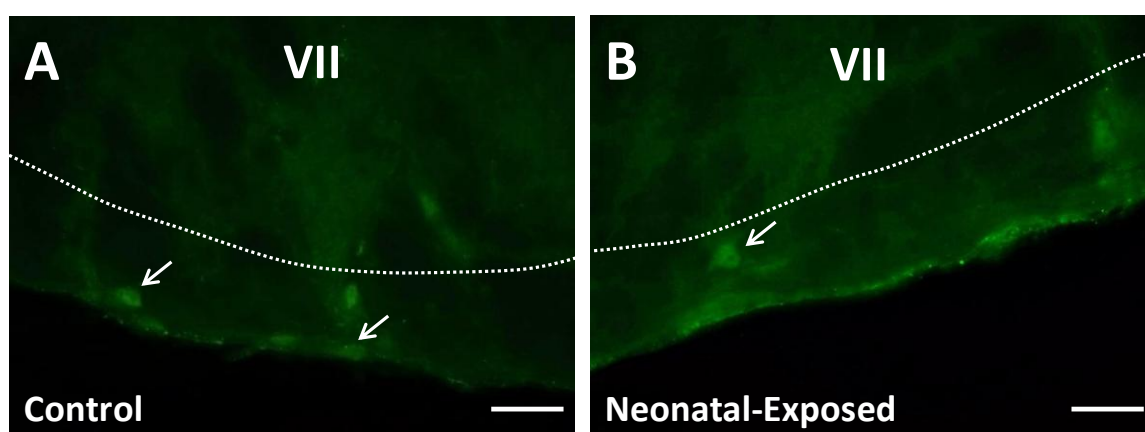


Figure 5-11. Fluorescent images showing Phox2b expressing cells within the RTN/pFRG of control (A) and neonatal-exposed (B) mice. In both control and neonatal-exposed mice, Phox2b expressing cells were found within the RTN/pFRG, in the region directly ventral to the VII (delineated by dotted line) and on the ventral medullary edge. Arrows show Phox2b immunopositive cells (nuclear staining). The coronal sections imaged were 960 μ m rostral to the LRN. Scale bar = 20 μ m. Images were acquired using an epifluorescent microscope.

5.4 Discussion

The aim of study 6 was to ascertain if repeated exposure to fentanyl during neonatal life in the mouse induces long-lasting histological changes within a section of the VRC comprising the preBötC and the RTN/pFRG. This was an attempt to unravel some of the fundamental mechanisms that may underlie the long term respiratory effects observed in the *in vivo* physiology experiments carried out in study 4 (chapter 4). The number of NK1R and μ opioid receptor immunopositive cells found through the VRC were counted and compared between control and neonatal-exposed mice. The distribution of NK1R expressing cells throughout the VRC was comparable between control and neonatal-exposed mice with a high level of expression found through the whole region examined. Neonatal-exposed mice did however exhibit significantly less NK1R expressing cells in a region believed to be the preBötC. The most striking consequence of neonatal fentanyl exposure was its long-term effect on μ opioid receptor expression throughout the VRC. Neonatal-exposed mice exhibited a dramatic reduction in the number of μ opioid receptor expressing cells in the preBötC and the region of the BC. This reduced level of μ opioid receptor expression within the preBötC could be fully or partially attributable to the respiratory effects reported in the neonatal-exposed mice from study 4, particularly the altered respiratory responsiveness to fentanyl observed in adulthood.

5.4.1 Neonatal-exposed mice exhibited a reduction in NK1R expression within the preBötC

NK1R expressing cells were present throughout the entire region of the VRC analysed in both control and neonatal-exposed mice. This finding is congruent with previous studies which have reported that NK1R immunoreactivity can be used as a marker for preBötC and RTN/pFRG neurons (Gray et al., 1999; Guyenet and Wang, 2001; Wang et al., 2001a; Guyenet et al., 2002; Onimaru et al., 2008; Pagliardini et al., 2008). It is important to highlight the fact that the exact rostrocaudal extent and anatomical boundaries of each of the respiratory groups (preBötC, BC and RTN/pFRG) has not been thoroughly investigated or identified in the adult mouse, with the majority of the work performed in the rat (Gray et al., 1999; Guyenet and Wang, 2001; Wang et al., 2001a). Their estimated positions were based on the adult mouse brain atlas by Franklin and Paxinos (Franklin and Paxinos, 2008). The method of analysing the area of the VRC that is estimated to encompassed the preBötC was comparable to that employed by Wang and colleagues (2001), who used

similar reference landmarks in the adult rat (Wang et al., 2001a). They reported that the region estimated to comprise the preBötC contained a higher number of NK1R expressing cells compared to the areas located directly rostral and caudal. The distribution pattern of NK1R expressing cells was similar in the present study for both control and neonatal-exposed mice. It is important to note that from NK1R expression alone it was difficult to anatomically delineate the area of the preBötC with great certainty. However, the large size of the counting box used (600 x 400 μm) meant that the area ventral to the scNA reported to encompass the preBötC was included in addition to the immediate surrounding area (see Figure 5-2 for illustration), ensuring preBötC neurons were definitely counted. It is therefore likely that an overestimation of the number of cells present within the preBötC was calculated, but given that the same method of cell counting was carried out for control and neonatal-exposed mice, the results can still be directly compared. A high level of NK1R expression was found within the area estimated to be the preBötC; with the greatest number of immunopositive cells in the medullary section located 480 μm from the LRN. Within this region, neonatal-exposed mice had significantly less NK1R expressing cells. This suggests that neonatal fentanyl exposure induces a long-term histological change within the preBötC. The physiological significance of this reduction in NK1R expression remains elusive but it may signify an alteration in the functioning of the preBötC. An *in vivo* study in the adult rat has found that systemically administered fentanyl induces a respiratory frequency depression by acting exclusively on NK1R expressing preBötC neurons (Montandon et al., 2011). Although not confirmed in this study, these neurons likely expressed the μ opioid receptor. Given that a subset of NK1R expressing preBötC neurons express the μ opioid receptor (Gray et al., 1999), it is possible that alterations in the μ opioid receptor also affected NK1R expression or the presence of the cell itself. Double immunostaining of NK1R and μ opioid receptor would help to elucidate this (further discussed in section 5.4.4). It is possible that a reduction in the number of preBötC NK1R expressing cells in the neonatal-exposed mice is responsible for the altered baseline respiratory activity reported in study 4, including the reduced respiratory frequency observed in the wakeful state (see section 4.3.2, chapter 4). In support of this theory, bilateral destruction of NK1R expressing preBötC neurons in the adult rat induces severe respiratory disturbances that are first observed during sleep then progress to wakefulness (McKay et al., 2005). The severe breathing abnormalities were due to the fact that the preBötC was anatomically ablated. In this study a less dramatic reduction in NK1R expressing cells within the preBötC was observed, which could induce more subtle changes in respiratory activity such as those exhibited by the neonatal-exposed mice

(chapter 4). Neonatal-exposed mice also displayed an increased occurrence of augmented breaths under anaesthesia (section 4.3.6, chapter 4). As previously discussed in section 4.5.3.1 of chapter 4, it is intriguing to speculate that the high frequency of augmented breaths exhibited by the neonatal-exposed mice could be an indication of an altered preBötC function, which generates an unstable respiratory pattern. This theory is further supported by the histological change detected within the region of the preBötC suggesting the functional capacity could be altered somewhat. It is important to highlight that further work is required before conclusions can be drawn relating to the impact of fentanyl exposure on the functional activity of the preBötC (see section 4.5.6, chapter 4 for examples of future experimentations).

5.4.2 NK1R expression within the RTN/pFRG was unaltered

Cells within the region of the RTN/pFRG were also found to express the NK1R, which is consistent with previous reports (Onimaru et al., 2008). Neonatal fentanyl exposure did not evoke any long-term changes in NK1R expression within the RTN/pFRG. The RTN/pFRG has been proposed to function as the principal central chemosensory site in the adult rodent (Mulkey et al., 2004; Guyenet et al., 2005; Takakura et al., 2008; Marina et al., 2010). The fact that neonatal-exposed mice exhibited a normal chemosensory response to hypercapnia when awake (section 4.3.4, chapter 4), together with the unaltered NK1R expression within the RTN/pFRG in this present study, suggests that neonatal fentanyl exposure does not induce lasting effects on the functioning of this neuronal group. Direct recording of RTN/pFRG neurons in response to hypercapnia in more reduced brainstem-spinal cord preparations in both control and neonatal-exposed mice would further assess the influence of fentanyl exposure on neural activity.

5.4.3 Neonatal-exposed mice exhibited a striking reduction in μ opioid receptor expression within the VRC

The most notable long-term consequence of neonatal fentanyl exposure was a reduction in μ opioid receptor expression within the VRC. In the area of the RTN/pFRG there were no μ opioid receptor expressing cells present in both experimental groups, which is congruent with previous studies (Gray et al., 1999). This finding is also consistent with previous studies that demonstrated RTN/pFRG neurons are insensitive to opioids (Takeda et al., 2001; Mellen et al., 2003) and supports the theory that fentanyl does not directly perturb

RTN/pFRG function *in vivo*. This absence of expression within the RTN/pFRG also serves as a negative control, indicating an adequate specificity of the primary antibody. In the control mice, the μ opioid receptor was highly expressed within the area estimated to contain the preBötC and the BC, which has been shown previously in the adult rat (Lonergan et al., 2003). The facial motor nucleus was also found to contain a dense cluster of μ opioid receptor expressing cells. Interestingly, neonatal-exposed mice displayed strikingly less μ opioid receptor expressing cells throughout the VRC, including the preBötC. The exact mechanism resulting in this reduced expression is unknown. It is possible that this reduction in μ opioid receptor expression is due to a downregulation of the receptor induced by repeated fentanyl exposure. As discussed in chapter 3, section 3.7.1, changes at the level of the μ opioid receptor are believed to underlie the development of tolerance to the effects of μ opioid receptor agonists, including fentanyl, after chronic exposure. Several radioligand binding studies have revealed that repeated exposure to μ opioid receptor agonists in rodents evoke downregulation of the μ opioid receptor within the brain through receptor internalisation (Bhargava and Gulati, 1990; Bernstein and Welch, 1998; Stafford et al., 2001), thereby reducing the number of functional receptors and inducing tolerance. Conversely, internalisation and downregulation of the μ opioid receptors evoked by repeated exposure has been suggested to actually prevent or delay tolerance (Koch et al., 2005). The results from this current study support the theory that repeated opioid exposure elicits downregulation of the receptor given the reduced level of expression detected by IHC in neonatal-exposed mice. Importantly, this study is the first to examine the long-term effects of fentanyl on receptor regulation. It is an intriguing possibility that fentanyl exposure in neonatal life elicits a long lasting downregulation of the μ opioid receptor which could account for the altered respiratory response to subsequent fentanyl administered in adult life observed in study 4. An *in vivo* study in the adult rat has found that systemically administered fentanyl induces a respiratory frequency depression by acting exclusively on preBötC neurons (Montandon et al., 2011). If the number of available functional μ opioid receptors within the preBötC is reduced in neonatal-exposed mice, then it is plausible that fentanyl's respiratory depressive actions would be attenuated. When in the wakeful state, neonatal-exposed mice did exhibit a reduced sensitivity to fentanyl (study 4, section 4.3.3), which fits with this theory and suggests that the development of tolerance to fentanyl could be associated with receptor downregulation. It is important to highlight however that based on the IHC data we cannot conclude that receptor downregulation has in fact occurred. It is possible that the reduced μ opioid receptor expression could indicate a loss of the cells themselves. Given the

widespread and substantial reduction of μ opioid receptor expression observed in the neonatal-exposed mice, it is unlikely that this represents cellular depletion as it would likely have a very profound impact on breathing which could be fatal. When baseline breathing was examined in the wakeful state, neonatal-exposed mice did not display any respiratory abnormalities (section 4.3.2). This idea of cell loss cannot however be ruled out. In order to investigate this, the study could be repeated and brain sections counterstained with a primary antibody against neuronal nuclei (NeuN). NeuN is a neuron-specific nuclear protein that is used as a general neuronal marker (Mullen et al., 1992). If the reduction in μ opioid receptor expression is also accompanied by a reduction in NeuN expression then this would indicate that there is neuronal loss. Likewise, no change in NeuN expression would suggest a downregulation of the μ opioid receptor. The utilisation of NeuN immunostaining would also help to dissociate between glial and neuronal cells.

It is important to highlight the fact that changes in receptor expression were not selective to the preBötC. A reduced number of μ opioid receptor expressing cells were also found in the area believed to be the BC as well as the facial motor nucleus. This suggests that the effects of repeated fentanyl exposure are complex and fentanyl may target multiple neuronal groups directly or indirectly. It is therefore likely that the respiratory changes observed in the neonatal-exposed mice in study 4 are due to complex network effects that cannot be elucidated from this study alone. Due to the extensive area of the VRC displaying a reduced number of μ opioid receptor expressing cells, it was of interest to determine if an area outside the VRC was also affected. We examined an area of the hypoglossal nucleus located in the dorsomedial medulla. This motor nucleus contains the hypoglossal motoneurons that innervate the GG muscle and is known to express the μ opioid receptor (Xia and Haddad, 1991). Furthermore, hypoglossal motor output is suppressed by μ opioid receptor agonists *in vitro* (Lorier et al., 2010) and *in vivo* (Hajiha et al., 2009) and is therefore targeted by fentanyl. Although no quantification was carried out, both control and neonatal-exposed mice exhibited a large cluster of μ opioid immunopositive cells within the hypoglossal, suggesting μ opioid expressing cells within this nucleus were not affected by neonatal fentanyl exposure. This finding is consistent with the physiological examination of the GG in study 4 (section 4.3.5), where neonatal-exposed mice exhibited no change in baseline GG muscle activity. The presence of μ opioid receptor expressing cells within the hypoglossal nucleus indicates that fentanyl exposure in neonatal life does not induce a global reduction in μ opioid expression throughout the medulla.

The influence of anaesthesia on the respiratory actions of fentanyl observed in the neonatal-exposed mice is an added complexity that is difficult to fully explain based on the histological results of this study. When anaesthetised, neonatal-exposed mice exhibited an enhanced susceptibility to fentanyl-induced respiratory depression (study 4, section 4.3.7), which was in direct contrast to the response observed when awake. The fact that fentanyl induced a profound respiratory depression suggests that it was acting on the μ opioid receptor to bring about the physiological response. In this study, the reduction in μ opioid receptor expression observed throughout the VRC, including that of the preBötC is inconsistent with this physiological response to fentanyl. Fentanyl has been shown to act on the μ_1 receptor subtype to induce its respiratory effects (Colman and Miller, 2001). The primary antibody used in the present study targets the μ_1 receptor subtype, indicating a specific reduction of the μ_1 opioid receptor in the neonatal-exposed mice. The effect of neonatal fentanyl exposure on the long-term expression of the μ_2 receptor subtype was not analysed. It is possible that in the absence of μ_1 receptors, fentanyl mediates its actions via this second μ opioid receptor subtype to induce the marked respiratory depression seen under anaesthesia. An assessment of μ_2 receptor immunoreactivity throughout the VRC could be carried out to determine the extent of its expression. Additionally, application of a μ_2 receptor antagonist prior to fentanyl administration *in vivo* would also determine if the respiratory depression was mediated via the μ_2 receptor in the neonatal-exposed mice.

It is interesting to speculate that the change in μ opioid receptor expression exhibited by the neonatal-exposed mice could be related to increased anxiety levels. As previously discussed in section 4.5.2.1 in chapter 4, it is possible that neonatal-exposed mice may have heightened anxiety in adulthood that could make them more sensitive to stressful events including injections. Prior to perfusion fixation, mice were anaesthetised with an i.p injection of pentobarbital. It is possible that the injection caused an augmented stress response in the neonatal-exposed mice. It is well established that exposure to stress evokes a release of endogenous opiates (Amir et al., 1980; Murua and Molina, 1990; Ruiz-Gayo et al., 1992). It is therefore possible that a greater release of endogenous opiates occurred in response to the pentobarbital injection in neonatal-exposed mice. In theory, the endogenous opiates could have activated the μ opioid receptors causing an acute internalisation. As a consequence of this, a reduction in μ opioid receptor expression would be detected using IHC. If this is the case, then the change in the number of μ opioid receptor expressing cells may not be directly related to fentanyl exposure per se and

therefore may not represent a long-term change in receptor expression caused by neonatal exposure. This theory also fits with the physiological data from study 4. Neonatal-exposed mice were insensitive to fentanyl when awake, which could be due to a stress-induced release of endogenous opiates caused by the fentanyl injection, thereby reducing the number of available μ opioid receptors for fentanyl to subsequently act on. On the contrary, when anaesthetised and stress responses were abolished, fentanyl induced a profound respiratory depression in neonatal-exposed mice, suggesting the availability of a sufficient number of μ opioid receptors. If the reduced receptor density within the VRC is due to an anxiety-induced release of endogenous opiates then it would be expected that a uniform reduction throughout the brain would be observed. However, as previously discussed, there was no apparent reduction in μ opioid receptor expression within the hypoglossal nucleus, indicating that the effects were not global, which is inconsistent with this theory of endogenous opiate release. It is important to highlight that these potential anxiety-related respiratory effects are merely speculative at present, thus it is imperative to first establish if neonatal-exposed mice display augmented anxiety. Potential further studies to investigate this are detailed in section 4.5.2.1 of chapter 4.

5.4.4 Study limitations and technical issues

One of the main limitations of study 6 was the fact that double staining for NK1R and μ opioid receptor was not carried out. The preBötC is known to express the NK1R, and a subset of these neurons also express the μ opioid receptor (Gray et al, 1999). It was difficult to define the anatomical boundaries of the preBötC using either the NK1R or the μ opioid receptor alone. Employing double immunostaining would help to further delineate the precise location of the preBötC. Furthermore, double immunostaining would provide additional information on the proportion of cells throughout the VRC that coexpress NK1R and μ opioid receptor. The number of NK1R expressing cells that exhibit downregulation of the μ opioid receptor could also be calculated. Double immunostaining was not employed in the present study as both NK1R and μ opioid receptor primary antibodies were raised in the rabbit and both fluorescent signals required amplification. To allow for double staining a guinea pig anti-NK1R primary antibody was originally tested, however it was found to produce inadequate staining. It would be beneficial to optimise a protocol allowing for double staining with both rabbit primary antibodies and an amplification of both immunofluorescent signals.

From the outset of study 6, sections were immunostained for VGLUT2 and ChAT. VGLUT2 is a marker for both preBötC and RTN/pFRG neurons, and thus would help to identify these neurons. ChAT is expressed in motor neurons and was used to delineate the facial motor nucleus, which was one of the reference landmarks. The immunofluorescence protocol utilised failed to produce VGLUT2 or ChAT staining. The reason(s) for this is unknown. It is possible that the concentration of the primary antibodies was too low or a longer incubation time of either the primary or secondary antibodies may be required. The addition of a tyramide amplification step may also improve the fluorescent signal. Further investigation is certainly necessary to optimise the staining protocol. The quality of Phox2b staining varied significantly between brains. Given that an identical staining protocol was utilised for every brain, the inconsistencies may be related to differences in the perfusion quality of the tissue. It is possible that the Phox2b primary antibody is highly sensitive to the quality of the fixed tissue.

All imaging and analysis of brain sections was performed using an epifluorescent microscope. It would have been advantageous to utilise confocal microscopy, which has several advantages over fluorescent microscopy. Confocal microscopy produces images that are of a higher resolution with greater contrast due to a reduction in background fluorescence and improved signal-to-noise (Sandison and Webb, 1994). Furthermore, the laser scanning confocal microscope has the ability to collect serial optical sections through the specimen allowing the tissue to be analysed to a greater depth. Using an epifluorescent microscope to quantify cells within the VRC would have resulted in an underestimation of the total number of cells present. However, given that the same method of imaging and analysis was performed for both control and neonatal-exposed tissue, adequate comparisons were made. The use of confocal microscopy would therefore not alter the conclusions drawn from this study.

5.4.5 Immunohistochemical analysis of juvenile-exposed brains

Taken together, the neonatal and juvenile exposure studies detailed in chapter 4 established that the postnatal age of fentanyl-exposure influenced the long-term respiratory effects. It appears that repeated neonatal fentanyl exposure is more detrimental to respiratory control. Thus, it was of interest to determine if repeated exposure to fentanyl during juvenile life in the mouse induces long-lasting changes in receptor expression within the VRC and if these differ from those found in the present study (study 6). This study was carried out with the

same experimental design and protocol as utilised in study 6. Mice were repeatedly administered fentanyl during juvenile life from P9-P13. They received a single i.p dose of 0.04 mg/kg on each postnatal day and IHC procedures were performed when mice reached adulthood. As mentioned previously (section 5.1.1), this study proved to be problematic and as a consequence insufficient data was generated. Immunostaining of the NK1R was weak and variable and μ opioid receptor staining failed for both control and juvenile-exposed tissue. As a result no data is shown. The fact that staining was variable in the control tissue suggests that the problems were due to technical issues. Since the same immunostaining protocol as described for study 6 was employed, it is difficult to determine the reasons for the failed staining but some possible explanations can be offered. The variability in the quality of NK1R staining could be due to sub optimal tissue fixation in some of the brains. The complete lack of μ opioid receptor staining may have also been due to problems with the tyramide amplification step. It is possible that the tyramide may have expired thus resulting in poor or no staining. This is consistent with the complete lack of staining in both control and juvenile-exposed tissue. Further IHC studies within the research group utilised a fresh batch of tyramide and obtained adequate NK1R and μ opioid receptor staining suggesting this may have been the source of the problem. Due to time constraints, the study was not repeated; however it is imperative that these investigations are conducted to help unravel the effects of postnatal age of fentanyl exposure on the long-term respiratory alterations. The addition of this study will also help to further explore the theory of developmental plasticity proposed from study 4 and 5 (see section 4.5.5, chapter 4). In light of these technical issues it would be beneficial to increase the number of neonatal-exposed and control brains analysed in study 6 to confirm the validity of the data.

5.4.6 Summary

Repeated fentanyl exposure during neonatal life evokes long-term changes in respiratory activity as well as altering the respiratory responsiveness to fentanyl (chapter 4). The fundamental mechanisms giving rise to these respiratory alterations are not fully understood, however the data from this study suggests that a substantial reduction in μ opioid receptor expression throughout the VRC, including that of the preBötC, could underlie these changes. Importantly, the alterations in the level of receptor expression reported here do not fully explain the influence that behavioural state has on fentanyl's respiratory actions in neonatal-exposed mice. This complex relationship between

behavioural state and the potency of fentanyl-induced respiratory depression certainly requires further investigation. Nonetheless, this study has generated novel data regarding the effects of repeated neonatal fentanyl exposure on receptor expression within the VRC.

Chapter 6.
General Conclusions

For decades, researchers have endeavoured to uncover the underlying neural mechanisms of respiratory rhythm generation. The lack of understanding of respiratory rhythmogenesis during early postnatal life provided the motivation for conducting some of the work detailed in this thesis. In addition, understanding the consequences of external perturbations on the respiratory rhythm generating networks has important clinical implications. The immaturity of the respiratory system and resultant fragile nature of breathing patterns immediately after birth in mammals could potentially make this period of life vulnerable to the lasting effects of respiratory depressants and is therefore an interesting time period to study.

The studies presented in this thesis utilised the μ opioid receptor agonist, fentanyl, to investigate respiratory control *in vivo*. Fentanyl was originally employed as a pharmacological tool to selectively target the opiate-sensitive preBötC whilst leaving the opiate-insensitive RTN/pFRG unperturbed. This was an attempt to tease apart the functioning of these two proposed respiratory oscillators during early postnatal life and determine the level of involvement of the preBötC in respiratory rhythm generation *in vivo*. The respiratory sensitivity to fentanyl during early postnatal life was examined to test the hypothesis that the preBötC functions as the dominant respiratory rhythm generator after a maturation of respiratory patterns has occurred.

6.1 Critical respiratory maturational time window

One of the main aims of this thesis was to increase the understanding of the respiratory control system and the influence of postnatal development on central respiratory control *in vivo*. The first study presented in this thesis demonstrated that the mouse respiratory system is immature at birth and generates an irregular respiratory pattern, potentially making this time period vulnerable to respiratory perturbations. The postnatal evolution of respiratory behaviour in the mouse was characterised and a substantial maturation of respiratory patterns was found between P2 and P3. A striking transformation in respiratory activity from an unstable pattern consisting of apnoeas and hyperpnoeic episodes, to a regular and rhythmic pattern devoid of respiratory abnormalities with a greater respiratory frequency occurred. Consequently, a critical developmental time period when the respiratory system undergoes a significant step in maturity was identified in the mouse. The identification of this short window of respiratory maturation represented an intriguing

developmental time period to investigate central respiratory control as well as the susceptibility of the immature respiratory system to insults.

6.2 Repeated exposure induces an acute respiratory tolerance to fentanyl

Initially, fentanyl was administered repeatedly throughout early life (P1-P5, P9 and P11) to determine age-dependent changes in the respiratory sensitivity to fentanyl and test the hypothesis that the preBötC functions as the dominant respiratory rhythm generator post-maturation. However a rapid desensitisation to the respiratory depressive effects of fentanyl occurred. It is probable that the repeated fentanyl administration induced a tolerance to the respiratory actions of the drug. The mechanism(s) that underlie this tolerance cannot be deduced from this study alone. Previous studies have suggested that the processes leading to the development of tolerance to μ opioid receptor agonists including fentanyl occur at the level of the receptor. Downregulation of the μ opioid receptor within the brain through receptor internalisation has been suggested as a mechanism of tolerance (Bhargava and Gulati, 1990; Bernstein and Welch, 1998; Stafford et al., 2001). Conversely it has been demonstrated that changes in the regulation of μ opioid receptors in response to repeated fentanyl administration occurs independently of the development of tolerance and is related to the dose itself, with both upregulation and downregulation occurring (Yoburn et al., 1993). Additionally, μ opioid receptor phosphorylation and desensitisation has been implicated in the development of opioid tolerance (Pitcher et al., 1998; Liu and Anand, 2001). It is likely that a complex set of cellular and molecular processes are involved in the development of respiratory tolerance observed in the study presented in this thesis, however this was not investigated. These unanticipated findings sparked further investigations designed to uncover the long-term respiratory effects of such exposure, particularly during early postnatal life when the respiratory system undergoes significant maturational changes.

6.3 Fentanyl-induced respiratory depression is age-dependent

To prevent repeated exposure to fentanyl and the consequential development of respiratory tolerance, a separate study was conducted whereby different mice were studied on each postnatal day throughout postnatal development. This allowed our hypothesis to be fully

tested. A trend towards an age-dependent increase in sensitivity to fentanyl induced respiratory frequency depression after the postulated respiratory maturation step was observed i.e. increased sensitivity from P3 onwards, as hypothesised. This finding lends support to the hypothesis that the preBötC functions as the dominant respiratory oscillator post-maturation. It is also congruent with the findings from previous *in vivo* studies that have explored the acute respiratory effects of riluzole throughout postnatal life in mice (Dr Leanne McKay, personal communication, SFN abstract 2009). Riluzole, which depresses RTN/pFRG activity, also exerted age-dependent respiratory depressive actions. Riluzole was reported to induce the greatest magnitude of respiratory depression in early life (P1-P3), which is in direct contrast to the age-dependent respiratory effects of fentanyl. Taken together, the fentanyl and riluzole experiments suggest that the level of involvement of the RTN/pFRG and the preBötC in respiratory rhythm generation change with postnatal development, with the RTN/pFRG functioning as the dominant respiratory oscillator in early life when the respiratory system is immature, and the preBötC functioning as the principal respiratory oscillator driving breathing rhythm after the respiratory system has matured. It is however important to consider the high degree of variability in the data from both the control and fentanyl experiments reported in this thesis. Increasing the number of mice studied at each postnatal age would help to reveal clearer data trends as well as increase the validity of the data, which is essential before definitive conclusions can be drawn. Furthermore, it should be highlighted that fentanyl's actions *in vivo* are widespread and not limited to the preBötC, which should also be considered when interpreting the effects of fentanyl and the high level of variability in the data.

6.4 Neonatal life is vulnerable to repeated fentanyl exposure

Developing a complete understanding of the effects of exogenous opioids on the highly complex respiratory system is desirable and has many clinical implications. Despite the profound respiratory depressive actions of μ opioids, the long-term respiratory effects of repeated opioid exposure remains to be fully explored both clinically and pre-clinically. The longitudinal fentanyl exposure studies detailed in this thesis (studies 4 and 5) have demonstrated that a non-destructive, pharmacological depression of the respiratory system in early neonatal life using fentanyl can induce long-term changes in baseline respiratory behaviour as well as evoke a change in the sensitivity to future fentanyl challenges in adulthood. Surprisingly, the change in sensitivity to fentanyl was state-dependent, where mice exhibited a reduced susceptibility to a further fentanyl challenge when awake but

displayed hypersensitivity under anaesthesia, in that fentanyl evoked a complete respiratory failure. This data indicates that anaesthesia represents a particularly vulnerable state to opioid-induced respiratory depression. Interestingly, identical exposure during juvenile life did not evoke the same long-term effects, with the most notable difference being the absence of the lasting hypersensitivity to fentanyl-induced respiratory depression under anaesthesia. The mechanisms underlying these long-term breathing changes and state-dependent fentanyl effects can only be hypothesised at present. Our findings are consistent with the idea that manipulations to the developing respiratory system can have profound, lasting changes in respiratory activity, and suggests fentanyl exposure during the neonatal period induces developmental plasticity. As previously described in this thesis, developmental plasticity in terms of respiratory control is defined as long-term changes in the mature respiratory system that are induced by experiences occurring during a critical developmental time period, whereas the same experiences after this critical time window evoke little or no lasting changes (Carroll, 2003; Bavis and Mitchell, 2008). Collectively our data suggests that the first five days of life in the mouse signifies a critical developmental time period highly susceptible to opioid-induced developmental plasticity. This theory is also congruent with our finding that a significant respiratory maturation step occurs between P2 and P3, which could be affected by fentanyl exposure. If repeated fentanyl exposure during the neonatal period induces lasting alterations to the function of the preBötC remains to be elucidated and certainly warrants further investigation.

Importantly, these studies raise many questions regarding the long-term implications of opioid therapy in neonatal humans. The data from this thesis suggests that long-term opioid therapy in neonatal humans could predispose a patient to respiratory anomalies later in life that may initially manifest in depressed behavioural states e.g. during sleep. Moreover, repeated exposure in the neonatal period could induce a lasting and dangerous hypersensitivity to the respiratory depressive actions of opioid drugs under depressed behavioural states, consequently limiting their therapeutic usefulness. Similar clinical longitudinal studies have never been conducted; therefore the clinical risks of opioid treatment in humans can only be speculated at this time.

6.5 Fentanyl exposure in neonatal life induces long-term changes in μ opioid receptor expression within the VRC

The long-term effects of neonatal fentanyl exposure on the expression of NK1R and μ opioid receptor expression throughout the VRC were analysed to begin to uncover potential mechanisms that underlie the documented long-term respiratory changes of such exposure. Neonatal-exposed mice exhibited a significant reduction in NK1R expressing cells within the preBötC. However, the most striking consequence of neonatal fentanyl exposure was the dramatic reduction in the number of μ opioid receptor expressing cells within the VRC including the preBötC seen in adult life. The reduced number of μ opioid receptor expressing cells could represent a long-term receptor downregulation. The physiological significance of this reduced expression is not fully understood, however it could be fully or partially attributable to the respiratory effects reported in the neonatal-exposed mice in adult life, particularly the altered respiratory responsiveness to fentanyl. The impact of arousal state on receptor regulation remains elusive. It is important to highlight that investigations of the long-term effects of juvenile fentanyl exposure on receptor expression is required to help explain the differences in the respiratory effects exhibited by the neonatal and juvenile-exposed mice. This would also enable the theory of developmental plasticity to be further investigated.

6.6 Behavioural state and respiratory activity

Respiratory differences between neonatal and juvenile-exposed mice including baseline breathing patterns and the striking difference in respiratory response to fentanyl only became apparent when the mice were in the anaesthetised state. In terms of respiratory function and fentanyl effects during wakefulness, there were only subtle differences between the two groups of mice. Studying breathing in the wakeful state alone would have drawn a different interpretation of the long-term respiratory effects of fentanyl. This highlights the complexity of respiratory control and opioid respiratory depression and the fact that in order to gain a full analysis of opioid depression and its effects on respiratory control *in vivo*, respiratory activity must be explored under varying behavioural states.

6.7 Future Directions

As previously discussed, to complement the work carried out in the whole animal, it would be advantageous to utilise more reduced experimental preparations that maintain respiratory-like rhythmic activity allowing for direct recordings from preBötC neurons. This is particularly important for determining the long-term effects of repeated fentanyl exposure on the rhythm generating capacity of the preBötC. The use of *in vitro* preparations including the medullary slice and *en bloc* preparation as well as the working heart-brainstem *in situ* preparation would enable a more comprehensive analysis of preBötC activity and respiratory motor output to further aid in the elucidation of the complex opioid-induced effects of the central respiratory system. A combination of both *in vitro* and *in vivo* study approaches could be the key to unravelling the mechanisms underlying the long-term respiratory effects of opioid exposure.

In keeping with the clinical relevance of establishing the long-term respiratory effects of repeated opioid exposure, investigating the effects of repeated exposure during the prenatal period is a possible avenue for further research. Opioid drugs are commonly abused during pregnancy (Kaltenbach et al., 1998) therefore determining the potential respiratory effects of this prenatal exposure on postnatal breathing is desirable. Given that the preBötC becomes rhythmically active at E15.5 in the mouse (Thoby-Brisson et al., 2005) it would be particularly interesting to determine the effects of fentanyl-exposure during this small time window in prenatal development. Pregnant dams could be injected with fentanyl thus also exposing developing fetuses and breathing activity of offspring examined in early postnatal life and through to adulthood, under both wakefulness and anaesthesia.

6.8 Concluding remarks

The studies detailed in this thesis have generated novel data regarding both the acute and lasting effects of opioid-induced respiratory depression. A critical postnatal maturation of breathing patterns has been identified in early life and our data provides supports for the hypothesis that the preBötC functions as the dominant respiratory rhythm generator post-maturation. Furthermore, the neonatal period appears to be particularly vulnerable to the long-term detrimental impact of repeated opioid exposure. Long-term alterations in the respiratory responsiveness to fentanyl after repeated neonatal exposure may be due to

downregulation of the μ opioid receptor within the preBötC. Importantly, the studies documented in this thesis have provided a solid basis for future research investigating the neural control of breathing and in particular opioid-induced alterations of respiratory control.

References

- Abbott SB, Stornetta RL, Coates MB, Guyenet PG (2011) Phox2b-expressing neurons of the parafacial region regulate breathing rate, inspiration, and expiration in conscious rats. *J Neurosci* 31:16410-16422.
- Abbott SB, Stornetta RL, Fortuna MG, Depuy SD, West GH, Harris TE, Guyenet PG (2009) Photostimulation of retrotrapezoid nucleus phox2b-expressing neurons in vivo produces long-lasting activation of breathing in rats. *J Neurosci* 29:5806-5819.
- Abdala AP, Dutschmann M, Bissonnette JM, Paton JF (2010) Correction of respiratory disorders in a mouse model of Rett syndrome. *Proc Natl Acad Sci U S A* 107:18208-18213.
- Alheid GF, Jiao W, McCrimmon DR (2011) Caudal nuclei of the rat nucleus of the solitary tract differentially innervate respiratory compartments within the ventrolateral medulla. *Neuroscience* 190:207-227.
- Aliverti A, Cala SJ, Duranti R, Ferrigno G, Kenyon CM, Pedotti A, Scano G, Sliwinski P, Macklem PT, Yan S (1997) Human respiratory muscle actions and control during exercise. *Journal of applied physiology (Bethesda, Md : 1985)* 83:1256-1269.
- Amir S, Brown ZW, Amit Z (1980) The role of endorphins in stress: evidence and speculations. *Neuroscience and biobehavioral reviews* 4:77-86.
- Anand KJ, Hansen DD, Hickey PR (1990) Hormonal-metabolic stress responses in neonates undergoing cardiac surgery. *Anesthesiology* 73:661-670.
- Antkowiak B (2001) How do general anaesthetics work? *Die Naturwissenschaften* 88:201-213.
- Arai AC, Xia YF, Suzuki E (2004) Modulation of AMPA receptor kinetics differentially influences synaptic plasticity in the hippocampus. *Neuroscience* 123:1011-1024.
- Arata S, Amano K, Yamakawa K, Arata A (2010) Central respiratory failure in a mouse model depends on the genetic background of the host. *Advances in experimental medicine and biology* 669:21-24.

- Arnold JH, Truog RD, Scavone JM, Fenton T (1991) Changes in the pharmacodynamic response to fentanyl in neonates during continuous infusion. *The Journal of pediatrics* 119:639-643.
- Aserinsky E (1965) Periodic respiratory pattern occurring in conjunction with eye movements during sleep. *Science* 150:763-766.
- Bailey CP, Connor M (2005) Opioids: cellular mechanisms of tolerance and physical dependence. *Current opinion in pharmacology* 5:60-68.
- Baldwin DN, Suki B, Pillow JJ, Roiha HL, Minocchieri S, Frey U (2004) Effect of sighs on breathing memory and dynamics in healthy infants. *Journal of applied physiology* (Bethesda, Md : 1985) 97:1830-1839.
- Balkowiec A, Katz DM (1998) Brain-derived neurotrophic factor is required for normal development of the central respiratory rhythm in mice. *J Physiol* 510 (Pt 2):527-533.
- Ballanyi K, Onimaru H, Homma I (1999) Respiratory network function in the isolated brainstem-spinal cord of newborn rats. *Progress in neurobiology* 59:583-634.
- Barnes BJ, Tuong CM, Mellen NM (2007) Functional imaging reveals respiratory network activity during hypoxic and opioid challenge in the neonate rat tilted sagittal slab preparation. *J Neurophysiol* 97:2283-2292.
- Bartlett D, Jr. (1971) Origin and regulation of spontaneous deep breaths. *Respiration physiology* 12:230-238.
- Bavis RW, Kilgore DL, Jr. (2001) Effects of embryonic CO₂ exposure on the adult ventilatory response in quail: does gender matter? *Respiration physiology* 126:183-199.
- Bavis RW, Mitchell GS (2008) Long-term effects of the perinatal environment on respiratory control. *Journal of applied physiology* (Bethesda, Md : 1985) 104:1220-1229.
- Bavis RW, Olson EB, Jr., Vidruk EH, Fuller DD, Mitchell GS (2004) Developmental plasticity of the hypoxic ventilatory response in rats induced by neonatal hypoxia. *J Physiol* 557:645-660.

- Bell HJ, Azubike E, Haouzi P (2011) The "other" respiratory effect of opioids: suppression of spontaneous augmented ("sigh") breaths. *Journal of applied physiology* (Bethesda, Md : 1985) 111:1296-1303.
- Bell SG, Ellis LJ (1987) Use of fentanyl for sedation of mechanically ventilated neonates. *Neonatal network* : NN 6:27-31.
- Berkenbosch A, Teppema LJ, Olievier CN, Dahan A (1997) Influences of morphine on the ventilatory response to isocapnic hypoxia. *Anesthesiology* 86:1342-1349.
- Bernard DG, Li A, Nattie EE (1996) Evidence for central chemoreception in the midline raphe. *Journal of applied physiology* (Bethesda, Md : 1985) 80:108-115.
- Bernstein MA, Welch SP (1998) mu-Opioid receptor down-regulation and cAMP-dependent protein kinase phosphorylation in a mouse model of chronic morphine tolerance. *Brain research Molecular brain research* 55:237-242.
- Bhargava HN, Gulati A (1990) Down-regulation of brain and spinal cord mu-opiate receptors in morphine tolerant-dependent rats. *European journal of pharmacology* 190:305-311.
- Biancardi V, Bicego KC, Almeida MC, Gargaglioni LH (2008) Locus coeruleus noradrenergic neurons and CO₂ drive to breathing. *Pflugers Archiv : European journal of physiology* 455:1119-1128.
- Blain GM, Smith CA, Henderson KS, Dempsey JA (2010) Peripheral chemoreceptors determine the respiratory sensitivity of central chemoreceptors to CO₂. *J Physiol* 588:2455-2471.
- Blanchi B, Kelly LM, Viemari JC, Lafon I, Burnet H, Bevençut M, Tillmanns S, Daniel L, Graf T, Hilaire G, Sieweke MH (2003) MafB deficiency causes defective respiratory rhythmogenesis and fatal central apnea at birth. *Nat Neurosci* 6:1091-1100.
- Booker P (1999) *Paediatric Anaesthesia*. New York: Oxford University Press.
- Bouvier J, Thoby-Brisson M, Renier N, Dubreuil V, Ericson J, Champagnat J, Pierani A, Chedotal A, Fortin G (2010) Hindbrain interneurons and axon guidance signaling critical for breathing. *Nat Neurosci* 13:1066-1074.

- Bradley SR, Pieribone VA, Wang W, Severson CA, Jacobs RA, Richerson GB (2002) Chemosensitive serotonergic neurons are closely associated with large medullary arteries. *Nat Neurosci* 5:401-402.
- Bradley TD, Floras JS (2003) Sleep apnea and heart failure: Part II: central sleep apnea. *Circulation* 107:1822-1826.
- Bragg P, Zwass MS, Lau M, Fisher DM (1995) Opioid pharmacodynamics in neonatal dogs: differences between morphine and fentanyl. *Journal of applied physiology* (Bethesda, Md : 1985) 79:1519-1524.
- Brill S (2013) Managing surgical pain in long-term opioid patients. *Journal of pain & palliative care pharmacotherapy* 27:185-187.
- Brockhaus J, Ballanyi K (1998) Synaptic inhibition in the isolated respiratory network of neonatal rats. *The European journal of neuroscience* 10:3823-3839.
- Caplan RA, Ready LB, Oden RV, Matsen FA, 3rd, Nessly ML, Olsson GL (1989) Transdermal fentanyl for postoperative pain management. A double-blind placebo study. *Jama* 261:1036-1039.
- Carroll JL (2003) Developmental plasticity in respiratory control. *Journal of applied physiology* (Bethesda, Md : 1985) 94:375-389.
- Chapin JL (1954) Ventilatory response of the unrestrained and unanesthetized hamster to CO₂. *The American journal of physiology* 179:146-148.
- Chapuis C, Autran S, Fortin G, Simmers J, Thoby-Brisson M (2014) Emergence of sigh rhythmogenesis in the embryonic mouse. *J Physiol* 592:2169-2181.
- Chen ML, Keens TG (2004) Congenital central hypoventilation syndrome: not just another rare disorder. *Paediatric respiratory reviews* 5:182-189.
- Chen SW, Maguire PA, Davies MF, Beatty MF, Loew GH (1996) Evidence for mu1-opioid receptor involvement in fentanyl-mediated respiratory depression. *European journal of pharmacology* 312:241-244.
- Chevillard L, Megarbane B, Risede P, Baud FJ (2009) Characteristics and comparative severity of respiratory response to toxic doses of fentanyl, methadone, morphine, and buprenorphine in rats. *Toxicology letters* 191:327-340.

- Chiocchio SR, Hilton SM, Tramezzani JH, Willshaw P (1984) Loss of peripheral chemoreflexes to hypoxia after carotid body removal in the rat. *Respiration physiology* 57:235-246.
- Choe CH, Smith FL (2000) Sedative tolerance accompanies tolerance to the analgesic effects of fentanyl in infant rats. *Pediatric research* 47:727-735.
- Coates EL, Li A, Nattie EE (1993) Widespread sites of brain stem ventilatory chemoreceptors. *Journal of applied physiology* (Bethesda, Md : 1985) 75:5-14.
- Colman AS, Miller JH (2001) Modulation of breathing by mu1 and mu2 opioid receptor stimulation in neonatal and adult rats. *Respiration physiology* 127:157-172.
- Colman AS, Miller JH (2002) mu-1 opioid receptor stimulation decreases body temperature in conscious, unrestrained neonatal rats. *Experimental biology and medicine* (Maywood, NJ) 227:377-381.
- Dahlstrom A, Fuxe K (1964) Localization of monoamines in the lower brain stem. *Experientia* 20:398-399.
- Davis MP and Pasternak GW (2009) Opioid receptors and opioid pharmacodynamics. In: *Opioids in cancer pain* (Davis MP, Glare PA, Hardy J, Quigley C, ed), pp1-28. Oxford: Oxford University Press.
- Del Negro CA, Koshiya N, Butera RJ, Jr., Smith JC (2002) Persistent sodium current, membrane properties and bursting behavior of pre-botzinger complex inspiratory neurons in vitro. *J Neurophysiol* 88:2242-2250.
- Del Negro CA, Morgado-Valle C, Hayes JA, Mackay DD, Pace RW, Crowder EA, Feldman JL (2005) Sodium and calcium current-mediated pacemaker neurons and respiratory rhythm generation. *J Neurosci* 25:446-453.
- Dellemijn PL, van Duijn H, Vanneste JA (1998) Prolonged treatment with transdermal fentanyl in neuropathic pain. *Journal of pain and symptom management* 16:220-229.
- Desrosiers G (2006) When opioid analgesia kills. *Perspective infirmiere : revue officielle de l'Ordre des infirmieres et infirmiers du Quebec* 4:6-9.

- Dobbins EG, Feldman JL (1994) Brainstem network controlling descending drive to phrenic motoneurons in rat. *The Journal of comparative neurology* 347:64-86.
- Drorbaugh JE, Fenn WO (1955) A barometric method for measuring ventilation in newborn infants. *Pediatrics* 16:81-87.
- Dubreuil V, Ramanantsoa N, Trochet D, Vaubourg V, Amiel J, Gallego J, Brunet JF, Goridis C (2008) A human mutation in *Phox2b* causes lack of CO₂ chemosensitivity, fatal central apnea, and specific loss of parafacial neurons. *Proc Natl Acad Sci U S A* 105:1067-1072.
- Dubreuil V, Thoby-Brisson M, Rallu M, Persson K, Pattyn A, Birchmeier C, Brunet JF, Fortin G, Goridis C (2009) Defective respiratory rhythmogenesis and loss of central chemosensitivity in *Phox2b* mutants targeting retrotrapezoid nucleus neurons. *J Neurosci* 29:14836-14846.
- Durand E, Dager S, Pattyn A, Gaultier C, Goridis C, Gallego J (2005) Sleep-disordered breathing in newborn mice heterozygous for the transcription factor *Phox2b*. *Am J Respir Crit Care Med* 172:238-243.
- Dutschmann M, Herbert H (2006) The Kolliker-Fuse nucleus gates the postinspiratory phase of the respiratory cycle to control inspiratory off-switch and upper airway resistance in rat. *The European journal of neuroscience* 24:1071-1084.
- Dutschmann M, Morschel M, Kron M, Herbert H (2004) Development of adaptive behaviour of the respiratory network: implications for the pontine Kolliker-Fuse nucleus. *Respir Physiol Neurobiol* 143:155-165.
- Eichenwald EC, Aina A, Stark AR (1997) Apnea frequently persists beyond term gestation in infants delivered at 24 to 28 weeks. *Pediatrics* 100:354-359.
- Ezure K, Tanaka I, Miyazaki M (1998) Pontine projections of pulmonary slowly adapting receptor relay neurons in the cat. *Neuroreport* 9:411-414.
- Ezure K, Tanaka I, Kondo M (2003) Glycine is used as a transmitter by decrementing expiratory neurons of the ventrolateral medulla in the rat. *J Neurosci* 23:8941-8948.
- Farney RJ, Walker JM, Cloward TV, Rhondeau S (2003) Sleep-disordered breathing associated with long-term opioid therapy. *Chest* 123:632-639.

- Feldman JL, Gautier H (1976) Interaction of pulmonary afferents and pneumotaxic center in control of respiratory pattern in cats. *J Neurophysiol* 39:31-44.
- Feldman JL, Smith JC (1989) Cellular mechanisms underlying modulation of breathing pattern in mammals. *Annals of the New York Academy of Sciences* 563:114-130.
- Feldman JL, Del Negro CA (2006) Looking for inspiration: new perspectives on respiratory rhythm. *Nature reviews Neuroscience* 7:232-242.
- Feldman JL, Mitchell GS, Nattie EE (2003) Breathing: rhythmicity, plasticity, chemosensitivity. *Annual review of neuroscience* 26:239-266.
- Fenner A, Schalk U, Hoenicke H, Wendenburg A, Roehling T (1973) Periodic breathing in premature and neonatal babies: incidence, breathing pattern, respiratory gas tensions, response to changes in the composition of ambient air. *Pediatric research* 7:174-183.
- Ferguson LM, Drummond GB (2006) Acute effects of fentanyl on breathing pattern in anaesthetized subjects. *British journal of anaesthesia* 96:384-390.
- Ferguson SS, Downey WE, 3rd, Colapietro AM, Barak LS, Menard L, Caron MG (1996) Role of beta-arrestin in mediating agonist-promoted G protein-coupled receptor internalization. *Science* 271:363-366.
- Filosa JA, Dean JB, Putnam RW (2002) Role of intracellular and extracellular pH in the chemosensitive response of rat locus coeruleus neurones. *J Physiol* 541:493-509.
- Fisher JT, Mortola JP, Smith JB, Fox GS, Weeks S (1982) Respiration in newborns: development of the control of breathing. *The American review of respiratory disease* 125:650-657.
- Fitzgerald LW, Teitler M (1993) Quantitative autoradiographic analysis of [³H]carfentanil binding to mu opiate receptors in the rat brain. *Synapse (New York, NY)* 14:154-159.
- Fong AY, Corcoran AE, Zimmer MB, Andrade DV, Milsom WK (2008) Respiratory rhythm of brainstem-spinal cord preparations: Effects of maturation, age, mass and oxygenation. *Respir Physiol Neurobiol* 164:429-440.

- Franklin KBJ, Paxinos G (2008) *The mouse brain in stereotaxic coordinates*. 3rd ed. New York: Elsevier.
- Funk GD, Smith JC, Feldman JL (1993) Generation and transmission of respiratory oscillations in medullary slices: role of excitatory amino acids. *J Neurophysiol* 70:1497-1515.
- Gang S, Sato Y, Kohama I, Aoki M (1995) Afferent projections to the Botzinger complex from the upper cervical cord and other respiratory related structures in the brainstem in cats: retrograde WGA-HRP tracing. *Journal of the autonomic nervous system* 56:1-7
- García-Pérez D, Laorden ML, Milanés MV, Núñez, C (2012) Glucocorticoids Regulation of FosB/ Δ FosB Expression Induced by Chronic Opiate Exposure in the Brain Stress System. *PLoS ONE* 7: e50264
- Glogowska M, Richardson PS, Widdicombe JG, Winning AJ (1972) The role of the vagus nerves, peripheral chemoreceptors and other afferent pathways in the genesis of augmented breaths in cats and rabbits. *Respiration physiology* 16:179-196.
- Gourlay GK, Kowalski SR, Plummer JL, Cherry DA, Szekely SM, Mather LE, Owen H, Cousins MJ (1990) The efficacy of transdermal fentanyl in the treatment of postoperative pain: a double-blind comparison of fentanyl and placebo systems. *Pain* 40:21-28.
- Gray PA, Rekling JC, Bocchiaro CM, Feldman JL (1999) Modulation of respiratory frequency by peptidergic input to rhythmogenic neurons in the preBotzinger complex. *Science* 286:1566-1568.
- Gray PA, Janczewski WA, Mellen N, McCrimmon DR, Feldman JL (2001) Normal breathing requires preBotzinger complex neurokinin-1 receptor-expressing neurons. *Nat Neurosci* 4:927-930.
- Gray PA, Hayes JA, Ling GY, Llona I, Tupal S, Picardo MC, Ross SE, Hirata T, Corbin JG, Eugenin J, Del Negro CA (2010) Developmental origin of preBotzinger complex respiratory neurons. *J Neurosci* 30:14883-14895.
- Greer JJ, Ren J (2009) Ampakine therapy to counter fentanyl-induced respiratory depression. *Respir Physiol Neurobiol* 168:153-157.

- Greer JJ, Smith JC, Feldman JL (1991) Role of excitatory amino acids in the generation and transmission of respiratory drive in neonatal rat. *J Physiol* 437:727-749.
- Greer JJ, Carter JE, al-Zubaidy Z (1995) Opioid depression of respiration in neonatal rats. *J Physiol* 485 (Pt 3):845-855.
- Guimaraes L, Dominguez-del-Toro E, Chatonnet F, Wrobel L, Pujades C, Monteiro LS, Champagnat J (2007) Exposure to retinoic acid at the onset of hindbrain segmentation induces episodic breathing in mice. *The European journal of neuroscience* 25:3526-3536.
- Gulemetova R, Kinkead R (2011) Neonatal stress increases respiratory instability in rat pups. *Respir Physiol Neurobiol* 176:103-109.
- Guyenet PG, Wang H (2001) Pre-Botzinger neurons with preinspiratory discharges "in vivo" express NK1 receptors in the rat. *J Neurophysiol* 86:438-446.
- Guyenet PG, Sevigny CP, Weston MC, Stornetta RL (2002) Neurokinin-1 receptor-expressing cells of the ventral respiratory group are functionally heterogeneous and predominantly glutamatergic. *J Neurosci* 22:3806-3816.
- Guyenet PG, Mulkey DK, Stornetta RL, Bayliss DA (2005) Regulation of ventral surface chemoreceptors by the central respiratory pattern generator. *J Neurosci* 25:8938-8947.
- Guyenet PG, Bayliss DA, Stornetta RL, Fortuna MG, Abbott SB, DePuy SD (2009) Retrotrapezoid nucleus, respiratory chemosensitivity and breathing automaticity. *Respir Physiol Neurobiol* 168:59-68.
- Hajiha M, DuBord MA, Liu H, Horner RL (2009) Opioid receptor mechanisms at the hypoglossal motor pool and effects on tongue muscle activity in vivo. *J Physiol* 587:2677-2692.
- Haldane JS, Priestley JG (1905) The regulation of the lung-ventilation. *J Physiol* 32:225-266.
- Hara K, Harris RA (2002) The anesthetic mechanism of urethane: the effects on neurotransmitter-gated ion channels. *Anesthesia and analgesia* 94:313-318.

- Hiatt IM, Hegyi T, Indyk L, Dangman BC, James LS (1981) Continuous monitoring of PO₂ during apnea of prematurity. *The Journal of pediatrics* 98:288-291.
- Hilaire G, Duron B (1999) Maturation of the mammalian respiratory system. *Physiological reviews* 79:325-360.
- Hoch B, Bernhard M, Hinsch A (1998) Different patterns of sighs in neonates and young infants. *Biology of the neonate* 74:16-21.
- Hodges MR, Richerson GB (2010) The role of medullary serotonin (5-HT) neurons in respiratory control: contributions to eupneic ventilation, CO₂ chemoreception, and thermoregulation. *Journal of applied physiology (Bethesda, Md : 1985)* 108:1425-1432.
- Hodges MR, Best S, Richerson GB (2011) Altered ventilatory and thermoregulatory control in male and female adult Pet-1 null mice. *Respir Physiol Neurobiol* 177:133-140.
- Hodges MR, Wehner M, Aungst J, Smith JC, Richerson GB (2009) Transgenic mice lacking serotonin neurons have severe apnea and high mortality during development. *J Neurosci* 29:10341-10349.
- Hodges MR, Opansky C, Qian B, Davis S, Bonis J, Bastasic J, Leekley T, Pan LG, Forster HV (2004) Transient attenuation of CO₂ sensitivity after neurotoxic lesions in the medullary raphe area of awake goats. *Journal of applied physiology (Bethesda, Md : 1985)* 97:2236-2247.
- Hodges MR, Tattersall GJ, Harris MB, McEvoy SD, Richerson DN, Deneris ES, Johnson RL, Chen ZF, Richerson GB (2008) Defects in breathing and thermoregulation in mice with near-complete absence of central serotonin neurons. *J Neurosci* 28:2495-2505.
- Horner RL (2008) Neuromodulation of hypoglossal motoneurons during sleep. *Respir Physiol Neurobiol* 164:179-196.
- Huang YH, Brown AR, Costy-Bennett S, Luo Z, Fregosi RF (2004) Influence of prenatal nicotine exposure on postnatal development of breathing pattern. *Respir Physiol Neurobiol* 143:1-8.

- Iizuka M, Fregosi RF (2007) Influence of hypercapnic acidosis and hypoxia on abdominal expiratory nerve activity in the rat. *Respir Physiol Neurobiol* 157:196-205.
- Jacquin TD, Borday V, Schneider-Maunoury S, Topilko P, Ghilini G, Kato F, Charnay P, Champagnat J (1996) Reorganization of pontine rhythmogenic neuronal networks in Krox-20 knockout mice. *Neuron* 17:747-758.
- Janczewski WA, Feldman JL (2006) Distinct rhythm generators for inspiration and expiration in the rat. *Journal of Physiology* 15:407-420.
- Janczewski WA, Onimaru H, Homma I, Feldman JL (2002) Opioid-resistant respiratory pathway from the preinspiratory neurones to abdominal muscles: in vivo and in vitro study in the newborn rat. *J Physiol* 545:1017-1026.
- Jansen AH, Chernick V (1983) Development of respiratory control. *Physiological reviews* 63:437-483.
- Javed RR, Dewey WL, Smith PA, Smith FL (2004) PKC and PKA inhibitors reverse tolerance to morphine-induced hypothermia and supraspinal analgesia in mice. *European journal of pharmacology* 492:149-157.
- Jiang C, Lipski J (1990) Extensive monosynaptic inhibition of ventral respiratory group neurons by augmenting neurons in the Botzinger complex in the cat. *Experimental brain research* 81:639-648.
- Jiang M, Alheid GF, Calandriello T, McCrimmon DR (2004) Parabrachial-lateral pontine neurons link nociception and breathing. *Respir Physiol Neurobiol* 143:215-233.
- Johnson SM, Smith JC, Funk GD, Feldman JL (1994) Pacemaker behavior of respiratory neurons in medullary slices from neonatal rat. *J Neurophysiol* 72:2598-2608.
- Kaltenbach K, Berghella V, Finnegan L (1998) Opioid dependence during pregnancy. Effects and management. *Obstet Gynecol Clin North Am* 25:139-151
- Kang BJ, Chang DA, Mackay DD, West GH, Moreira TS, Takakura AC, Gwilt JM, Guyenet PG, Stornetta RL (2007) Central nervous system distribution of the transcription factor Phox2b in the adult rat. *The Journal of comparative neurology* 503:627-641.

- Karlsson KA, Blumberg MS (2002) The union of the state: myoclonic twitching is coupled with nuchal muscle atonia in infant rats. *Behavioral neuroscience* 116:912-917.
- Khoo MC, Kronauer RE, Strohl KP, Slutsky AS (1982) Factors inducing periodic breathing in humans: a general model. *Journal of applied physiology: respiratory, environmental and exercise physiology* 53:644-659.
- Kitterman JA (1988) Physiological factors in fetal lung growth. *Canadian journal of physiology and pharmacology* 66:1122-1128.
- Kivell BM, Day DJ, McDonald FJ, Miller JH (2004) Developmental expression of mu and delta opioid receptors in the rat brainstem: evidence for a postnatal switch in mu isoform expression. *Brain research Developmental brain research* 148:185-196.
- Kobayashi K, Lemke RP, Greer JJ (2001) Ultrasound measurements of fetal breathing movements in the rat. *Journal of applied physiology (Bethesda, Md : 1985)* 91:316-320.
- Koch T, Widera A, Bartzsch K, Schulz S, Brandenburg LO, Wundrack N, Beyer A, Grecksch G, Hollt V (2005) Receptor endocytosis counteracts the development of opioid tolerance. *Molecular pharmacology* 67:280-287.
- Kornick CA, Santiago-Palma J, Moryl N, Payne R, Obbens EA (2003) Benefit-risk assessment of transdermal fentanyl for the treatment of chronic pain. *Drug safety : an international journal of medical toxicology and drug experience* 26:951-973.
- Krause KL, Forster HV, Kiner T, Davis SE, Bonis JM, Qian B, Pan LG (2009) Normal breathing pattern and arterial blood gases in awake and sleeping goats after near total destruction of the presumed pre-Botzinger complex and the surrounding region. *Journal of applied physiology (Bethesda, Md : 1985)* 106:605-619.
- Laferriere A, Colin-Durand J, Moss IR (2005) Ontogeny of respiratory sensitivity and tolerance to the mu-opioid agonist fentanyl in rat. *Brain research Developmental brain research* 156:210-217.
- Lahiri S, Mokashi A, Mulligan E, Nishino T (1981) Comparison of aortic and carotid chemoreceptor responses to hypercapnia and hypoxia. *Journal of applied physiology: respiratory, environmental and exercise physiology* 51:55-61.

- Lalley PM (2003) Mu-opioid receptor agonist effects on medullary respiratory neurons in the cat: evidence for involvement in certain types of ventilatory disturbances. *American journal of physiology Regulatory, integrative and comparative physiology* 285:R1287-1304.
- Lalley PM (2006) Opiate slowing of feline respiratory rhythm and effects on putative medullary phase-regulating neurons. *American journal of physiology Regulatory, integrative and comparative physiology* 290:R1387-1396.
- Lara JP, Parkes MJ, Silva-Carvalho L, Izzo P, Dawid-Milner MS, Spyer KM (1994) Cardiovascular and respiratory effects of stimulation of cell bodies of the parabrachial nuclei in the anaesthetized rat. *J Physiol* 477 (Pt 2):321-329.
- Lavezzi AM, Maturri L (2008) Functional neuroanatomy of the human pre-Botzinger complex with particular reference to sudden unexplained perinatal and infant death. *Neuropathology* 28:10-16.
- Law PY, Erickson LJ, El-Kouhen R, Dicker L, Solberg J, Wang W, Miller E, Burd AL, Loh HH (2000) Receptor density and recycling affect the rate of agonist-induced desensitization of mu-opioid receptor. *Molecular pharmacology* 58:388-398.
- LeGallois CJJ (1813) *Experiments on the Principles of Life*. Philadelphia: M. Thomas.
- Leino K, Mildh L, Lertola K, Seppala T, Kirvela O (1999) Time course of changes in breathing pattern in morphine- and oxycodone-induced respiratory depression. *Anaesthesia* 54:835-840.
- Lieske SP, Ramirez JM (2006a) Pattern-specific synaptic mechanisms in a multifunctional network. I. Effects of alterations in synapse strength. *J Neurophysiol* 95:1323-1333.
- Lieske SP, Ramirez JM (2006b) Pattern-specific synaptic mechanisms in a multifunctional network. II. Intrinsic modulation by metabotropic glutamate receptors. *J Neurophysiol* 95:1334-1344.
- Lieske SP, Thoby-Brisson M, Telgkamp P, Ramirez JM (2000) Reconfiguration of the neural network controlling multiple breathing patterns: eupnea, sighs and gasps [see comment]. *Nat Neurosci* 3:600-607.

- Liu JG, Anand KJ (2001) Protein kinases modulate the cellular adaptations associated with opioid tolerance and dependence. *Brain research Brain research reviews* 38:1-19.
- Liu Q, Lowry TF, Wong-Riley MT (2006) Postnatal changes in ventilation during normoxia and acute hypoxia in the rat: implication for a sensitive period. *J Physiol* 577:957-970.
- Liu X, Sood S, Liu H, Nolan P, Morrison JL, Horner RL (2003) Suppression of genioglossus muscle tone and activity during reflex hypercapnic stimulation by GABA(A) mechanisms at the hypoglossal motor nucleus in vivo. *Neuroscience* 116:249-259.
- Liu YY, Ju G, Wong-Riley MT (2001) Distribution and colocalization of neurotransmitters and receptors in the pre-Botzinger complex of rats. *Journal of applied physiology* (Bethesda, Md : 1985) 91:1387-1395.
- Loeschcke HH (1982) Central chemosensitivity and the reaction theory. *J Physiol* 332:1-24.
- Lonergan T, Goodchild AK, Christie MJ, Pilowsky PM (2003) Mu opioid receptors in rat ventral medulla: effects of endomorphin-1 on phrenic nerve activity. *Respir Physiol Neurobiol* 138:165-178.
- Lorier AR, Funk GD, Greer JJ (2010) Opiate-induced suppression of rat hypoglossal motoneuron activity and its reversal by ampakine therapy. *PLoS One* 5:e8766.
- Lotsch J, Skarke C, Schneider A, Hummel T, Geisslinger G (2005) The 5-hydroxytryptamine 4 receptor agonist mosapride does not antagonize morphine-induced respiratory depression. *Clinical pharmacology and therapeutics* 78:278-287.
- Lumsden T (1923) Observations on the respiratory centres in the cat. *J Physiol* 57:153-160.
- Lundberg JM, Hokfelt T, Fahrenkrug J, Nilsson G, Terenius L (1979) Peptides in the cat carotid body (glomus caroticum): VIP-, enkephalin-, and substance P-like immunoreactivity. *Acta physiologica Scandinavica* 107:279-281.

- Maggi CA, Meli A (1986) Suitability of urethane anesthesia for physiopharmacological investigations in various systems. Part 2: Cardiovascular system. *Experientia* 42:292-297.
- Manzke T, Guenther U, Ponimaskin EG, Haller M, Dutschmann M, Schwarzacher S, Richter DW (2003) 5-HT₄(a) receptors avert opioid-induced breathing depression without loss of analgesia. *Science* 301:226-229.
- Marder E, Calabrese RL (1996) Principles of rhythmic motor pattern generation. *Physiological reviews* 76:687-717.
- Marina N, Abdala AP, Trapp S, Li A, Nattie EE, Hewinson J, Smith JC, Paton JF, Gourine AV (2010) Essential role of Phox2b-expressing ventrolateral brainstem neurons in the chemosensory control of inspiration and expiration. *J Neurosci* 30:12466-12473.
- Marshall JM, Metcalfe JD (1988) Cardiovascular changes associated with augmented breaths in normoxia and hypoxia in the rat. *J Physiol* 400:15-27.
- Mathew OP (2011) Apnea of prematurity: pathogenesis and management strategies. *Journal of perinatology : official journal of the California Perinatal Association* 31:302-310.
- Matrot B, Durand E, Dauge S, Vardon G, Gaultier C, Gallego J (2005) Automatic classification of activity and apneas using whole body plethysmography in newborn mice. *Journal of applied physiology (Bethesda, Md : 1985)* 98:365-370.
- Matthes HW, Maldonado R, Simonin F, Valverde O, Slowe S, Kitchen I, Befort K, Dierich A, Le Meur M, Dolle P, Tzavara E, Hanoune J, Roques BP, Kieffer BL (1996) Loss of morphine-induced analgesia, reward effect and withdrawal symptoms in mice lacking the mu-opioid-receptor gene. *Nature* 383:819-823.
- McKay LC, Feldman JL (2008) Unilateral ablation of pre-Botzinger complex disrupts breathing during sleep but not wakefulness. *Am J Respir Crit Care Med* 178:89-95.
- McKay LC, Janczewski WA, Feldman JL (2005) Sleep-disordered breathing after targeted ablation of preBotzinger complex neurons. *Nat Neurosci* 8:1142-1144.

- McQueen DS, Ribeiro JA (1980) Inhibitory actions of methionine-enkephalin and morphine on the cat carotid chemoreceptors. *British journal of pharmacology* 71:297-305.
- Mellen NM, Janczewski WA, Bocchiaro CM, Feldman JL (2003) Opioid-induced quantal slowing reveals dual networks for respiratory rhythm generation. *Neuron* 37:821-826.
- Montandon G, Bairam A, Kinkead R (2006) Long-term consequences of neonatal caffeine on ventilation, occurrence of apneas, and hypercapnic chemoreflex in male and female rats. *Pediatric research* 59:519-524.
- Montandon G, Qin W, Liu H, Ren J, Greer JJ, Horner RL (2011) PreBotzinger complex neurokinin-1 receptor-expressing neurons mediate opioid-induced respiratory depression. *J Neurosci* 31:1292-1301.
- Morgado-Valle C, Feldman JL (2004) Depletion of substance P and glutamate by capsaicin blocks respiratory rhythm in neonatal rat in vitro. *J Physiol* 555:783-792.
- Morgado-Valle C, Baca SM, Feldman JL (2010) Glycinergic pacemaker neurons in preBotzinger complex of neonatal mouse. *J Neurosci* 30:3634-3639.
- Mortola JP (1984) Breathing pattern in newborns. *Journal of applied physiology: respiratory, environmental and exercise physiology* 56:1533-1540.
- Mortola JP (2001) *Respiratory Physiology of Newborn Mammals, a Comparative Perspective*. USA: The Johns Hopkins University Press.
- Mortola JP, Frappell PB (1998) On the barometric method for measurements of ventilation, and its use in small animals. *Canadian journal of physiology and pharmacology* 76:937-944.
- Moss IR, Brown KA, Laferriere A (2006) Recurrent hypoxia in rats during development increases subsequent respiratory sensitivity to fentanyl. *Anesthesiology* 105:715-718.
- Mulkey DK, Stornetta RL, Weston MC, Simmons JR, Parker A, Bayliss DA, Guyenet PG (2004) Respiratory control by ventral surface chemoreceptor neurons in rats. *Nat Neurosci* 7:1360-1369.

- Mullen RJ, Buck CR, Smith AM (1992) NeuN, a neuronal specific nuclear protein in vertebrates. *Development (Cambridge, England)* 116:201-211.
- Murua VS, Molina VA (1990) An opiate mechanism involved in conditioned analgesia influences forced swim-induced immobility. *Physiology & behavior* 48:641-645.
- Niane LM, Bairam A (2011) Selecting representative ages for developmental changes of respiratory irregularities and hypoxic ventilatory response in rats. *Open J Mol Integr Physiol* 1:1-7.
- Niane LM, Bairam A (2012) Age-dependent changes in breathing stability in rats. *Advances in experimental medicine and biology* 758:37-41.
- Niane LM, Joseph V, Bairam A (2012) Systemic blockade of nicotinic and purinergic receptors inhibits ventilation and increases apnoea frequency in newborn rats. *Experimental physiology* 97:981-993.
- Niesters M, Overdyk F, Smith T, Aarts L, Dahan A (2013) Opioid-induced respiratory depression in paediatrics: a review of case reports. *British journal of anaesthesia* 110:175-182.
- Okubo S, Mortola JP (1988) Long-term respiratory effects of neonatal hypoxia in the rat. *Journal of applied physiology (Bethesda, Md : 1985)* 64:952-958.
- Onimaru H, Homma I (2003) A novel functional neuron group for respiratory rhythm generation in the ventral medulla. *J Neurosci* 23:1478-1486.
- Onimaru H, Ikeda K, Kawakami K (2008) CO₂-sensitive preinspiratory neurons of the parafacial respiratory group express Phox2b in the neonatal rat. *J Neurosci* 28:12845-12850.
- Pagliardini S, Ren J, Greer JJ (2003) Ontogeny of the pre-Botzinger complex in perinatal rats. *J Neurosci* 23:9575-9584.
- Pagliardini S, Gosgnach S, Dickson CT (2013) Spontaneous sleep-like brain state alternations and breathing characteristics in urethane anesthetized mice. *PLoS One* 8:e70411.
- Pagliardini S, Greer JJ, Funk GD, Dickson CT (2012) State-dependent modulation of breathing in urethane-anesthetized rats. *J Neurosci* 32:11259-11270.

- Pagliardini S, Janczewski WA, Tan W, Dickson CT, Deisseroth K, Feldman JL (2011) Active expiration induced by excitation of ventral medulla in adult anesthetized rats. *J Neurosci* 31:2895-2905.
- Pagliardini S, Ren J, Gray PA, Vandunk C, Gross M, Goulding M, Greer JJ (2008) Central respiratory rhythmogenesis is abnormal in *lhx1*-deficient mice. *J Neurosci* 28:11030-11041.
- Paton JF (1996a) A working heart-brainstem preparation of the mouse. *J Neurosci Methods* 65:63-68.
- Paton JF (1996b) The ventral medullary respiratory network of the mature mouse studied in a working heart-brainstem preparation. *J Physiol* 493 (Pt 3):819-831.
- Paton JF, Richter DW (1995) Maturation changes in the respiratory rhythm generator of the mouse. *Pflugers Archiv : European journal of physiology* 430:115-124.
- Paton JF, Abdala AP, Koizumi H, Smith JC, St-John WM (2006) Respiratory rhythm generation during gasping depends on persistent sodium current. *Nat Neurosci* 9:311-313.
- Patroniti N, Foti G, Cortinovis B, Maggioni E, Bigatello LM, Cereda M, Pesenti A (2002) Sigh improves gas exchange and lung volume in patients with acute respiratory distress syndrome undergoing pressure support ventilation. *Anesthesiology* 96:788-794.
- Pattinson KT (2008) Opioids and the control of respiration. *British journal of anaesthesia* 100:747-758.
- Pena F, Parkis MA, Tryba AK, Ramirez JM (2004) Differential contribution of pacemaker properties to the generation of respiratory rhythms during normoxia and hypoxia. *Neuron* 43:105-117.
- Phillipson EA, Bowes G (1986) Control of breathing during sleep. In: *Handbook of Physiology*, pp 649–989. Bethesda, MD: American Physiological Society.
- Picardo MC, Weragalaarachchi KT, Akins VT, Del Negro CA (2013) Physiological and morphological properties of *Dbx1*-derived respiratory neurons in the pre-Botzinger complex of neonatal mice. *J Physiol* 591:2687-2703.

- Pitcher JA, Freedman NJ, Lefkowitz RJ (1998) G protein-coupled receptor kinases. Annual review of biochemistry 67:653-692.
- Putnam RW, Filosa JA, Ritucci NA (2004) Cellular mechanisms involved in CO₂ and acid signaling in chemosensitive neurons. American journal of physiology Cell physiology 287:C1493-1526.
- Ramirez JM, Schwarzacher SW, Pierrefiche O, Olivera BM, Richter DW (1998) Selective lesioning of the cat pre-Botzinger complex in vivo eliminates breathing but not gasping. J Physiol 507 (Pt 3):895-907.
- Razi NM, DeLauter M, Pandit PB (2002) Periodic breathing and oxygen saturation in preterm infants at discharge. Journal of perinatology : official journal of the California Perinatal Association 22:442-444.
- Read DJ, Henderson-Smart DJ (1984) Regulation of breathing in the newborn during different behavioral states. Annual review of physiology 46:675-685.
- Rekling JC, Feldman JL (1998) PreBotzinger complex and pacemaker neurons: hypothesized site and kernel for respiratory rhythm generation. Annual review of physiology 60:385-405.
- Rekling JC, Champagnat J, Denavit-Saubie M (1996) Electroresponsive properties and membrane potential trajectories of three types of inspiratory neurons in the newborn mouse brain stem in vitro. J Neurophysiol 75:795-810.
- Remmers JE, deGroot WJ, Sauerland EK, Anch AM (1978) Pathogenesis of upper airway occlusion during sleep. Journal of applied physiology: respiratory, environmental and exercise physiology 44:931-938.
- Ren J, Ding X, Greer JJ (2012a) Respiratory depression in rats induced by alcohol and barbiturate and rescue by ampakine CX717. J Appl Physiol 113:1004-1011.
- Ren J, Ding X, Funk GD, Greer JJ (2012b) Anxiety-related mechanisms of respiratory dysfunction in a mouse model of Rett syndrome. J Neurosci 32:17230-17240.
- Ren J, Poon BY, Tang Y, Funk GD, Greer JJ (2006) Ampakines alleviate respiratory depression in rats. Am J Respir Crit Care Med 174:1384-1391.

- Renolleau S, Dauger S, Autret F, Vardon G, Gaultier C, Gallego J (2001) Maturation of baseline breathing and of hypercapnic and hypoxic ventilatory responses in newborn mice. *American journal of physiology Regulatory, integrative and comparative physiology* 281:R1746-1753.
- Richerson GB (1995) Response to CO₂ of neurons in the rostral ventral medulla in vitro. *J Neurophysiol* 73:933-944.
- Robinson DM, Kwok H, Adams BM, Peebles KC, Funk DG (2000) Development of the ventilatory response to hypoxia in Swiss CD-1 mice. *J Appl Physiol* 88:1907-1914.
- Robinson L, Guy J, McKay L, Brockett E, Spike RC, Selfridge J, De Sousa D, Merusi C, Riedel G, Bird A, Cobb SR (2012) Morphological and functional reversal of phenotypes in a mouse model of Rett syndrome. *Brain : a journal of neurology* 135:2699-2710.
- Romberg R, Sarton E, Teppema L, Matthes HW, Kieffer BL, Dahan A (2003) Comparison of morphine-6-glucuronide and morphine on respiratory depressant and antinociceptive responses in wild type and mu-opioid receptor deficient mice. *British journal of anaesthesia* 91:862-870.
- Rong W, Gourine AV, Cockayne DA, Xiang Z, Ford AP, Spyer KM, Burnstock G (2003) Pivotal role of nucleotide P2X₂ receptor subunit of the ATP-gated ion channel mediating ventilatory responses to hypoxia. *J Neurosci* 23:11315-11321.
- Rose MF, Ren J, Ahmad KA, Chao HT, Klisch TJ, Flora A, Greer JJ, Zoghbi HY (2009) *Math1* is essential for the development of hindbrain neurons critical for perinatal breathing. *Neuron* 64:341-354.
- Ruiz-Gayo M, Baamonde A, Turcaud S, Fournie-Zaluski MC, Roques BP (1992) In vivo occupation of mouse brain opioid receptors by endogenous enkephalins: blockade of enkephalin degrading enzymes by RB 101 inhibits [3H]diprenorphine binding. *Brain research* 571:306-312.
- Rybak IA, Shevtsova NA, Paton JF, Dick TE, St-John WM, Morschel M, Dutschmann M (2004) Modeling the ponto-medullary respiratory network. *Respir Physiol Neurobiol* 143:307-319.

- Saarenmaa E, Huttunen P, Leppaluoto J, Meretoja O, Fellman V (1999) Advantages of fentanyl over morphine in analgesia for ventilated newborn infants after birth: A randomized trial. *The Journal of pediatrics* 134:144-150.
- Salmoiraghi GC, Burns BD (1960) Localization and patterns of discharge of respiratory neurones in brain-stem of cat. *J Neurophysiol* 23:2-13.
- Sandison DR, Webb WW (1994) Background rejection and signal-to-noise optimization in confocal and alternative fluorescence microscopes. *Applied optics* 33:603-615.
- Sapru HN, Krieger AJ (1977) Carotid and aortic chemoreceptor function in the rat. . *Journal of Applied Physiology* 42:344-348.
- Sauerland EK, Harper RM (1976) The human tongue during sleep: electromyographic activity of the genioglossus muscle. *Experimental neurology* 51:160-170.
- Sceniak MP, Maciver MB (2006) Cellular actions of urethane on rat visual cortical neurons in vitro. *J Neurophysiol* 95:3865-3874.
- Schwarzacher SW, Rub U, Deller T (2011) Neuroanatomical characteristics of the human pre-Botzinger complex and its involvement in neurodegenerative brainstem diseases. *Brain : a journal of neurology* 134:24-35.
- Severson CA, Wang W, Pieribone VA, Dohle CI, Richerson GB (2003) Midbrain serotonergic neurons are central pH chemoreceptors. *Nat Neurosci* 6:1139-1140.
- Shea SA (1997) Life without ventilatory chemosensitivity. *Respiration physiology* 110:199-210.
- Shen L, Duffin J (2002) Caudal expiratory neurones in the rat. *Pflugers Archiv : European journal of physiology* 444:405-410.
- Shvarev YN, Lagercrantz H (2006) Early postnatal changes in respiratory activity in rat in vitro and modulatory effects of substance P. *The European journal of neuroscience* 24:2253-2263.
- Sin DD, Fitzgerald F, Parker JD, Newton G, Floras JS, Bradley TD (1999) Risk factors for central and obstructive sleep apnea in 450 men and women with congestive heart failure. *Am J Respir Crit Care Med* 160:1101-1106.

- Smith JC, Ellenberger HH, Ballanyi K, Richter DW, Feldman JL (1991) Pre-Botzinger complex: a brainstem region that may generate respiratory rhythm in mammals. *Science* 254:726-729.
- Smith JC, Abdala AP, Koizumi H, Rybak IA, Paton JF (2007) Spatial and functional architecture of the mammalian brain stem respiratory network: a hierarchy of three oscillatory mechanisms. *J Neurophysiol* 98:3370-3387.
- Spengler CM, Gozal D, Shea SA (2001) Chemoreceptive mechanisms elucidated by studies of congenital central hypoventilation syndrome. *Respiration physiology* 129:247-255.
- Spyer KM (2009) To breathe or not to breathe? That is the question. *Experimental physiology* 94:1-10.
- Stafford K, Gomes AB, Shen J, Yoburn BC (2001) mu-Opioid receptor downregulation contributes to opioid tolerance in vivo. *Pharmacology, biochemistry, and behavior* 69:233-237.
- Stornetta RL, Sevigny CP, Guyenet PG (2003a) Inspiratory augmenting bulbospinal neurons express both glutamatergic and enkephalinergic phenotypes. *The Journal of comparative neurology* 455:113-124.
- Stornetta RL, Rosin DL, Wang H, Sevigny CP, Weston MC, Guyenet PG (2003b) A group of glutamatergic interneurons expressing high levels of both neurokinin-1 receptors and somatostatin identifies the region of the pre-Botzinger complex. *The Journal of comparative neurology* 455:499-512.
- Stornetta RL, Moreira TS, Takakura AC, Kang BJ, Chang DA, West GH, Brunet JF, Mulkey DK, Bayliss DA, Guyenet PG (2006) Expression of Phox2b by brainstem neurons involved in chemosensory integration in the adult rat. *J Neurosci* 26:10305-10314.
- Swarm RA, Karanikolas M, Kalauokalani D (2001) Pain treatment in the perioperative period. *Current problems in surgery* 38:835-920.
- Szewczak JM, Powell FL (2003) Open-flow plethysmography with pressure-decay compensation. *Respir Physiol Neurobiol* 134:57-67.

- Takakura AC, Moreira TS, Colombari E, West GH, Stornetta RL, Guyenet PG (2006) Peripheral chemoreceptor inputs to retrotrapezoid nucleus (RTN) CO₂-sensitive neurons in rats. *J Physiol* 572:503-523.
- Takakura AC, Moreira TS, Stornetta RL, West GH, Gwilt JM, Guyenet PG (2008) Selective lesion of retrotrapezoid Phox2b-expressing neurons raises the apnoeic threshold in rats. *J Physiol* 586:2975-2991.
- Takeda S, Eriksson LI, Yamamoto Y, Joensen H, Onimaru H, Lindahl SG (2001) Opioid action on respiratory neuron activity of the isolated respiratory network in newborn rats. *Anesthesiology* 95:740-749.
- Tan W, Pagliardini S, Yang P, Janczewski WA, Feldman JL (2010) Projections of preBotzinger complex neurons in adult rats. *The Journal of comparative neurology* 518:1862-1878.
- Tan W, Janczewski WA, Yang P, Shao XM, Callaway EM, Feldman JL (2008) Silencing preBotzinger complex somatostatin-expressing neurons induces persistent apnea in awake rat. *Nat Neurosci* 11:538-540.
- Tan W, Sherman D, Turesson J, Shao XM, Janczewski WA, Feldman JL (2012) Reelin demarcates a subset of pre-Botzinger complex neurons in adult rat. *The Journal of comparative neurology* 520:606-619.
- Tavani A, Robson LE, Kosterlitz HW (1985) Differential postnatal development of mu-, delta-and chi-opioid binding sites in mouse brain. *Brain research* 355:306-309.
- Thoby-Brisson M, Ramirez JM (2001) Identification of two types of inspiratory pacemaker neurons in the isolated respiratory neural network of mice. *J Neurophysiol* 86:104-112.
- Thoby-Brisson M, Trinh JB, Champagnat J, Fortin G (2005) Emergence of the pre-Botzinger respiratory rhythm generator in the mouse embryo. *J Neurosci* 25:4307-4318.
- Thoby-Brisson M, Karlen M, Wu N, Charnay P, Champagnat J, Fortin G (2009) Genetic identification of an embryonic parafacial oscillator coupling to the preBotzinger complex. *Nat Neurosci* 12:1028-1035.

- Thompson SA, Wafford K (2001) Mechanism of action of general anaesthetics--new information from molecular pharmacology. *Current opinion in pharmacology* 1:78-83.
- Thornton SR, Smith FL (1997) Characterization of neonatal rat fentanyl tolerance and dependence. *The Journal of pharmacology and experimental therapeutics* 281:514-521.
- Thornton SR, Smith FL (1998) Long-term alterations in opiate antinociception resulting from infant fentanyl tolerance and dependence. *European journal of pharmacology* 363:113-119.
- Thornton SR, Compton DR, Smith FL (1998) Ontogeny of mu opioid agonist antinociception in postnatal rats. *Brain research Developmental brain research* 105:269-276.
- Tian GF, Peever JH, Duffin J (1998) Botzinger-complex expiratory neurons monosynaptically inhibit phrenic motoneurons in the decerebrate rat. *Experimental brain research* 122:149-156.
- Tobias JD (1999) Sedation and analgesia in paediatric intensive care units: a guide to drug selection and use. *Paediatric drugs* 1:109-126.
- van den Hoogen RH, Colpaert FC (1986) Respiratory effects of morphine in awake unrestrained rats. *The Journal of pharmacology and experimental therapeutics* 237:252-259.
- Viscusi ER, Reynolds L, Chung F, Atkinson LE, Khanna S (2004) Patient-controlled transdermal fentanyl hydrochloride vs intravenous morphine pump for postoperative pain: a randomized controlled trial. *Jama* 291:1333-1341.
- Voituron N, Zanella S, Menuet C, Lajard AM, Dutschmann M, Hilaire G (2010) Early abnormalities of post-sigh breathing in a mouse model of Rett syndrome. *Respir Physiol Neurobiol* 170:173-182.
- Wallen-Mackenzie A, Gezelius H, Thoby-Brisson M, Nygard A, Enjin A, Fujiyama F, Fortin G, Kullander K (2006) Vesicular glutamate transporter 2 is required for central respiratory rhythm generation but not for locomotor central pattern generation. *J Neurosci* 26:12294-12307.

- Walsh M, Smith GA, Yount RA, Ferlic FJ, Wieschhaus MF (1991) Continuous intravenous infusion fentanyl for sedation and analgesia of the multiple trauma patient. *Annals of emergency medicine* 20:913-915.
- Wang H, Stornetta RL, Rosin DL, Guyenet PG (2001a) Neurokinin-1 receptor-immunoreactive neurons of the ventral respiratory group in the rat. *The Journal of comparative neurology* 434:128-146.
- Wang W, Tiwari JK, Bradley SR, Zaykin RV, Richerson GB (2001b) Acidosis-stimulated neurons of the medullary raphe are serotonergic. *J Neurophysiol* 85:2224-2235.
- Wang X, Hayes JA (2014) Laser ablation of Dbx1 neurons in the pre-Botzinger complex stops inspiratory rhythm and impairs output in neonatal mice. *3:e03427*.
- West JB (2007) *Respiratory Physiology: The Essentials*. Philadelphia: Lippincott Williams & Wilkins.
- Wree A (1990) Principles of the 2-deoxyglucose method for the determination of the local cerebral glucose utilization. *European journal of morphology* 28:132-138.
- Xia Y, Haddad GG (1991) Ontogeny and distribution of opioid receptors in the rat brainstem. *Brain research* 549:181-193.
- Yoburn BC, Billings B, Duttaroy A (1993) Opioid receptor regulation in mice. *The Journal of pharmacology and experimental therapeutics* 265:314-320.

Appendix I

Details of solution preparation for perfusion fixation and immunohistochemistry.

4% Paraformaldehyde solution (1 litre)

40 g of paraformaldehyde was added to 400 ml of distilled water (heated to approximately 68°C). NaOH was then added drop by drop until all the paraformaldehyde was dissolved and the solution became clear. The solution was then filtered into a 1L volumetric flask. 500 ml of 0.2M phosphate buffer solution was added and made up to 1L with distilled water.

30% sucrose solution

30 g of sucrose dissolved in 100 ml PBS.

0.2M Phosphate Buffer (PB)

17.47 g sodium di-hydrogen phosphate (NaH_2PO_4) and 40.75 g di-sodium hydrogen phosphate (Na_2HPO_4) were dissolved in 2 L distilled water.

0.3M Phosphate Buffered Saline (PBS)

72 g of sodium chloride (NaCl) was dissolved in 200 ml 0.2M PB and 1800 ml distilled water.

0.3M Phosphate Buffered Saline and 0.3% Triton X-100 (0.3% PBST)

500 ml 0.3M PBS + 1.5 ml triton X-100